

Université de Montréal

**La régulation génique chez *Solanum chacoense*: de la
pollinisation jusqu'à l'embryogenèse**

par

Faiza Tebbji

Département des sciences biologiques

Faculté des arts et des sciences

Thèse présentée à la Faculté des études supérieures
en vue de l'obtention du grade de Philosophiæ doctor (Ph.D)
en Sciences biologiques

Juillet, 2010

© Faiza Tebbji, 2010

Université de Montréal
Faculté des études supérieures

Cette thèse intitulée :

La régulation génique chez *Solanum chacoense*: de la pollinisation jusqu'à l'embryogenèse

Présentée par :
Faiza Tebbji

a été évaluée par un jury composé des personnes suivantes :

Mohamed Hijri, président-rapporteur
Daniel Philippe Matton, directeur de recherche
André Nantel, co-directeur
David Morse, membre du jury
Patrick Gulick, examinateur externe
Mohamed Hijri, représentant du doyen de la FES

Résumé

Chez les végétaux supérieurs, l'embryogenèse est une phase clé du développement au cours de laquelle l'embryon établit les principales structures qui formeront la future plante et synthétise et accumule des réserves définissant le rendement et la qualité nutritionnelle des graines. Ainsi, la compréhension des événements moléculaires et physiologiques menant à la formation de la graine représente un intérêt agronomique majeur. Toutefois, l'analyse des premiers stades de développement est souvent difficile parce que l'embryon est petit et intégré à l'intérieur du tissu maternel. *Solanum chacoense* qui présente des fleurs relativement grande facilitant l'isolation des ovules, a été utilisée pour l'étude de la biologie de la reproduction plus précisément la formation des gamètes femelles, la pollinisation, la fécondation et le développement des embryons. Afin d'analyser le programme transcriptionnel induit au cours de la structuration de ces étapes de la reproduction sexuée, nous avons mis à profit un projet de séquençage de 7741 ESTs (6700 unigènes) exprimés dans l'ovule à différents stades du développement embryonnaire. L'ADN de ces ESTs a été utilisé pour la fabrication de biopuces d'ADN. Dans un premier temps, ces biopuces ont été utilisé pour comparer des ADNc issus des ovules de chaque stade de développement embryonnaire (depuis le zygote jusqu'au embryon mature) versus un ovule non fécondé. Trois profils d'expression correspondant au stade précoce, intermédiaire et tardive ont été trouvés. Une analyse plus approfondie entre chaque point étudié (de 0 à 22 jours après pollinisation), a permis d'identifier des gènes spécifiques caractérisant des phases de transition spécifiques. Les annotations Fonctionnelles des gènes différentiellement exprimés nous ont permis d'identifier les principales fonctions cellulaires impliquées à chaque stade de développement, révélant que les embryons sont engagés dans des actifs processus de différenciation. Ces biopuces d'ADN ont été par la suite utilisé pour comparer différent types de pollinisation (compatible, incompatible, semi-compatible et inter-espèce) afin d'identifier les gènes répondants à plusieurs stimuli avant l'arrivé du tube pollinique aux ovules (activation à distance). Nous avons pu démontrer que le signal perçu

par l'ovaire était différent et dépend de plusieurs facteurs, incluant le type de pollen et la distance parcourue par le pollen dans le style. Une autre analyse permettant la comparaison des différentes pollinisations et la blessure du style nous a permis d'identifier que les programmes génétiques de la pollinisation chevauchent en partie avec ceux du stress. Cela était confirmé en traitant les fleurs par une hormone de stress, méthyle jasmonate. Dans le dernier chapitre, nous avons utilisé ces biopuces pour étudier le changement transcriptionnel d'un mutant sur exprimant une protéine kinase FRK2 impliqué dans l'identité des ovules. Nous avons pu sélectionner plusieurs gènes candidat touchés par la surexpression de cette kinase pour mieux comprendre la voie de signalisation.

Ces biopuces ont ainsi servi à déterminer la variation au niveau transcriptionnelle des gènes impliqués lors de différents stades de la reproduction sexuée chez les plantes et nous a permis de mieux comprendre ces étapes.

Mots-clés: *Solanum chacoense*, biopuces d'ADN, pollinisation, fécondation, embryogenèse, activation à distance, gamétophyte femelle, ovule, ovaire, guidage, MAPK.

Abstract

In higher plants, embryogenesis is a key phase of development during which the embryo establishes the main structures that will form the future plant, synthesizes, and accumulates the reserves that will define the yield and nutritional quality of the seeds. Thus, understanding the molecular and physiological events leading to the formation of the seed is of major agronomic interest. However, analysis of early stages of development is often difficult because the embryo is small and integrated within the maternal tissue. *Solanum chacoense*, whose relatively large flowers facilitate the isolation of ovules, was used to study the biology of reproduction, in particular the formation of female gametes, pollination, fertilization and embryo development. To analyze the transcriptional program induced during these stages of sexual reproduction, we produced amplicon-derived microarrays with 7741 ESTs isolated from ovules bearing embryos from different developmental stages. These chips were first used to compare cDNA of unfertilized ovule with ovule cells of each stage of embryonic development (from zygote to mature embryo). During embryogenesis, three major expression profiles corresponding to early, middle and late stages of embryo development were identified. Further analysis, of time points taken every 2 days from 0 to 22 days after pollination allowed the identification of a subset of stage-specific and transition-specific genes. Functional annotation of differentially expressed genes allowed us to identify the major cell processes implicated at each stage of development and revealed that embryos are engaged in active differentiation. The DNA microarrays were then used to compare different types of pollination (compatible, incompatible, semi-compatible and inter-species) to identify genes responding to various stimuli before the pollen tube reach the ovules (activation at distance). We found that the signal received by the ovary was different and depended on several factors including the pollen source and the distance traveled by the pollen in the style. Another analysis comparing different pollinations with wounding of the style showed that the genetic programs of pollination overlap with those of stress. This was confirmed by treating the

flowers with a stress hormone, methyl jasmonate. lastly, we used the microarrays to study transcriptional changes in mutant ScFRK2. The over expression of FRK2 affect the ovule identity. We were able to select several candidate genes that may have a role in ovules identity signaling.

These chips were used to determine the variation in transcription of genes involved at various stages of sexual reproduction in plants and has allowed us to better understand these steps at the transcriptional level.

Keywords: *Solanum chacoense*, DNA microarray, pollination, fertilization, embryogenesis, activation at distance, female gametophyte, ovule, ovary, guidance, MAPK.

Table des matières

Résumé.....	iii
Abstract	v
Liste des tableaux.....	ix
Liste des figures	xii
Liste des sigles et abréviations	xxi
Remerciements	xxxii
Introduction	1
1 Le développement des gamétophytes femelles et mâles.....	1
1.1 La fleur	1
1.1.1 Induction du méristème floral: transition du stade végétatif au stade reproductif	2
1.1.2 Les gènes d'identité d'organes floraux	5
1.2 Développement de l'ovule	9
1.2.1 Spécification et formation du placenta.....	9
1.2.2 L'identité des ovules	10
1.2.3 Développement du sac embryonnaire	11
1.3 Développement du pollen	14
1.4 La pollinisation	16
1.5 Attraction des tubes polliniques	17
1.6 La double fécondation et l'embryogenèse	20
2- Génomique et contrôle génétique de l'embryogenèse végétale.....	22
3- Modèle génétique et fonctionnel de l'établissement des patrons embryonnaires chez <i>A. thaliana</i>	28
Problématique et projet de recherche.....	34
Chapitre 1.....	37

Transcription profiling of fertilization and early seed development events in a solanaceous species using using a 7.7K cDNA microarray from <i>Solanum chacoense</i> ovules	37
Abstract	38
Background	40
Methods.....	43
Results.....	49
Discussion	70
Conclusion	85
Acknowledgements	85
Chapitre 2.....	86
Pollination type recognition from a distance by the ovary is revealed by a global transcriptomic analysis.....	86
Abstract	87
Introduction	88
Materials and Methods	90
Results.....	95
Discussion	113
Chapitre 3.....	124
Loss of ovule identity induced by overexpression of the Fertilization-Related Kinase 2 (ScFRK2), a MAPKKK from <i>Solanum chacoense</i>	124
Abstract	125
Introduction	127
Material and Methods	130
Results	135
Discussion	156
Discussion et perspectives.....	166
Conclusion	178
Bibliographie.....	180

Liste des tableaux

Tous les tableaux sont accessibles sur le site:
https://www.webdepot.umontreal.ca:443/xythoswfs/webui/_xy-6277605_1-t_soOnkV9V

Chapitre 1 :

Supplemental Table 1: Primer sequences used in the real time quantitative PCR expression analysis of selected genes representing candidates from the early, middle and late embryogenesis stages shown in figure 9.

Supplemental Table 2: Differential expression of 1024 genes during *S. chacoense* embryogenesis

Supplemental Table 3: Differential expression of genes in anthers, style, and leaf tissues compared to unfertilized ovules.

Supplemental Table 4: Differential expression of genes during embryo development showing the up or less 10 fold changes.

Supplemental Table 5: Differential expression of genes amongst the three major stages (early, middle and late) of embryogenesis

Supplemental Table 6: Differential expression of stage-specific genes during each point of the embryo development (2 to 22 DAP).

Chapitre 2:

Supplemental Table 1: Differential expression of regulated genes at 6, 24 and 48 hours after pollination between compatible pollination (SC), incompatible pollination (SI), semi-compatible pollination (SeC) and interspecific pollination (IS).

Supplemental Table2: Differential expression of genes in compatible pollination at 6, 24 and 48 hours after pollination.

Supplemental Table 3:: Differential expression of genes in incompatible pollination at 6, 24 and 48 hours after pollination.

Supplemental Table 4: Differential expression of regulated genes at 6, 24 and 48 hours after pollination or wounding between compatible pollination (SC), incompatible pollination (SI), and wounding.

Supplemental Table 5: Differential expression of regulated genes at 6, 24 and 48 hours after pollination or wounding between semi-compatible pollination (SeC), interspecific pollination (IS), and wounding.

Supplemental Table 6: Differential expression of regulated genes at 6, 24 and 48 hours between compatible pollination (SC), incompatible pollination (SI), MeJA treatment, and style wounding.

Chapitre 3:

Supplemental Table 1: Differential expression of regulated genes that showed a statistically significant difference in transcript abundance between the WT and the *ScFRK2*-

overexpressing ovules. A Welch *t*-test ($P < 0.05$) with a 1.5-fold variation was used to compare the profiles from the *ScFRK2* versus control.

Liste des figures

Chapitre 1:

Figure 1: Gene expression profiling of unfertilized and fertilized ovule samples.

Scatter plots comparing the average fluorescence intensities in microarray experiments measuring the change in transcript abundance between A, pooled control and individual control; or B, 16 DAP pollinated ovules versus unfertilized ovules. The individual control samples were different from the pooled one that is used as the universal control in all our experiments. Black transversal lines show the ± 2 fold change.

Figure 2: Transcriptional changes in *S. chacoense* ovules across an embryo developmental time course. The level of expression is compared to unfertilized ovules.

A, Each line represents a probe that was spotted on the microarray while each time points of embryo developmental stage are represented in X-axis. The Y-axis shows the log of the normalized fluorescence ratios. Indicated in red are the genes expressed to levels higher than the median value. Genes indicated in blue are expressed to lower levels than the median value. The corresponding embryo developmental stage for each time point was ascertain by ovule clearings and observed by DIC microscopy and represented with a schematic figure. B Cluster analysis using unsupervised hierarchical clustering of 1024 genes that exhibit a statistically significant change between all samples ($P < 0.01$). The analysis was performed using condition tree clustering on all samples. Each row represents a different gene, and each column displays gene expressions at each time point (0 to 22 DAP). Each experimental data point is colored according to the change in fluorescence ratio at that time point: data values displayed as red and blue represent increased and reduced expression, respectively while data values in yellow are not differentially expressed when compared to unfertilized ovules.

Figure 3: Tissue-specific comparison between ovule, style, anther and leaf tissues. The level of expression is compared to unfertilized ovules.

A, Cluster analysis of the transcriptional profiles obtained from leaves, styles, and anthers. The clustering was performed using condition tree clustering on all samples. Each row represents a different gene, and each column displays gene expressions at different tissues (UO, style, leaf and anther). Data values displayed as red and blue represent elevated and reduced expression, respectively. A total of 601 genes with a statistically significant change in transcript abundance of ≥ 2 -fold in at least one tissue compared to unfertilized ovules (FDR <0.01) are found. B, Venn diagram showing overlap between lists of genes differentially expressed in anther, style and leaf tissues. C, Principal Components Analysis (PCA) of various tissue types (A: Anthers; S: Styles; Le: Leaves; C: unfertilized ovules. E, M, L: early, middle and late stages of embryo development, respectively) based on the expression profile of 1376 genes including 558 that are differentiellly expressed in at least one tissue from styles, leaves and anthers and 1024 transcripts that are regulated in ovule which resulted in a clear differentiation distributed between 7 classifications.

Figure 4: Venn diagram showing overlap between gene lists that show significant changes in transcript abundance during the three major embryo development stages (early, middle and late stages). The level of expression is compared to unfertilized ovules.

Figure 5: Functional annotations of the 955 genes (passing the significance filter: $P < 0.01$ and 2 fold cut-off) during the three major embryo developmental stages. The color keys show the designated gene class annotations.

Figure 6: Graphical representation of the number of stage-specific genes identified at each time points of embryo development. The level of expression is compared to unfertilized ovules. (Volcano plot using Student's t-test analysis taking FDR <0.01 and 2 fold cut off). To find specific genes in each time, a Venn diagram was used between each time point and

the total of genes remaining in the other stages. Numbers in the inner circle are genes shared by at least another time point. Numbers in the outer circle are genes considered stage-specific by the Volcano analysis.

Figure 7: Distribution of 558 differentially expressed (by 2 fold-change, $P < 0.01$) genes in anthers styles and leaves in various biological process categories. The level of expression is compared to unfertilized ovules. The color key shows the designated gene class annotations.

Figure 8: Quantitative real-time PCR (qRT-PCR) of selected genes representing the early, middle and late stage of embryo development. qRT-PCR was performed with two independent samples at each point .

Figure 9: K-means clustering using Pearson Correlation (GeneSpring version 7.2) during an embryo development time course. A, Models of dynamic gene expression patterns representing all the nine different pattern founded based on the three point time (early, middle and late). B, Clustering of specific differentially expressed genes in the ovules based on 15 clusters representing all the stages of embryonic development from 0 to 22 DAP. The black discontinues line represent the average of gene profile.

Chapitre 2:

Figure 1: Pollen tube growth measurments after manual pollination and aniline blue staining of the styles from 6 to 48 hours after pollination. Pollen tube growth were measured in 4 different pollination types including compatible pollination (SC), incompatible pollination (SI), semi-compatible pollination (SeC) and interspecific pollination (IS). All the observations and measurments were taken by fluorescent

microscope (Zeiss AxioImager M1 fluorescent microscope equipped with an AxioCam HRc camera).

Figure 2: Venn diagram analysis of regulated genes at 6, 24 and 48 hours after pollination between compatible pollination (SC), incompatible pollination (SI), semi-compatible pollination (SeC) and interspecific pollination (IS).

Figure 3: Venn diagram showing overlap between gene lists that show significant changes in transcript abundance at 6, 24 and 48HAP during: A- compatible pollination (SC). B- Incompatible pollination (SI). C- Semi-compatible pollination (SeC) and D- interspecific pollination (IS).

Figure 4: Cluster analysis using unsupervised hierarchical clustering of gene lists that show significant changes in transcript abundance ($P < 0.05$). During compatible pollination (SC), incompatible pollination (SI), semi-compatible pollination (SeC) and interspecific pollination (IS) at 6, 24 and 48HAP. The analysis was performed using condition tree clustering on all samples. Each row represents a different gene, and each column displays gene expressions at each pollination experiment (SC, SI, SeC, and IS). Each experimental data point is colored according to the change in expression ratio at that time point: data values displayed as yellow and blue represent increased and reduced expression, respectively while data values in yellow are not differentially expressed when compared to unfertilized ovules.

Figure 5: Venn diagram showing overlap between gene lists that show significant changes in transcript abundance during :A- compatible pollination (SC), incompatible pollination (SI), and wounding at 6 HAP/HAW. B- Compatible pollination (SC), incompatible pollination (SI), and wounding at 24 HAP/HAW. C- Compatible pollination (SC), incompatible pollination (SI), and wounding at 48 HAP/ HAW. D- Semi-compatible

pollination (SeC), interspecific pollination (IS), and wounding at 6 HAP/ HAW. E- Semi-compatible pollination (SeC), interspecific pollination (IS), and wounding at 24 HAP/ HAW. F- Semi-compatible pollination (SeC), interspecific pollination (IS), and wounding at 48 HAP/ HAW.

Figure 6: Venn diagram showing overlap between gene lists that show significant changes in transcript abundance during wounding treatment at 6, 24, and 48 HAW.

Figure 7: Venn diagram showing overlap between gene lists that show significant changes in transcript abundance during :A- compatible pollination (SC), methyl jasmonate (MeJA), and wounding (W) at 6 hours. B- Incompatible pollination (SI), methyl jasmonate (MeJA), and wounding (W) at 6 hours. C- Compatible pollination (SC), methyl jasmonate (MeJA), and wounding (W) at 24 hours. D- Incompatible pollination (SI), methyl jasmonate (MeJA), and wounding (W) at 24 hours. E- Compatible pollination (SC), methyl jasmonate (MeJA), and wounding (W) at 48 hours. F- Incompatible pollination (SI), methyl jasmonate (MeJA), and wounding (W) at 48 hours.

Figure 8: Summary of Pollination and wound effect at a distance in the ovary.

Chapitre 3

Figure 1. Sequence analyses of ScFRK1 and ScFRK2. A. Sequence alignment of the deduced protein sequences from *S. chacoense* ScFRK1 and ScFRK2, and with the three most similar MAPKKK from *A. thaliana*. Kinase subdomains are identified with thick black lines and were defined as described by Hanks and Hunter (1995), where alpha helices and beta sheets were deduced by four different prediction tools (see materials and methods). **B.** Phylogenetic tree obtained with the neighbor-joining method from uncorrected distances. Bootstrap support values from 1000 replicates are indicated beside

the branches. All *A. thaliana* sequences were directly obtained from the TAIR website (<http://www.arabidopsis.org/>). The phylogenetic analysis was performed using the catalytic kinase domain. Tree branch length is proportional to the number of substitutions and the scale bar represents the expected number of substitution per site.

Figure 2. Transcript profile of *ScFRK2*. **A.** DNA gel blot analysis of the *ScFRK2* gene. Genomic DNA (10 µg) isolated from *S. chacoense* leaves was digested with Bam HI, Eco RI, Nco I or Xba I restriction enzyme, transferred onto membranes and probed with the complete 1.1 kb *ScFRK2* cDNA. Estimated molecular weights of the fragments obtained appear on the left of each DNA blot. **B.** RNA gel blot analysis of *ScFRK2* gene. All tissues were collected from greenhouse-grown plants. Pollen tubes were germinated *in vitro*. Fertilized ovules were dissected from ovaries 2 to 6 days after pollination (DAP). Pistils at 2 to 4 DAP were separated into styles and ovaries. Ten µg of total RNA isolated from *S. chacoense* tissues were blotted and probed using the full-length *ScFRK2* cDNA (upper panel). Membranes were stripped and re-probed using a partial 18S ribosomal RNA to ensure equal loading of each RNA sample (lower panel). **C.** *In situ* localization of *ScFRK2* transcripts in mature ovaries. I and II, unfertilized mature ovary sections. III and IV, ovary sections 2 DAP (approximately 12 h post-fertilization). V and VI, magnifications of III and IV, respectively. VII and VIII, magnification of ovary sections 2 DAP showing staining in the zygote. I, III, V, and VII, control sense probe. II, IV, VI and VIII, antisense sense probe. Digoxigenin labeling is visible as red to purple staining. All hybridizations used 10 µm-thick sections and an equal amount of either *ScFRK2* sense or antisense probe. Scale bars, 250 µm (I to IV); 125 µm (V and VI); 20 µm (VII and VIII). In, integument; ov, ovule; ow, ovary wall (pericarp); p, placenta; zy, zygote.

Figure 3. Analyses of *ScFRK2* transgenic plants carrying sense constructs. **A.** RNA gel blot analyses of *ScFRK2* mRNA (upper panel) and 18S rRNA (lower panel) of ovary tissues derived from wild-type plants (WT), overexpression lines S2 and S17, and

cosuppression line S20. **B.** Comparison of fruit slices. Scale bar, 1 cm. **C.** Growth in fruit size after pollination.

Figure 4. Fruit and ovule development of *ScFRK2-OX* plants. A and B. wild-type (**A**) and transgenic (**B**) ovaries. Ovary wall has been removed to expose ovules. The white arrow in **B** points to a normal ovule. **C-Q.** SEM images from wild-type (**C, H, J, L, N, and P**) and transgenic (**D-G, I, K, M, O and Q**) plants. **C.** Ovules from wild-type plant. **D and E.** Ovules from *ScFRK2-OX* plants, where **D** showing milder phenotype than **E**. **F.** Enlargement of emerging carpelloid structure (CS). **G.** Enlargement of an elongated CS. **H.** Papillae on wild-type stigma. **I.** Papillae on the CS extremity. **J.** Enlargement of stigmatic papillae. **K.** Enlargement of papillae on the CS extremity. **L.** Style cortex epidermis of a wild-type plant. **M.** Epidermis of the stylar section of CS. **N.** Small papillae on a wild-type style three days before anthesis. **O.** Small papillae from the stylar section of CS. In **N** and **O**, papillar cells are indicated by dark arrows. **P.** Enlargement of papillar ornamentations from the style of a wild-type plant. **Q.** Enlargement of papillar ornamentations from CS of a transgenic plant. **R through U.** Light microscopy of wild-type (**R**) and transgenic (**S-U**) plants. **R.** Ovary from a wild-type plant (only one locule shown). **S.** Ovary from a *ScFRK2-OX* plant (only one locule shown). **T.** Transverse section of a style from wild-type plant. The arrow indicates the transmitting tract. **U.** Transverse section of CS showing dense cells resembling the transmitting tract (indicated by arrows). **V.** Developing ovary from a wild-type plant. Section was taken from a flower bud approximately 2 mm in length. **W.** Enlargement of an ovule shown in **V**. The black arrow indicates the ovule integument and the white arrow indicates the megasporocyte. **X.** Developing ovary from a *ScFRK2-OX* plant. Section was taken from a flower bud approximately 2 mm in length. The black arrows indicate developing CSs. **Y.** Enlargement of the tip of CSs shown in **X**. The black arrow indicates the integument. Integuments were often enlarged. The white arrow indicates the megasporocyte. Scale bars, 1 mm (A and B); 100 µm (C , D, F-H, L-O, U, V,

and X); 500 µm (E); 50 µm (I and T); 10 µm (J, K, P and Q); 250 µm (R and S); 20 µm (W and Y).

Figure 5. In situ RNA hybridization analyses in developing ovules.

A to E. *ScFRK2* expression in wild-type plants **A.** Sense probe. **B to E.** Antisense probe. **A and B.** Developing ovary showing ovule primordia arising from the placenta. Sections were taken from a flower bud approximately 1.5 mm in length. **C.** Ovary at a later stage showing developing ovule with growing integuments. The section was taken from a flower bud approximately 2 mm in length. As ovules mature, the signal in the megasporocyte became weaker while the signal in the integument became stronger, particularly at the growing tip. **D.** Enlargement of B showing an intense *ScFRK2* mRNA signal in the megasporocyte. **E.** Enlargement of C. **F to I.** Comparison of *ScFRK2* expression between wild-type and *ScFRK2*-OX plants. *In situ* RNA hybridization was performed simultaneously using identical conditions to allow direct comparison. Sections were taken from ovaries at a similar stage as shown in C. **F.** Sense probe. **G-I.** Antisense probe. **F and G.** Wild-type plant. **H.** *ScFRK2*-OX plant. Arrow heads show developing CSs. Although signals are almost absent from the stalk, intense signals remain strong at the tip. **I.** Enlargement of H, showing the megasporocyte at the tip of the developing CS. The signal in the megasporocyte remains strong. **J to M.** *ScFBP11* expression in developing ovules. Tissue sections were taken from ovaries about the same stage as those in C-I. *In situ* RNA hybridization was performed simultaneously using identical conditions to allow direct comparison. **J.** Sense probe. **K to M.** Antisense probe. **J and K.** Wild-type plant. **K.** Diffuse signals were detected from the ovule integument while little signals were detected from the megasporocyte. **L.** Ovary from a *ScFRK2*-OX plant. Strong signals were detected in ovules that appear normal and also at the tip of the developing CS. Very little signals were detected in the stalk of CS. **M.** Enlargement of K. showing absence of signal in the megasporocyte. **N.** Enlargement of L, showing intense signals in the megasporocyte of CS..

cs, carpelloid; in, integument; mmc, megasporocyte; op, ovule primodium; ov, ovule; ow, ovary wall; p, placenta. Scale bars, 100 μ m (A - C, F – H, J - L); 20 μ m (D, E, I, M and N).

Figure 6. Schematic representation of *ScFRK2* mRNA distribution during wild-type and *ScFRK2-OX* ovule development.

ScFRK2 *in situ* RNA hybridization signal distribution is represented by the gray scale, where black is strongest, and decreasing intensity of gray corresponds to lower expression levels. **Wild-type.** *ScFRK2* mRNA accumulates in the megasporocyte during ovule primordium formation. As ovules mature, *ScFRK2* mRNA levels decrease in megasporocyte and increase near the growing tip of the ovule's integument. When ovule reaches maturity, *ScFRK2* mRNA is only detected in the integument. ***ScFRK2-OX.*** In general, *ScFRK2* mRNA accumulates more than wild-type but the accumulation pattern during ovule primordium formation is identical to wild-type (i.e. accumulation mostly found in megasporocyte). *ScFRK2* mRNA remains abundant in megasporocyte during ovule/CS formation. Also, *ScFRK2* mRNA accumulates at the tip of overgrowing integument, whereas no or little *ScFRK2* mRNA is detected in the overgrowing funiculus (stalk of CS).

Liste des sigles et abréviations

Sauf si mentionné, le gène et son abréviation proviennent de l'espèce *Arabidopsis thaliana*. Le mutant est écrit dans le texte en minuscule et en italique, mais dans la liste des abréviations il est représenté par le nom du gène.

%	pourcentage
χ^2	test statistique
°C	degré Celcius
μg	microgramme
μl	microlitre
μm	micromètre
μM	micromolaire
ABA	acide abscicique
ABI	Applied Biosystems
Abs	absorbance
ACR4	gène CRINKLY4
ADN	acide desoxiribonucléique
AG	gène <i>AGAMOUS</i>
<i>AGL11</i>	gène <i>AGAMOUS like 11</i>
<i>AGL15</i>	gène <i>AGAMOUS like 15</i>
<i>AGL2</i>	gène <i>AGAMOUS like 2</i>
<i>AGL4</i>	gène <i>AGAMOUS like 4</i>
<i>AGL9</i>	gène <i>AGAMOUS like 9</i>
<i>AGP</i>	arabinogalactan protein
ANOVA	analysis of variance
<i>ANT</i>	gène <i>AINTEGUMENTA</i>
<i>API</i>	gène <i>APETALA 1</i>

<i>AP2</i>	gène <i>APETALA 2</i>
<i>AP3</i>	gène <i>APETALA 3</i>
AREs	auxin response elements
ARFs	auxine response factors
ARN	acide ribonucléique
ARNm	ARN messager
<i>AS1</i>	gène <i>ASYMETRIC LEAVES 1</i>
ATP	adénosine triphosphate
ATPase	adénosine triphosphatase
<i>ATS1</i>	gène <i>ARABIDOPSIS THALIANA SEED 1</i>
<i>ATS3</i>	gène <i>ARABIDOPSIS THALIANA SEED 3</i>
<i>BDL</i>	gène <i>BODENLOS</i>
BLAST	Basic Local Alignment Search Tool
bp	base pair
BSA	bovine serum albumin
CA	California
<i>CAL</i>	gène <i>CAULIFLOWER</i>
CDK	cyclin dependant kinase
cDNA	complementary DNA
CDPK	calcium dependent protein kinase
<i>CLF</i>	gène <i>CURLY LEAF</i>
<i>CLV1</i>	gène <i>CLAVATA1</i>
<i>CLV2</i>	gène <i>CLAVATA2</i>
<i>CLV3</i>	gène <i>CLAVATA3</i>
cm	centimètre
<i>CO</i>	gène <i>CONSTANT</i>
<i>CR4</i>	gène <i>CRINKLY 4</i>
<i>CRC</i>	gène CRABS CLAW

<i>CTR1</i>	gène <i>CONSTITUTIVE TRIPLE RESPONSE 1</i>
<i>CUC 2</i>	gène <i>CUP-SHAPED COTYLEDON 2</i>
<i>CUC 3</i>	gène <i>CUP-SHAPED COTYLEDON 3</i>
<i>CUC1</i>	gène <i>CUP-SHAPED COTYLEDON 1</i>
Cy	cyanine
d	day
d(T)/ dT	deoxythymidine
DAP	days after pollination
dATP	déoxyadénosine triphosphate
dCTP	déoxycytidine triphosphate
DE	Delaware
<i>DEF</i>	gène <i>DEFICIENS</i> chez <i>A. majus</i>
<i>DEK</i>	gène <i>DEFECTIVE-KERNEL</i>
DIC	differential interference contrast
DMSO	Dimethylsulfoxide
DNA	deoxyribonucleic acid
dNTP	deoxyribonucleotide triphosphate/désoxyribonucléotide triphosphate
Dr.	Docteur
DTT	dithiothreitol
<i>ECE1</i>	gène <i>Extent of Cell Elongation</i> chez <i>Candida albicans</i> (orf19.3374)
ECM	matrice extracellulaire
email	electronic mail
<i>EMB</i>	gène <i>EMBRYO-DEFECTIVE</i>
<i>EMF1</i>	gène <i>EMBRYONIC FLOWER 1</i>
<i>EMF2</i>	gène <i>EMBRYONIC FLOWER 2</i>
EMS	Ethyl Methhyl Sulfonate
<i>EMS1</i>	gène <i>EXCESS MICROSPOROCYTES 1</i>
ENP	gène <i>ENHANCER OF PINOID</i>

EST	expressed sequence tag
EXS	extrasporogenous cells
EXS	gène <i>EXTRA SPOROGENOUS</i>
FAA	Formaldehyde-Acid Alcohol
FAR	gène <i>FARINELLI</i> chez <i>A. majus</i>
<i>FBP11</i>	gène <i>FLORAL BINDING PROTEIN 11</i> chez <i>Pétunia</i>
<i>FBP7</i>	gène <i>FLORAL BINDING PROTEIN 7</i> chez <i>Pétunia</i>
<i>FEM1</i>	gène <i>FEMALE GAMETOPHYTE 1</i>
<i>FEM2</i>	gène <i>FEMALE GAMETOPHYTE 2</i>
<i>FER</i>	gène <i>FERONIA</i> chez <i>Torenia fournieri</i>
FGS	gamétophytique femelle spécifique
<i>FIE</i>	gène <i>FERTILIZATION INDEPENDENT-ENDOSPERM</i>
<i>FIE1</i>	gène <i>FERTILIZATION INDEPENDENT-ENDOSPERM 1</i>
<i>FIE2</i>	gène <i>FERTILIZATION INDEPENDENT-ENDOSPERM 2</i>
<i>FIE3</i>	gène <i>FERTILIZATION INDEPENDENT-ENDOSPERM 3</i>
Fig.	figure
FQRNT	Fonds Québécois de la Recherche sur la Nature et les
FRK1	gène <i>FERTILIZATION RELATED KINASE 1</i> chez <i>S. chacoense</i>
FRK2	gène <i>FERTILIZATION RELATED KINASE 2</i> chez <i>S. chacoense</i>
<i>FT</i>	gène <i>FLOWERING LOCUS T</i>
<i>FUS</i>	gène <i>FUSCA</i>
G4	lignée G4 de <i>Solanum chacoense</i>
GA	Gibberillin
GABA	γ-amino butyric acide
<i>GDR</i>	gène <i>GROUDED</i>
GEO	Gene Expression Omnibus
<i>GF</i>	gène <i>GAMETOPHYTIC FACTOR</i>
<i>GF2</i>	gène <i>GAMETOPHYTIC FACTOR 2</i>

<i>GF3</i>	gène <i>GAMETOPHYTIC FACTOR 3</i>
<i>GF4</i>	gène <i>GAMETOPHYTIC FACTOR 4</i>
<i>GF5</i>	gène <i>GAMETOPHYTIC FACTOR 5</i>
<i>GF7</i>	gène <i>GAMETOPHYTIC FACTOR 7</i>
GG	gamétophytique générale
<i>GK</i>	gène <i>GURKE</i>
<i>GLO</i>	gène <i>GLOBOSA (GLO)</i> chez <i>A. majus</i>
GMC	guard mother cell
<i>GN</i>	gène <i>GNOM</i>
GO	Gene Ontology
GUS	gène glucuronidase permettant une coloration
h	hour/heure
HAIP	heure après pollinisation incompatible
HAP	hours after pollination
<i>HDD</i>	gène <i>HADAD</i>
<i>HYD1</i>	gène <i>Hydra1</i>
<i>IAA12</i>	gène <i>AUXIN/INDOLEACETIC ACID- INDUCED PROTEIN 12</i>
<i>IAA13</i>	gène <i>AUXIN/INDOLEACETIC ACID- INDUCED PROTEIN 13</i>
<i>ICU2</i>	gène <i>INCURVATA2</i>
<i>IG 1</i>	gène <i>INDETERMINATE GAMETOPHYTE 1</i>
IRBV	Institut de Recherche en Biologie Végétale
IS	pollinisation inter-espèce
K ⁺	ion potassium
K ₃ PO ₄	Potassium phosphate
kb	kilobase
kDa	kiloDalton
<i>KNOX</i>	gène <i>KNOTTED1</i> -like homeobox
L/l	litre

<i>LEC1</i>	gène <i>LEAFY COTYLEDON 1</i>
<i>LePRK1</i>	gène codant pour un récepteur like kinases 1 chez la tomate
<i>LePRK2</i>	gène codant pour un récepteur like kinases 2 chez la tomate
<i>LePRK3</i>	gène codant pour un récepteur like kinases 3 chez la tomate
<i>LFY</i>	gène <i>LEAFY</i>
<i>LIP1</i>	gène <i>LIPLESS 1</i>
<i>LIP2</i>	gène <i>LIPLESS 2</i>
<i>LO2</i>	gène <i>LETHAL OVULE2</i>
LOWESS	locally weighted scatterplot smoothing
LRR	leucine-rich repeat
LTP	lipid transfer protein
<i>LUG</i>	gène <i>LEUNIG</i>
M	molaire
MA	Massachusetts
<i>MAA3</i>	gène <i>MAGATAMA 3</i>
MADS-box	doamine de facteur de transcription conservé trouvé initialement dans les membres des familles MCM1, AGAMOUS, DEFICIENS et SRF (serum response factor).
MAPK	protéine Mitogen activated protein kinase
MAPKKK	mitogen activaed protein kinase kinase kinase
MeJA	methyle jasmonate
MeOH	methanol
mg	miligramme
MgCl ₂	clorure de magnésium
Min	minute
ml	milliliter
mm	milimètre
mM	milimolaire

<i>MP</i>	gène <i>MONOPTEROS (MP)</i>
<i>MPK3</i>	gène <i>MITOGEN ACTIVATED KINASE 3</i>
<i>MPK6</i>	gène <i>MITOGEN ACTIVATED KINASE 6</i>
mRNA	messenger RNA
MW	molecular weight
<i>MYB98</i>	gène <i>MYB98</i>
n	nombre d'échantillon/ d'acide nucléique
N	unité de concentration; Normal
Na ⁺	ion sodium
NAC	gènes NAM (no apical meristem), ATAF1 (Arabidopsis transcription activator factore1) and CUC2 (CUP-SHAPED COTYLEDON 2)
NaOH	hydroxyde de sodium
NCBI	National Center for Biological Information
ng	nanogramme
nm	nanomètre
nmol	nanomole
no.	number/numéro
<i>NPH4</i>	gène <i>NONPHOTOTROPIC HYPOCOTYL4</i>
NRC	National Research Council
NRSP	National Research Support Program
NY	New York
ON	Ontario
OX	ligné surexprimante
P	valeur statistique FDR (False discovery rate)
PCR	polymerase chain reaction
PE	Perkin Elmer
pEce1	plasmid ECE1
Ph D	Philosophiæ doctor

pH	potentiel hydrogène
<i>PI</i>	gène <i>PISTILLATA</i>
<i>PID</i>	gène <i>PINOID</i>
<i>PIN7</i>	gène <i>PINFORMED7</i>
PIR	Protein Information Resource
<i>PLE</i>	gène <i>PLENA</i> chez <i>A. majus</i>
PMC	Pollen Mother Cell
<i>POP2</i>	gène <i>POLLEN-PISTIL INTERACTION 2</i>
<i>PRI</i>	gène <i>PROLIFERA 1</i>
p-value	valeur statistique
QC	Québec
QPCR	quantitative PCR
RALF	gène Rapid alcalinization factor
RNA	ribonucleic acid
RNAi	ARN d'interference
Rpm	rotation par minute
RT-PCR	reverse transcription polymerase chain reaction
S	allèle d'auto incompatibilité
SAM	shoot apical meristem
SC	self-compatible
ScFRK1	<i>Solanum chacoense</i> fertilization related kinase 1
SD	standard deviation
SDS	Sodium Dodecyl Sulfate
sec	secondes
SeC	semi-compatible
<i>SEP</i>	gène <i>SEPALLATA</i>
<i>SER</i>	gène <i>SIRENE</i>
SERK	gène somatic embryogenesis receptor kinase

SGMD	Soybean Genomics and Microarray Database
<i>SHP1</i>	gène <i>SHATTERPROOF 1</i>
<i>SHP2</i>	gène <i>SHATTERPROOF 2</i>
SI	self-incompatible
<i>SMT1</i>	gène <i>STEROL METHYL-TRANSFERASE</i> de même que <i>CPH</i>
<i>SOC1</i>	gène <i>SUPPRESSOR OF CONSTANT1</i>
<i>SPT</i>	gène <i>SPATULA</i>
S-RNA	RNAse associé au locus S
SSC	salt sodium citrate buffer
<i>SSP</i>	gène <i>SHORT SUSPENSOR</i>
<i>STK</i>	gène <i>SEEDSTICK</i>
<i>STM</i>	gène <i>SHOOT MERISTEMLESS</i>
<i>SUP</i>	gène <i>SUPERMAN</i>
TAIR	The Arabidopsis Information Resource
tel	téléphone
tRNA	ARN totaux
<i>TSL</i>	gène <i>TOUSLED</i>
TTS	transmiting tissue-specific
UO	Unfertilized ovules
USA	United States of America
USDA	united states department of agriculture
UV	ultraviolet
V	volt
V22	génotype comportant les allèles d'incompatibilité S ₁₂ ,S ₁₄
W	blessure
<i>WOL</i>	gène <i>WOODEN LEG</i>
WT	wild type (témoin, type sauvage)
<i>YDA</i>	gène <i>YODA</i>

ZLL

gène *ZWILLE*

ZmEA1

gène *Zea mays EGG APPARATUS 1* de *Zea mays*

$\Delta\Delta Ct$

Delta Delta cycle threshold

« A toi mon cher papa qui arrêtait pas de demander depuis ma première année: quand est ce que tu fini ton doctorat? Et à toi mon petit poussin d'amour inattendu Imrane. Ton arrivé à changer tout mon programme et à laisser traîner ma thèse beaucoup plus longtemps que prévu.»

Remerciements

Tout d'abord je tiens à remercier chaleureusement mon directeur le Dr. Daniel Philippe Matton qui m'a accueilli dans son laboratoire, qui m'a encadré durant ces quatre années et qui m'a offert toutes les possibilités pour avoir une formation la plus complète possible, incluant non seulement le travail à la paillasse, la réflexion scientifique et la rédaction des articles mais aussi l'encadrement, l'enseignement, la préparation des examens et les corrections. Je ne te serai jamais assez reconnaissante de toute la confiance que tu m'as faite et je ne pourrai jamais assez te remercier. Merci pour tout.....

Je tiens aussi à remercier mon adorable co-directeur André Nantel à l'IRB. Merci de m'avoir ouvert les portes de ton laboratoire et m'avoir donné tout le matériel nécessaire pour réaliser mon travail dans les meilleures conditions sans aucune exigence. Merci de ton soutien au niveau transcriptomique, tes conseils et ta façon de faire. Crois-moi si je te dis que tout le monde aimera avoir un boss comme toi, si gentil, si humain.

Un merci si spécial à Jean Sébastien Denault mon complice à l'IRB et mon ami. Merci de ton aide et de l'ambiance de travail. Le laboratoire est vide sans toi. Un grand merci aussi à Hervé Hogue. Merci beaucoup pour ton aide au niveau informatique, je te suis très reconnaissante pour tout ce que t'as fait pour moi. Merci beaucoup Hervé.

Merci au comité d'évaluation de cette thèse, je vous doit en partie mon avenir.
Merci.

Merci à toi Édith pour ton aide pour la récolte des ovules et pour le partage de tous les événements si importants dans notre vie. Je ne t'oublierai jamais. Un grand merci à l'expert de récoltes des ovules, à toi, Théo qui a pas mal arraché les pauvre fruits pour les mesurer. Merci à tous mes collègues de laboratoire à l'IRBV et l'IRB, ceux qui sont partis et ceux qui y sont encore, merci pour votre aide, votre humour et votre ambiance. Je vous

souhaite tout le succès que vous méritez. Faire parti d'une telle équipe offre un plan de carrière sans pareil....

Un merci si spécial à l'homme de ma vie, mon mari Adnane Sellam, Merci pour ton amour et ton soutien pendant toutes ces années, merci pour ton aide et pour la confiance que tu m'as toujours fait. J'espère être à la hauteur. Je t'aime.

Un merci à toute ma famille, spécialement maman et papa. J'aimerai tellement être à la hauteur de votre fierté. Vous êtes des parents uniques. Merci mille fois.

Merci aussi aux organismes subventionnaires: FQRNT, FES et le fond de Marie Victorin et celui de Zeiss.

Et finalement, aux membres de l'IRBV, professeurs, chercheurs et étudiants. Merci pour l'ambiance familiale. Restez comme vous êtes ne changez rien.

Merci !!!!

Introduction

Les angiospermes, ou plantes à fleurs présentent le système reproductif le plus évolué des végétaux. Leur cycle biologique alterne entre deux phases: une phase gamétophytique haploïde réduite (n) et une phase sporophytique diploïde dominante ($2n$) (Figure. 1). La première correspond à la production des gamètes au cours de laquelle, suite à la méiose, les spores se spécifient en grains de pollen (gamète mâle) et en sac embryonnaire (gamète femelle). Pour sa part, la phase sporophytique débute avec la formation du zygote et de l'albumen (tissu nutritif de la graine) issus de la fusion des gamètes mâle et femelle. Ce stade, englobant les étapes d'embryogenèse et de germination de la graine, se poursuit avec le développement de la plante mature, l'établissement des organes végétatifs et reproducteurs puis s'étend jusqu'à la production des gamètes (Esau 1977). Le contrôle de ces deux phases via plusieurs mécanismes de régulation géniques orchestrant le développement de l'ovule, les événements de pollinisation et d'embryogenèse afin d'établir les générations gamétophytique et sporophytique.

Les dernières décennies ont été très révélatrices sur la compréhension de ces mécanismes et ce, en combinant plusieurs approches biochimiques, génétiques, moléculaires et cellulaires.

1 Le développement des gamétophytes femelles et mâles

1.1 La fleur

À l'exception de certaines plantes comme les orchidées, la plupart des fleurs contiennent quatre différents organes disposés en quatre spirales. La première spirale se compose des sépales, la deuxième des pétales, la troisième des étamines et, finalement, la quatrième des carpelles (Figure. 2). Le développement des organes floraux nécessite des mécanismes moléculaires hautement conservés. Après la période de croissance végétative, la combinaison entre les signaux environnementaux et endogènes induit le développement floral (Simpson and Dean 2002). Durant la transition florale, le méristème apical devient un

méristème végétatif et ce dernier se transforme en méristème floral. Le développement floral peut être divisé en 3 étapes :

1- La réponse aux signaux environnementaux et endogènes permet à la plante de passer d'un stade de croissance végétative à une croissance reproductive. Ce processus est contrôlé par des gènes appelés des gènes d'intégration.

2- Les signaux des différentes voies font intégrés et mènent à l'activation d'un groupe de gènes qui confèrent l'identité florale au meristème.

3- Les gènes d'identité de méristème activent les gènes d'identité d'organes floraux dans des régions distinctes de la fleur. Ces derniers activent des gènes en aval qui spécifient les tissus constituant la fleur.

1.1.1 Induction du méristème floral: transition du stade végétatif au stade reproductif

La transition florale est un changement majeur ayant lieu au cours de la vie d'une plante. Son apparition au cours de l'évolution a eu des impacts considérables. Aujourd'hui, la vaste majorité des espèces végétales possèdent des fleurs. Cette transition est contrôlée par des facteurs environnementaux comme la photopériode et l'exposition au froid (vernalisation) de même que des facteurs endogènes tels l'âge de la plante ou les phytohormones. L'ensemble de ces signaux conduit à l'activation d'un groupe de gènes (les intégrateurs floraux) qui provoqueront la formation des jeunes fleurs (méristèmes floraux) au niveau de l'apex de la plante.

Pour déclencher la floraison chez *Arabidopsis*, deux gènes d'identité du méristème floral sont nécessaires et suffisants: *APETALA1* (*API*) et *LEAFY* (*LFY*). Ces gènes codent pour des facteurs de transcription (Riechmann, Krizek et al. 1996; Parcy, Nilsson et al. 1998) et ont un rôle partiellement redondant dans la spécificité du méristème floral (Weigel, Alvarez et al. 1992). *LFY* contrôle la transition florale par une induction de l'expression de *API*, une cible directe de *LFY* (Wagner et al., 1999; Wagner et al., 2004;

William et al., 2004). Ces gènes sont sous le contrôle des gènes d'intégration, *FLOWERING LOCUS T (FT)* et *SUPPRESSOR OF CONSTANT1 (SOC1)* (Komeda 2004).

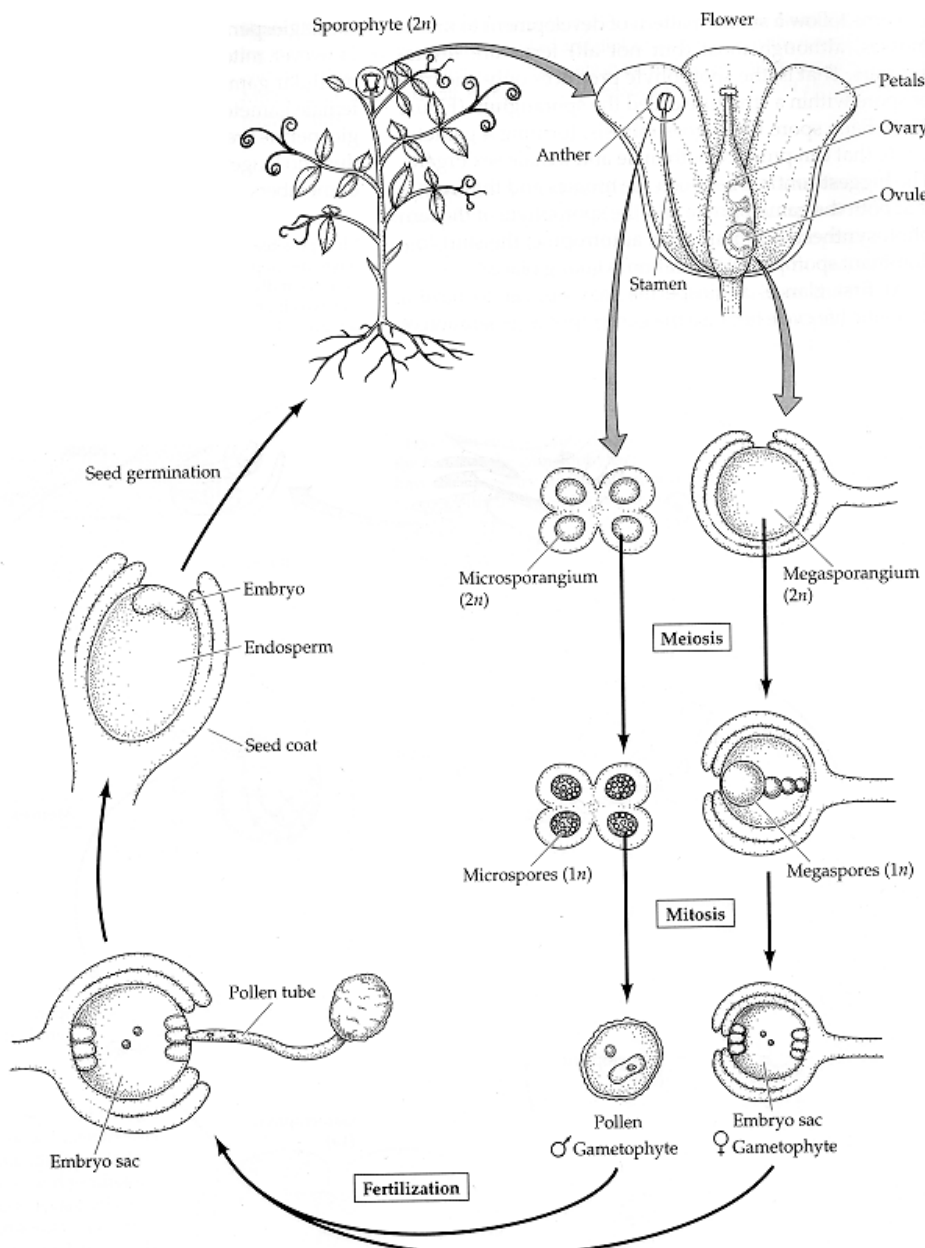


Figure 1: Cycle de vie des angiospermes.

Image tirée de <http://zygote.swarthmore.edu/phyto1.html>

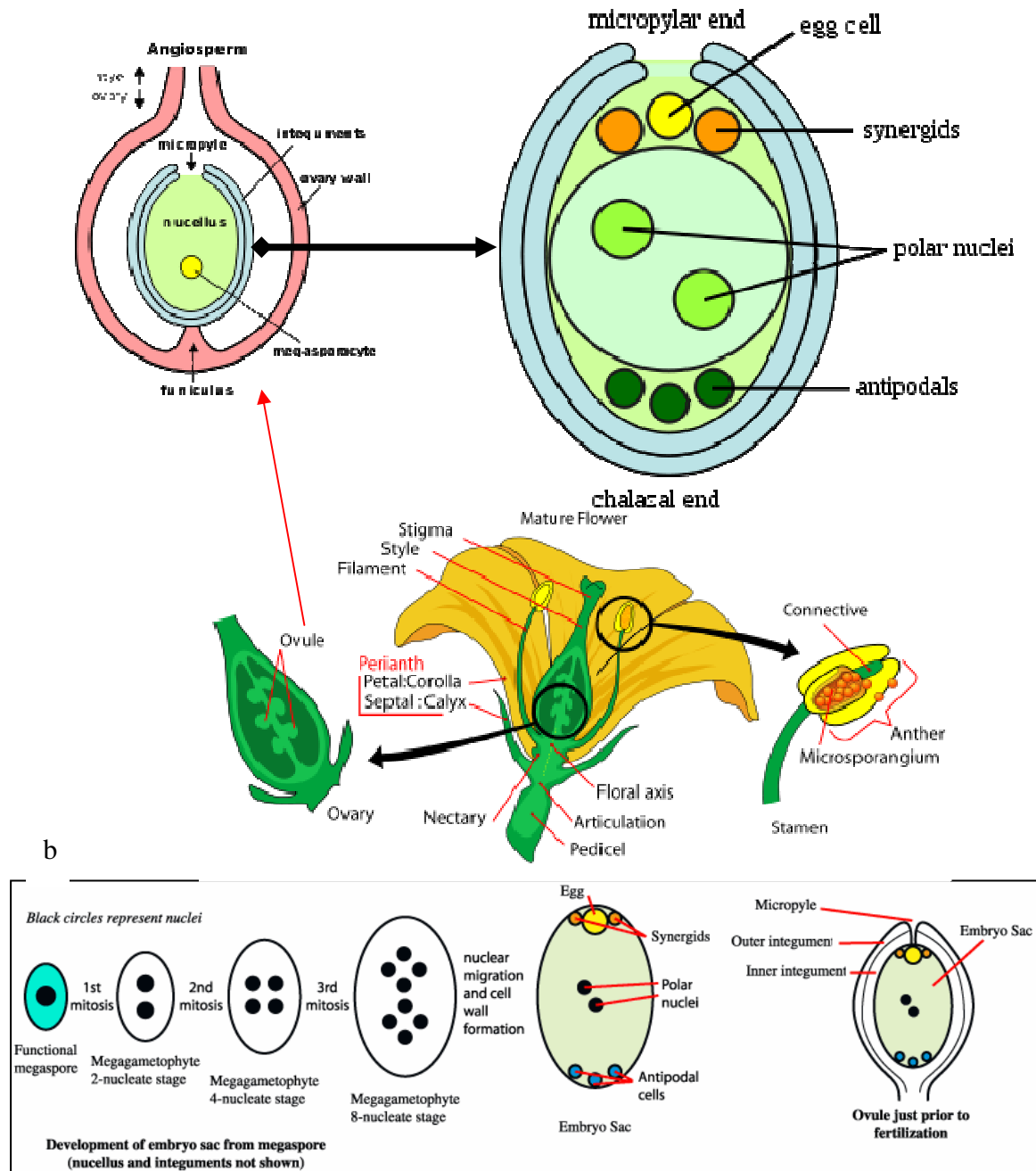


Figure 2: Représentation de l'organe reproducteur chez les plantes à fleurs. 2a: Représentation schématique de la fleur et de l'ovule. 2b: Mégagamétogénèse chez les angiospermes de type *Polygonum*. Image tirées : http://upload.wikimedia.org/wikipedia/commons/thumb/7/7f/Mature_flower_diagram.svg/450px-Mature_flower_diagram.svg.png. http://www.google.ca/images?hl=en&source=imghp&q=ovule+of+a+flower&gbv=2&aq=1&aqi=g2g-m4&aql=&oq=ovule&gs_rfai=

Ces derniers sont eux-mêmes sous le contrôle d'un des régulateurs central de la voie de la photopériode, *CONSTANT (CO)* qui code pour un facteur de transcription à doigts de zinc (Putterill, Robson et al. 1995; Kardailsky, Shukla et al. 1999; Kobayashi, Kaya et al. 1999; Samach, Onouchi et al. 2000). Alors que quelques scientifiques ont montré que CO active à la fois *SOC1* et *FT* dans deux voies parallèles (Samach, Onouchi et al. 2000), une étude plus récente suggère que CO active *SOC1* par l'intermédiaire de *FT* (Yoo et al., 2005). Bien que *LFY* et *API* soient les gènes centraux de l'identité du méristème floral, d'autres gènes comme *CAULIFLOWER (CAL)* (Bowman, Alvarez et al. 1993), *FRUITFULL (Gu, Ferrandiz et al. 1998)* et *AP2* (Jofuku, den Boer et al. 1994; Okamuro, den Boer et al. 1996) jouent un rôle secondaire dans la spécification de l'identité du méristème floral. Des expériences de biopuces d'ADN et d'immunoprécipitation ont permis d'identifier des gènes cibles de *LFY*, tel que le déjà connu *API* ainsi que *CAL* et *SEPALLATA (SEP)*, deux nouveaux candidats directement induits par l'activité de *LFY* (Schmid, Uhlenhaut et al. 2003; William, Su et al. 2004).

1.1.2 Les gènes d'identité d'organes floraux

La principale fonction des gènes d'identité du méristème floral est l'activation des gènes qui spécifient l'identité des organes floraux. Ces derniers furent originalement identifiés chez *Arabidopsis thaliana* et *Antirrhinum majus* sur la base des phénotypes de mutants qui présentent des transformations homéotiques de leurs organes floraux. Les analyses génétiques de ces mutants homéotiques ont permis l'élaboration du "modèle classique ABC" (Coen and Meyerowitz 1991). Ce modèle suppose que les trois fonctions A, B et C agissent en combinaison pour conférer l'identité des organes floraux dans chaque spirale (Fig. 3). Les gènes homéotiques de la classe A, c'est-à-dire *API* et *AP2* chez *A. thaliana* et *LIPLESS1 (LIP1)* et *LIP2* chez *A. majus*, spécifient l'identité des sépales. Les gènes de la classe B, soient *AP3* et *PISTILLATA (PI)* chez *A. thaliana* et *DEFICIENS (DEF)* et *GLOBOSA (GLO)* chez *A. majus*, spécifient l'identité des pétales lorsque

exprimés avec les gènes de la classe A. Les gènes de la classe C, *AGAMOUS* (*AG*) chez *A. thaliana* et *PLENA* (*PLE*) et *FARINELLI* (*FAR*) chez *A. majus*, spécifient l'identité des étamines lorsque exprimés avec les gènes de la classe B. Finalement, la fonction C à elle seule spécifie l'identité des carpelles et confère aussi le déterminisme floral. De plus, les protéines de type A et C s'excluent mutuellement en réprimant l'expression de l'autre (Weigel and Meyerowitz 1994). Plus récemment, des études génétiques ont permis d'identifier une nouvelle classe E comprenant les gènes d'identité d'organes floraux *AGAMOUS like 2* (*AGL2*), *AGL4* et *AGL9*.

Les expériences de co-suppression menées chez *Pétunia* ont été la première indication que ces gènes joueraient un rôle important dans l'identité des pétales, carpelles et étamines (Angenent, Franken et al. 1994). Le triple mutant *agl2-agl4-agl9* se compose de seulement de sépales et ce phénotype explique le changement de nom de ces gènes pour *SEPALLATA1* (*SEPI*), *SEP2* et *SEP3* (Pelaz, Ditta et al. 2000). Le phénotype du triple mutant *sep1/2/3* est similaire au double mutant *bc*, indiquant que les gènes d'identité d'organes B et C sont inactifs dans le triple mutant et par conséquent, la fonction E est nécessaire pour l'activation des gènes B et C (Pelaz, Ditta et al. 2000). Plus récemment, le nouveau gène *SEP4* a été caractérisé et il a été montré qu'il fonctionne avec les autres gènes de la classe E. Il contribue également au développement des quatre organes floraux: sépales, pétales, étamines et carpelles (Ditta, Pinyopich et al. 2004). Une mutation de ces quatre gènes ensemble montre une transformation de tous les organes floraux en structure semblable aux feuilles. Ce phénotype ressemble à celui du triple mutant *ap2/ap3/ag* (Bowman, Smyth et al. 1991).

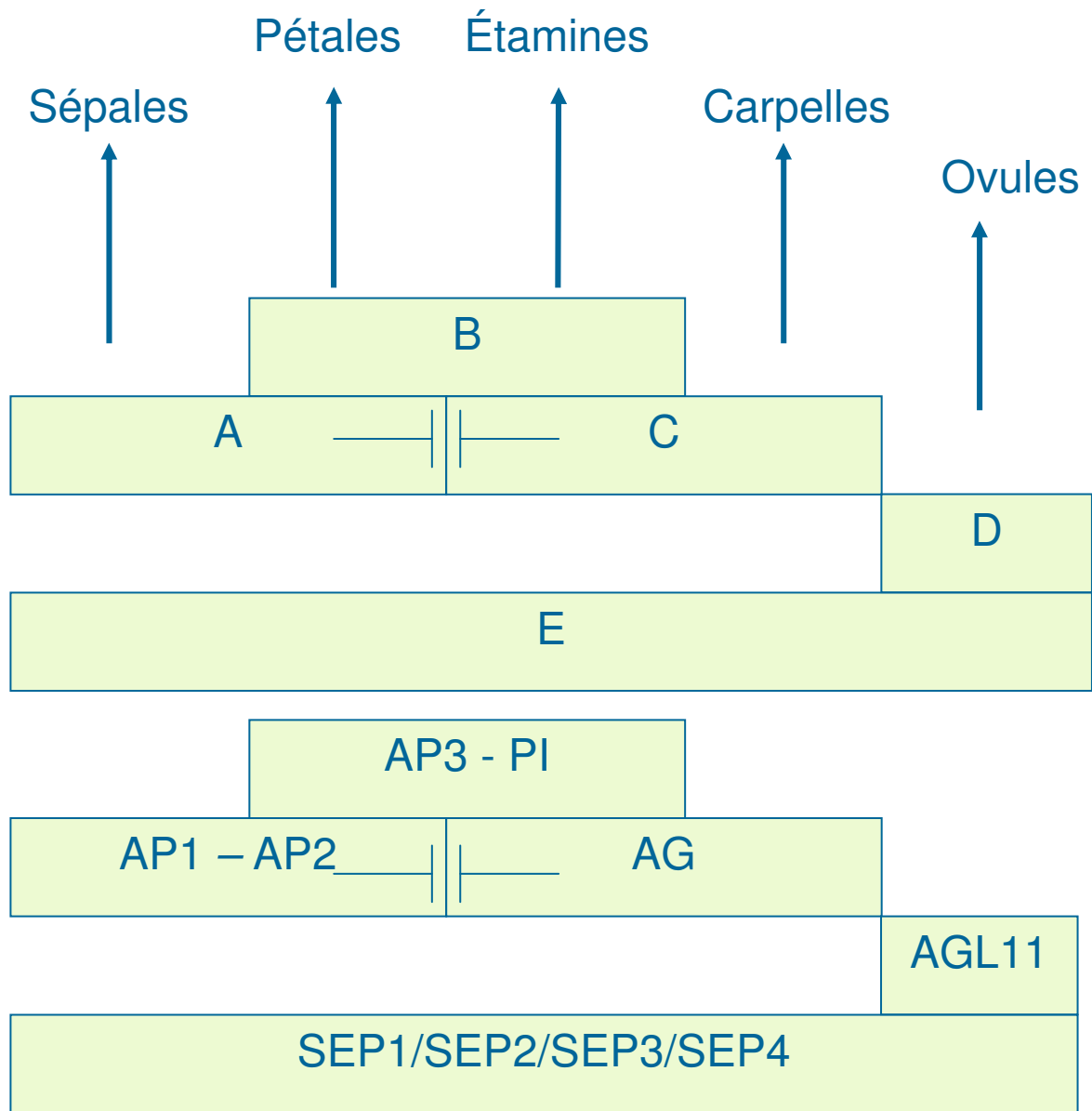


Figure 3: Le modèle ABCDE et déterminisme de l'identité des organes floraux

Les gènes *SEP* ont été désignés sous le nom de la classe E plutôt que de la classe D puisqu'un autre groupe de gènes, précédemment caractérisés chez *Pétunia*, sont nommés des gènes de classe de D (Colombo, Franken et al. 1995). Ensuite, les deux gènes *FLORAL BINDING PROTEIN 7 (FBP7)* et *FBP11* de la classe D confèrent l'identité des ovules chez *Pétunia*. La co-suppression de ces gènes cause un remplacement des ovules par des structures carpelloïdes. Cependant, l'expression constitutive du FBP11 est suffisante pour induire la formation des ovules. La similarité de séquence suggère que le gène correspondant chez *A. thaliana* serait *AGL11* (Angenent and Colombo 1996). Ce gène a été récemment renommé *SEEDSTICK (STK)* (Pinyopich, Ditta et al. 2003). STK fonctionne avec AG, SHATTERPROOF1 (SHP1) et SHP2 pour spécifier l'identité des ovules. Avec une fonction similaire aux gènes *FBP7* et *FBP11* chez *Pétunia* dans la spécification de l'identité d'ovule, les gènes *STK*, *SHP1* et *SHP2* peuvent être considérés comme des gènes de la classe D. Pour leur part, les gènes *SEP* sont aussi nécessaires à formation des ovules (Favaro, Pinyopich et al. 2003). Ainsi, suite à la découverte de nouvelles fonctions, le modèle classique ABC a perdu sa simplicité. Bien que beaucoup d'études portaient sur l'implication des gènes ABCDE au niveau floral, beaucoup d'autres gènes sont nécessaires à la formation des fleurs et la régulation des gènes d'identité d'organes floraux. Parmi eux, notons les gènes *EMBRYONIC FLOWER1 (EMF1)*, *EMF2* et *FERTILIZATION INDEPENDANT ENDOSPERM (FIE)* qui répriment l'expression des gènes d'identité d'organes floraux pendant les stades précoce du développement végétatif (Krizek and Fletcher 2005; Calonje, Sanchez et al. 2008). D'autres gènes, comme *CURLY LEAF (CLF)* (Goodrich, Puangsomlee et al. 1997) et *INCURVATA2 (ICU2)* (Chanvivattana, Bishopp et al. 2004) fonctionnent aussi pendant le développement végétatif pour maintenir le patron de répression des gènes homéotiques. Finalement, *SUPERMAN (SUP)* est nécessaire pour le maintien des limites entre étamines et carpelles (Bowman, Sakai et al. 1992), alors que *ROXY1* (Xing, Rosso et al. 2005), *RABBIT EARS* (Takeda, Matsumoto et al. 2004) et *PETAL LOSS* (Griffith, da Silva Conceicao et al. 1999) assurent le développement des pétales.

1.2 Développement de l'ovule

Les ovules jouent un rôle central dans la reproduction sexuée des plantes, incluant la formation des mégagamétophytes, la fécondation, l'embryogenèse et finalement la formation des graines. Les ovules dérivent de régions à potentiel méristématique du placenta (Robinson-Beers, Pruitt et al. 1992), qui se différencie le long du septum divisant l'ovaire en deux loges. La région centrale du septum constitue le tissu transmissif alors que les tissus périphériques sont fusionnés avec la couche interne de la paroi des ovaires.

Les ovules des angiospermes contiennent trois ou quatre structures morphologiquement distinctes (Fig. 2a). Le nucelle est la région terminale de l'ovule et correspond au site de la formation du sac embryonnaire. Le nucelle est entouré par un ou deux tissus sporophytiques qui l'encaissent, nommés téguments internes et externes. Ces structures latérales pourraient jouer un rôle dans le développement de l'embryon et de l'albumen. Les téguments sont fusionnés à l'apex du nucelle mais présentent une ouverture, le micropyle, à travers lequel le tube pollinique peut accéder au sac embryonnaire. La partie basale de l'ovule est le funicule, ou la tige, qui attache l'ovule à la région placentaire à l'intérieur du carpelle. Le développement de l'ovule et du carpelle peut être dissociable et indépendant, un fait supporté par la possibilité d'obtenir la formation d'ovules ectopique hors du contexte du carpelle (Colombo, Franken et al. 1995; Pinyopich, Ditta et al. 2003).

1.2.1 Spécification et formation du placenta

Le placenta se différencie le long du septum à l'intérieur de l'ovaire. Le primordium d'ovule apparaît à partir des régions placentaires au stade 9 (stade de différentiation des pétales) du développement de la fleur (Smyth, Bowman et al. 1990). Malgré l'importance du placenta dans le développement d'ovule, les événements moléculaires qui mènent au

développement placentaire ne sont pas encore bien compris. Le carpelle représente un scénario complexe pour le modelage et le maintien de cellules méristématiques. L'allongement et la différenciation du primordium du carpelle doivent se maintenir pour assurer la production de nouvelles régions méristématiques - les placentas - qui produiront par la suite le primordium d'ovule. Alors que le cylindre s'allonge, le domaine du milieu du gynécée (gynoecium) reste dans un état relativement non différencié comparativement aux domaines latéraux. Cet état est nécessaire pour permettre le développement postérieur des tissus marginaux, y compris l'activité méristématique du placenta. *SHOOT MERISTEMLESS* (STM), *CUP-SHAPED COTYLEDONS1* (CUC1) et CUC2 sont exprimés dans les sites d'initiation des ovules et sont reconnus comme étant impliqués dans le maintien des cellules méristématiques (Aida et al., 1999; Takada et al., 2001).

Le facteur de transcription AINTEGUMENTA (ANT) avec le répresseur transcriptionnel LEUNIG (LUG) jouent un grand rôle dans le développement du domaine interne de l'ovaire. Le double mutant *ant lug* montre un phénotype caractérisé par la perte totale du septum, du placenta et des ovules (Conner and Liu, 2000; Liu et al., 2000). D'autres gènes, comme les facteurs de transcription CRABS CLAW (CRC) et SPATULA (SPT) ainsi que la sérine/thréonine kinase TOUSLED (TSL), influencent également la structure du placenta et affectent la production des ovules (Roe, Rivin et al. 1993; Roe, Durfee et al. 1997; Roe, Nemhauser et al. 1997; Alvarez and Smyth 1999; Lee, Baum et al. 2005). L'inactivation de ces gènes aboutie à une réduction de la formation d'ovules en modifiant le développement des régions du placenta où les ovules tirent origine.

1.2.2 L'identité des ovules

Des études génétiques et moléculaires ont permis d'identifier plusieurs gènes impliqués dans l'identité des ovules. Parmi ces gènes, la famille des facteurs de transcription de type MADS-box est la plus étudiée. Tel que mentionné précédemment, la

classe D du modèle ABCDE, incluant *FBP11*, le facteur de transcription de type MADS chez *Pétunia* et orthologue de *AtSTK*, est impliquée dans l'instauration de l'identité de l'ovule (Angenent, Franken et al. 1995; Colombo, Franken et al. 1995; Pinyopich, Ditta et al. 2003). La surexpression de ce facteur provoque la production des ovules sur les sépales et les pétales tout comme la surexpression de *AtSTK* chez *Arabidopsis*. Dans le même groupe de famille, le triple mutant *sep1/2/3* produit des organes floraux avec une transformation des ovules en structures semblables au carpelle (Favaro, Pinyopich et al. 2003). Il en est de même pour le triple mutant *shatterproof1/2* (*shp1/2*) et *seedstick* (*stk*) (Pinyopich, Ditta et al. 2003). L'importance de *AGAMOUS* (*AG*), un autre gène de la famille MADS-box dans la détermination de l'identité des ovules a été étudié (Western and Haughn 1999). La perte de *AG* mène à une diminution dans le nombre d'ovules matures, suggérant que le produit de gène *AG* agit tôt dans le développement d'ovule d'une façon à déterminer son identité. De plus, des expériences de double hybride et de co-immunoprécipitation ont démontré que les protéines MADS box peuvent se lier *in vitro* en formant un complexe multimérique (Honma and Goto 2001; Favaro, Pinyopich et al. 2003). Ces complexes contiennent les combinaisons des protéines de type MADS-box *AGAMOUS* (*AG*), *SEEDSTICK* (*STK*), *SHATTERPROOF1* (*SHP1*), *SHP2* et le *SEP1*, *SEP2* et des protéines *SEP3* pour maintenir l'identité des ovules. Un autre facteur de transcription, *BEL1*, codant pour une protéine à homéodomaine, agit en parallèle avec *AG* pour spécifier l'identité des ovules (Western and Haughn 1999). Dans le mutant *bell*, les téguments de l'ovule cessent de croître et forment un collet autour de ce dernier. Quant à l'ovule, il se transforme en une structure ressemblant au carpelle (Robinson-Beers, Pruitt et al. 1992; Modrusan, Reiser et al. 1994; Ray, Robinson-Beers et al. 1994; Reiser, Modrusan et al. 1995; Western and Haughn 1999).

1.2.3 Développement du sac embryonnaire

Chez les angiospermes, le développement du gamétophyte femelle ou sac embryonnaire

consiste en deux processus successifs: la mégasporogenèse et la mégagamétogenèse (Maheshwari and Johri, 1950; Willemse and van Went, 1984; Yadegari and Drews, 2004). Plus d'une quinzaine de modèles différents de développement ont été décrits ces dernières années. Ces modèles se basent principalement sur les variations dans la cytokinèse pendant la méiose, sur le nombre et le mode des divisions mitotiques ainsi que sur le mode de cellularisation. La forme de développement observée chez plus de 70% des angiospermes suit une mégasporogenèse de type monosporique avec un noyau méiotique combinée à une mégagamétogenèse de type *Polygonum*, ainsi nommé puisqu'originellement décrit chez *Polygonum divaricatum* (Maheshwari and Johri 1950; Yadegari and Drews 2004). Durant la mégasporogenèse, le nucelle fournit la cellule initiale pour la différentiation du mégasporocyte (cellule mère du mégaspore). Cette dernière se divise en quatre mégaspores haploïdes généralement disposées linéairement (phases diade et tétrade). Chez la plupart des dicotylédones et chez quelques monocotylédones, trois des quatre mégaspores avortent par mort cellulaire programmée suite à la méiose femelle. L'unique spore survivante (mégaspore fonctionnelle) se situe dans la partie opposée au micropyle, soit la zone chalazale, et se différencie en une cellule mononucléée hautement vacuolée (Rees-Leonard 1935; Jongedijk 1985; Lersten 2004). Cette mégaspore fonctionnelle représente le début de la mégagamétogenèse (Fig. 2b). Lors de cette étape, la mégaspore subit un ou plusieurs cycles de mitose sans cytokinèse, aboutissant à un syncytium multinucléé. Par la suite, les parois cellulaires se forment autour de ces noyaux, aboutissant à la formation du sac embryonnaire mature. Dans le modèle *Polygonum*, le noyau de la mégaspore entreprend trois divisions mitotiques, ce qui aboutit à la création de huit noyaux répartis en deux groupes égaux séparés par une grande vacuole. L'un des groupes se retrouve à l'extrémité micropylaire et le second, à l'opposé, à l'extrémité chalazale. Immédiatement après la troisième division mitotique, les noyaux polaires (un noyau de chaque groupe), migrent vers le centre de la cellule octanucléé en se dirigeant vers le pôle micropylaire. Concomitamment à cette migration, les autres noyaux subissent une cellularisation en modifiant considérablement le sac embryonnaire. À maturité, le sac embryonnaire

comprend huit noyaux et sept cellules (hepta-cellulaire) localisées d'une manière polarisée et définissant ainsi la forme de type *Polygonum*: une cellule œuf et deux synergides à l'extrémité micropylaire, une cellule centrale à deux noyaux et trois cellules antipodales à l'extrémité chalazale (Maheshwari, 1950; Maheshwari and Johri, 1950; Willemse and van Went, 1984; Mansfield and Briarty, 1991; Kay Schneitz, 1995; Baroux et al., 2002). Le gamétophyte femelle de type *Polygonum* peut être modifiée par des événements de mort cellulaire programmée ou de prolifération cellulaire chez différentes espèces. Par exemple, chez *Arabidopsis*, les cellules antipodales subissent la mort cellulaire immédiatement avant la fécondation, tandis que chez le maïs, ces mêmes cellules prolifèrent (Maheshwari 1950; Huang and Russella 1992; Kay Schneitz 1995; Drews, Lee et al. 1998). Cependant, la fonction des antipodales demeure méconnue.

Le développement du gamétophyte femelle et celui des tissus sporophytiques de l'ovule semblent intimement liés. En effet, la présence de plasmodesmes à travers les parois latérales des mégaspores, indique qu'il peut y avoir une communication entre les cellules nucellaires (tissues sporophytiques) et la mégasporre fonctionnelle, permettant probablement un flux nutritif (Bajon, Horlow et al. 1999). De plus, durant son développement, le gamétophyte femelle acquiert une polarité au long de l'axe chalaza-micropilaire, correspondant à un développement asymétrique des tissus sporophytiques de l'ovule. Ceci suggère que la polarité du gamétophyte femelle serait régulée, au moins en partie, par les tissus sporophytiques de l'ovule (Yadegari and Drews 2004).

Au cours des années précédentes, les chercheurs ont découvert deux grandes classes de mutations qui exposent des modèles de ségrégation fondamentalement différents, sporophytiques et gamétophytiques. Les mutations sporophytiques affectent sporophytiquement les gènes exprimés et exposent généralement des modèles de ségrégation mendélienne 3:1. Les mutations gamétophytiques, cependant, affectent gamétophytiquement l'expression des gènes et ne sont pas transmis par l'oosphère et/ou le

pollen. En conséquence, ces mutations exposent des modèles de ségrégation non-mendélienne et peuvent passer d'une génération à une autre sous forme d'hétérozygotes (Drews, Lee et al. 1998). Les mutations gamétophytiques se divisent en deux classes. Les mutations dites femelle-spécifique (FGS) affectent uniquement les gamétophytes femelles alors que les mutations gamétophytiques générales (GG) s'associent aux gamétophytes mâle et femelle (Drews, Lee et al. 1998). Les mutations *ctrl1, female gametophyte1 (fem1), fem2, fertilization independant-endosperm 1 (fie1), fie2, fie3, indeterminate gametophyte1 (ig1)* et *prolifera (prl)* représentent quelques exemples du groupe gamétophytique-spécifique. Pour leur part, *fem3, fem4, gametophytic factor (Gf), gfa2, gfa3, gfa4, gfa5, and gfa7, hadad (hdd), lethal ovule2 (lo2)* sont des mutants gamétophytiques généraux. Ces mutants manifestent une grande variété de phénotypes à différents stades de la mégagaméto-génèse. Ces derniers sont reliés aux divisions mitotiques, à la formation des vacuoles, à la fusion nucléaire et à la cellularisation (Redei 1965; Kermicle 1971; Huang and Sheridan 1994; Springer, McCombie et al. 1995; Ohad, Margossian et al. 1996; Chaudhury, Ming et al. 1997; Christensen, King et al. 1997; Feldmann, Coury et al. 1997; Moore JM, Calzada JP et al. 1997; William F. Sheridan 1997; Christensen, Subramanian et al. 1998; Drews, Lee et al. 1998; Chaudhury, Koltunow et al. 2001; Christensen, Gorsich et al. 2002)

1.3 Développement du pollen

Le pollen ou microgamétophyte (du grec: plante produisant de petites gamètes, sperme) est une structure très petite, haploïde, non photosynthétique, de courte durée de vie et qui se compose de 2 ou 3 cellules. Le développement du pollen comprend plusieurs stades (Tableau 1). Initialement, les cellules sporogéniques prolifèrent par mitose. Chaque cellule sécrète ensuite une couche de callose qui l'enrobe ; on parle alors de PMC (Pollen Mother Cell). Chaque cellule PMC subit deux divisions méiotiques caractérisées par la formation de la paroi après la deuxième division. Ceci aboutit à la formation de microspores en tétrade (Regan and Moffatt 1990). La callose entourant la tétrade est

digérée après mésiose, libérant des microspores individuelles non matures à l'intérieur du sac pollinique. La paroi des microspores s'épaissie par la déposition d'exine et ceux-ci s'élargissent par la formation d'une vacuole (Regan and Moffatt 1990). Par la suite, une mitose crée une large cellule végétative et une petite cellule germinale. Cette dernière migre dans la cellule végétative et des réserves nutritives commencent à s'accumuler dans le grain de pollen. La vacuole dégénère et la cellule germinale se divise pour former deux cellules spermatiques. Le pollen est finalement relâché lorsque les cellules qui entourent le stomium de l'anthere se séparent.

Tableau 1: Stades de développement des gamétophytes mâles et des étamines.

Stade floral	Stade de développement du pollen	Morphologie des étamines
7	Division des cellules sporogéniques	Les régions des filaments et anthères sont distinctes
8	Différenciation des PMC	Apparition du lobe du côté adaxial de l'anthere
9	Engobage des PMC par la callose et Formation de tétrades	Les trois couches de l'anthere (l'endothélium, la couche médiane et le tapetum) sont évidentes
10	Libération et maturation des microspores	Élongation des filaments
11-12	Division mitotique des microspores et dessiccation des grains de pollen	Dégénérescence du tapetum

1.4 La pollinisation

La pollinisation est le processus par lequel le pollen est transferé sur le stigmate de la fleur suite à sa libération après déhiscence de l'anthère. Une pollinisation réussie dépend de l'acheminement des cellules spermatiques vers sa cible finale, l'ovule. La croissance du tube pollinique, ou le grain de pollen germé, au cours de ce trajet dépend d'interactions complexes et régulées avec les cellules diploïdes de l'appareil reproducteur femelle. Ces interactions peuvent affecter toutes les étapes du développement du tube pollinique, en commençant par l'adhérence et l'hydratation du grain de pollen, la germination du tube pollinique à travers le stigmate, le style et l'ovaire pour finalement effectuer la fécondation de l'ovule (Sanchez, Bosch et al. 2004; Weterings and Russell 2004). En vue de ces interactions, le pistil agit non seulement comme un conduit passif aux tubes polliniques, mais aussi comme une passoire de pré-fécondation sélective pour examiner les différents types de grains de pollen. Ceci permet la germination et la croissance de grains appropriés et empêche le développement des grains inopportuns. Le pistil joue donc un rôle central dans la prévention de la fusion entre gamétophytes sexuels interspécifiques de même que pour les gamétophytes sexuels intraspécifiques, dans le cas de plantes possédant un système d'auto-incompatibilité (voir ci-dessous).

Les angiospermes ont développé plusieurs stratégies pour éviter l'autofécondation, promouvant ainsi la fécondation croisée (interfécondation) ou allogamie, augmentant ainsi le brassage et la diversité génétique. Certaines espèces, comme le houx, exposent des fleurs unisexuées mâles et femelles sur des plants séparés (dioécie), ce qui écarte l'autofécondation. D'autres espèces, par exemple le maïs, portent des fleurs unisexuées mâles et femelles sur le même individu (monocécie), ce qui réduit, mais n'empêche pas l'autofécondation. La majorité des angiospermes, cependant, ont des fleurs hermaphrodites dans lesquelles les organes mâles et femelles se développent l'un près de l'autre. D'autres espèces, comme l'érythrina à sucre, utilisent la séparation temporelle entre la maturation des

stigmates et celle des anthères promouvant aussi la fécondation croisée (out-crossing), réduisant ainsi les occasions d'autofécondation. Chez d'autres plantes, l'autofécondation est empêchée et le croisement externe est assuré par les systèmes d'auto-incompatibilité génétiques (Herr 1995; Rea and Nasrallah 2008). Chez les Solanaceae, l'auto-incompatibilité est dite gamétophytique et survient lorsque le locus d'auto-incompatibilité du grain de pollen, ou locus S, contient un allèle qui correspond à l'un des deux locus retrouvé dans le tissu maternel. Lors d'une telle réaction, l'hydratation et la germination du grain de pollen ont lieu, mais la croissance des tubes polliniques à l'intérieur du tissu transmissif est ralentie et peut même être rapidement paralysée. Une glycoprotéine pourvue d'une activité ribonucléase (S-RNases) est codée par le locus S. Elle est sécrétée au niveau du stigmate et tout au long du style afin d'inhiber la croissance de tubes polliniques d'une même espèce ou d'un partenaire incompatible (Dodds, Clarke et al. 1996).

1.5 Attraction des tubes polliniques

Suivant l'hydratation et la germination du grain de pollen, le tube pollinique doit percer le style. Dépendamment du type de stigmate, deux situations sont observées concernant l'acheminement du tube pollinique. Dans le cas d'un stigmate dit sec, l'adhérence du grain de pollen sur les papilles stigmatiques détermine le point d'entrée du tube pollinique dans le tissu transmissif du style. Dans un stigmate dit humide, la situation est différente. Le tube pollinique peut croître dans la matrice extracellulaire (MEC) couvrant la surface du stigmate avant de pénétrer dans le style (Lord 2003). Chez *Nicotiana tabacum*, la matrice extracellulaire de nature lipidique fournit un gradient hydraulique qui agit en tant que signal directionnel pour la croissance des tubes polliniques dans le stigmate (Lush, Grieser et al. 1998; Wolters-Arts, Lush et al. 1998). Chez d'autres espèces, l'évidence d'un signal chimique assurant le guidage directionnel a été rapportée (Mascarenhas and Machlis 1999).

En général, l'attraction des tubes polliniques peut se diviser en deux phases: la phase sporophytique et la phase gamétophytique. Durant la phase sporophytique, le tissu transmissif sécrète divers nutriments essentiels à la croissance des tubes polliniques, tels des sucres, des acides aminés, des polysaccharides, des glycolipides, des glycoprotéines et des lipides (Labarca and Loewus 1972; Swanson, Edlund et al. 2004). Diverses enzymes sont probablement nécessaires pour faciliter l'entrée entre les cellules sécrétoires via les espaces intercellulaires. Plusieurs ont été décrites dans le pollen ou dans le stigmate et semblent impliquées dans ce processus. Parmi elles, notons les polygalacturonases (Dearnaley and Daggard 2001; Kim, Shiu et al. 2006), les serines esterases (Hiscock, Bown et al. 2002), les pectines esterases (Mu, Stains et al. 1994), les glucanases (Kotake, Li et al. 2000; Doblin, De Melis et al. 2001), les expansines/LTP (Nieuwland, Feron et al. 2005) et les endoxylanases (Bih, Wu et al. 1999). Toutes ces enzymes pourraient jouer un rôle dans la modification de la MEC du stigmate et du style et pourraient également agir sur la paroi du pollen lui-même (Lord 2003). Plusieurs molécules ont été proposées en tant que candidates agissant comme un signal directionnel de la croissance du tube pollinique. Des études chez la tomate ont mis en évidence des récepteur kinases (LePRK1, LePRK2 et LePRK3) et leurs ligands comme des médiateurs potentiels de la croissance du tube pollinique et la communication pollen-stigmate (Muschietti, Eyal et al. 1998; Kaothien, Ok et al. 2005). Chez *Nicotiana tabacum*, l'arabinogalactane (AGP), spécifique au pistil et désigné par “transmitting tissue-specific” TTS, agit comme un signal dirigeant la croissance vers l'ovaire (Wang, Wu et al. 1993; Cheung, Wang et al. 1995; Wu, Wang et al. 1995). La caractérisation moléculaire chez *Arabidopsis* du gène *POP2* (pollen–pistil interaction 2), codant une transaminase qui convertie le GABA (γ -amino butyric acide) en semi-aldéhyde succinique, a révélé l'implication de cette molécule. Connue chez les animaux comme un neurotransmetteur, GABA agirait comme un signal potentiel dans le guidage du tube pollinique (Palanivelu, Brass et al. 2003). Cependant, le GABA ne semble pas être le seul signal du guidage. En effet, une petite molécule basique, la chemocyanine, semble

également agir comme attractant chemotropique le long du style (Kim, Mollet et al. 2003; Kim, Dong et al. 2004).

Durant la phase gametophytique, d'autres signaux sont responsables de guider le tube pollinique jusqu'au gamétophyte femelle. La caractérisation des mutants *feronia* (*fer*) (Huck, Moore et al. 2003) et *sirène* (*ser*) (Rotman, Rozier et al. 2003) a démontré que le guidage et la réception du tube pollinique sont également contrôlés par le gamétophyte femelle. La mise en évidence d'un système semi-*in vivo* chez *Torenia fournieri* combiné à des expériences d'ablation au laser de cellules spécifiques a permis de préciser plus spécifiquement que les synergides représentent la source d'un signal diffusible agissant sur une courte distance et de façon directe sur le guidage du tube pollinique (Higashiyama, Kuroiwa et al. 1998). De plus, la présence d'une seule synergide intacte semble suffisante à cette attraction (Higashiyama, Yabe et al. 2001). Les synergides ont une implication à plusieurs niveaux. En plus de leur rôle dans le guidage, leur dégénérescence est essentielle au relâchement des composantes du tube pollinique (van Went JL and MTM 1984; Went and Cresti 1988) et à la réorganisation du cytosquelette qui facilitera la migration des cellules spermatiques jusqu'à la cellule centrale et l'œuf (Russell 1993; Russell 1996). L'étude du mutant *gfa2* (*gametophytic factor2*) a montré que leur dégénérescence est indépendante du guidage puisque la mort cellulaire des synergides s'initie après que le tube pollinique soit parvenu au gamétophyte femelle, mais avant sa décharge (Sandaklie-Nikolova, Palanivelu et al. 2007). Ces données soutiennent un modèle dans lequel une cascade de signalisation déclenchée par le contact entre les cellules du tube pollinique et les synergides induit la mort cellulaire des synergides (Sandaklie-Nikolova, Palanivelu et al. 2007). Ce rôle des synergides est également supporté chez *A. thaliana* par les études réalisées sur le gène *MYB98*, exprimé à la base de ces cellules. Ces études concluent que la structure filiforme des synergides (appareil filiforme) est nécessaire entre autre à la sécrétion d'un attractant aux tubes polliniques (Kasahara, Portereiko et al. 2005). Dans le même ordre d'idées, le gène *EGG APPARATUS1* (*ZmEAI*), isolée chez le maïs, est

exprimé dans les synergides et est impliqué dans le guidage du tube pollinique. Très récemment, il a été reporté que des peptides isolés des cellules synergides chez *T. fournieri* codant pour des protéines riche en cystéine (CRPs, « cysteine-rich proteins ») de la sous-famille de protéines « defensin-like ») et nommées LUREs par les auteurs sont des attractants du tube pollinique (Okuda, Tsutsui et al. 2009). D'autres études démontrent également la contribution de la cellule centrale (Shimizu and Okada 2000; Chen, Li et al. 2007) et/ou de l'oosphère (Dresselhaus, Lörz et al. 1994; Marton, Cordts et al. 2005) dans l'attraction des tubes polliniques. Il a été reporté que le gène *Matagama3* (*MAA3*), codant pour une hélicase, régule la production de molécules d'ARN responsables du guidage des tubes polliniques par les synergides et/ou les autres cellules du sac embryonnaire (Shimizu, Ito et al. 2008).

1.6 La double fécondation et l'embryogenèse

La fécondation et l'embryogenèse sont des événements cruciaux pour le développement d'une plante. Comprendre ces mécanismes, c'est comprendre comment un organisme multicellulaire telle une plante se développe à partir d'une seule cellule: le zygote. Au cours des dernières années, plusieurs analyses génétiques et moléculaires ont été rapportées portant sur le développement des ovules chez *Arabidopsis* et chez d'autres espèces. Le développement des ovules nécessite les mêmes processus cellulaires de base nécessaires à la formation d'autres organes, tel que, l'initiation et la spécification de primordium, la division et l'expansion cellulaire de même que la croissance et la différentiation asymétrique. Cependant, les ovules diffèrent des autres structures végétatives par leur fonction reproductive et leur origine évolutive (Herr 1995). Les chercheurs utilisent aujourd'hui la richesse des connaissances botaniques et les nouvelles approches moléculaires pour mieux comprendre ce système reproductif. En effet, plusieurs études génétiques ont contribué à des avancées majeures en révélant des voies et des mécanismes de régulation impliqués dans le développement embryonnaire des plantes.

La double fécondation a été décrite dès 1898 par Navashin (cité dans la revue (Chaudhury, Koltunow et al. 2001)). À la suite de la libération des grains de pollen après déhiscence de l'anthère, ceux-ci se déposent sur le stigmate de la fleur au cours de la pollinisation. Ce mécanisme nécessite plusieurs molécules pour l'interaction initiale du pollen avec le stigmate (Dickinson, Doughty et al. 1998; Dickinson 2000). Chez la plante modèle *A. thaliana*, les molécules lipophiles dans le pollen servent comme médiaterices à l'adhérence pollen-stigma (Zinkl, Zwiebel et al. 1999). Après son adhérence, le pollen s'hydrate, puis germe en tube pollinique. Celui-ci passe à travers le tissu sporophytique du carpelle pour arriver au tissu gamétophytique. Le tube pollinique pénètre le gamétophyte femelle via le micropyle et fusionne avec une des synergides. Le contenu du tube pollinique, soit les deux noyaux spermatiques haploïdes et le noyau végétatif, se déverse dans la synergide qui dégénère peu après. C'est alors que se produit la double fécondation au cours de laquelle l'un des noyaux spermatiques fusionne avec le noyau haploïde de l'oosphère formant ainsi le zygote diploïde. Le second noyau mâle s'unit aux deux noyaux polaires haploïdes de la cellule centrale pour former l'albumen, un tissu triploïde qui a pour rôle de fournir des nutriments à l'embryon et/ou à la plantule.

Suivant la fécondation, le zygote entame les étapes de l'embryogenèse. En premier lieu, il subit une division asymétrique qui résulte en une petite cellule apicale et une grande cellule basale. Cette première division asymétrique fournit la polarité à l'embryon. La majeure partie de la plante se développe à partir de la cellule apicale. Le suspenseur, dont le développement s'initie à partir de la cellule basale, constitue le point d'ancrage de l'embryon à l'endosperme et sert de conduit nutritif à l'embryon en développement. Par la suite, il subit de nombreuses divisions en passant par plusieurs stades pour finalement se transformer en graine.

Les différents stades de l'embryogenèse sont schématisés à la figure 4a. L'embryogenèse des végétaux supérieurs comprend trois phases qui se déroulent de manière successive lors de la formation de la graine (Fig. 4 b):

- La **phase d'embryogenèse précoce**, depuis le zygote jusqu'au stade cœur (ou cordiforme), correspond à une étape d'établissement du patron d'organisation et de la morphogenèse de la plantule.
- La **phase d'embryogenèse intermédiaire**, qui s'étend jusqu'au stade cotylédonaire, correspond à la phase de maturation de l'embryon et est caractérisée par l'accumulation des réserves.
- Enfin, la **phase d'embryogenèse tardive** correspond à la phase de la dessiccation de la graine et de l'embryon qui se prépare à la phase d'arrêt de développement et à la phase de dissémination. Cette phase s'accompagne d'un ralentissement de l'activité physiologique de la graine qui entre tranquillement en dormance (état de repos végétatif). Chez *A. thaliana* l'embryogenèse est rapide. Les stades précoce et intermédiaire sont complétés 11 ou 12 jours après fécondation. Le dernier stade est rapidement effectué 2 jours après (14 jours après fécondation) (Lindsey and Topping 1993).

2- Génomique et contrôle génétique de l'embryogenèse végétale

Vu la petite taille des embryons et leur localisation pendant les stades précoces du développement embryonnaire, les études approfondies qui ont été menées depuis plusieurs années ont porté principalement sur la phase tardive de ce processus. Ces recherches ont mené à l'identification de nombreux gènes impliqués dans la formation des réserves de même que des gènes induits par l'acide abscissique (hormone impliquée dans la déshydratation de la graine) (Galau, Hughes et al. 1986; Galau, Bijaisoradat et al. 1987; Skriver and Mundy 1990; Espelund, Saeboe-Larsen et al. 1992). Ainsi, depuis longtemps,

les seules alternatives pour l'étude des gènes impliqués dans les stades précoce sconsistaient à analyser l'induction de l'embryon somatique (Zimmerman 1993). Par la suite, les approches fonctionnelles par mutagenèse menées chez *A. thaliana* et le maïs ont permis d'identifier des mutants létaux affectés dans l'embryogenèse précoce et ainsi déterminer leur fonction pendant le début de ce processus (Meinke 1985; Clark and Sheridan 1991; Jürgens G 1991; Meinke 1991). L'ensemble des mutants isolés peuvent être groupés en trois grandes catégories: i) mutants embryonnaires létaux chez qui l'embryogenèse est arrêtée, tel que les mutants *emb* (*embryo-defective*) (Clark and Sheridan 1991); ii) mutants de plantules anormales avec une pigmentation altérée, tel que le mutant *fusca* (Feldmann 1991; Jürgens G 1991); et iii) mutants de plantules anormales avec une morphologie altérée, tel que le mutant *gnom* (Mayer, Buttner et al. 1993). Basé sur le taux des mutants létaux trouvés par les approches de mutagenèse, différentes estimations du nombre de gènes essentiels impliqués dans l'embryogenèse ont été effectuées. Ainsi, Meinke évalue à environ 500 le nombre de gènes *EMB* chez *A. thaliana* (Meinke 1991), alors que Jürgens estime que 4000 gènes seraient essentiels au développement normal de l'embryon parmi lesquels environ 40 gènes seraient responsables de la mise en place du patron morphologique (Jürgens 1991). Toutefois, les informations disponibles de nos jours ne sont pas suffisantes pour élucider l'ensemble des mécanismes moléculaires et physiologiques menant à la formation de la graine.

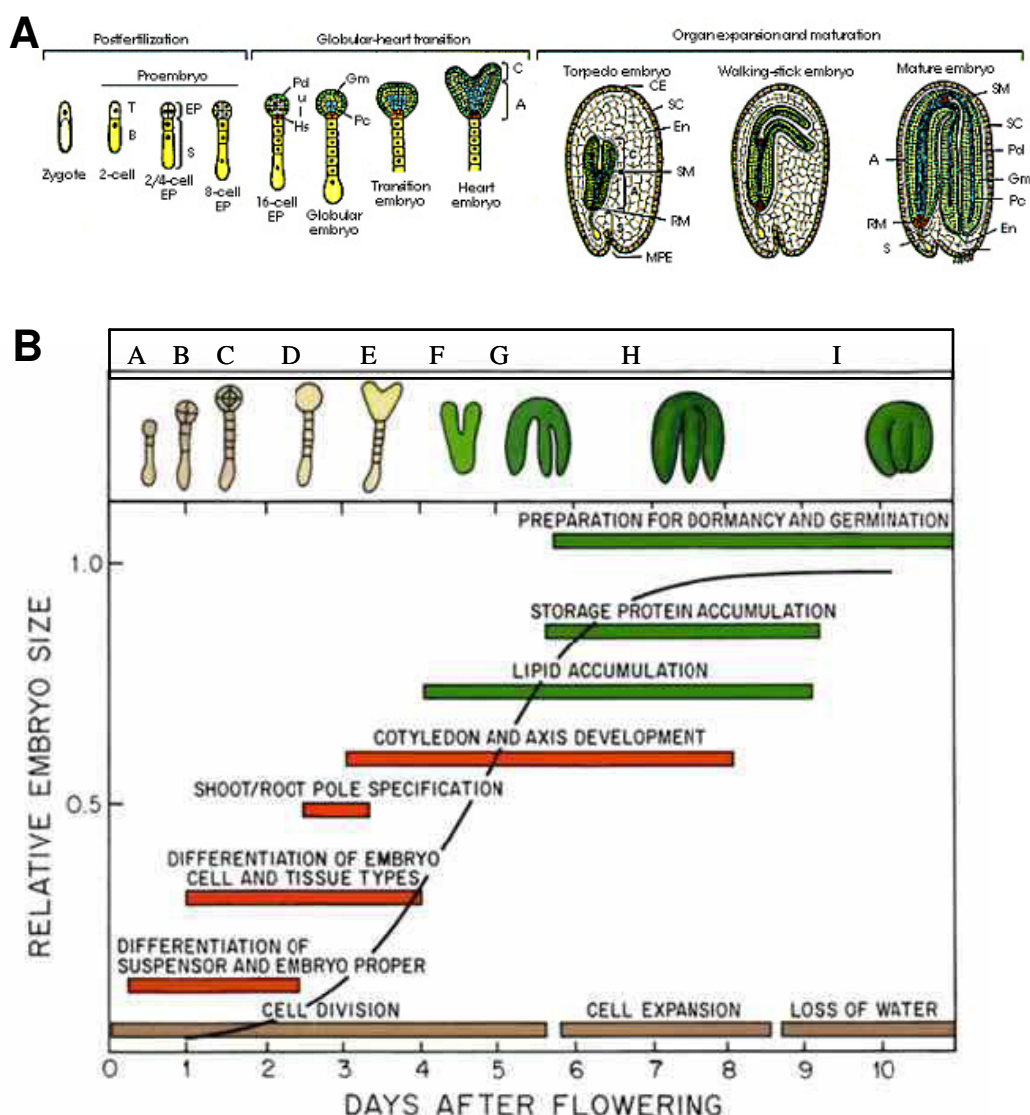


Figure 4: l'organisation cellulaire lors des différents stades de l'embryogenèse chez les plantes. 4a: Représentation schématiques des différents stades de développement embryonnaire chez *Arabidopsis thaliana*. 4b: Représentation des trois principales phases (la morphogenèse, la maturation, et la dessiccation) lors du développement normal de la graine chez *Arabidopsis thaliana*.

Image tirée du <http://www.mcdb.ucla.edu/Research/Goldberg/research/interests-index.htm>

Image tirée : http://www.bio.miami.edu/dana/pix/plant_embryogenesis.jpg

A = Embryon une cellule

B = Stade octant

C = Stade dermatogène

G-I = Stade cotylédonaire

D = Stade globulaire

E = Stade cordiforme

F = Stade torpille

La majorité des connaissances concernant le programme génétique induit au cours de l'embryogenèse des végétaux supérieurs provient de l'étude de mutants. Plusieurs mutants du développement embryonnaire ont été identifiés chez différentes espèces végétales (*A. thaliana*, *maïs*, *riz*...) par divers types de mutagenèses (chimique par EMS, insertionnelle ou aux rayons X). Par exemple, chez le *maïs*, les mutants *dek* (*defective-kernel*: grain altéré) (Neuffer and Sheridan 1980; Sheridan and Neuffer 1980; Scanlon, Stinard et al. 1994) sont altérés simultanément au niveau de l'embryon et de l'albumen et les mutants *emb* (Clark and Sheridan 1991), pour lesquels seul l'embryon est affecté, ont été identifiés. Chez *A. thaliana*, plus de 2000 mutants ont été identifiés par mutagenèse (Meinke 1985; Errampalli, Patton et al. 1991; Mayer, Ruiz et al. 1991; Goldberg, de Paiva et al. 1994; Altmann, Felix et al. 1995; Devic, Albert et al. 1996; McElver, Tzafrir et al. 2001).

L'analyse de mutants a déjà permis la caractérisation de plusieurs gènes jouant des rôles clés dans le développement embryonnaire végétal. Cependant, cette approche ne permet pas l'accès à l'ensemble des gènes potentiellement impliqués dans l'embryogenèse. Cela est dû d'une part à l'existence de redondance fonctionnelle au sein du génome et, d'autre part, par une forte prépondérance d'effets létaux de ces mutations agissant à un stade aussi critique du développement. De ces limitations découle le recours à d'autres méthodes telles que la transcriptomique qui permet de visualiser l'expression différentielle des gènes de manière spatiale, temporelle ou conditionnelle, à plus ou moins grande échelle.

Depuis une douzaine d'années, plusieurs techniques de criblage différentiel ont permis de caractériser des gènes différentiellement exprimés pendant l'embryogenèse. Ainsi, Nuccio et Thomas (1999) ont pu isoler par « differential display » deux gènes embryon-spécifiques, *ATS1* et *ATS3* (*Arabidopsis thaliana seed 1* et *3*) (Nuccio and Thomas 1999). En 1995, Heck et ses collaborateurs ont caractérisé, par la même technique,

le gène *AGL15* (*Agamous like 15*), une protéine de type MADS box (Heck, Perry et al. 1995). Aujourd’hui, la progression des méthodes d’analyse de l’expression génique par séquençage des banques EST (expressed sequence tags) à haut débit, l’utilisation de la technologie des puces à ADN (microarray) et, plus récemment, les techniques dites de « deep sequencing » comme le pyroséquençage (454 sequencing), ou l’amplification en phase solide (Solexa, Illumina), ou la prochaine génération de séquençage (Metzker 2010) ont permis de réaliser des études approfondies et simultanées de l’expression de la totalité du génome au cours du développement embryonnaire. Cependant, les difficultés rencontrées pour collecter les tissus à partir de jeunes embryons ont longtemps été responsables d’un manque dans les données génomiques concernant les stades précoce du développement embryonnaire végétal. Chez *Arabidopsis*, les premiers EST obtenus à partir des graines immatures ont été publiés en 2000 (White, Todd et al. 2000), avec 10 500 séquences s’appliquant à des stades encore trop tardifs de l’embryogenèse (de 5 à 10 jours après floraison). Chez le maïs (*Zea mays*), la première banque d’ADNc de tissus reproducteurs a été construite en 1995 à partir d’embryons au stade de transition (Breton, Chaboud et al. 1995). Plus récemment, une approche utilisant la technologie des biopuces d’ADN a permis d’obtenir un aperçu sur les différentes voies métaboliques impliquées au cours du développement embryonnaire chez le maïs (entre 5 et 40 jours après fécondation) en s’appuyant sur les profils d’expression de 1 500 gènes (Lee, Williams et al. 2002). Plusieurs autres travaux visant à caractériser les programmes transcriptionnels régulés lors des différents stades reproducteurs plus précoce ont aussi été menés au cours des dernières années (Lee, Williams et al. 2002; Hennig, Gruisse et al. 2004; Lan, Chen et al. 2004; Alba, Payton et al. 2005; Casson, Spencer et al. 2005; Zhang, Feng et al. 2005; Becerra, Puigdomenech et al. 2006; Spencer, Casson et al. 2007). Une des études réalisées a porté sur des boutons floraux pendant trois stades de développement des fleurs et des fruits: le premier stade juste avant pollinisation, le deuxième à partir de fleurs pollinisées et le troisième grâce à des siliques récoltées deux jours après fécondation. À l’aide de biopuces à ADN comptant plus de 22 000 gènes, Hennig et ses collaborateurs ont identifiés 1043

gènes spécifiquement exprimés pendant les stades reproductifs. Parmi ces gènes, plusieurs composantes des voies de transduction de signaux tel que des récepteurs de type «receptor-like protein kinase», des protéines phosphatases et des facteurs de transcription ont été enrichis dans les profils transcriptionnels obtenus (Hennig, Gruisse et al. 2004). Cependant, toutes ces études, conduites à partir d'un mélange de tissus reproductifs (tissus embryonnaires, albumen et enveloppe de la graine) et non d'embryons isolés à un stade précis du développement, ne permettent pas de décrire précisément les gènes exprimés de manière spécifique au sein des tissus embryonnaires. Une autre étude chez le riz à l'aide d'une puce d'ADNc contenant 10 000 gènes uniques a été réalisée à partir de pistils non pollinisés, de pistils pollinisés cinq heures après pollinisation et 5 jours après pollinisation, d'étamines, de pousses, de racines, d'embryons et d'endospermes 10 jours après pollinisation (Lan, Chen et al. 2004). Cette étude a permis d'identifier 253 gènes différenciellement exprimés pendant la pollinisation et la fécondation. Les plus grandes catégories fonctionnelles modulées par la pollinisation et la fécondation sont le stress, la défense, la transduction des signaux et le métabolisme des glucides.

Récemment, une étude utilisant des biopuces d'ADN et réalisée sur des embryons d'*A. thaliana* disséqués au laser a permis une comparaison fine et à grande échelle des transcriptomes des régions apicales et basales d'embryons aux stades globulaire et cœur (Casson, Spencer et al. 2005). Jusqu'à 65% du génome serait exprimé dans l'embryon en formation. Cette étude a également démontré que les régions basales et apicales au stade cœur seraient caractérisées par une plus grande complexité en terme de profils transcriptionnels par rapport au stade globulaire. Ceci serait probablement lié à la complexité de l'activité cellulaire au cours de la transition entre ces deux stades critiques du développement. Le même groupe a étendu ses études pour couvrir aussi le stade torpille (Spencer, Casson et al. 2007). L'analyse de regroupement par « clustering » a montré que la différence spatiale de l'expression des gènes était moins significative que l'expression temporelle. L'analyse du profil transcriptionnel au cours de ce stade de développement a

révélé une dynamique et une complexité de l'expression génique tant dans la région apicale que basale de l'embryon en développement. La transition du stade globulaire au stade cordiforme est associée en particulier à une surexpression des gènes impliqués dans le cycle cellulaire, la régulation transcriptionnelle, l'énergie et le métabolisme. La transition du stade cœur à torpille est caractérisée par une répression des gènes du cycle cellulaire et une surexpression des gènes codant pour des protéines de réserves et des voies de croissance cellulaire, d'énergie et du métabolisme.

Ces études transcriptomiques à grande échelle ont permis d'élucider une image globale des mécanismes cellulaires impliqués durant l'embryogenèse végétale, mais également de comparer ces processus entre différentes espèces. Cependant, les fonctions biologiques d'un grand nombre de gènes restent à déterminer. Le défi pour la recherche future sera d'assigner une fonction à ces gènes. En révélant des gènes jouant potentiellement un rôle clé au cours de cette phase critique du développement et en apportant des informations sur les principales fonctions cellulaires et les voies de régulation engagées, nous constituerons la première étape vers la compréhension des processus moléculaires et physiologiques contrôlant le développement embryonnaire et ainsi le développement des végétaux.

3- Modèle génétique et fonctionnel de l'établissement des patrons embryonnaires chez *A. thaliana*

Suite à la fécondation, le zygote d'*A. thaliana* se divise en une petite cellule apicale et une large cellule basale. La cellule apicale et ses cellules filles adoptent un patron de croissance isotropique et se divisent longitudinalement et transversalement. La cellule basale continue à s'allonger et se divise transversalement pour former les cellules filles. La cellule apicale de ces dernières, appelée hypophyse, devient une partie du méristème primaire racinaire alors que les autres cellules forment le suspenseur. Ces cellules ne

diffèrent pas seulement par leur position et leur forme, mais aussi par leur profil d'expression.

La division asymétrique du zygote produit deux cellules filles avec des propriétés différentes. En effet, le gène *YODA* (*YDA*), codant pour une kinase de type MAPKKK régule le développement de la cellule basale et ses cellules filles (Lukowitz, Roeder et al. 2004). Une mutation dans *YDA* mène à un patron de division anormal. La perte de fonction de *YDA* supprime la formation du suspenseur. La perte de fonction de *MPK3* et *MPK6* (des MAP kinases) a un effet semblable au mutant *yda* au niveau de la formation du suspenseur (Wang, Ngwenyama et al. 2007). Le même phénotype est observé au niveau de la division asymétrique et l'élongation du suspenseur chez les mutants *ssp* (*short suspensor*) et *gdr* (*grounded*) (Lukowitz, Roeder et al. 2004). Le devenir du suspenseur serait également dépendant du gène *LEAFY COTYLEDON 1* (*LEC1*) (Lotan, Ohto et al. 1998) puisque l'inactivation de ce gène aboutit à la formation d'un suspenseur anormal.

La division asymétrique du zygote produit une cellule basale qui transporte l'auxine et une cellule apicale qui répond à cette hormone. Ce gradient d'activité apico-basal d'auxine déclenche la spécification des structures de l'embryon apical. Il est, de plus, activement maintenu par une composante d'efflux auxinique PIN7 (PINFORMED7) qui est localisée apicalement dans la cellule basale (Friml, Vieten et al. 2003). Le mutant *pin7* a plusieurs phénotypes différents. Dans le cas le plus extrême, l'embryon perd la polarité ou bien le proembryon disparaît, aboutissant seulement à une file de cellules. Ces observations suggèrent que l'auxine joue un rôle complémentaire avec la protéine *YDA* et promeut le développement normal des cellules apicales en proembryon; alors que *YDA* promeut le développement des cellules basales en suspenseur (Jenik, Gillmor et al. 2007).

L'auxine a un profond effet sur les gènes régulant l'activité transcriptionnelle. Ces réponses transcriptionnelles sont assurées par la famille des ARFs (Auxin Response

Factors) qui se lient à des éléments sur les promoteurs de gènes inductibles par l'auxine (AREs, Auxin Response Elements). La mise en place du schéma d'organisation de l'embryon et des tissus vasculaires nécessite les gènes de la famille ARFs tels que *MONOPTEROS (MP)* et *NONPHOTOTROPIC HYPOCOTYL4 (NPH4)* et des gènes de la famille *AUX/IAA* comme *IAA12/BODENLOS (BDL)* et *IAA13* (Hardtke and Berleth 1998; Hamann, Mayer et al. 1999; Hamann, Benkova et al. 2002; Hardtke, Ckurdumova et al. 2004; Weijers, Benkova et al. 2005). Le traitement des embryons de *Brassica* avec de l'auxine exogène ou des inhibiteurs de transport d'auxine induit la formation d'un seul cotylédon entourant l'apex (Liu, Xu et al. 1993; Hadfi, Speth et al. 1998). Les cotylédons disparaissent complètement dans les doubles mutants *mp/nph4* et *pinoid (pid)/pin1*, PID codant pour une protéine kinase exprimée dans le domaine périphérique de l'embryon au stade globulaire (Aida, Vernoux et al. 2002; Furutani, Vernoux et al. 2004).

Plusieurs autres gènes sont impliqués dans l'initiation du primordium. C'est en effet le cas de *SHOOT MERISTEMLESS (STM)* chez *A. thaliana*, qui est un facteur de transcription appartenant à la famille de gènes *KNOX (KNOTTED1-like homeobox)* et de *ASYMETRIC LEAVES 1 (AS1)* qui est également un facteur de transcription de type MYB. Le mutant *as1* est affecté dans la formation d'organes latéraux en maintenant les cellules dans un état méristématique (Byrne, Barley et al. 2000). Le gène *AS1* est négativement régulé par *STM*. L'inactivation du gène *STM* semble donc indispensable à la formation des primordia foliaires. Un autre réseau de gènes incluant *CUP-SHAPED COTYLEDON 1, 2 et 3 (CUC1, 2 et 3)*, codant pour des facteurs de transcription de type NAC, permet de définir les limites des primordia et de mener à la formation d'organes distincts (Aida, Ishida et al. 1999; Vroemen, Mordhorst et al. 2003). Ces gènes interagissent avec les gènes *STM*, *PIN1* et *MP* pour réguler l'initiation des primordia. *PIN1* et *MP*, qui sont impliqués dans la voie de signalisation auxinique, influencent le patron d'expression spatial de *CUC1* en inactivant ce gène au niveau des cotylédons, alors qu'ils activent *CUC2* à la frontière méristème-cotylédons (Aida, Vernoux et al. 2002). En revanche, les gènes *CUC* initient l'expression de *STM*, un gène nécessaire à la formation du méristème apical (Aida, Ishida et al. 1999).

Au cours des phases tardives d'embryogenèse, *STM* régulerait à son tour le profil d'expression des gènes *CUC*. La formation du méristème apical et racinaire est soumise à un système de régulation complexe. En ce qui concerne le méristème apical, plusieurs autres mutants chez *A. thaliana* ont été identifiés. Les mutants *clavata 1, 2 et 3* (*clv1, 2 et 3*) présentent plusieurs phénotypes caractérisés par une surcroissance des méristèmes apical et floral (Clark, Running et al. 1993; Clark, Running et al. 1995; Clark, Jacobsen et al. 1996; Clark, Williams et al. 1997; Kayes and Clark 1998; Clark 2001). Ces gènes codent respectivement pour un récepteur kinase (*CLV1*) (Clark, Williams et al. 1997), un récepteur-like protéine de type leucine-rich repeats (*CLV2*) (Jeong, Trotochaud et al. 1999) et un petit peptide secrété jouant le rôle du ligand (*CLV3*) (Fletcher, Brand et al. 1999; Rojo, Sharma et al. 2002). L'expression de *CLV3* est induite par le gène *WUSHEL* (*WUS*), gène qui code pour un facteur de transcription et qui est nécessaire à la maintenance des cellules souches du méristème. À son tour, *CLV3* induit l'inhibition de *WUS* par rétrocontrôle négatif, assurant ainsi le maintien de l'identité des cellules souches et la différenciation des cellules (Brand, Fletcher et al. 2000; Schoof, Lenhard et al. 2000; Carles and Fletcher 2003).

Des centaines d'autres gènes sont impliqués dans l'embryogenèse. Un résumé de quelques gènes impliqués dans ce processus biologique est présenté au tableau 2 ci-dessous.

Table 2: Description des fonctions biologiques des gènes liés au développement des embryons.

Mutant	Protéine	Phénotype	Référence
<i>Auxin resistant 6</i>	Sous-unité de la ligase de l'ubiquitine SKP1/CULLIN/F-BOX	Pas de racine, un seul cotylédon, défauts dans les tissus vasculaires	(Hobbie, McGovern et al. 2000)
<i>Crinkly4</i>	Récepteur kinase de type LRR	Mal formation de l'embryon à différent degré	(Long, Woody et al. 2002) (Tanaka, Watanabe et al. 2002)
<i>doppelwurzel</i>		Duplication polaire du patron embryogénèse et formation de deux plantes d'un seul ovule	(Jurgens G 1991)
<i>Excess microsporocytes (EMS1)/Extra sporogenous (EXS)</i>	Récepteur kinase de type LRR	cellules embryonnaires plus petites, le développement d'embryon retardé et des embryos mature plus petits	(Canales, Bhatt et al. 2002)
<i>Fackel (fk)</i>	Stérol C-14 réductase	Plantules avec hypocotyle très raccourcie Les cotylédons sont directement attachés à la radicule	(Mayer, Ruiz et al. 1991; Schrick, Mayer et al. 2000)
<i>Gnom/emb30</i>	ARF-GEF associé à la Membrane	Perturbation de la polarité du zygote et de l'embryon en développement	(Mayer, Buttner et al. 1993)
<i>Gurke (gk)</i>	acetyl-CoA carboxylase	Mal formation du méristème embryonnaire apical	(Torres-Ruiz, Lohner et al. 1996)
<i>Hydra1 (hyd1)</i>	Isomérase	Divisions et des expansions cellulaires anormales au cours de la transition entre les stades globulaire et cœur	(Topping, May et al. 1997)

Mutant	Protéine	Phénotype	Référence
<i>Meristem layer 1 (ATML1)/ Protodermal2 (pdf2)</i>	Facteur de transcription de type HD-Zip	Défauts dans le développement des cotylédons	(Abe, Katsumata et al. 2003; Takada and Jurgens 2007)
<i>mp</i> <i>bdl</i>	Facteur de transcription	Perturbation de l'initiation des racines	(Mayer, Ruiz et al. 1991; Hamann, Mayer et al. 1999)
	Protéine IAA12	Perturbation de l'initiation des racines	
<i>Short root (shr) et scarecrow (scr)</i>	Facteurs de transcription de la famille GRAS (GIBBERELLIN-INSENSITIVE, REPRESSOR of gal-3, SCARECROW)	La division asymétrique du tissu parenchymateux générant le cortex et l'endoderme n'a pas lieu	(Scheres, Di Laurenzio et al. 1995)
<i>Sterol methyl-transferase 1(smt1/CPH)</i>	C-24 sterol methyl transférase	Divisions et expansions cellulaires anormales au cours de l'embryogenèse	(Diener, Li et al. 2000)
<i>Topless</i>	Répresseur de transcription	Délétion du méristème apicale Fusion des cotylédons Production des racines à la place des pousses	(Long, Woody et al. 2002)
<i>Wooden leg (wol)</i>	Récepteur kinase de type histidine	Réduction du nombre des cellules d'hypocotyle et du système vasculaire dû à une réduction de division périclinale des cellules précurseurs du système vasculaire	(Mahonen, Bonke et al. 2000)
<i>Zwille (zll)</i>	Protéine de la famille PIWI/ARGONAUTE	Différenciation de diverses structures à la place du méristème apical embryonnaire	(Lynn, Fernandez et al. 1999; Newman, Fernandez et al. 2002)

Problématique et projet de recherche

Les mécanismes moléculaires et cellulaires contrôlant l'embryogenèse sont encore très peu connus jusqu'à maintenant. Ceci s'explique par des difficultés au niveau des manipulations, compte tenu de la petitesse des embryons et spécialement ceux d'*A. thaliana*. Jusqu'à très récemment, la grande majorité des connaissances et des mécanismes moléculaires régulant le développement embryonnaire chez les végétaux provenait d'études de mutants menées sur quelques plantes telles qu'*Arabidopsis thaliana*, le riz ou le maïs. Bien que l'analyse par mutagenèse soit très prolifique, elle connaît aussi quelques inconvénients et limites. Du fait de l'existence de redondances génétiques et fonctionnelles ne permettant pas la visualisation phénotypique relié aux mutations et du fort taux de létalité entraîné par des mutations à des stades critiques du développement, cette approche ne permet pas d'identifier tous les gènes essentiels au développement embryonnaire et d'élucider l'ensemble des processus nécessaires à la formation de la graine. De nos jours, le développement des techniques permettant l'analyse simultanée de l'ensemble du génome à partir d'échantillons réduits a permis d'intensifier les recherches portant sur cette étape du développement végétal qui revêt un intérêt biologique et agronomique évident. Cela permet également d'accélérer les découvertes concernant les gènes impliqués dans la formation de l'embryon, celles-ci restant toutefois encore insuffisantes et trop parcellaires. Malgré les études transcriptomiques élucidées jusqu'à maintenant chez différentes espèces, aucune étude de ce genre n'a été entreprise sur la grande famille des Solanacées, bien qu'elle ait un rôle agronomique crucial.

Solanum chacoense Bitter, la plante à l'étude dans ce présent travail, s'insère dans la sous-famille des Solanoideae, elle-même comprise dans la grande famille des Solanaceae. Regroupant près de 1700 espèces, le genre *Solanum* est le principal représentant de cette famille, et l'un des plus étudié. En effet, il comprend de nombreuses

espèces économiquement importantes, dont la pomme de terre (*S. tuberosum*), la tomate (*S. lycopersicum*) et l'aubergine (*S. melongena*) et des plantes ornementales, comme la morelle faux jasmin (*Solanum jasminoides*). L'inflorescence de *Solanum chacoense* est une cyme. Ces fleurs hermaphrodites sont de couleur blanche, chacune comporte cinq sépales et pétales soudés entre eux. Son fruit est une baie, semblable d'une petite tomate ronde renfermant de nombreuses graines. Le gynécée est qualifié de supère, c'est-à-dire que l'ovaire se situe au-dessus du niveau des autres insertions.

Lors de la fécondation, plusieurs gènes impliqués dans le développement embryonnaire sont activés et certains le sont avant même que la fécondation n'ait lieu. Ces gènes activés répondent soit à la présence du pollen sur le stigmate, soit à la croissance des tubes polliniques dans le tissu transmetteur du style, soit à des signaux émis lors de la mort cellulaire des cellules du tissu transmetteur du style causée par la croissance des tubes polliniques. Actuellement, peu de données répartissant les composantes de la voie de signalisation lors la pollinisation sont connues. La majorité des études reportées s'appuient sur un signal à courte distance. Aucune d'entre elles ne porte sur la signalisation longue distance dans l'ovaire afin de mieux comprendre comment l'ovaire perçoit le signal d'une pollinisation et comment il se prépare pour réagir à ce signal. Dans le même ordre d'idées, jusqu'à tout récemment, les données existantes sur la façon dont le tube pollinique trouve son chemin restent encore parcellaires.

Dans le but d'ouvrir des perspectives pour une meilleure compréhension des mécanismes de régulation lors de la reproduction sexuée chez les végétaux, nous avons mené des études géniques de la pollinisation jusqu'au développement embryonnaire et nous avons analysé l'effet de la surexpression (*ScFRK2*) de protéine kinase, impliquée dans l'identité des ovules sur la régulation transcriptomique dans les ovules de *Solanum chacoense*, une espèce de pomme de terre sauvage.

Dans le premier chapitre traitant le développement embryonnaire, nous avons évalué le changement transcriptomique dans les ovules de *S. chacoense* de type sauvage après différents temps de pollinisation (2, 4, 6, 8, 10, 12, 14, 16, 18, 20 et 22 jours après pollinisation, ou du zygote à l'embryon mature) tout en les comparant aux ovules collectés à partir de plantes non pollinisées. Dans le but de sélectionner les gènes spécifiques aux ovules, une analyse comparative entre les gènes régulés dans l'ovule et ceux régulés dans les feuilles, étamines et styles a été réalisée conjointement.

Dans le deuxième chapitre, l'accent porte sur les changements qu'entraîne la pollinisation au niveau de l'ovaire, avant même l'arrivée du tube pollinique. Il s'agit donc d'un mécanisme de signalisation à distance nécessitant l'émission et la réception des molécules mobiles. Une de ces molécules est le méthyle jasmonate (MeJA). Les patrons de transcription entre différents types de pollinisation (compatibles, incompatibles, semi-compatibles, et interspécifiques), des traitements au jasmonate de méthyle (MeJA) et une réponse à une blessure au niveau du style (imitant la croissance physique des tubes polliniques) sont comparés à différents stades (12, 24 et 48 heures après traitement) afin d'identifier les gènes répondants à ces stimuli.

Dans le troisième chapitre, nos analyses portent sur l'isolation des gènes dont l'expression est modifiée par la surexpression de *ScFRK2*, *Solanum chacoense* Fertilization Related Kinase 2. Le mutant *frk2* montre une transformation homéotique des ovules en structure carpelloïdes filiformes, réitérant de ce fait le programme de développement du style. Le but était d'isoler des gènes candidats pour l'identité des ovules et comprendre la voie de signalisation en identifiant les gènes touchés par la sur-expression de cette kinase.

Chapitre 1.

Transcription profiling of fertilization and early seed development events in a solanaceous species using a 7.7K cDNA microarray from *Solanum chacoense* ovules

By Faiza Tebbji ^{1,2}, André Nantel ², and Daniel P. Matton ¹

¹Institut de recherche en biologie végétale, Département de sciences biologiques, Université de Montréal, 4101 rue Sherbrooke est, Montréal, Québec, Canada, H1X 2B2.

²Biotechnology Research Institute, National Research Council, 6100 Royalmount Avenue, Montreal, QC, Canada, H4P 2R2.

Accepté à BMC plant biology

Abstract

Background: To provide a broad analysis of gene expression changes in developing embryos from a solanaceous species, we produced amplicon-derived microarrays with 7741 ESTs isolated from *Solanum chacoense* ovules bearing embryos from all developmental stages. Our aims were to: 1) identify genes expressed in a tissue-specific and temporal-specific manner; 2) define clusters of genes showing similar patterns of spatial and temporal expression; and 3) identify stage-specific or transition-specific candidate genes for further functional genomic analyses.

Results: We analyzed gene expression during *S. chacoense* embryogenesis in a series of experiments with probes derived from ovules isolated before and after fertilization (from 0 to 22 days after pollination), and from leaves, anthers, and styles. From the 6374 unigenes present in our array, 1024 genes were differentially expressed ($\geq \pm 2$ fold change, FDR ≤ 0.01) in fertilized ovules compared to unfertilized ovules and only limited expression overlap was observed between these genes and the genes expressed in the other tissues tested, with more than three quarters of the fertilization-regulated genes specifically or predominantly expressed in ovules (955 genes). During embryogenesis three major expression profiles corresponding to early, middle and late stages of embryo development were identified. From the early and middle stages, a large number of genes corresponding to cell cycle, DNA processing, signal transduction, and transcriptional regulation were found. Defense and stress response-related genes were found in all stages of embryo development. Protein biosynthesis genes, genes coding for ribosomal proteins and other components of the translation machinery were highly expressed in embryos during the early stage. Genes for protein degradation were overrepresented later in the middle and late stages of embryo development. As expected, storage protein transcripts accumulated predominantly in the late stage of embryo development.

Conclusion: Our analysis provides the first study in a solanaceous species of the transcriptional program that takes place during the early phases of plant reproductive development, including all embryogenesis steps during a comprehensive time-course. Our comparative expression profiling strategy between fertilized and unfertilized ovules identified a subset of genes specifically or predominantly expressed in ovules while a closer analysis between each consecutive time points allowed the identification of a subset of stage-specific and transition-specific genes.

Background

Angiosperm sexual reproduction starts when pollen is transferred from the anther to the stigma. After hydration and germination, the pollen tube carrying two sperm cells enters the embryo sac through the micropyle of the ovule and penetrates one of the synergid where it discharges its contents. One sperm cell fuses with the egg cell and the resultant zygote develops into the embryo. The central cell unites with the second sperm cell to form a triploid primary endosperm cell that develops into the endosperm (Nawaschin 1898; Guignard 1899; Russell 1992; Russell 1996; Drews and Yadegari 2002). Thus, the double fertilization event initiates the development of two interconnected multicellular structures, the diploid embryo and the triploid endosperm. Embryogenesis patterning starts with an asymmetric cell division that produces a small apical cell that ultimately becomes the embryo, and a large basal cell (leading to the suspensor) that functions to provide nutrients from the endosperm to the growing embryo (Mansfield and Briarty 1991). Embryogenesis in higher plants can be divided conceptually into three overlapping phases (Goldberg, Barker et al. 1989; Thomas 1993; West and Harada 1993). The first phase involves morphogenesis and pattern formation, during which the polar axis of the plant body is defined by specification of the shoot and root apices, and the embryonic tissue and organ systems are formed (pattern formation/cell proliferation/cell division). During the second phase (maturation), storage reserves start to accumulate in the maturing embryo, and, in the third phase, the embryo prepares for desiccation and enters a period of developmental arrest. Successful embryogenesis thus leads to seed development. In *Arabidopsis* embryogenesis is rapid, requiring only 14 days after pollination to produce the desiccated mature seed (Lindsey and Topping 1993). In solanaceous species, embryogenesis spans a much longer period. For example, in *Solanum phureja*, embryo maturation, excluding desiccation, is only completed 27 days after pollination (Dnyansagar and Cooper 1960).

Classification of gene expression patterns associated with specific stages of embryo and seed development and functional understanding of the encoded genes are critical for

understanding the molecular and biochemical events associated with embryogenesis. Most of the knowledge concerning the genetic program activated during embryogenesis of higher plants comes from the study of mutants. Several mutants affecting embryonic development were identified in numerous plant species including *A. thaliana*, maize, rice, and tomato through various mutagenesis strategies (Neuffer and Sheridan 1980; Sheridan and Neuffer 1980; Clark and Sheridan 1991; Scanlon, Stinard et al. 1994; Tzafrir, Pena-Muralla et al. 2004; Gomez, Baud et al. 2006; Gray-Mitsumune, O'Brien et al. 2006; Chandler, Cole et al. 2007; Griffith, Mayer et al. 2007; Jenik, Gillmor et al. 2007; Lahmy, Guilleminot et al. 2007; Vidaurre, Ploense et al. 2007; Boisson-Dernier, Frietsch et al. 2008; Colombo, Masiero et al. 2008; Liu, Zhang et al. 2008). These analyses enabled the identification and characterization of several genes that play key roles in plant embryonic development. However, mutagenesis strategies alone cannot identify all of the genes that are potentially involved in a biological process.

In the past few years, several differential screening techniques (including differential display, subtracted libraries, differential hybridization, etc.) have made it possible to characterize genes differentially expressed during embryogenesis (Heck, Perry et al. 1995; Nuccio and Thomas 1999). More recently, other methods such as transcriptional profiling have allowed us to visualize global changes in transcript abundance in a spatial, temporal or conditional way. Genome-wide transcription profiling is an important and powerful tool leading to the generation of testable hypotheses for novel processes not yet characterized at the molecular level. Its usefulness has been demonstrated in the investigation of transcriptional programs occurring in a variety of developmental processes such as fruit ripening, seed development, flower development, embryo development, defense response to pathogens, and the response to wounding (Spellman, Sherlock et al. 1998; Girke, Todd et al. 2000; Harmer and Kay 2000; Schenk, Kazan et al. 2000; Aharoni, Keizer et al. 2002; Cheong, Chang et al. 2002; Lee, Williams et al. 2002; Becker, Boavida et al. 2003; Honys and Twell 2003; Hennig, Gruisse et al. 2004; Lan, Chen et al. 2004; Wellmer, Riechmann et al. 2004; Casson, Spencer et al. 2005; Zhang,

Feng et al. 2005; Wellmer, Alves-Ferreira et al. 2006; Spencer, Casson et al. 2007). Now that the technology has matured, microarray data are routinely correlated with other methods that measure RNA expression levels (Desikan, S et al. 2001; Perez-Amador, Lidder et al. 2001).

Recently we completed a medium scale EST sequencing project from normalized cDNA libraries made from *Solanum chacoense* ovules in order to identify signal transduction components involved in fertilization and early seed development (Germain, Rudd et al. 2005). *Solanum chacoense*, a diploid ($2n=4$) and self-incompatible close relative of the potato and tomato, produces both large numbers of easily isolated ovules inside a fleshy tomato-like fruit, and tubers in the roots, like potatoes. *Solanum chacoense* belongs to the Solanaceae family which includes between 3000 and 4000 species. This family is of great economic importance since it contains many ornamental plants (petunia, datura, tobacco ...), industrial plants(tobacco), and especially many fruits and vegetables (tomatoes, eggplants, peppers, potatoes ...). The flowers of *S. chacoense* are bisexual and actinomorphic. The pistil is composed of a wet-type stigma, an elongated style and a bilocular ovary superior to central placentation containing type ovules anatropous. The presence of a gametophytic self-incompatibility barrier was used to dissect the molecular events occurring at precise time points following pollination and fertilization since it enables synchronization of fertilization. These EST were used to construct cDNA microarrays consisting of 7,741 cDNAs spotted in duplicate, which were used to investigate the regulation of gene expression during fertilization and early seed development events from 0 to 22 days after pollination (DAP). Our aims were to: 1) identify genes expressed in a tissue-specific and temporal-specific manner; 2) define clusters of genes showing similar patterns of spatial and temporal expression; and 3) identify stage-specific or transition-specific candidate genes for further functional analyses.

Methods

Solanum chacoense cDNA clones and inserts amplification

We have previously used a subtraction screen on two cDNA libraries covering embryo development from early fertilization events (6-12 hours post-fertilization) to ovules bearing late torpedo stage embryos as a method to produce an EST pool enriched for weakly expressed messenger RNAs. From roughly 50,000 colonies spotted on nylon membranes, 8000 colonies that displayed a hybridization signal corresponding to the lowest 20% were selected for further analyses. 7741 good sequences were obtained and these comprised 6374 unigenes (Germain, Rudd et al. 2005). Inserts of these cDNA clones were PCR amplified using flanking primers complementary to vector sequences upstream and downstream of the cDNA inserts. Plasmid templates (1-2 ng) were added to 100 µl PCR mixture containing 0.2 mM of each nucleotide, 1 µM of each primer, 1.5 mM of MgCl₂ and 10 units of Taq DNA Polymerase. Inserts were amplified for 36 cycles (95 °C for 30 sec, 54 °C for 30 sec, 72 °C for 2 min), with an initial denaturation at 95 °C for 2 min and final extension at 72 °C for 6 min. Two (2) µl of each reaction were separated on 1.5% agarose gels to confirm amplification quantity and quality. PCR products were purified using MultiScreen® PCR₉₆ filter plates (Millipore, Billerica, MA, USA), and lyophilized. In general, the amount of each PCR product was greater than 5 µg and the average insert size was around 1000 bp.

cDNA microarray preparation

PCR products were resuspended in 10 µl of 50% DMSO and arrayed from 384 well microtiter plates onto UltraGAPS™ slides (Corning incorporated, Corning, NY, USA). A total of 7741 ESTs spotted in duplicate along with a variety of controls, including buffer-only spots and a dilution series of a plasmid harboring the *Candida albicans Ece1* gene.

Plant materials and RNA isolation

The diploid ($2n=2x=24$) and self-incompatible wild potato species *Solanum chacoense* Bitt. was greenhouse grown with an average photoperiod of 14-16h per day. The genotypes used were originally obtained from the USDA Agricultural Research Service, NRSP-6 Potato Genebank (Potato Introduction Station, Sturgeon Bay, WI, USA). Plant material was collected from female progenitor, *S. chacoense* genotype G4 (S₁₂ and S₁₄ self-incompatibility alleles) (Van Sint Jan, Laublin et al. 1996). For fertilization-related events, the fully compatible *S. chacoense* genotype V22 (S₁₁ and S₁₃ self-incompatibility alleles) was used as pollen donor. Plants were hand pollinated and ovules were collected between 0 and 22 days after pollination (DAP) and used for RNA extraction and probe preparations. Leaf, style and anther tissues were collected from plant genotype G4 grown under the same conditions as above. All samples for RNA preparation were quick-frozen in liquid nitrogen and ground to a powder with a mortar and pestle. Total RNA was extracted using the TRIzol® Reagent according to the manufacturer's protocol (Invitrogen, Burlington, ON, Canada). The yield and purity of RNA were assessed by determination of absorbance at both 260 nm and 280 nm. RNA was only used when the ratio Abs_{260 nm}/Abs_{280 nm} was higher than 1.7. RNA integrity was checked by both agarose gel 1% and with the RNA 6000 Nano Assay Kit and the Agilent 2100 Bioanalyzer. RNA from unfertilized ovules served as control.

Design of microarray experiments

To monitor the expression pattern from genes involved in fertilization and embryogenesis processes, flowers were hand-pollinated and ovules were isolated every two days during a 22 days period after pollination. Four independent biological replicates were produced from each time points. In addition, to isolate genes specifically or predominantly expressed in ovules, four biological replicates of leaf, anther, and style tissue mRNA preparations were individually hybridized against unfertilized ovule mRNAs and compared with the data obtained using unfertilized and fertilized ovule cDNA prepared at various

time points after pollination. To estimate reproducibility and to produce control data for statistical analysis, a large number of unfertilized ovules were isolated and separated between six independent control groups. RNA from randomly selected pairs of control was hybridized on six microarrays.

Preparation of fluorescent probes

Thirty (30) µg of total RNA, 1.5 µl oligo (dT)₂₁ (100 pmol/µl), and water in a final volume of 36 µl was denatured at 65°C for 10 min and cooled to room temperature for 5 min. The reverse transcription reaction was performed at 42°C for 2 h after addition of 3 µl dNTP-minus dCTP (6.67 mM each), 1 µl dCTP (2 mM), 4 µl DTT (100 mM), 8 µl 5× first strand buffer (Invitrogen), 2 µl of cyanine 3-dCTP (1 mM) or cyanine 5-dCTP (1 mM; Perkin Elmer-Cetus/NEN, Boston, MA, catalog # NEL999) and 2 µl of SuperScript II (200 units/µl, Invitrogen). After incubation at 42 ° C, 0.05 units each of RNase A and RNase H (Invitrogen) were, added and the reaction mix was incubated at 37 °C for 30 min. The probes were then purified using CyScribe GFX Purification Kit (GE Healthcare Bio-Sciences Inc., Baie d'Urfé, QC, Canada) according to the manufacturer's instructions. Incorporation efficiency of the CyDye probes was, measured using the ND-1000 Nano drop spectrophotometer (NanoDrop, Wilmington, DE, USA). In general, optimal amounts are 20 pmol of dye incorporated with an incorporation efficiency of between 20-50 labeled nucleotides per 1000 nucleotides. Probes were then air-dried.

Hybridization

Slides were prehybridized at 42°C for at least 1 hour, with 50 µl of a solution containing 5× SSC, 0.1% SDS and 1% BSA. The two cDNAs to be compared were pooled together, and mixed with the hybridization buffer to a volume of 50 µl with Dig Ease Hybridization buffer (Roche Applied Science, Mississauga, ON, Canada), 2.5 µl tRNA (Roche Applied Science) and 2.5 µl of Sonicated Salmon Sperm DNA (10 mg/ml; Invitrogen). The hybridization solution was heat denatured at 95°C for 3 min, cooled to

room temperature, and applied onto the DNA microarray slides for overnight hybridization at 42°C. To account for the possibility of dye bias, half of the hybridizations were performed in the Cy3/Cy5 configuration, and half in the Cy5/Cy3 configuration. The microarray slides were covered with a 24 × 60-mm glass coverslip (Fisher Scientific, Ottawa, ON, Canada). During all hybridization steps the hybridization chamber was kept at high humidity level. Immediately before hybridization, the DNA microarray slides were washed twice with 0.1× SSC at room temperature for 5 min and once with water for 30 sec and centrifuged at 800 rpm for 3 min. The DNA microarray slides were kept dry for a minimal amount of time before hybridization. Afterward, slides were completely immersed in a large volume of washing buffer, and the coverslips were carefully removed before washing twice for 10 min at 42°C with 1× SSC, 0.1% SDS, twice for 10 min at 37°C with 0.1× SSC, 0.1% SDS, and finally, with quick consecutive washes in three 0.1× SSC baths. DNA chips were air dried and stored protected from light until scanning.

Microarray scanning and data analysis

The DNA microarray slides were scanned with a ScanArray Lite microarray scanner (Perkin Elmer-Cetus, Wellesley, CA) at 10- μ m/pixel resolution. The fluorescence intensities were quantified with QuantArray software (Perkin Elmer-Cetus; versions 2.0 and 3.0). Microarray data normalization and analysis was performed in GeneSpring GX software version 7.3 (Agilent Technologies, Santa Clara, CA, USA). Raw intensities were normalized with a Lowess curve using 20% of the data to fit each point. To identify transcripts with a significant change in abundance, the fluorescence ratios from each time point were compared to the fluorescence ratios from 6 control hybridizations using the Welch t-test and the Benjamini and Hochberg False Discovery Rate. We selected genes with a p-value ≤ 0.01 and further restricted the lists to transcripts whose change in abundance was greater than 2-fold. The use of such a stringent gene selection method that uses both multiple testing correction and a fold-change cutoff did not significantly affect our conclusions. GeneSpring GX was also used for hierarchical clustering and to detect

significant overlaps between gene lists. Gene annotation was based on blastX with e value cut-off of 10^{-10} . Functional categorization was performed according to the Gene Ontology (GO) Consortium and Arabidopsis consortium information (<http://www.geneontology.org/>). Translated *S. chacoense* sequences were sorted into 15 functional categories by sequence comparison. The data discussed in this publication have been deposited in NCBI's Gene Expression Omnibus (Edgar et al., 2002) and are accessible through GEO Series accession number GSE21552 (<http://www.ncbi.nlm.nih.gov/geo/query/acc.cgi?acc=GSE21552>).

Real-time PCR

cDNA samples were synthesized from 2 µg of 2 independent preparations of total RNA using the SuperScript® II Reverse Transcriptase (Invitrogen). The RNA was denatured at 70°C for 10 min. The total volume was adjusted to 40 µl by adding 8 µl of 5× RT buffer, 2 pmoles of oligo dT 25 primer, 4 µl of 0.1 mM DTT, 2 µl of 10 mM dNTP, 200 units of SuperScript® II Reverse Transcriptase and 19 µl of water. The mixture was then incubated 1 hour at 42°C. The resulting first strand cDNA was used for real-time PCR amplification experiments. Ovule RNAs from three different developmental stages (4, 12, and 22 days after pollination) were compared. RNAs from unfertilized ovules were used as the calibration tissue. Duplicate quantitative assays for each tissue were performed with the SYBR Green Master mix (Invitrogen) according to the manufacturer's instructions. For real-time PCR amplification, the following PCR program was used: 50°C for 2 min, 95 °C for 10 min, 95 °C for 15 s, 60 °C for 1 min; steps 3 and 4 were repeated 40 times in Mx4000® Multiplex QPCR System (Stratagene, La Jolla, CA, USA). The relative quantification analysis was performed using the comparative $\Delta\Delta Ct$ method. To evaluate the gene expression level, the results were normalized using an ubiquitin gene (DN977330) as control. Primer sequences used in real time quantitative PCR are summarized in [Supplemental Table 1](#).

Tissue fixation and optical microscopy observation

Ovules were fixed in FAA for 24 h at 4°C (50% ethanol, 1.35% formaldehyde, and 5% glacial acetic acid). Samples were then dehydrated in an increasing series of ethanol baths (from 30% to pure ethanol). Microscopic observations were taken on an AxioImager M1 microscope equipped with an Axio Cam MRm camera (Carl Zeiss Canada, Toronto, ON, Canada).

Results

Microarray spotting and evaluation

We have previously generated expressed sequence tags (ESTs) derived from fertilized ovule cDNA libraries covering embryo development from zygote to late torpedo stages in *Solanum chacoense* Bitt. (Germain, Rudd et al. 2005) The 7741 ESTs corresponded to weakly expressed mRNAs obtained through a subtraction selection screen that produced a highly enriched unigene set (6374 unigenes) corresponding to 82% of the total ESTs sequenced. To provide a glimpse into the ovule transcriptome during embryogenesis in a solanaceous species and to identify a subset of ovule-specific and stage-specific genes comprising this transcriptome, these ESTs were used to construct amplicon-based cDNA microarrays. In the present study, we used a comparative expression profiling strategy to analyze gene expression profiles in ovules from 0 to 22 days after pollination.

For microarray production, the ESTs were amplified by PCR with vector-specific primers. The PCR products were purified, verified for single clone amplification, normalized, and arrayed onto aminosilane-coated glass surfaces. To increase the reliability of the detected signals, each PCR sample was spotted twice resulting in 15,482 data points for each array. Several controls were also spotted to verify the reliability of our hybridization. After each spotting runs, samples of printed arrays were visualized with a fluorescent dye to control evenness of DNA deposition and spot morphology.

Sixty-two (62) hybridizations corresponding to 15 experiments were performed (see material and methods for details). Eleven experiments each an average of four hybridizations, consisted of the comparison of ovule tissues harvested at 2, 4, 6, 8, 10, 12, 14, 16, 18, 20 and 22 days after pollination (DAP) with unfertilized ovules (control, 0 DAP). To determine the percentage of genes specifically or predominantly expressed in ovules, three experiments that compared RNA from unfertilized ovules to either leaf, style, or anther tissues were also conducted in quadruplicate. Due to the large amount of control tissue material needed for each time point comparison and for each replicate (unfertilized

ovules corresponding to 0 DAP), the control RNA obtained were pooled from different replicates and used for comparison with the various time points and other tissues. Pooling RNA before labeling has the advantage of reducing the variation due to biological replication and sample handling (Churchill 2002). To estimate this variation our last experiment competitively hybridized cDNA probes from six additional control samples collected from unfertilized ovule against the pooled control. The six individual control samples were different from the pooled one that was used as the universal control in all our experiments. The correlation coefficient between the normalized intensities of the two channels was of 0.98, and only few spots showed occasional differences in intensities above 2-fold ([Figure 1a](#)). This very high correlation coefficient gives a strong indication that biological replication is not a significant source of variation. For each experiment, four biological replicates were collected from the same greenhouse and from a large number of plants. For each individual replicate, all the necessary material was collected at once. Each hybridization was performed against the pooled control sample from unfertilized ovules (UO). To account for the possibility of dye bias, half of the hybridizations were performed in the Cy3/Cy5 configuration and half in the Cy5/Cy3 configuration.

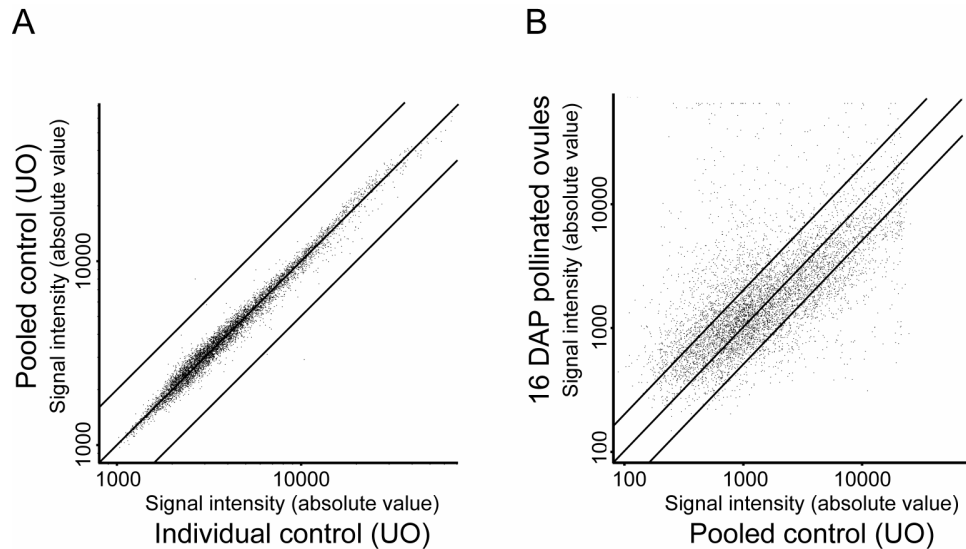


Figure 1. Gene expression profiling of unfertilized and fertilized ovule samples.

Scatter plots comparing the average fluorescence intensities in microarray experiments measuring the change in transcript abundance between A, pooled control and individual control; or B, 16 DAP pollinated ovules versus unfertilized ovules. The individual control samples were different from the pooled one that is used as the universal control in all our experiments. Black transversal lines show the ± 2 fold change.

Expression profiling of genes involved in fertilization and embryogenesis

To monitor gene expression profiles during fertilization and early embryogenesis, total RNA samples from UO to 22 DAP were isolated, labeled, and hybridized to the 7.7K microarray. A fraction of the ovules from each sample was set aside and fixed. These ovules were cleared and analyzed by differential interference contrast (DIC) microscopy to ensure that homogenous developmental stages were used in the various developmental time points. Strict pollination timing was accomplished through manual pollinations with pollen from a fully compatible *S. chacoense* genotype on anthesis day. Fertilization occurs between 36 and 42 hours following pollination in *S. chacoense* (Chantha, Emerald et al. 2006). Since *S. chacoense* is a self-incompatible species this prevents self-fertilization and eliminates the need for emasculation, which could induce a bias in gene expression through a wounding response. Furthermore, since anther dehiscence is not completed at the time of anthesis while the pistil is already fully receptive, this reduces the risk of self-pollen landing on the stigma that could trigger a self-incompatible response.

For each time point, four biological replicates were used, with two labeled as Cy3 cDNA probes and the other two as Cy5 cDNA probes. Using ANOVA testing, along with a Benjamini and Hochberg multiple testing correction algorithm, 1997 transcripts showed a statistically significant change in abundance ($p \leq 0.01$) in at least one of the time points compared to the control hybridizations (Figure 2A). Amongst those, 1024 showed a greater than ± 2 -fold variation in expression in at least one of the time points (Supplemental Table 2). These differentially expressed genes were grouped according to the similarity of their expression profiles using two dimensional hierarchical clustering (Figure 2B) (Fowlkes and Mallows 1983). These results clearly segregate the dataset amongst three major groups of genes that specify early (494 genes), middle (604 genes), and late (203 genes) stages of embryogenesis (Figure 2A and B). Embryonic stages as determined by ovule clearing and microscopical observation encompassing each time points are schematically represented (Figure 2A). From 0 to 6 DAP (early stage), embryo development corresponded to the post fertilization stages that include embryos from the zygotic stage to 8-celled embryo proper.

From 8 to 16 DAP (middle stage) ovules mainly bore embryos from the 16 cell to heart stages, and from 18 to 22 DAP (late stage) embryo developmental stages encompassed torpedo, walking stick, and mature embryos.

Figure 2 presents the global profiling during all stages of embryogenesis. In order to better illustrate the dynamic and magnitude of these changes in gene expression, and the distribution of the signal intensities obtained from each probe, an example of a scatter plot representing the data from a single time point comparing pollinated ovule (16 DAP) versus unfertilized ovule is shown in [Figure 1B](#). This representation shows the global distribution of all the genes spotted on the microarray slide at 16 DAP vs. UO. The scatter plot showed a positive correlation between fertilized ovules at 16 DAP vs. unfertilized ovule for most of the genes, with the majority of the genes analyzed showing a lesser than ± 2 fold difference in expression when compared to UO across the full intensity range. Genes that show a greater than ± 2 fold expression difference (735 genes) are also evenly distributed across the intensity range (up to 150 fold change) with a group of genes that show signal saturation. Comparing each time point scatter plots against the UO experiment ([Figure 1](#)) clearly showed that, for each time point, a group of genes are significantly modulated. All time point scatter plot comparisons gave similar distributions (data not shown).

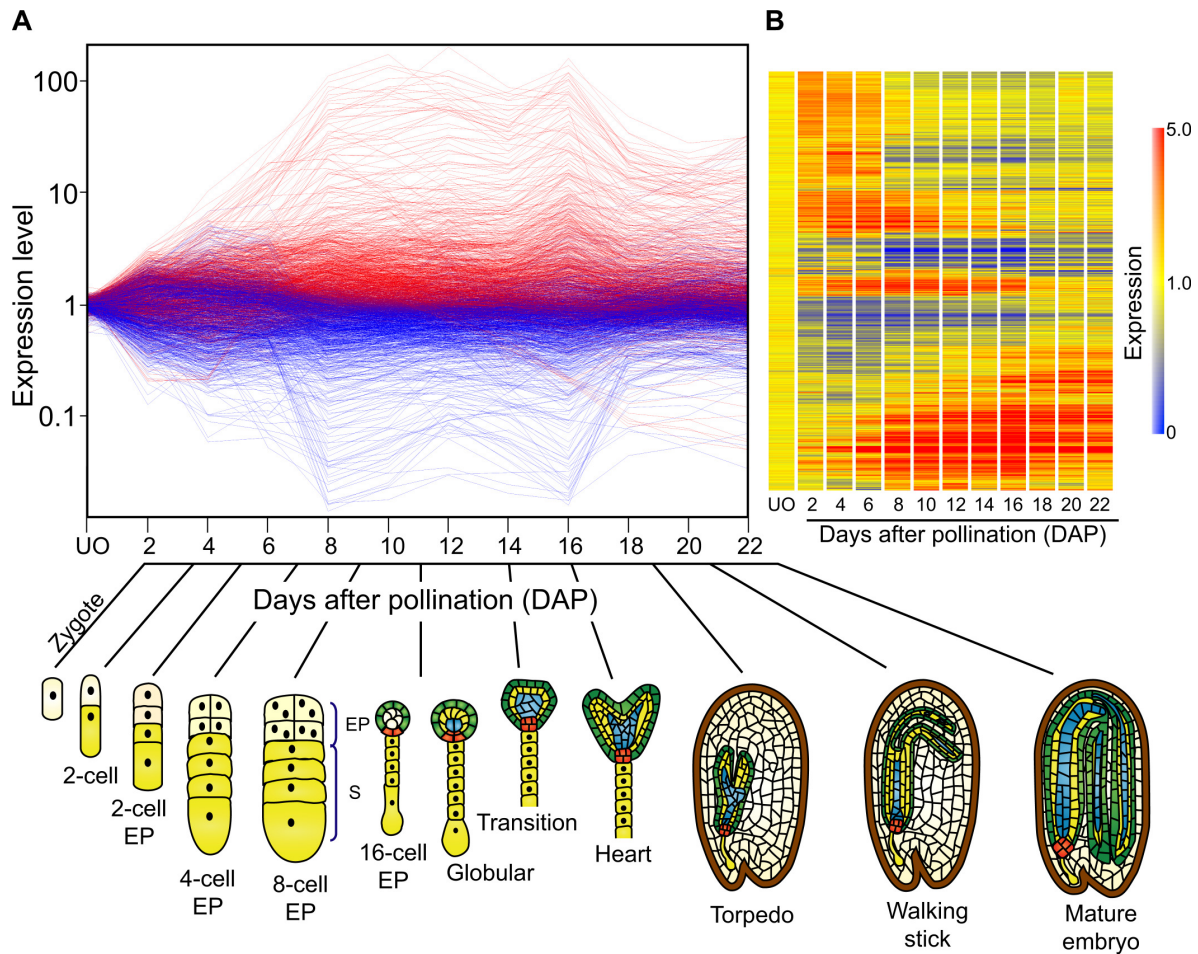


Figure 2. Transcriptional changes in *S. chacoense* ovules across an embryo developmental time course. The level of expression is compared to unfertilized ovules

A, Each line represents a probe that was spotted on the microarray while each time points of embryo developmental stage are represented in X-axis. The Y-axis shows the log of the normalized fluorescence ratios. Indicated in red are the genes expressed to levels higher than those in UO. Genes indicated in blue are expressed to lower levels than those found in UO. The corresponding embryo developmental stage for each time point was ascertain by ovule clearings and observed by DIC microscopy and represented with a schematic figure.

B Cluster analysis using unsupervised hierarchical clustering of 1024 genes that exhibit a statistically significant change between all samples ($P < 0.01$). The analysis was performed using condition tree clustering on all samples. Each row represents a different gene, and

each column displays gene expressions at each time point (0 to 22 DAP). Each experimental data point is colored according to the change in fluorescence ratio at that time point: data values displayed as red and blue represent increased and reduced expression, respectively, while data values in yellow are expressed similarly to unfertilized ovules.

Analysis of genes specifically or predominantly expressed in ovule tissues

To determine the percentage of ovule-specific genes in our EST pool, RNA samples from leaf, anther, and style tissues of *S. chacoense* were compared to UO pool sample. Each microarray experiment was performed four times using, in all cases, independently isolated RNA samples as starting material (four biological replicates). Statistical analyses showed that 558 genes (out of all ESTs) showed a significant variation in transcript abundance ($\geq\pm 2$ -fold coupled with FDR, false discovery rate ≤ 0.01) in at least one tissue (leaf, style, or anther) when compared to UO (Figure 3A). A Venn diagram analysis of modulated genes from leaves, anthers, and styles shows that, from the 558 genes, 3 genes were differentially expressed in all tissues compared to ovules; 322 genes are differentially expressed only in anthers; 10 genes are differentially expressed only in leaves; and 115 genes are differentially expressed only in styles. Four (4) genes are co-regulated in leaves and styles; 5 genes are co-regulated in leaves and anthers; and 99 genes are co-regulated in anthers and styles (Figure 3B).

From these 558 genes, 262 genes were up-regulated (≥ 2 -fold variation) and 296 genes were down-regulated (≤ 2 -fold change) when compared to UO (Supplemental Table 3). We thus considered that the transcripts corresponding to these 296 genes were predominantly expressed in UO. From the 262 transcripts that were more highly in styles, anthers, or leaves, 69 genes were also differentially expressed in ovules after pollination but with an induction level less than the one observed in the other tissues tested (< 2 -fold). A principal components analysis of these genes clearly indicates that the subset of genes expressed in non-ovule tissues is quite different than those expressed in ovules (Figure 3C). Thus, these results confirm that a large number of the ESTs on our microarrays can be considered ovule-specific or ovule-predominant. Out of the 1024 genes that showed more than ± 2 -fold variation in expression after fertilization, 955 (1024 - 69, or 93.2%) are considered specifically or predominantly expressed in ovule tissues.

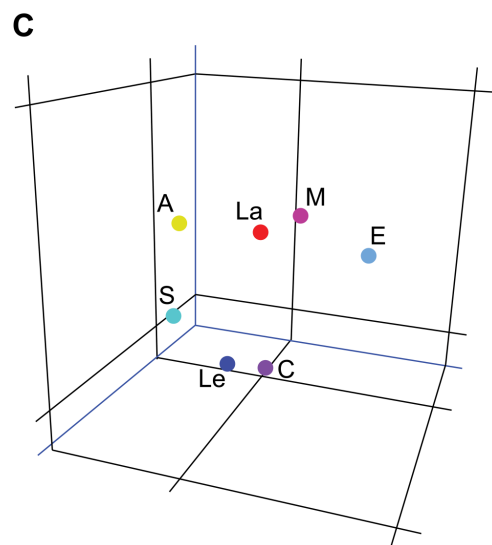
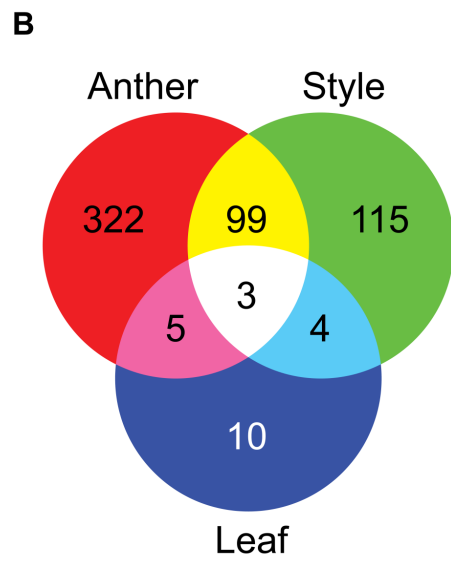
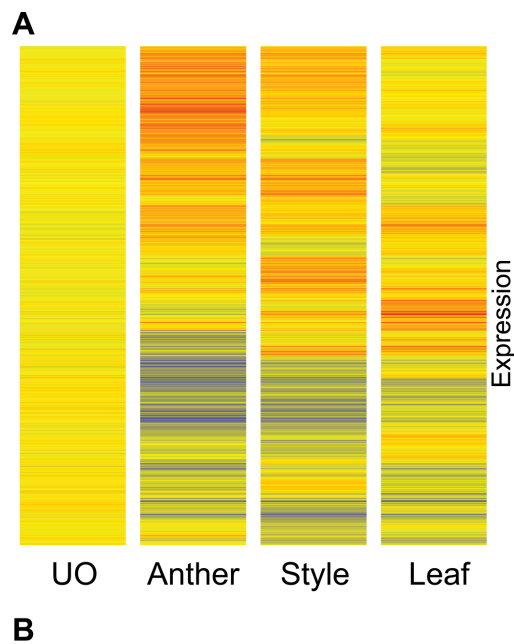


Figure 3. Tissue-specific comparison between ovule, style, anther and leaf tissues. The level of expression is compared to unfertilized ovules

A, Cluster analysis of the transcriptional profiles obtained from leaves, styles, and anthers was performed using condition tree clustering on all samples. Each row represents a different gene, and each column displays different tissues (UO, style, leaf and anther). Data values displayed as red and blue represent elevated and reduced expression, respectively. A total of 558 genes with a statistically significant change in transcript abundance of ≥ 2 -fold in at least one tissue compared to unfertilized ovules (FDR <0.01) are found. B, Venn diagram showing overlap between lists of genes differentially expressed in anther, style and leaf tissues. C, Principal Components Analysis (PCA) of various tissue types (A: Anthers; S: Styles; Le: Leaves; C: unfertilized ovules. E, M, L: early, middle and late stages of embryo development, respectively) based on the expression profile of 1376 genes including 558 that are differentiellly expressed in at least one tissue from styles, leaves and anthers and

1024 transcripts that are regulated in ovule which resulted in a clear differentiation distributed between 7 classifications.

Amongst these genes, a small group (1.15 %) was modulated by more than 100-fold during embryogenesis, 2.1 % of the genes were modulated by \pm 50 to 100-fold, 4.8 % between \pm 20 and 50-fold, and 6.1 % between \pm 10 and 20-fold (Supplemental Table 4). The most highly up-regulated genes comprised almost exclusively genes involved in proteolysis and peak transcript accumulation occurred between 8 and 16 DAP (Figure 2A). Genes involved in proteolytic function were also highly represented in the \geq 50 to 100-fold and \geq 20 to 50-fold up-regulated genes and covered various classes of proteases including serine-type peptidases (carboxypeptidases, subtilases or subtilisin-like serine protease), aspartic-type peptidases, and cysteine-type peptidases. Apart from genes involved in proteolysis, other highly up-regulated genes (\geq 10-100 fold) included numerous lipid transfer proteins (LTP) and non-specific lipid transfer proteins (nsLTP) that are involved in various biological processes including plant defense, pollen tube adhesion and guidance, embryo patterning and cell wall biogenesis (Vroemen, Langeveld et al. 1996; Kader 1997; Wolters-Arts, Lush et al. 1998; Park, Jauh et al. 2000; Nieuwland, Feron et al. 2005; Sarowar, Kim et al. 2009), as well as proteinase inhibitor, that are involved in plant defense responses and early seed development (Peña-Cortes, Sanchez-Serrano et al. 1988; Johnson, Narvaez et al. 1989).

Amongst the genes found to be strongly repressed in the following combined categories (from \geq 10 to 20, \geq 20 to 50, \geq 50 to 100-fold), most corresponded to genes classified as being involved in stress responses with a high representation of metallocarboxypeptidase inhibitor (MCPI) genes. One such MCPI was characterized by Martineau et al. (1991) as being highly expressed in anthesis stage ovaries in tomato (*Solanum lycopersicum*) while decreasing quite rapidly during fruit development, with an estimated 10-fold drop (Martineau, McBride et al. 1991; Josep, Francesc et al. 1998). The three most similar *S. chacoense* orthologs to the tomato MCPI were also found in the 10 to 20-fold down-regulated genes (Supplemental Table 4).

Functional classification of differentially expressed genes during fertilization and early seed development

The hierarchical gene clustering presented in Figure 2B showed that, following fertilization, the ovule-expressed gene pool could be clearly divided into three major groups that specified early, middle, and late stages of embryogenesis. A Venn diagram analysis of

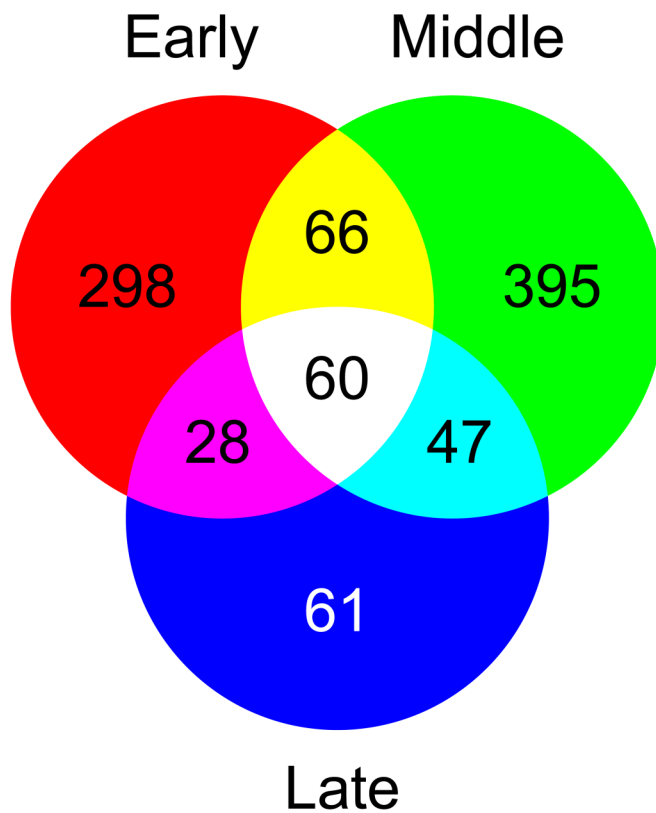


Figure 4. Venn diagram showing overlap between gene lists that show significant changes in transcript abundance during the three major embryo development stages (early, middle and late stages). The level of expression is compared to unfertilized ovules.

the genes predominantly expressed in fertilized ovules indicates that 298 genes are differentially expressed during the early developmental stage, 395 genes only during the middle stage, and 61 genes only during the late stage ([Figure 4](#)). Sixty-six (66) genes are differentially expressed in early and middle stages, 28 genes in early and late stages and 47 genes in middle and late stages. Sixty (60) genes are differentially expressed in all embryo development stages ([Supplemental Table 5](#)). Since the ESTs used to build the microarray were isolated from ovules harvested at various time following pollination, they encompass all different developmental stages of the embryo. The microarray analysis was thus sensitive enough to separate them between the major developmental transitions. This also suggests a highly specific expression program for each separate stage, with little overlap between the three major stages defined.

To determine whether the differentially expressed genes were involved in similar biological processes, transcript profiling data was correlated with the Gene Ontology classification based on both the *S. chacoense* sequences and their closest orthologs in *Arabidopsis thaliana*. The functional categories of these genes are given in [Figure 5](#). As expected, the largest category in every stage consisted of genes with unknown function or genes with no significant homology/no hit (29.8 %), as observed in fully sequenced genomes (Berardini, Mundodi et al. 2004). For the early and middle stages, the largest functional categories included metabolism (49 and 83 genes respectively), regulation of transcription (28 and 22 genes respectively), energy (11 and 18 transcripts respectively),

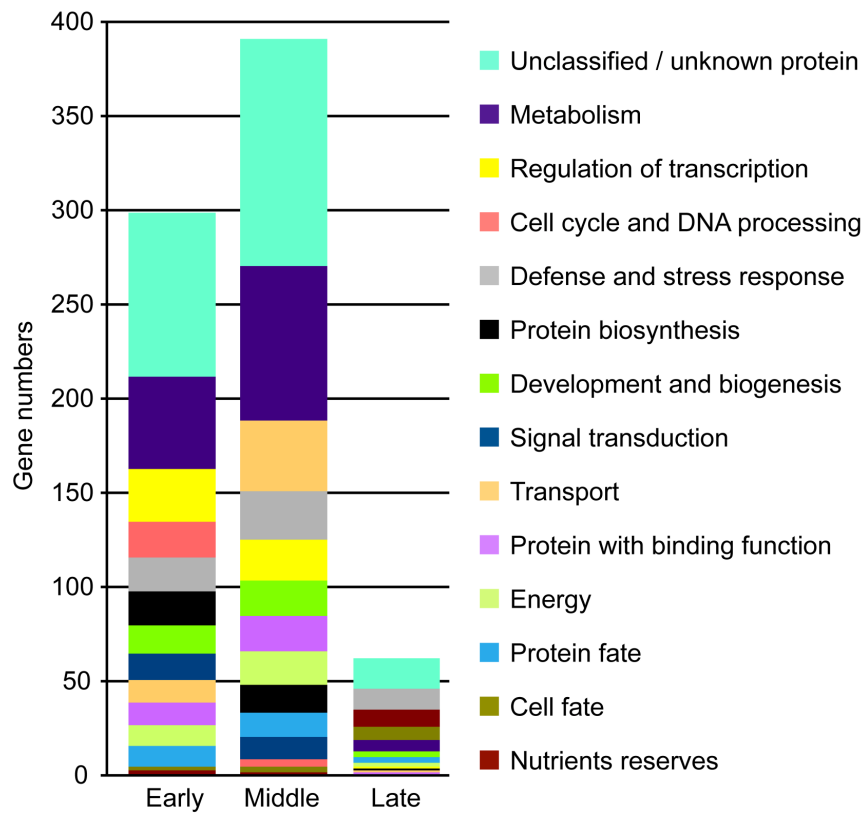


Figure 5. Functional (GO) annotations of the 955 genes (passing the significance filter: $P < 0.01$ and 2 fold cut-off) during the three major embryo developmental stages. The color keys show the designated gene class annotations.

signal transduction (14 and 12 transcripts respectively), protein fate (11 and 13 transcripts respectively) and proteins with binding functions (12 and 19 transcripts respectively).

One functional category of genes that was highly overrepresented in the early stage compared to the middle and late stages corresponded to genes related to the cell cycle & DNA processing category (19 in early stage, with 18 transcripts up-regulated, and 4 in middle stage with 3 genes up-regulated), probably reflecting the high cell division activity observed in the endosperm that precedes the development of the embryo. In solanaceous species, embryo division starts when the endosperm has reached 24-48 cells (Dnyansagar and Cooper 1960). For the protein biosynthesis category, 18 genes were differentially expressed in early stage with a large proportion of up-regulated genes (14 transcripts). An inverse situation was found in the middle stage, where only 3 transcripts were up-regulated out of 15 genes for this functional category. Interestingly, for the protein fate group, 3 genes out of the 11 found were up-regulated in the early stage, while 9 genes out of 13 were up-regulated in the middle stage, suggesting a coordinate inverse regulation of protein biosynthesis and fate during these two stages. For the following gene categories corresponding to development and biogenesis (15 in early and 19 in middle), and transport (12 in early and 38 in middle), the number of transcribed genes was higher in the middle stage when compared to the early stage.

Genes associated with nutrient reserves were up regulated in the late stage, as expected. The defense and stress responses category was important in all three stages. Differentially expressed genes associated with signal transduction and regulation of transcription classes were almost nonexistent in the late stage, comprising only 0.13 % (1 out of 754 genes) of the transcripts while they comprised 5.57 % (42 out of 754 genes) and 6.36 % (48 out of 754 genes) in early and middle stages respectively.

Isolation of stage-specific genes

To characterize in more detail the transcriptional changes taking place between developmental stages, a different analysis was undertaken for each time point during

embryogenesis from 0 to 22 DAP. A Volcano Plot with Student's t-test analysis was used to identify genes that were specifically expressed at only one time point when compared to UO (2 DAP vs UO, 4 DAP vs UO, etc) during embryogenesis, with a FDR ≤ 0.01 and $\geq \pm 2$ fold cut-off. Depending on the time point chosen, from 217 to 735 genes were significantly modulated at any single time point and between 3 and 194 genes were specifically modulated during a single time point ([Figure 6](#)). Genes expressed only at a single time represent candidates for stage-specific or stage-predominant expressed genes. Interestingly, four time points (2, 4, 8 and 16 DAP) had a high proportion (from 1/8 to 1/4) of their genes specifically modulated only at the observed time point. In the early zygotic phase at 2 DAP, 56 of 257 modulated genes (22%) were only expressed at this stage. At 4 DAP, when ovules bear embryos with a 2-cell embryo proper, 86 of 458 modulated genes (19%) were stage-specific. The last two time points enriched in stage-specific genes are found at the beginning and the end of the middle phase at 8 and 16 DAP, respectively. At 8 DAP, when ovules bear mostly embryos undergoing transition from a 4-cell to an 8-cell embryo proper

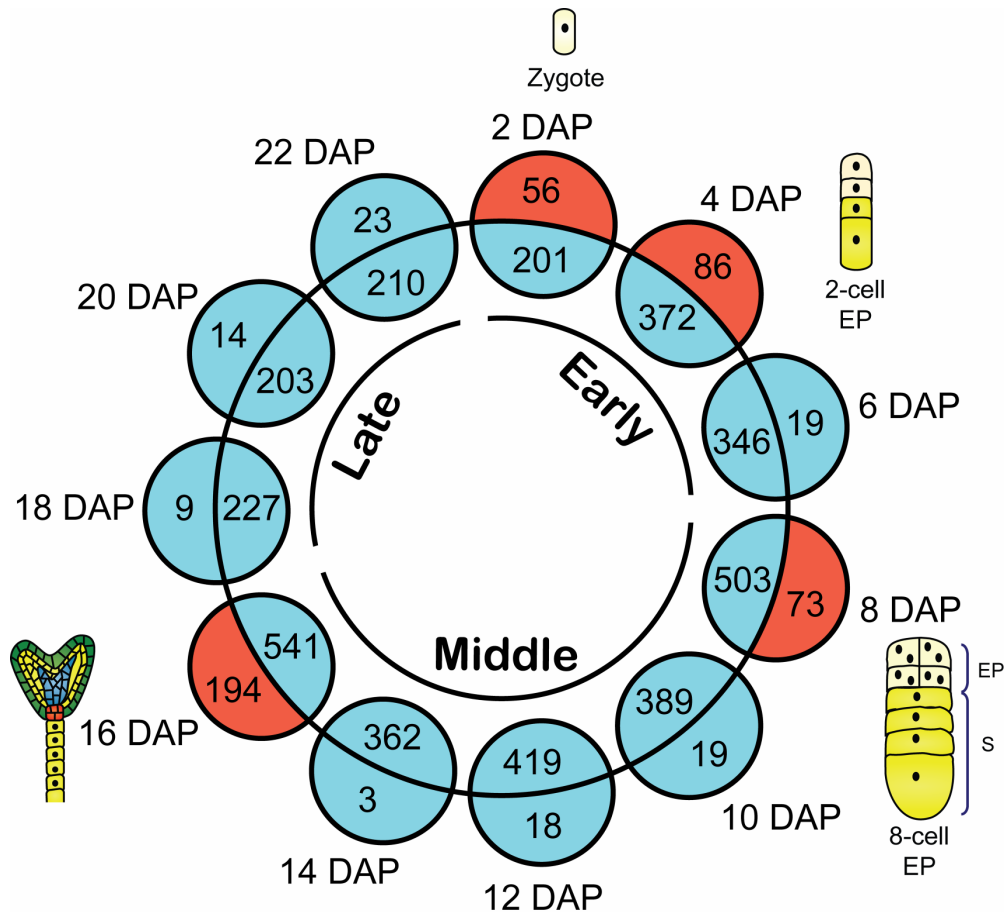


Figure 6. Graphical representation of the number of stage-specific genes identified at each time points of embryo development. The level of expression is compared to unfertilized ovules (Volcano plot using Student's t-test with FDR <0.01 and a 2 fold cut off). To find specific genes in each time, a Venn diagram was used between each time point and the total of genes remaining in the other stages. Numbers in the inner circle are genes shared by at least another time point. Numbers in the outer circle are genes considered stage-specific by the Volcano analysis.

73 of 576 genes modulated genes (13%) were stage-specific while at 16 DAP, when ovules bear mostly heart-stage embryos, 194 of the 735 modulated genes (26%) were stage-specific. Thus, although the majority of the genes were differentially expressed during several embryo stages, genes differentially expressed only at a single time point were also found for all stages in variable numbers. Supplemental [Table 6](#) provides the list of these stage-specific genes. At 2 DAP, half the stage-specific modulated genes were classified as part of the functional category covering translation. At 4 DAP, we noted the accumulation of the stress and defense related genes including heat shock proteins (12.34 %) and genes coding for protein with binding function (9.87 %). The major functional category represented at 8 DAP was related to energy (12.12 %). A specific group of cell cycle regulation (3.03 %) and chromosome organization and biogenesis (6.06 %) were also found. Finally, the 16 DAP time point was specially enriched in three gene ontology (GO) categories: hormone related genes (4.84 %), signal transduction (6.06 %) and transport (6.06 %).

Functional classification of differentially expressed genes in style, anther and leaf

The 558 genes that were differentially expressed in other tissues when compared to UO were grouped into different functional categories ([Supplemental Table 3](#)) according to their predicted gene products, based on the Gene Ontology (GO) Consortium through *S. chacoense* sequences and their closest orthologs in *Arabidopsis* ([Figure 7](#)). Apart from a large class of unknown and unclassified proteins (22.14 %), the largest functional groups

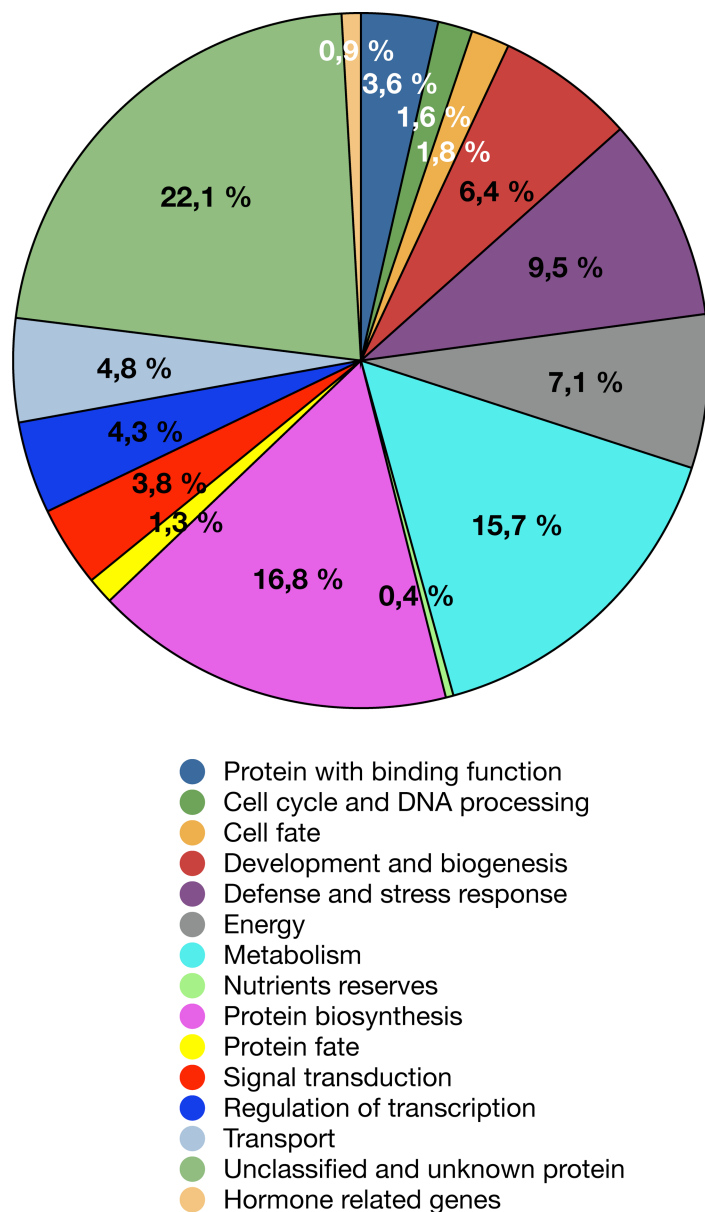


Figure 7. Distribution of 558 differentially expressed (by 2 fold-change, $P < 0.01$. The level of expression is compared to unfertilized ovules) genes in anthers styles and leaves in various biological process categories. The color key shows the designated gene class annotations.

observed were protein synthesis (16.78 %), metabolism (15.71 %), energy (7.14%), stress and defense related genes (9.46 %), development and biogenesis (6.42 %), transport (4.82 %), regulation of transcription (4.28 %), signal transduction (3.75 %), protein with binding function (3.57 %), cell cycle and DNA processing (1.6 %), protein fate (1.25 %).

Comparison of the categories found in these tissues and in ovules showed a completely different enrichment in functional categories (compares [Figures 5 and 7](#)). Whereas globally in ovule tissues (all stages taken together), we observed a large proportion of genes related to signal transduction and transcription, a very active cell cycle, and an up-regulation of genes associated with protein synthesis, in the other tissues tested these categories were less represented and even in the most represented category, protein biosynthesis, almost all genes were down-regulated (92 out of 94 genes).

Validation of microarray data by real-time PCR

In order to confirm the validity of differentially expressed genes identified by cDNA microarray analysis, we performed real time RT-PCR experiments on candidates from the three major groups of genes that specify early, middle, and late stages of embryogenesis. Quantitative RT-PCR analyses were performed on RNA extracted from ovules four days after pollination corresponding to the early stage of embryo development; from ovules 12 days after pollination corresponding to the middle stage; and from ovules 22 days after pollination corresponding to the late stage. Unfertilized ovules were used as the calibration tissue and the ubiquitin amplicon as the internal control to normalize the data. Quantitative RT-PCR confirmed the expression pattern for all the nine genes chosen from the microarray analysis: DN980725, DN981910, DN978427, and DN983138 that specify the early stage of the embryo development; DN976716, DN983239, and DN978469 which specify the middle stage; DN979177 and DN976898 which specify the late stage ([Figure 8](#)). In all cases, the quantitative RT-PCR validation indicated that differential expression detected by microarray experiment was highly reliable.

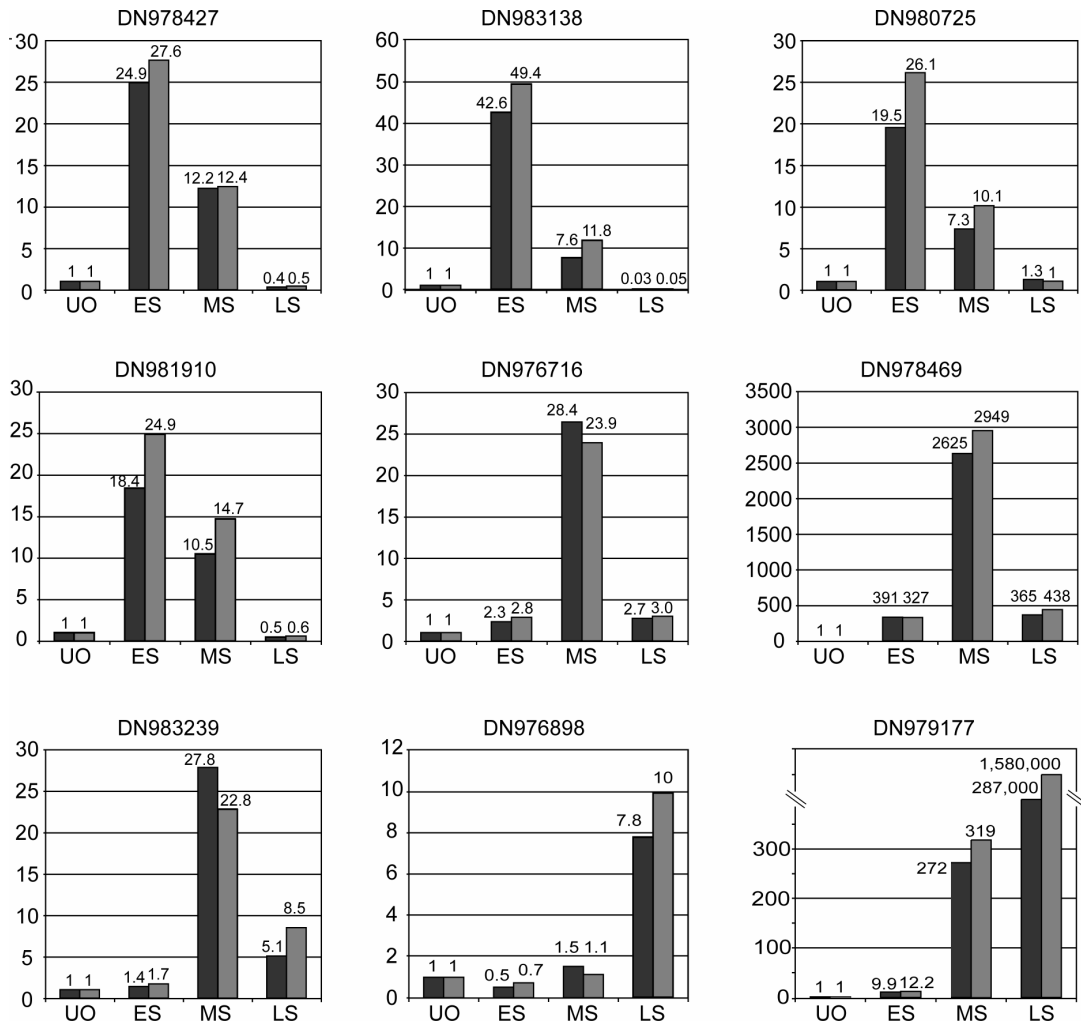


Figure 8. Quantitative real-time PCR (qRT-PCR) of selected genes representing the early, middle and late stage of embryo development. QRT-PCR was performed with two independent samples at each point.

Discussion

Until recently, most methodologies used to study the molecular mechanism involved in plant embryogenesis were based on mutagenesis approaches, and were mainly conducted in a few plant species, namely, *Arabidopsis*, rice and maize. These have allowed the characterization of numerous and informative mutants affecting early embryogenesis (Sheridan and Neuffer 1980; Meinke 1985; Clark and Sheridan 1991; Errampalli, Patton et al. 1991; Jurgens 1991; Mayer, Ruiz et al. 1991; Goldberg, de Paiva et al. 1994; Altmann, Felix et al. 1995; Devic, Albert et al. 1996; Elster, Bommert et al. 2000; Tzafrir, Pena-Muralla et al. 2004). In recent years, candidate gene studies involving gene-profiling technologies have enabled the global visualization of spatial and temporal differential gene expression patterns, thus being complementary to mutagenesis approaches while also being able to characterize new key genes inaccessible through mutant screens. Only few such studies targeting plant embryogenesis have been conducted (Lee, Williams et al. 2002; Hennig, Gruissem et al. 2004; Lan, Chen et al. 2004; Casson, Spencer et al. 2005; Spencer, Casson et al. 2007). In this study, we have analyzed for the first time a large transcriptomic dataset of temporal gene expression in ovules from a solanaceous species, *S. chacoense*, by comparing the gene expression profiles of fertilized ovules versus unfertilized ovules. We have covered the whole embryo development process from zygote to mature embryo and have identified 955 genes ($\geq\pm 2$ -fold change, $p\leq 0.01$) that are specifically or predominantly expressed in ovules compared to their expression profile in leaves, styles or anthers. Many differentially expressed genes encode proteins with putative regulatory functions, and most of them have not yet been characterized. Overall, in ovules, a large proportion of genes related to transport, signal transduction and regulation of transcription were modulated, and an up-regulation of genes associated with cell cycle and protein synthesis was noticed. In the other tissues tested (style, anthers and leaves), these categories were poorly represented and, even in the most represented category of protein biosynthesis, almost all genes were

down-regulated (92 from 94 genes). The data obtained indicates that some gene categories are overrepresented in some tissues or organs. Interestingly, we found that expression of MADS-box, MYB, AP2-EREBP and YABBY transcription factor families were overrepresented in the transcriptional regulation groups during the early and middle stages of embryo development as well as in anthers, but were absent in the leaves and style. This suggests that these genes might play an important role in defining structural and functional identity of reproductive tissues. Consistent with this, many transcription factors from the abovementioned gene families have been previously shown to play major roles during plant reproduction (Rounsley, Ditta et al. 1995; Hennig, Gruissem et al. 2004) and floral organ development (Bowman, Smyth et al. 1991; Golz and Hudson 1999; Bowman 2000; Theissen, Becker et al. 2000; Ng and Yanofsky 2001). Therefore, genes identified as being preferentially expressed in a given tissue probably have an important function in this tissue (Yanofsky, Ma et al. 1990; Jack, Brockman et al. 1992; Azumi, Liu et al. 2002; Vroemen, Mordhorst et al. 2003; Colombo, Masiero et al. 2008).

Specific functional category enrichment in the three major embryonic developmental stages

Differentially expressed genes in ovules were grouped according to the similarity of their expression profiles using unsupervised hierarchical clustering algorithms. Clustering results segregated the dataset amongst three major groups of genes that specified early (from zygote to 16-cell stage), middle (16-cell to heart stage) and late (heart to mature embryo) stages of embryogenesis ([Figure 2](#)). There is a clear distinction in transcriptional profiles between early, middle and late stages of embryogenesis, as determined by principal components analysis ([Figure 3](#)), by the little overlap seen between the modulated genes ([Figure 4](#)), as well as by the specific enrichment in the corresponding functional categories ([Figure 5](#)). K-means clustering using Pearson correlation was also used to separate the expression patterns during the embryo's developmental time course. Considering that three

major expression profiles are found, representing early, middle and late stages of embryonic development, a maximum of nine patterns can be expected ([Figure 9a](#)). Hennig et al. (2004) also proposed nine models of dynamic expression patterns for genes involved in reproductive development in *Arabidopsis* based on three different stages: before, during and after pollination (Hennig, Gruisse et al. 2004). Spencer et al. (2007) found that seven distinct expression patterns were present within the apical and basal section of the embryo during the globular, heart, and torpedo stage embryos (Spencer, Casson et al. 2007). The two missing profiles are most probably the consequence of the absence of earlier stages, before the globular stage. When considering less global trends, as depicted in [Figure 6](#) for stage-specific genes, a higher number of specific and slightly

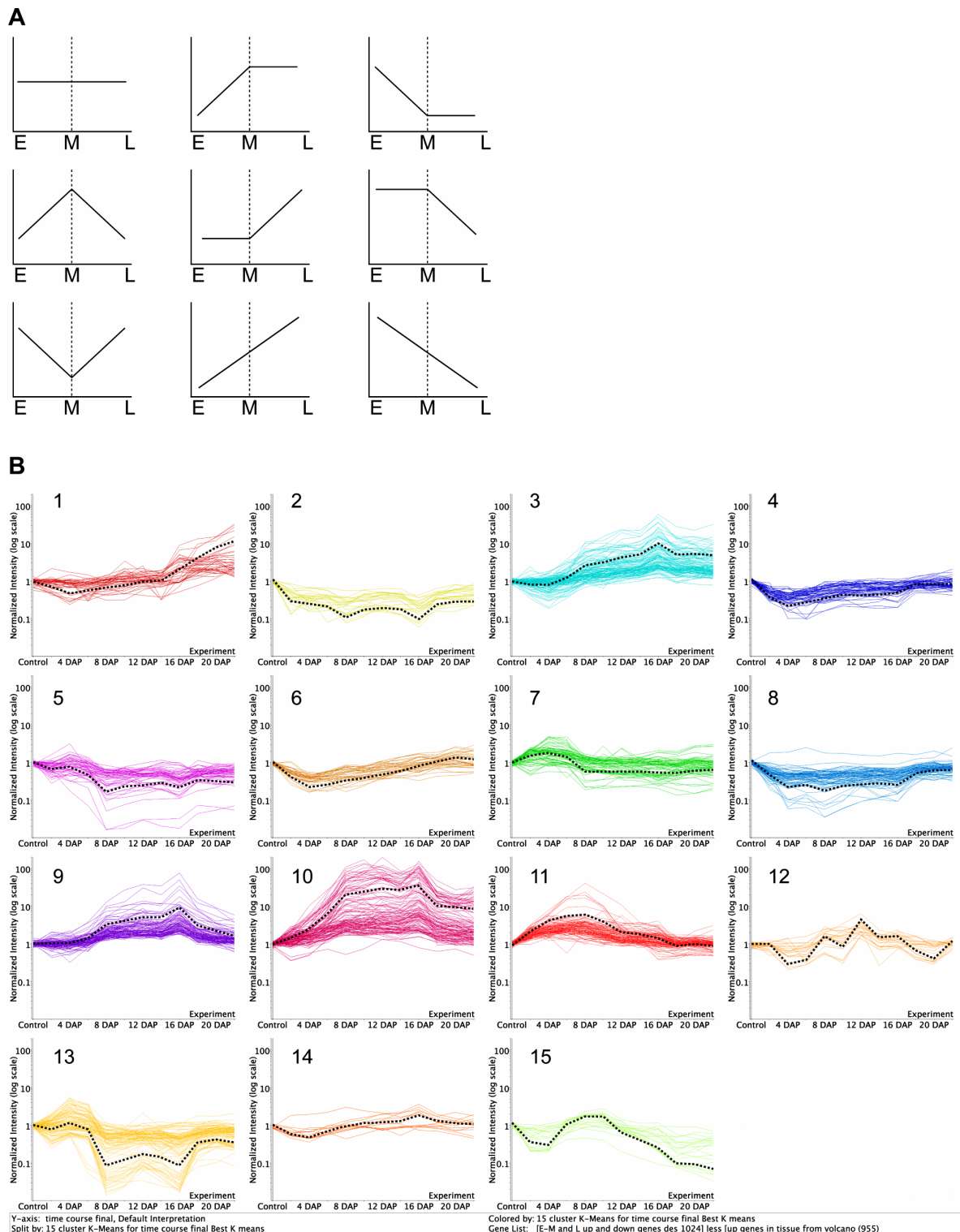


Figure 9. K-means clustering using Pearson Correlation (GeneSpring version 7.2) during an embryo development time course. A, Models of dynamic gene expression patterns representing all the nine different pattern founded based on the three point time (early, middle and late). B, Clustering of specific differentially expressed genes in the ovules based on 15 clusters representing all the stages of embryonic development from 0 to 22 DAP. The black discontinues line represent the average of gene profile.

different patterns can be obtained, based on the 12 individual time points. [Figure 9b](#) depicts 15 such patterns that can be derived from the analysis of our time-course every second day from 0 to 22 DAP and that include the nine possible dynamic expression patterns. Although the majority of functional groups are shared between several stages, some of these clusters show specific functional categories enrichment ([Supplemental Table 6](#)). The first cluster (cluster 1) includes genes involved in protein storage and are expressed during the late stages of embryogenesis. Cluster 7 corresponds to the early stage (2 and 4 DAP) and is enriched in genes classified in the protein biosynthesis category. Cluster 11 shows a peak at 8 DAP and is enriched in genes of the nucleosome assembly and cell cycle regulation group. Clusters 3 and 9 show a profile with a pronounced peak at 16 DAP, corresponding to the transition from heart to torpedo stages. These two clusters are enriched in functional categories corresponding to proteins with binding function, lipid metabolism, transport and genes implicated in development and biogenesis. Cluster 10 represent the transition of the early stage to middle (8 DAP) and middle to the late (16 DAP) and is characterized by a large number of genes involved in proteolysis, lipid metabolism and transport, development and protein folding.

Based on the global trend from the three major clusters specifying early, middle and late stages of embryogenesis, we found that the transcriptional pattern of some functional categories was specific to certain embryo developmental stages. These included metabolism, transcriptional regulation, cell cycle, protein biosynthesis, defense and stress response, development and cell growth, signal transduction, transport, protein with binding function, protein fate and energy, which are represented in early and/or the middle stage. The late embryonic stage was characterized, in addition to some groups found in the early and middle stages, by the cell fate and nutrient reserves functional categories ([Figure 5](#)). A comparison with the closest study published by Spencer and collaborators (2007) in *Arabidopsis*, shows that a larger representation of functional groups is present in our dataset. Spencer and colleagues found 1872 and 1226 differentially expressed genes in the apical and basal tissue time course, respectively, using a FDR of 0.05 for genes whose

expression was significantly different from a value of 1. They then choose the 200 most highly expressed genes (100 in apical and 100 in basal tissues) between the developmental stages studied. In contrast, we used, a FDR of 0.01 and a cut off of $\geq\pm 2$ fold in each time point compared to the same control. Our GO groups were assigned to all the genes that were specific and differentially expressed in the early (zygote to 16 cell), middle (globular to heart) and late (torpedo to mature embryo) stages of embryogenesis. In the published *Arabidopsis* data (Spencer, Casson et al. 2007) the transition from globular to heart stage is characterized by the up regulation of genes involved in energy production, metabolism, protein biosynthesis, signal transduction and transcription. While in our dataset, the middle stage, which includes this transition, is enriched in the same functional groups except for the protein biosynthesis category which was instead found in the early embryonic stage (from zygote to almost the globular stage). In addition, other enriched functional categories were up-regulated in the middle stage, including proteins with binding function, development and cell growth, protein fate and transport. The late stage was characterized by the up-regulation of the nutrient reserve category. It was reported that the storage proteins typically accumulate only from the mid-maturation phase onwards, when cell division is completed and the basic form of the embryo has developed (Lindsey and Topping 1993). Given that the plant body pattern is already established and that the seedling continues to mature, it was expected to have similar transcriptional profile from torpedo to mature embryo and have a up regulation of nutrient reserves at all these late stages, which is indeed what we observed. Thus, during embryo development, some functional groups characterized specific stages while other groups are shared between different embryogenesis stages. Indeed, the up regulation of genes related to cell cycle and protein biosynthesis characterized the early stage; proteins with binding function, protein fate, cell-cell communication and transcription specified the middle stage; and reserve proteins were more abundant in late stage. Energy and transport functional groups were represented in the early and middle stages while stress and defense related genes were highly represented during all developmental stages.

Protein biosynthesis, including ribosomal proteins (RP) and components of the translation machinery, were up-regulated in the early embryonic stage but then down-regulated in the middle stage. Spencer and colleagues (Spencer, Casson et al. 2007) found a similar trend but it appeared to be delayed compared to our data as it shows a significant up-regulation of genes involved in protein synthesis between the heart stage and the torpedo stage in their apical embryo time course, and between the globular and the heart stage in their basal embryo time course. These embryo developmental stages would be included in our middle stage, where we observed a decrease in protein synthesis components when compared to our early stage. This could be representative of the transition from early embryogenesis to the maturation and protein accumulation phase typical of the later embryogenesis stages (Lindsey and Topping 1993). Conversely, protein fate genes were down-regulated in the early stage but up-regulated in the middle stage. Genes belonging to the cell cycle category were exclusively up-regulated in the early stage. Up-regulation of the protein biosynthesis category specified the second and fourth day after pollination, afterward, these genes were either down-regulated or showed no differential expression during the later time points. This finding reflects the need to produce sufficient amounts of these essential proteins and the indispensability of protein synthesis in the actively developing seeds. Conversely, genes involved in protein degradation were overrepresented later in middle and late stages. Spencer et al. (2007), found the same enrichment order, with an up regulation of protein biosynthesis from the globular to the heart stage, followed by overrepresentation of the protein fate group in the heart to the torpedo stage in which the protein biosynthesis group was absent. The over-expression of these particular categories of genes illustrates the high energetic requirements of embryo tissue and suggests that other regulatory mechanisms at the post-transcriptional and posttranslational levels are important during the embryogenesis. Consistent with this, other interesting genes were found including genes coding for ubiquitin, and proteinase inhibitors. Indeed, transcriptional and post-transcriptional control have been described for the proteinase inhibitors of soybean (Walling, Drews et al. 1986) and other legume seed

proteins (Gatehouse, Evans et al. 1986); and ubiquitination was already found to be an important post-translational regulatory process of the unfertilized egg cell in wheat (Sprunck, Baumann et al. 2005).

Examination of the cell cycle and DNA processing categories revealed a prevalence of gene up-regulation from 2 to 16 DAP. B-type cyclin-dependant kinases (CDKs) involved in the control of the G₂/M transition in plants (Porceddu, Stals et al. 2001) as well as a large number of S-phase markers such as Histone 1, 2, 3 and 4 (Tanimoto, Rost et al. 1993; Gown, Jiang et al. 1996; Breyne, Dreesen et al. 2002) were significantly enriched and up-regulated. This is not unexpected since cell division in the embryo starts after fertilization and continues until the heart stage (West and Harada 1993). It has also been shown that protein synthesis and the cell cycle are associated at two levels (Cormier 2000). On the one hand, protein synthesis is required for entry and progression through the cell cycle; on the other hand, protein biosynthesis is itself modified during cell division steps. This finding is in line with our data set. In the early stage, the up-regulation of ribosomal proteins, translation and elongation factors coincide with the overexpression of histones. Markedly, in the middle stage, proteolysis genes represented by a large number of ubiquitine/proteasome-related genes, proteases, peptidases, and subtilases, were activated, suggesting active degradation of proteins by proteolysis, while proteins biosynthesis genes remain expressed at a basal, non-modulated level. Ubiquitin/proteasome-related genes during embryogenesis have also been reported to strongly affect the progression of the *Arabidopsis* embryo from the globular stage onward (Brukhin, Gheyselinck et al. 2005). Altogether, this suggests important post-translational regulation over cell cycle progression during embryogenesis.

The set of differentially expressed genes modulated during the early and middle phases during also contained many signal transduction components and transcriptional regulators. Among them were 24 signaling proteins and 50 transcriptional regulators. In the signal transduction category, one calmodulin, most similar to the *Arabidopsis* CaM7 (Kushwaha, Singh et al. 2008), and one calmodulin-like gene, most similar to the *AtCML24*

(Ma, Smigel et al. 2008) were found. Interestingly, three *Arabidopsis* SIP4 orthologs (SOS3 kinase-interacting protein 4 or CBL-interacting protein kinase 11 (CIPK11), also characterized in tobacco as ACRE216 - Avr9/Cf-9 rapidly elicited protein 216) (Durrant, Rowland et al. 2000; Navarro, Zipfel et al. 2004) and an ortholog of the *Arabidopsis* CBL-interacting protein kinase 5 (CIPK5) were also found, suggesting an important role for protein phosphorylation and calcium signaling during sexual reproductive development. Of the protein kinases modulated during embryogenesis, only one coded for a receptor-like kinase *ScORK11* (Germain, Rudd et al. 2005). Interestingly, from the EST pool that was used to make the cDNA microarray, we had previously isolated 30 different RLKs with 28 being predominantly expressed in ovary tissues or young developing fruits, and 23 being transcriptionally induced following fertilization (Germain, Rudd et al. 2005). This discrepancy highlights the different sensitivity of the methodologies used, e.g. microarray analyses (this study) vs. quantitative RT-PCR analysis (Germain, Rudd et al. 2005). A shaggy-like kinase gene similar to the *Arabidopsis* *ATSK41* (Benschop, Mohammed et al. 2007), an IRE-Like AGC kinase gene (Pislariu and Dickstein 2007) and an ortholog of the *Arabidopsis* RAB GTPase homolog B1C (Moore, Diefenthal et al. 1997) were also found. Most of these have been previously shown to be involved in various stress responses and none had been shown to play a role in embryogenesis. Considering the high number of differentially expressed genes (100/955) classified as involved in defense and/or stress response during all stages of embryogenesis, this also emphasize their potential roles in response to pollination and during reproductive development.

Several genes implicated in embryonic patterning were found in the first two major stages. Amongst these, PROTODERMAL FACTOR 1 (*PDF1*) and TOPLESS-RELATED 1 (*TPR1*) were up-regulated in the early and middle stages, respectively. *PDF1* is a predicted cell wall protein restricted to the protoderm of the embryo following tangential divisions between the 8 and 16-cell stages (Abe, Takahashi et al. 1999) and specifies the first element of the radial pattern (Jenik, Gillmor et al. 2007). Since the *S. chacoense* *PDF1* ortholog shares the same expression pattern as the *Arabidopsis* *PDF1* with an expression

peak at the 16-cell stage (2.24-fold at 8-cell and 3-fold at 16-cell stages) this protein most probably has the same function in solanaceous species as in the brassicaceae. The TPR1 gene is involved in maintenance of shoot fates during *A. thaliana* embryogenesis and in defining the apical pole of embryo (Long, Ohno et al. 2006). Transcriptional activation of this protein in our study suggests that the *S. chacoense* TPR1 ortholog is developmentally regulated during embryogenesis and might also act as a determinant of embryo polarity in solanaceous species.

Many members of the MADS box family are expressed at higher levels during embryogenesis (Lehti-Shiu, Adamczyk et al. 2005). Interestingly, a protein identified as an ortholog of the *A. thaliana* *AGL11/SEEDSTICK* gene was up-regulated during the middle stage. *AGL11/STK* is required for normal development of the funiculus, an umbilical-cord-like structure that connects the developing seed to the placenta, and for dispersal of the seeds when the fruit matures (Angenent, Franken et al. 1995; Pinyopich, Ditta et al. 2003). Furthermore, *AGL11/SEEDSTICK* is also expressed during embryogenesis in ovules as determined from publicly available microarray data (BAR, www.bar.utoronto.ca) with a high activity in stage 3 seeds (globular stage of embryo development). Then its expression decreases during the middle stage and increases again in the late stage of seed development. Rounsley et al. also showed that *AGL11/SEEDSTICK* expression is also maintained after pollination through late seed development (Rounsley, Ditta et al. 1995). MADS-box genes are known to act as homeotic selector genes determining floral organ identity and also as floral meristem identity genes (Golz and Hudson 1999; Bowman 2000; Theissen, Becker et al. 2000; Ng and Yanofsky 2001). Our profiling study highlights the potential role of MADS-box transcription factors during the early stages of reproductive development. Several others studies showed an important differential expression of transcription factors, including MADS-box, from various families during pollination, fertilization and seed development (Girke, Todd et al. 2000; Hennig, Gruissem et al. 2004; Lan, Chen et al. 2004; Sieber, Gheyselinck et al. 2004; Yu, Hogan et al. 2005; Zhang, Feng et al. 2005; Becerra, Puigdomenech et al. 2006; Spencer, Casson et al. 2007).

Biotic and abiotic stress-responsive genes

More than 100 genes out of the 955 differentially expressed genes are classified as potentially involved in defense and/or stress response during all stages. This suggests that these defense-related genes might also function in response to pollination and during embryo development, in addition to their contribution to defense against pathogens (Tung, Dwyer et al. 2005; Nielsen, Lok et al. 2006). Among the activated genes in our dataset, those corresponding to proteins of the subtilase family were induced by two- to 137-fold. An ortholog of the ARA12 Subtilisin-like serine protease showed a two- to 73-fold change in *S. chacoense*. Golldack and colleagues showed by *in situ* hybridization that the ARA12 subtilisin-like serine protease was present at higher level in pistils, ovules and anthers, but also responded to stress and pathogen stimuli (Golldack, Vera et al. 2003). Several other pathogenesis-related proteins were also up-regulated after pollination during embryo development, including proteinase inhibitors, Thaumatin-like protein, PR10, β -1,3-glucanase-like protein and elicitor-inducible chitinases. An important increase in transcript levels, from 2- to 118-fold, of non-specific lipid transfer proteins (nsLTPs) has been found during the middle and late stages. These proteins are member of a superfamily of seed protein called prolamins that, in addition to storage, plays important roles in plant defense responses (Blein, Coutos-Thevenot et al. 2002; Maldonado, Doerner et al. 2002). The nsLTPs have been reported in a number of plants, including solanaceous plants (Trevino and MA 1998), and are involved in lipid transfer and in the formation of a protective covering of cutin and suberin layers over plant surfaces. Proteomics analyses of embryo and endosperm from germinating tomato seeds revealed a high level of nsLTPs in the tomato endosperm suggesting a role in the mobilization of lipids from the endosperm to the embryo and probably in defense against infection during germination (Sheoran, Olson et al. 2005). Recently, Vriezen et al (2009) also reported 54 stress or defense-related genes that were expressed in tomato ovary tissues prior to fertilization with the vast majority (47/54) being down-regulated after fertilization. In our case, in 2 DAP ovaries compared to

unfertilized ovaries, 54 stress or defense-response genes were regulated with 34 being down-regulated. Furthermore, when looking at the whole profile from 2 to 22 DAP, a much more dynamic and variable profile for these genes is observed, precluding any global generalization over the whole time-course. The activation of defense-related genes during embryogenesis is probably due to the fact that the plant protects embryo development by increasing the activation of defense and stress related genes. Alternatively, some of these stress-related genes might exert other functions, as is the case for the POP2 gene that is also involved in pollen tube adhesion and growth (Wilhelmi and Preuss 1996; Palanivelu, Brass et al. 2003) and in oxidative stress response (Sweetlove, Heazlewood et al. 2002), and for the HSP70-1 chaperone, involved in development and abiotic stress responses in *Arabidopsis* (Cazale, Clement et al. 2009). Altogether, this suggests an overlap between fertilization/embryogenesis and stress and defense response pathways. This was also reported by Lan et al. in rice, revealing a cross talk in genetic programs controlling pollination/fertilization and stress responses (Lan, Li et al. 2005).

Identification of stage or transition specific candidate genes during embryo development

To identify stage specific or transition specific candidate gene we used a Volcano Plot analysis to identify genes that were specifically expressed at only one time point during embryogenesis with a FDR ≤ 0.01 and a $\geq \pm 2$ fold cut off. As mentioned before, 4 time points (2, 4, 8 and 16 DAP) had a high proportion of stage-specific or stage-predominant candidates genes. At 16 DAP, when ovules bear mostly heart-stage embryos, 26% of modulated genes were stage-specific and were enriched in up-regulated genes from the signal transduction, transport, and hormone-related genes gene ontology (GO) categories, when compared to the GO profiles of the other time points. Of the genes orthologous to the *Arabidopsis* EMB genes required in the normal embryo development (Tzafrir, Pena-Muralla et al. 2004), six (*EMB* 2171 - 2 DAP, *EMB* 1738 - 4 DAP, *EMB* 2473 - 4 DAP, *EMB* 1473 - 8 DAP, *EMB* 1345 - 16 DAP, and *EMB* 1990 - 16 DAP) were found to be

stage-specific in the Volcano analysis. *EMB 2171* and *EMB 1473* code for the mitochondrial targeted 60S L17 RP and the chloroplastic 50S L13 RP, respectively. *Arabidopsis* mutant plants corresponding to these genes display embryos arrested at the globular stage (<http://www.seedgenes.org/index.html>). These two genes had been previously shown to be highly expressed during early embryo development in *S. chacoense* (Chantha, Tebbji et al. 2007). *EMB 1738* codes for the *CYP51G1* obtusifoliol 14- α demethylase gene, a gene involved in lipid signaling (O'Brien, Chantha et al. 2005). In *emb 1738* plants, two-thirds of the embryos are arrested at the early transition to heart stage (Tzafrir, Pena-Muralla et al. 2004). *EMB 2473/MIRO1* codes for a GTPase required for embryogenesis that also affects pollen mitochondria morphology (Yamaoka and Leaver 2008). *MIRO1* mutants display embryos arrested at the zygotic to the 4-cell stage. *EMB 1345* codes for a WD40 protein, similar to the CIA1 protein involved in iron/sulfur protein biogenesis (Balk, Aguilar Netz et al. 2005), that interacts with the Willm's tumor suppressor protein WT1 (Johnstone, Wang et al. 1998). In *emb 1345* mutants, only 3% of the analyzed plants displayed globular embryos while the remaining plants had no detectable embryos (<http://www.seedgenes.org/index.html>). The *EMB 1990* gene codes for an chloroplastic putative integral membrane protein (Zybailov, Rutschow et al. 2008). In *emb 1990* mutants, two-thirds of the embryos are arrested at the globular stage while 13% have a cotyledon terminal phenotype (<http://www.seedgenes.org/index.html>).

Two families of auxin-regulated genes (the *Aux/IAA*, and *GH3* families) have been identified among the transcripts that were specifically found in 16 DAP heart-stage embryos. Auxins are important signaling molecules involved in many developmental processes in plants. Identification of embryo-defective mutants affected in the transport or the auxin signaling pathway indicates that auxins coordinate the organization of the embryo by providing positional information (Weijers, Benkova et al. 2005). During embryogenesis, auxin is particularly important in the specification of the apical cell after the first zygotic division (Friml, Vieten et al. 2003), the formation of the root meristem from the hypophysis (Jürgens 2001; Jürgens 2003; Weijers, Schlereth et al. 2006), and the establishment of

bilateral symmetry (Zimmerman 1993). Apical-to-basal transport of the hormone auxin is initiated at the early globular stage and plays a key role in regulation of many aspects of embryonic pattern formation in plant (Hadfi, Speth et al. 1998; Chen, Ullah et al. 2001). In dicots, auxin is first found in the endosperm and only later is it detectable in the embryo itself with a special distribution starting with a maximal accumulation in the apical cell until the 32-cell-embryo stage. At later stages an inverse pattern of auxin maxima is observed (Eeuwens and Schwabe 1975; Friml, Vieten et al. 2003; Tanaka, Dhonukshe et al. 2006). Amongst the auxin-regulated genes found in our transcriptomic analysis, we noticed the up-regulation of the *GH3* gene, *YDK1* (*YADOKARI* 1). Takase et al (2004), found a dwarf mutant, named *ya do Kari 1-D* (*ydk1-D*), which had a T-DNA insertion proximal this *GH3* gene. The *ydk1-D* mutant is dominant and has a short hypocotyl, a short primary root, reduced lateral root number, and reduced apical dominance, suggesting that *YDK1* may function as a negative component in auxin signaling by regulating auxin activity (Takase, Nakazawa et al. 2004). A second gene of interest is *IAA13*, a member of the auxin response factors family which is required for the axialization of the embryo (Jurgens, Torres Ruiz et al. 1994; Przemeck, Mattsson et al. 1996; Hardtke and Berleth 1998; Hamann, Mayer et al. 1999; Hamann, Benkova et al. 2002; Weijers, Benkova et al. 2005). Weijers et al. showed that stabilization of BDL/IAA12 or its sister protein IAA13, prevents MP/ARF5-dependent embryonic root formation. A dominant mutation that renders IAA13 insensitive to auxin-dependent degradation results in elimination of embryonic axis: the cell at the base of the proembryo divides abnormally and never elongates or become organized in files. The seedlings produce a short peg in place of the hypocotyl and root and also show fused cotyledons with reduced vasculature. *IAA13* is initially expressed in the apical daughter of the zygote and in all cells of the proembryo, but it becomes restricted to the provascular cells by the midglobular stage (Weijers, Benkova et al. 2005). Although the shoot apical meristem (SAM) gradually develops during embryogenesis, it appears as a distinct histological entity somehow late during embryogenesis (Barton and Poethig 1993), around the time where we observed peak expression of numerous auxin-related genes.

Conclusion

Our analysis provides the first study, to our knowledge of the transcriptional program that takes place during the early phases of plant reproductive development in a solanaceous species, including all embryogenesis steps. We used a comparative expression profiling strategy between fertilized and unfertilized ovules to provide insight into the embryo transcriptome in *S. chacoense*. Several potential regulators of fertilization and early seed development have been identified. We identified 1024 genes (955 genes were specifically expressed in ovules tissues when compared to others tissues) that were differentially regulated during these developmental stages, along with many highly stage-specific genes. Although the biological function of most genes remains to be determined, the identification of genes involved in reproductive processes in solanaceous species that produces embryos much more slowly than model species like *A. thaliana*, will enable the selection of stage-specific genes that will deepen our understanding of complex stage transition processes as well as pinpoint potential targets for improving yield and seed quality by conventional breeding or biotechnological approaches.

Acknowledgements

We thank Gabriel Téodorescu for plant care and maintenance. F. Tebbji was the recipient of a Ph. D. fellowships from the Fonds Québécois de la Recherche en Nature et Technologie (FQRNT). The Natural Sciences and Engineering Research Council of Canada (NSERC), FQRNT, and the Canada Research Chair program are also acknowledged for their financial support (D. P. Matton).

Chapitre 2.

Pollination type recognition from a distance by the ovary is revealed by a global transcriptomic analysis.

By Faiza Tebbji^{1,2}, André Nantel², and Daniel P. Matton¹.

¹Institut de recherche en biologie végétale, Université de Montréal, 4101 rue Sherbrooke est, Montréal, QC, Canada, H1X 2B2. ²Institut de recherche en biotechnologie, Conseil national de recherches du Canada, 6100 Avenue Royalmount, Montréal, QC, Canada, H4P 2R2.

Keywords: Interorgan signaling, compatible pollination, incompatible pollination, interspecific pollination, global transcriptomic analysis, ovule, pollen-pistil interactions.

Abstract

Sexual reproduction in flowering plants involves intimate interactions between the growing pollen tube and the female reproductive structure. These interactions start immediately after pollen landing on the stigma and continue during the pollen tube journey through the style and the ovary. Thus, well before fertilization, genes in the gynoecium are affected by the growing pollen tubes. Genes activated at a distance in the ovary before pollen tubes arrival represent one class of such genes. Using a global transcriptomic approach, expression profiles obtained from compatible (SC), incompatible (SI), semi-compatible (SeC) and interspecific (IS) pollinations revealed that these pollinations are perceived differently from a distance by the ovary. As the pollen tubes grow through the style, more and more genes became specific for each pollination type, although even early on, when no difference could be observed in pollen tube growth rates, each pollination type already displayed a specific signature of transcribed genes. Wounding experiments as well as methyl jasmonate treatment were also conducted to determine if transmitting tissue cell death caused by pollen tube growth in the style could also activate gene expression at distance in the ovary. Our data suggest that pollen tube growth in the style is at least partially perceived as a wounding aggression, and that a SI pollination is more akin to a wound response than the other pollination types tested, suggesting similarities in the signaling pathways controlling pollen recognition and stress responses. Similarly to what is observed in plant-pathogen interactions, our analysis reveals that pollination types are specifically recognized in the style and that this information is relayed from a distance to the ovary ahead of fertilization. We thus propose that pollen-borne compounds and/or the outcome of specific pollen-pistil interactions produce pollen-associated molecular patterns (PoAMP) that represent the diversity of pollen-type signatures.

Introduction

In angiosperms, sexual reproduction is initiated by pollen landing on the stigma papillae. After hydration, pollen grains produce a tube that grows through the internal tissue of the carpel, guided by physical as well as chemotropic cues originating from both the style and the ovary to finally deliver its two sperm cells to the female gametophyte (recently reviewed in (Berger, Hamamura et al. 2008). One sperm cell fuses with the egg cell forming the zygote while the second one fuses with the central cell forming the endosperm, which surrounds and provides nutrients to the developing embryo. From the onset of pollen grains landing on a receptive stigma surface until effective fertilization, multiple interactions are initiated and a complex and intricate cross talk between the pollen and the pistil is established (Hiscock and Allen 2008). The decision to accept or reject the pollen can be made at the stage of pollen capture and adhesion, as found in species expressing sporophytic self-incompatibility (SSI), such as in the Brassiceae family (Rea and Nasrallah 2008). In species expressing gametophytic self-incompatibility (GSI) systems, such as in the Papaveraceae and in the Solanaceae, pollen tube recognition and rejection occurs either soon after pollen germination (Wheeler, Vatovec et al. 2010) or later on during pollen tube growth in the transmitting tissue of the style (McClure 2009), respectively. Being highly specialized structures, pollen (Becker, Boavida et al. 2003; Honys and Twell 2003; Pina, Pinto et al. 2005; Wang, Zhang et al. 2008), stigma/style (Swanson, Clark et al. 2005; Tung, Dwyer et al. 2005; Li, Xu et al. 2007; Quiapim, Brito et al. 2009) and ovary (O'Brien, Chantha et al. 2005; Yu, Hogan et al. 2005; Peiffer, Kaushik et al. 2008; Vriezen, Feron et al. 2008; Tebbji, Nantel et al. 2010), all express a specific transcriptome.

During pollen-pistil interactions, continuous intimate contact and concomitant multiple signal exchanges are likely to modulate these transcriptomes. Indeed, numerous studies have reported cases where pollination-modulated genes were isolated from the interacting tissues, for example, the HT-B and S-RNAses stylar-expressed genes involved in self-

incompatibility (O'Brien, Kapfer et al. 2002; Liu, Morse et al. 2009); genes involved in phytohormone biosynthesis (Llop-Tous, Barry et al. 2000; Sanchez and Mariani 2002; Weterings, Pezzotti et al. 2002); as well as genes involved in various biological processeses and modulated during pollen-pistil interactions either in the stigma or style (Wang, Wu et al. 1996; Li and Gray 1997; van Eldik, Reijnen et al. 1997; Lantin, O'Brien et al. 1999; Pezzotti, Feron et al. 2002; Weterings, Pezzotti et al. 2002; Wang, Zhang et al. 2008). Only a few large scale transcriptomic studies have addressed this issue. For example, a study in rice pistils following pollination was conducted but could not clearly separate the contribution of pistil vs. pollen genes or if the modulated genes were pollination or fertilization modulated (Lan et al., 2004). In an other study, influence of the stigma and style on the pollen tube transcriptome was measured through a global gene expression profile comparison using excised pollen tubes growing out of a cut style in a semi *in vivo* system (Qin, Leydon et al. 2009). This analysis revealed major differences between the *in vivo* and *in vitro* grown pollen tubes transcriptomes, and confirmed the dynamic nature of pollen-pistil interactions prior to fertilization.

In the abovementioned studies, the modulated genes were isolated from the tissues in direct contact, but what goes on in distal structures or organs such as the ovules before pollen tubes arrive? Long-distance signaling during plant reproduction has been described almost 150 years ago with the discovery of pollination-induced ovule maturation in orchid species (Hildebrand 1863; Treub 1883; Guignard 1886). In most orchids, female gametophyte development is incomplete before pollination and pollination itself regulates ovule development and gametophyte initiation, in preparation for subsequent fertilization (O'Neill, Nadeau et al. 1993; Zhang and O'Neill 1993; O'Neill 1997). In numerous species, pollination is also known to affect various physiological processes including changes in flower pigmentation, senescence and abscission of floral organs, as well as growth and development of the ovary (reviewed in (O'Neill 1997). Some of the genes modulated from a distance following pollination are activated well before pollen tubes reach the ovules. These genes must therefore react to cues other than fertilization and some of these cues are

generated during pollen tube growth in the transmitting tissue of the style, either from the pollen itself, from the interaction between the pollen and the pistil, or from cell death in the transmitting tissue of the style that occurs during pollen tube growth (Wu and Cheung 2000). How precisely can the ovary interpret pollination from a distance in preparation for fertilization? Is recognition generic or sufficiently specific toward various pollination types to produce a distinctive response? To address these questions we have used a global transcriptomic approach with a 7.7K cDNA amplicon array representing roughly 6500 ovule-expressed unigenes (Germain, Rudd et al. 2005; Tebbji, Nantel et al. 2010) in the self-incompatible wild potato species *Solanum chacoense* Bitt. Expression profiles obtained from compatible (SC), incompatible (SI), semi-compatible (SeC) and interspecific (IS) pollinations as well as from wounded styles revealed precise and specific discrimination between pollination types from a distance in the ovary.

Materials and Methods

Plant materials and pollination conditions

The self-incompatible (SI) wild potato species *Solanum chacoense* ($2n=2x=24$) was greenhouse grown with an average photoperiod of 14-16 h per day. The genotypes used were originally obtained from the USDA Agricultural Research Service, NRSP-6 Potato Genebank (Potato Introduction Station, Sturgeon Bay, WI, USA). Plant material was collected from female progenitor, *S. chacoense* genotype G4 (S_{12} and S_{14} SI alleles) (Van Sint Jan, Laublin et al. 1996). To access the impact of pollination-related events, different genotypes were used as pollen donor. For fully compatible pollinations, *S. chacoense* genotype V22 (S_{11} and S_{13} SI alleles) was used to pollinate *S. chacoense* genotype G4 (S_{12} and S_{14} SI alleles). For fully incompatible pollinations, *S. chacoense* G4 was selfed. For semi-compatible pollinations, *S. chacoense* PI230582 (S_{13} and S_{14} SI alleles) was used. For interspecific pollinations, pollen from the self-incompatible *Solanum microdontum* (PI500041 from NRSP-6 Potato Genebank) was used. Control pollinations to detect and

eliminate touch-induced genes were accomplished by gently touching the stigmas with sterile 100 µm zirconia/silica beads (Biospec Products Inc., Bartlesville, OK, USA). Touch induced genes were subtracted from all subsequent analyses. For wounding experiments, the upper region of the style was slightly crushed with small forceps as described previously (Lantin, O'Brien et al. 1999). For methyl jasmonate treatment, 100 µl of 0.1M MeJA solution in methanol (MeOH) was added to a piece of Whatman paper suspended over the plant in a closed chamber of 10L volume. As controls, untreated plants in closed chambers and plants treated with 100 µl of MeOH were used (Lantin, O'Brien et al. 1999).

RNA isolation and microarray experimental Design

Ovules were collected at 6, 24 and 48 hours after each treatment and used for RNA extraction and probe preparation. All samples for RNA preparation were quick-frozen in liquid nitrogen and ground to a powder with a mortar and pestle. Total RNA was extracted using the TRIzol® Reagent according to the manufacturer's instructions (Invitrogen, Burlington, ON, Canada). The yield and purity of RNA were assessed by determination of absorbance at both 260 nm and 280 nm. RNA was only used when the ratio $\text{Abs}_{260 \text{ nm}}/\text{Abs}_{280 \text{ nm}}$ was higher than 1.7. RNA integrity was checked by both agarose gel 1% and with the RNA 6000 Nano Assay Kit and the Agilent 2100 Bioanalyzer. RNA from unfertilized ovules served as control.

To evaluate the reliability of the hybridization experiments, to detect the sensitivity limit and to have an additional controls for balancing the intensities of the two channels, several control elements were arrayed on the slides, including buffer only spots, and exogenous DNA with different dilutions (Undiluted, 1:2, 1:4, 1:8 and 1:16 dilution) from *Candida albicans* (*ECE1*, Extent of Cell Elongation gene). For each time point four independent biological replicates were produced. To estimate reproducibility and to produce control data for statistical analysis, a large number of unfertilized ovules were isolated and separated in seven independent control groups. RNA from randomly selected pairs of control was hybridized on six microarrays.

cDNA microarray preparation, preparation of fluorescent probes and hybridization

PCR products were resuspended in 10 µl of 50% DMSO and arrayed from 384 well microtiter plates onto UltraGAPS™ slides (Corning incorporated, Corning, NY, USA). A total of 7741 ESTs spotted in duplicate and a variety of control including buffer only spots and a dilution series of *Candida albicans* pEce1 plasmid were arrayed in a 770 mm² area of the UltraGAPS™ slides.

Thirty (30) µg of total RNA, 1.5 µl oligo (dT)₂₁ (100 pmol/µl), and water to a volume of 36 µl was denatured at 65°C for 10 min and cooled to room temperature for 5 min. The reverse transcription reaction was performed at 42°C for 2 h after addition of 3 µl dNTP-minus dCTP (6.67 mM each), 1 µl dCTP (2 mM), 4 µl DTT (100 mM), 8 µl 5× first strand buffer (Invitrogen), 2 µl of either cyanine 3-dCTP (1 mM) or cyanine 5-dCTP (1 mM; Perkin Elmer-Cetus/NEN, Boston, MA, catalog # NEL999) and 2 µl of SuperScript II (200 units/µl, Invitrogen). After incubation at 42°C, 0.05 units each of RNase A and RNase H (Invitrogen) were added and the reaction mix was incubated at 37°C for 30 min. The probes were then purified using CyScribe GFX Purification Kit (GE Healthcare Bio-Sciences Inc., Baie d'Urfé, Québec, Canada) according to the manufacturer's instructions. Incorporation efficiency of the CyDye probes was assessed using the ND-1000 Nano drop spectrophotometer (NanoDrop, Wilmington, DE, USA). In general, optimal amounts are 20 pmol of dye incorporated with an incorporation efficiency of between 20-50 labeled nucleotides per 1000 nucleotides. Probes were then air-dried.

Slides were prehybridized at 42°C for at least 1 hour, with 50 µl of a solution containing 5× SSC, 0.1% SDS and 1% BSA. The two labeled cDNA preparations were pooled together, and mixed with Dig Ease Hybridization buffer (Hoffmann-La Roche Limited, Mississauga, ON, Canada) to a volume of 50 µl, also containing 2.5 µl tRNA (10 mg/ml; Baker's yeast, Roche Applied Science) and 2.5 µl of Sonicated Salmon Sperm DNA (10 mg/ml; Invitrogen). The hybridization solution was heat denatured at 95°C for 3 min, cooled to room temperature, and applied onto the DNA microarray slides for an

overnight hybridization at 42°C. To account for the possibility of dye bias, half of the hybridizations were performed in the Cy3/Cy5 configuration, and half in the Cy5/Cy3 configuration. The microarray slides were covered with a 24 × 60-mm glass coverslip (Fisher Scientific, Ottawa, ON, Canada). During all hybridization steps the hybridization chamber was kept at high humidity level. Immediately before hybridization, the DNA microarray slides were washed twice with 0.1× SSC at room temperature for 5 min and once with water for 30 sec and centrifuged at 800 rpm for 3 min. The DNA microarray slides were kept dry for a minimal amount of time before hybridization. Afterward, slides were completely immersed in a large volume of washing buffer, and the coverslips were carefully removed before washing twice for 10 min at 42°C with 1× SSC, 0.1% SDS, twice for 10 min at 37°C with 0.1× SSC, 0.1% SDS, and finally, with quick consecutive washes in three 0.1× SSC baths. DNA chips were air dried and stored protected from light until scanning.

Microarray scanning and data analysis

The DNA microarray slides were scanned with a ScanArray Lite microarray scanner (Perkin Elmer-Cetus, Wellesley, CA; version 2.0) at 10- μ m resolution. The fluorescence intensities were quantified with QuantArray software (Perkin Elmer-Cetus; versions 2.0 and 3.0). Microarray data normalization and analysis was performed in GeneSpring GX software version 7.3 (Agilent Technologies, Santa Clara, CA, USA). Raw intensities were normalized with a Lowess curve using 20.0% of the data to fit each point. To identify transcripts with a significant change in abundance, the fluorescence ratios from each time point were compared to the fluorescence ratios from 6 control hybridizations using the volcano analysis. We selected genes with a p-value ≤ 0.05 and further restricted the lists to transcripts whose change in abundance was ≥ 1.5 -fold. The data discussed in this publication have been deposited in NCBI's Gene Expression Omnibus (Edgar et al., 2002) and are accessible through GEO Series accession number GSE21552.

(<http://www.ncbi.nlm.nih.gov/geo/query/acc.cgi?acc=GSE21957>). Gene annotation was based on blastX with e value cut-off of 10^{-10}

Pollen Tube Growth Assays and Aniline Blue Staining

Flowers were collected 6, 8 and 12 h after pollination and fixed in a 3:1 ethanol/glacial acetic acid solution overnight. Pistils were dissected and washed twice with water and then softened in 8 M NaOH one hour at 60 °C. The pistils were then washed three times in sterile distilled water, stained with 0.1% aniline blue in K₃PO₄ buffer (pH 7.5) and slightly squashed between a slide and a coverslip. Pictures were taken on a Zeiss AxioImager M1 fluorescent microscope equipped with an AxioCam HRc camera.

Results

Pollination types have been previously shown to differentially affect steady state mRNA levels of some specific genes, principally at the site of interaction, in the transmitting tract of the style. For example, in species expressing a gametophytic self-incompatibility breeding barrier (O'Brien, Bertrand et al. 2002; Feng, Chen et al. 2006; Liu, Morse et al. 2009), compatible and incompatible pollinations have an opposite effect on the transcript level of genes involved in pollen tube rejection, such as the S-RNases. In numerous species, pollination affects many other aspects of flower development including perianth senescence and floral pigmentation. In some species, pollination has also been shown to regulate the development of the female gametophyte, the ovary, and of apomictic embryogenesis (reviewed in (Zhang and O'Neill 1993; O'Neill 1997). In most cases, these effects have been investigated at the morphological and physiological levels, and interorgan modulation of gene expression at a distance from the interaction site has only rarely been reported during pollen-pistil interactions (Lantin, O'Brien et al. 1999). To determine on a more global scale if interorgan communication during pollen-pistil interactions is a widespread phenomenon and involves more than just a few specialized genes, we used a 7.7K cDNA microarray comprising ~6500 ovule-derived unigenes from *Solanum chacoense*, a self-incompatible wild potato species (Germain, Rudd et al. 2005), to conduct gene expression analyses through cDNA microarray hybridizations. Profiles obtained from compatible (SC), incompatible (SI), semi-compatible (SeC) and interspecific (IS) pollinations as well as from wounding treatments were all analyzed using the same minimal expression level criteria (fold change $\geq \pm 1.5$, $p < 0.05$).

Comparison between different pollination types reveals different signal perception

To understand how ovules perceive and discriminate between pollination signals during pollen tube growth in the transmitting tract of the style, an experimental design was set up to compare pollination types, including compatible (SC), incompatible (SI), semi-

compatible (SeC) and interspecific (IS) pollinations against unpollinated ovules (UO). Firstly, a time course of pollen tube growth *in vivo* in the style was performed ([Figure 1](#)). From the *in vivo* pollen tube growth curves ([Figure 1](#)), two obvious patterns can be clearly observed. For conspecific compatible pollinations (SC and SeC), pollen tube growth is fairly slow (~125 µm/h) until tubes reached roughly the mid-style region around 24 HAP. From this time onward, until pollen tubes exit the style to reach the apical portion of the ovary, the mean speed reached ~300 µm/h. Compared to this biphasic growth pattern, pollen tubes in SI or IS pollinations have a more steady but slower monophasic growth pattern. Although most of the SI pollen tubes stop before they reach half the length of the style, a few continue their growth but have mostly plateaued from 24 HAP. Pollen tubes from a heterospecific but compatible pollination, e. g., that are not stopped by the SI reaction as they share different S-alleles, but still facing suboptimal growth in the heterospecific style (incongruity), have a slow but steady monophasic growth pattern, at least during the time-course studied, ultimately leading to later fertilization than conspecific pollen.

Since most pollen tubes during an incompatible pollination are already arrested mid-style, around 24 hours after pollination (HAP), this time point was chosen as our reference time. Compatible pollen have not yet reached the ovary as they normally emerge from the end of the style around 28-30 HAP and reach the first available ovules around 36 HAP to effect fertilization. A late time point, 48 HAP, was also selected to determine pollination effects at a distance in the ovary for pollinations that did not reach the ovules (IS) and for comparison with the other abiotic treatments (see below). More critical was the selection of the earliest time point when all pollinations could be considered equal. Pollen tube growth was thus closely monitored after manual pollination and aniline blue staining of the styles ([Figure 1](#)). All four pollination types germinated equally and had undistinguishable growth until 6 HAP where they all had reached ~1.5 mm in length. As early as 8 HAP, significant tube length differences could be observed between the four pollination types and, by 12 HAP, these differences were clearly accentuated.

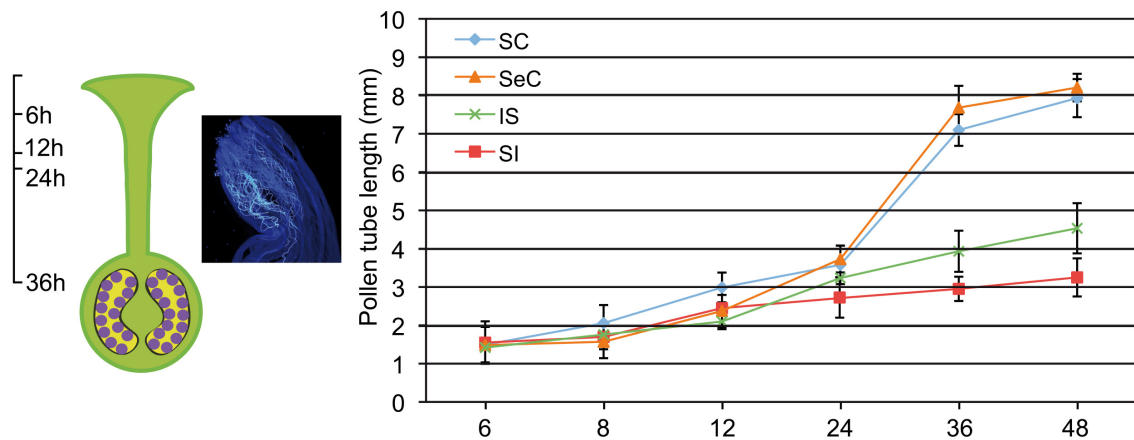


Figure 1: Pollen tube growth measurements after manual pollination and aniline blue staining of the styles from 6 to 48 hours after pollination. Pollen tube growth were measured in 4 different pollination types including compatible pollination (SC), incompatible pollination (SI), semi-compatible pollination (SeC) and interspecific pollination (IS). All the observations and measurements were taken using a fluorescent microscope.

To determine if the ovary could accurately discriminate between pollination types from a distance, irrelevant of the outcome of the interaction and before any visible differences in pollen tube growth, 6 HAP was chosen as the first time point to be evaluated.

Early pollination responses in the ovary

At 6 HAP, 125 genes showed a statistically significant change in abundance at a distance in the ovule in compatible (SC) pollinations, while 90 genes were modulated after incompatible (SI) pollinations. After the subtraction of the touch-modulated genes, 61 and 63 genes were specific to SC and SI reaction, respectively ([Figure 2](#)). From them, 38 transcripts were common and co-regulated between the two pollination types, representing A significant overlap (p value = 4.2e-70). Although more than half (~60%) the genes co-regulated at a distance were common in 6 HAP SI and SC pollinations, already a differential response could be observed in the ovary transcriptome with 23 and 25 genes specifically induced in SC and SI pollination, respectively. In terms of functional categories in the SC/SI common gene pool, genes corresponding to stress responses were the most abundant (26.3%, [Dataset S1](#)).

In the semi-compatible pollination (SeC), 120 genes were modulated at a distance in the ovary, roughly corresponding to the sum obtained from the SC and SI pollinations ([Figure 2](#)). When comparing the SeC pollination with the previous two profiles, 42 (41 co-regulated, p value = 7.5e-65) and 44 (43 co-regulated, p value= 1.5e-68) genes were in common with SC and SI, respectively, corresponding to 2/3 of the genes modulated in SC or SI pollinations. Globally, 32 genes (31 co-regulated) were common between the three pollination types, of which 1/3 corresponded to stress-related genes ([Figure 2](#) and [Dataset S1](#)).

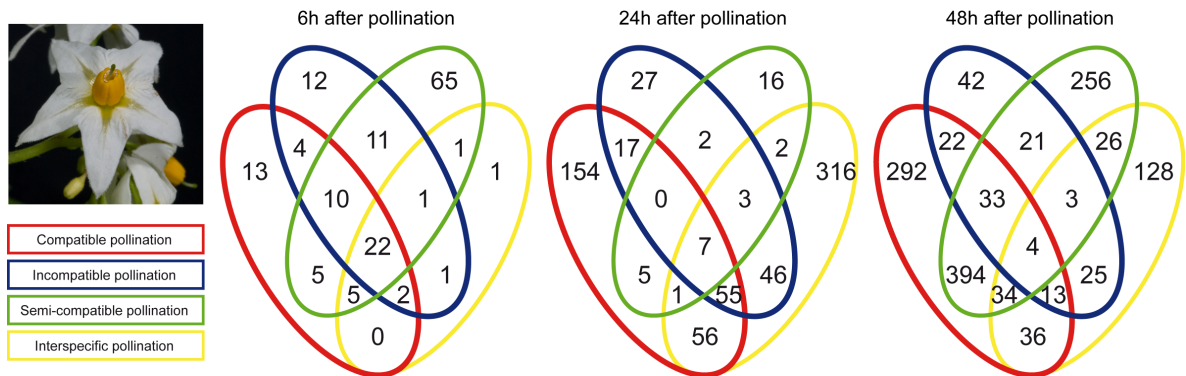


Figure 2: Venn diagram analysis of regulated genes at 6, 24 and 48 hours after pollination between compatible pollination (red), incompatible pollination (blue), semi-compatible pollination (green) and interspecific pollination (yellow).

These data suggest that, at 6 HAP, the ovary mostly perceives the signal from a SeC pollination as the sum of SC and SI pollinations, which indeed it is, although, as for the SC and SI pollinations, SeC pollination specific genes are already found at 6 HAP.

Next, the effect of insterspecific pollination (IS) was tested. To minimize incongruity problems we chose not to use pollen from another solaneceous genera, like *Nicotiana*, but focused on a closely related self-incompatible species, *Solanum microdontum*, that had been shown to make fertile hybrids with *S. chacoense* (Brucher 1953). This was further confirmed using two different *S. microdontum* accessions (PI 473171 and PI 500041, Lafleur, E. and Matton D. P., unpublished results). When using *S. microdontum* as the pollen donor, only 33 genes were modulated at a distance in the ovary with 29 common (p value = 1.4e-60; 28 co-regulated) genes with the SC pollination, 26 (p value = 4.8e-51; 25 co-regulated) with the SI pollination, and 29 (29 co-regulated) with the SeC pollination ([Figure 2 and Dataset S1](#)). Thus, in IS pollination, two third of the genes modulated (22/33) were common to all pollination types and only one gene was specific at 6 HAP.

Pollination response after completion of the SI reaction

At 24 HAP, the second time point chosen, the vast majority of the incompatible pollen tubes were arrested mid-style while compatible pollen tubes have reached slightly less than half of the style's length ([Figure 1](#)). Compared to 6 HAP, a much higher number of modulated genes were observed in all pollination types except during SeC pollination ([Figures 2](#)). Two hundred and ninety five genes (295) were modulated in SC pollination while 157 genes were modulated in SI pollination. Seventy-nine (79) genes were common to SC and SI pollinations reppresenting a significant overlap (p value = 1.4e-72), and including 70 co-regulated genes. A larger proportion of the modulated genes are now specific to SC (73% or 216/295) or SI (50% or 78/157) pollinations when compared to 6 HAP (SC 38% or 23/61; SI 40% or 25/63). Compared to 6 HAP, this suggests that the two pollination types are now perceived more distinctly with a higher percentage of specific vs.

common modulated genes. This is further supported by the detailed analysis of functional categories enrichment. While the translation, embryonic development-related genes (EMB genes), lipid transport, response to water deprivation, unidimensional cell growth, gibberellic acid and auxin signaling functional categories characterized the SC pollination, the SI pollination was characterized by the expression of stress-related genes including those regulated by ABA and ethylene and a group of abiotic stress-responsive genes (heat stress, osmotic stress, oxidative stress, metallocarboxypeptidase inhibitor) ([Dataset S1](#)). From the phytohormone-related genes found in our dataset, genes involved in the GA regulatory network, including GA-responsive genes and GA biosynthetic enzymes were regulated in SC pollination, suggesting the involvement of gibberellins in pollination-induced responses. This is supported by a microarray analysis of pollination and fertilization responses in rice that also revealed a cluster of genes both regulated by pollination and/or fertilization and GA (Lan, Li et al. 2005).

In semi-compatible pollination, surprisingly only 36 genes were modulated after 24 HAP. Thirteen (13) were common (9 co-regulated) with a SC pollination with p value overlap of 1.7e-10;, 12 were common (6 co-regulated) with SI pollination with p value overlap of 2.7e-12, and 13 were common (8 co-regulated) with an IS pollination (p value=1 e-07). Only 7 genes (3 co-regulated) were common between all pollination types ([Figure 2](#)).

For interspecific pollination, 486 genes were modulated at 24 HAP, a considerable increase compared to 6 HAP ([Figure 2](#)). One hundred and nineteen (119, p value=4.5e-69) were common (95 co-regulated) with SC pollination, 111 were common (p value=1e-100; 106 co-regulated) with SI pollination, and 13 were common (8 co-regulated) with SeC pollination. By comparison with SC, SI, and SeC pollinations, IS pollination showed the largest number (316) of specifically modulated genes at this time point ([Figure 2](#)). Functional categories analysis revealed that, apart from a large group of genes involved in metabolism (21%), stress-related genes represented the second most abundant functional category with 11%. Altogether these data suggest that, compared to 6 HAP, pollination types are definitively perceived as distinct stimuli by the ovary 24 HAP.

Fertilization and late pollination responses at 48 HAP

In *Solanum chacoense*, as in many *Solanum* species, conspecific fertilization takes place from 36 HAP until ~ 48 HAP. The first zygotic division happens only three to four days after pollination while the endosperm has already started to divide (Clarke 1940; Williams 1955). As expected, the highest number of ovule-modulated genes, 828, were isolated from a 48 HAP fully compatible pollination (SC) that lead to fertilization, thus includes a large number of genes regulated immediately following fertilization. Of these, one hundred and forty-seven genes were also modulated before fertilization at 6 and 24 HAP, suggesting a possible dual role for these genes before and after fertilization, during pollination and early embryogenesis ([Figure 3A](#) and [Dataset S2](#)). Profiling of the genes specifically expressed in compatibly pollinated *S. chacoense* ovules showed 56% (34/61) and 68% (201/295) of the genes were down-regulated in pollinated ovules after 6 hours and 24 hours, respectively, suggesting that gene repression in the ovary is a major form of gene regulation during the initial stages of pollination. By comparison many genes were found to be up- or down-regulated after fertilization.

For incompatible pollinations, 163 genes were modulated at 24 and 48 HAP, and although no significant change was observed in the total number of genes modulated, the nature of the modulated genes was strikingly different with 73.6 % (120/163) genes specifically expressed at 48 HAP and 70 % (114/163) specifically expressed at 24 HAP ([Figure 3B](#) and [Table S3](#)). Thus, even although most pollen tubes have stopped growing, the ovary expresses a different early and late response toward SI pollination, suggesting the perception of two different signals. To determine if the late (48 HAP) ovarian response toward SI pollination stems from a distinct signal or is due to a delayed or slowly propagated pollination response, the 120 genes specifically regulated in a 48 HAP SI pollination were compared with 24 and 48 HAP SC pollinations. Of the 295 regulated genes from a 24 HAP SC pollination, only 28 genes were common (p value=3.5e-15) and GO categories showed different functional groups enrichment. The comparison between 48

HAP SC and SI pollinations revealed 72 common genes (p value=1.3e-28). From those, 42 genes were co-regulated (36 down- and 6 up-regulated), representing 26% of SI modulated (163) genes. No functional group enrichment was found but 54 and 77% were common to wound and methyljasmonate modulated genes, respectively (see below), suggesting they correspond to a core of wound-regulated genes due to tube growth in the style.

In the case of SeC pollination, 771 genes were modulated at 48 HAP (Figure 3C and Table S1). As for the SC pollination, fertilization had taken place, as determined by aniline blue staining of the pollen tubes that had reached the ovules (Figure 1) and by the fertilization-induced activation of ribosomal protein synthesis. Steep accumulation of ribosomal protein mRNAs had been previously shown to be a good marker of fertilization (Chantha, Tebbji et al. 2007). As expected, since SeC pollination also leads to full seed set, it shared most of its modulated genes with the SC pollination (465/771, 60%, Figure 2 and Table S1). This is clearly illustrated when comparing expression profiles through hierarchical clustering of the expressed genes, showed in Figure 4. When compared to SC pollination, of the remaining 306 genes specifically regulated at 48 HAP in a SeC pollination, one would expect a high percentage shared with the ones specifically regulated in SI pollination 48 HAP (subtracting the genes already shared between the SI and SC pollination). However, this is not the case since only 24 genes are shared between 48 HAP SeC and SI pollinations, representing 26% of the SI specific genes (Figure 2). This suggests that a SeC pollination is more than the sum of a SC and a SI pollination, as already observed at 6 HAP.

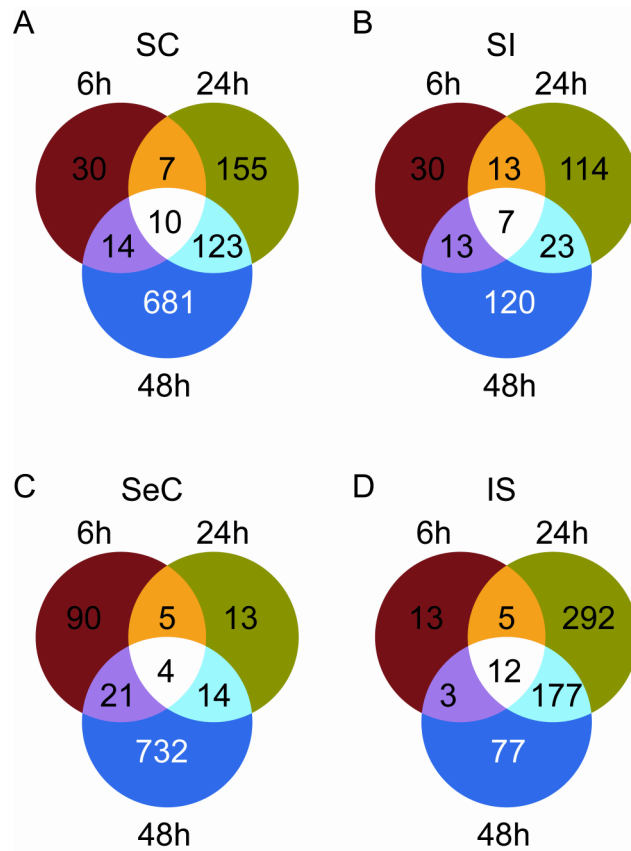


Figure 3: Venn diagram showing overlap between gene lists that show significant changes in transcript abundance at 6, 24 and 48 HAP during: A- compatible pollination (SC). B- Incompatible pollination (SI). C- Semi-compatible pollination (SeC) and D- interspecific pollination (IS).

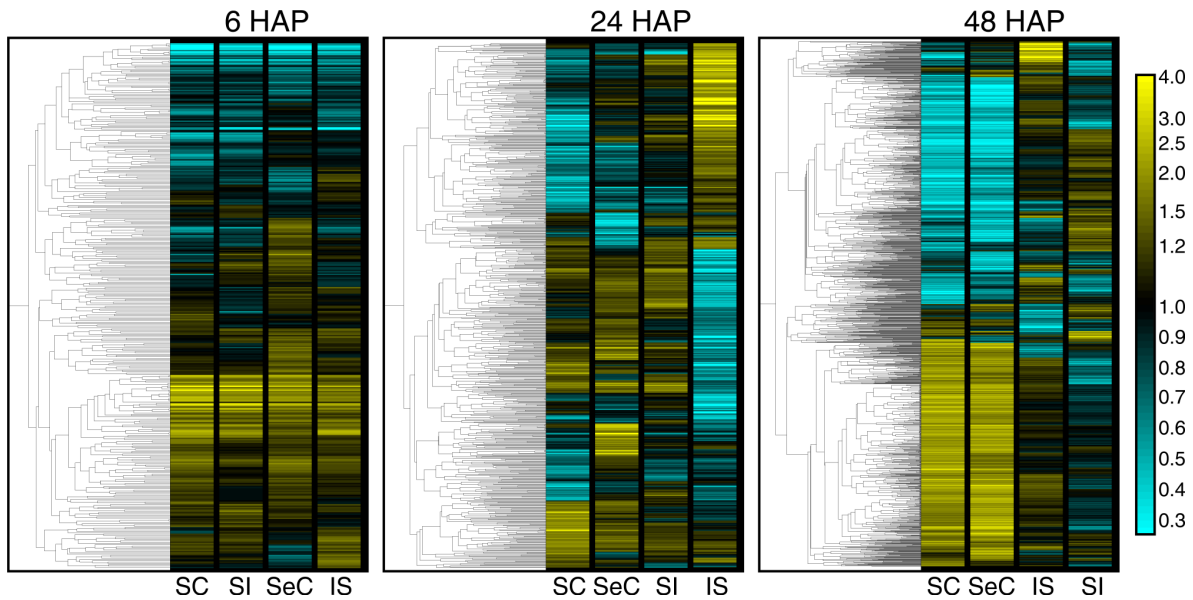


Figure 4: Cluster analysis using unsupervised hierarchical clustering of gene lists that show significant changes in transcript abundance ($P < 0.05$) during compatible pollination (SC), incompatible pollination (SI), semi-compatible pollination (SeC) and interspecific pollination (IS) at 6, 24 and 48 HAP. The analysis was performed using condition tree clustering on all samples. Each row represents a different gene, and each column displays gene expressions at each pollination experiment (SC, SI, SeC, and IS). Each experimental data point is colored according to the change in expression ratio at that time point: data values displayed as yellow and blue represent increased and reduced expression, respectively while data values in yellow are not differentially expressed when compared to unfertilized ovules.

When compared to SC and SeC pollinations, only 269 genes were modulated in IS pollination 48 HAP, a decrease from 24 HAP (Figures 2, 3D and Table S1). Importantly no RP genes were up-regulated at 48 HAP (out of 65 RP genes available on our cDNA microarray), indicating that fertilization had not yet taken place. This was confirmed by aniline blue staining of *S. microdontum* pollen tubes at 48 HAP, showing that most of the tubes had only traveled roughly 60% of the style's length (Figure 1). Interestingly, 70% (189/269) of the genes regulated at 48 HAP were common with the ones expressed at 24 HAP, a situation different from the three other pollination types where little overlap had been observed between successive time points (Figure 3A-C). Since fertilization had not yet taken place 48 HAP in both IS and SI pollinations, the transcriptomic profiles were compared. Of the 163 SI regulated genes, 45 were common (13 co-regulated) with the 269 IS regulated genes (Figure 2). Although *S. microdontum* is not affected by the SI response and viable hybrids can be produced between *S. chacoense* and *S. microdontum*, *S. microdontum* pollen tubes grow considerably slower than do conspecific *S. chacoense* pollen. Although each pollination type produced its own transcriptomic signature and was perceived differently at a distance in the ovary, a common component is the effect of pollen tube growth , which is known to induce cell death in the transmitting tissue of the style along the path of pollen tube growth (Cheung 1996; Wang, Wu et al. 1996). This component is further addressed in the next section with the application of abiotic stresses to the stigma and style.

Effect of stylar wounding on gene expression at a distance in the ovule

To determine if cellular death could also activate gene expression in the ovule from a distance and to what extent it contributes to the transcriptome pattern caused by pollen tube growth, we mimicked cell death by stylar wounding. At 6 HAW (hours after wounding), 70 genes were modulated. We used Venn diagram analysis, to examine possible cross-talk between wounding and different types of pollinations (Figure 5A-F). From wound modulated genes at 6 HAW, 45 genes were common and co-regulated with

those from a SC pollination while 38 genes were common (and co-regulated) with those from a SI pollination, representing 74% (45/61) and 60% (38/63) of their modulated genes, respectively ([Figure 5A](#)). Most of the common genes observed could be classified as being involved in stress and defense responses ([Table S4](#)), including numerous genes involved in protein folding, and the heat shock response, suggesting that early on, pollen tube growth in the style is partially perceived as wounding. At 24 HAW, 101 genes were regulated, a slight increase from 6 HAW ([Figure 5B](#)). Sixty-one (61) and 62 were common and co-regulated with SC and SI 24 HAP pollinations, respectively, representing two third of the wound-modulated genes and 38 genes were common between the three experiments ([Table S4](#)). These included genes related to carbohydrate metabolism, electron transport, transcriptional regulation, stress and defense responses, flavin mononucleotide binding (FMN) binding, Lipid Transfer Protein (LTP and LTP-like), transport, protein folding, calcium ion binding, proteolysis, hormone responsive genes. Compatible pollinations having already effected fertilization 48 HAP, and thus reprogrammed the ovule transcriptome toward embryo and seed development, the late effect of wounding or pollination not resulting in fertilization, e. g. SI pollination, were also compared ([Figure 5C](#)). Of the 163 genes modulated during SI pollination 48 HAP, 40% (66/163) were common with those modulated by wounding 48 HAW (37%, 66/177). These results confirm the suggestion that pollen tube growth in the style is at least partially perceived as a wounding aggression and suggests that SI pollination is more akin to a wound response since 40% of the genes modulated by SI pollination are also modulated by wounding, while only 20% of the genes modulated by SC pollination are wound-modulated. This is also clearly observed when stylar wounding is compared to IS and SeC pollinations ([Figure 5D-F](#), [Table S5](#)). At 6 HAP, 88% of the genes modulated (67% co-regulated) in an IS pollination and 34% (26% co-regulated) of the genes modulated by a SeC pollination are shared with the ones modulated by wounding.

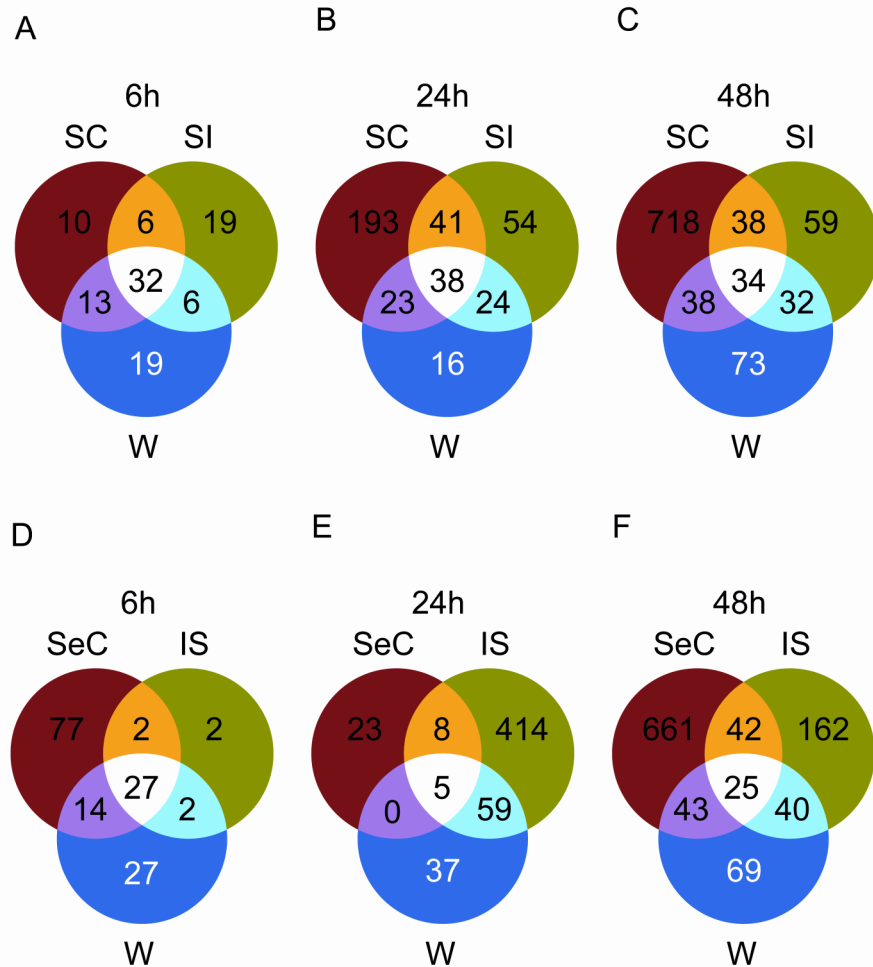


Figure 5: Venn diagram showing overlap between gene lists that show significant changes in transcript abundance during: A- compatible pollination (SC), incompatible pollination (SI), and wounding (W) at 6 HAP/HAW. B- at 24 HAP/HAW., and C- at 48 HAP/ HAW. D- Semi-compatible pollination (SeC), interspecific pollination (IS), and wounding at 6 HAP/ HAW. E- at 24 HAP/ HAW, and F- at 48 HAP/ HAW.

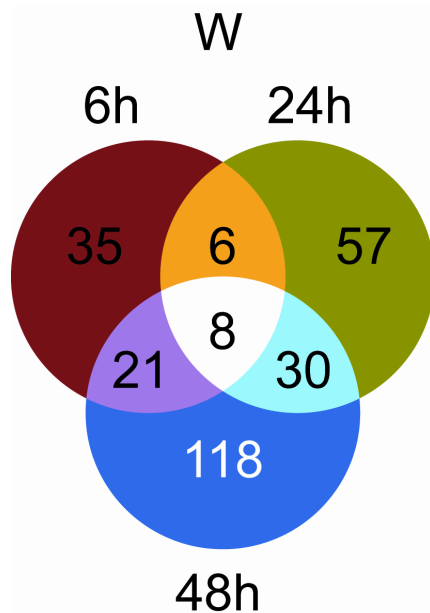


Figure 6: Venn diagram showing overlap between gene lists that show significant changes in transcript abundance during wounding treatment at 6, 24, and 48 HAW.

At 24 HAP, only 6% of the SeC modulated genes and 7% of the IS modulated genes are now shared and co-regulated with 24 HAW ([Table S5](#)). Since IS pollen tubes 48 HAP have not yet reached the ovules, this was also compared to 48 HAW ([Figure 5F](#)). At 48 HAP, 24% (65/269) of the genes regulated (20% co-regulated) in IS pollination are shared with the ones modulated by wounding. This situation is more akin to the one observed in a SC pollination.

Comparing wounding experiments between the three time points revealed an increasing number of specific genes (35 at 6 HAW, 57 at 24 HAW and 118 at 48 HAW) as well as a limited overlap between the time points ([Figure 6](#)). This suggests either the successive modulation of early to late wound-responsive genes through a single wounding event, or the conversion of the primary wounding signal into a late response to wound-induced cell death of the stigma/style region, as observed by slight oxidation and browning of the wounded tissue.

Effect of Methyl jasmonate (MeJA) on gene expression in the ovule

To determine if wound stress hormones could mediate the activation at a distance produced by the wounding effect of pollen tube growth in the style, flowers were treated in a closed chamber with the volatile wound hormone MeJA (Koo and Howe 2009). Since MeJA is used as a diluted solution in methanol and applied to a piece of absorbing paper in the closed chamber, a methanol control was used and subtracted in order to compare MeJA profiles with untreated ovules also collected from a similar closed chamber set-up. Profiles were produced as for the previous experiments with the same three time points 6, 24 and 48 hours after each treatment ([Figure 7](#)). At 6 hours, 416 genes were modulated, including 32, 25 and 32 genes in common with wounding, SC and SI respectively ([Table S6](#)); representing 45.7%, 40.9% and 50.7% of wounding, SC and SI regulated genes, respectively. At 24 hours after MeJA treatment, 599 were differentially expressed in ovules with 95 genes in common with SC pollination (32.2% of SC modulated genes), 66 genes in common with SI pollination (42% of SI modulated genes) and 37 genes in common with

wounding (36.6% of wound modulated genes) ([Table S6](#)). While, at 48 hours after MeJA treated plants, 362 genes were differentially expressed in ovules with 144 genes in common with SC pollination (17.3% of SC modulated genes), 54 common genes with SI pollination (30.5% of SI modulated genes) and 55 genes in common with wounding (31.7% of wound modulated genes) ([Table S6](#)). Although the numbers of genes modulated by MeJA is much higher than the ones obtained following pollinations, these data suggest that the stress hormone MeJA partially mimic the effect of pollination or wounding, at least during early pollination events, suggesting that the activation at distance in the ovule could partially be mediated by this phytohormones.

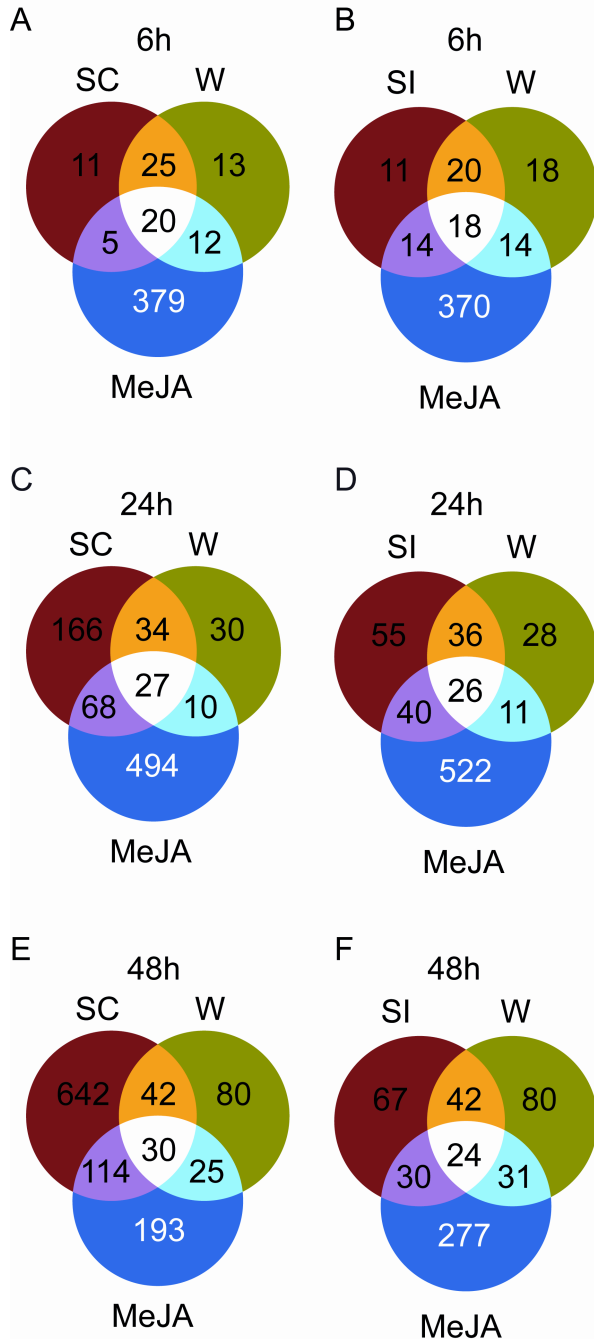


Figure 7: Venn diagram showing overlap between gene lists that show significant changes in transcript abundance during :A- compatible pollination (SC), methyl jasmonate (MeJA), and wounding at 6 hours. B- Incompatible pollination (SI), methyl jasmonate (MeJA), and wounding at 6 hours. C- Compatible pollination (SC), methyl jasmonate (MeJA), and wounding at 24 hours. D- Incompatible pollination (SI), methyl jasmonate (MeJA), and wounding at 24 hours. E- Compatible pollination (SC), methyl jasmonate (MeJA), and wounding at 48 hours. F- Incompatible pollination (SI), methyl jasmonate (MeJA), and wounding at 48 hours.

Discussion

Although numerous studies have been performed to better understand pollen-pistil and pollen-stigma interactions (Lantin, O'Brien et al. 1999; Tung, Dwyer et al. 2005; Yoshida, Endo et al. 2005; Li, Xu et al. 2007; Qin, Leydon et al. 2009; Quiapim, Brito et al. 2009), most focused on direct and close-contact interactions. Here, using a global transcriptomic approach with an amplicon-derived array representing ~6500 ovule-expressed unigenes (Germain, Rudd et al. 2005; Tebbji, Nantel et al. 2010), we addressed the issue of gene modulation at a distance from the interaction site to determine: 1) if pollination type recognition occurs at a distance, perhaps in preparation for fertilization and; 2) if this recognition is generic or sufficiently specific toward various pollination types to produce a unique imprint and thus a unique reaction.

In vivo pollen tube growth assessment

In species that shed bicellular pollen (containing a vegetative and a generative cell), like in the *Solanaceae*, pollen tube growth is generally biphasic (Stephenson, Travers et al. 2003). Phase one is characterized by a period of slow growth and is also termed the autotrophic phase, since pollen can generally germinate and grow in simple synthetic media (although not entirely autotrophic since pollen relies on water and sugars from the stigma and style). Phase two, termed the heterotrophic phase, is characterized by a much faster growth rate, and is spurred by the available nutritional resources from the transmitting tissue of the style. The transition between these two phases generally coincides with the division of the generative cell into two gametes (sperm cells) and, in many species, with the passage through the stigma/style transition, imposing a physical constriction where the pollen tubes must grow (Hormanza and Herrero 1994). Our *in vivo* results confirm this biphasic growth pattern for conspecific compatible pollinations (SC and SeC) with a slow growth phase and a mean speed of ~125 µm/h for the first 24 hours and a fast growth phase with a mean speed ~300 µm/h for the following 12 hours. However, considering the small size of the stigma (~1mm long), the transition from autotrophic to heterotrophic growth

cannot coincide with the passage through the stigma/style zone since the major shift in growth speed occurs at 24 HAP when the pollen tubes have already reached roughly 40% of the style's length ([Figure 1](#)). In species expressing S-RNase-based gametophytic self-incompatibility, like in the *Solanaceae*, this transition zone was also identified as the area with the greatest attrition of incompatible self-pollen tubes (Herrero and Hormaza 1996). Again, this is clearly not the case since numerous SI pollen had reached ~70% of the length of SC pollen by 24 HAP ([Figure 1](#)). In contrast to SC and SeC pollen, SI pollen tubes showed a monophasic slow growth profile, with some tubes continuing their growth until late after pollination but never reaching more than half the style's length. IS pollen also showed a monophasic slow growth profile during the 48h span of our time-course. Considering that without fertilization *S. chacoense* flowers will abscise five to six days after pollination, and that the mean speed of *S. microdontum* pollen tubes between 24 and 48 HAP was ~54 $\mu\text{m}/\text{h}$, to reach the same length as SC pollen at this speed would require another ~64 h (2 1/2 day), suggesting that in IS pollination, a monophasic slow growth would suffice to effect late fertilization (≥ 96 HAP) before flower abscission. The fact that by 48 HAP IS pollen have not effected fertilization and are still midway through the style also account for the large overlap between the genes expressed at 24 and 48 HAP (70%) in IS pollination ([Figure 3D](#)), suggesting the continuous perception of a single pollination event.

Early responses to pollination

At 6 HAP, all pollen types had germinated equally and pollen tubes had reached all ~1.5mm. The comparison between differentially expressed genes in different pollination types showed that ~60% were common and co-regulated between SC and SI. Two-thirds of the expressed genes in SC and SI were in common with those expressed in SeC pollination and the vast majority of the IS regulated genes were also in common to the other pollination types. When placed into GO categories, the most abundant functional grouping in all pollination types corresponded to stress responses, especially wound responses,

suggesting that the early response following pollination corresponds to the perception of a wounding aggression due to the penetration and growth of the pollen tubes. Indeed, this holds true for all different pollinations type tested ([Dataset S1](#)). It has been proposed that the primary pollination signal results from physical contact between the pollen and the stigma, from pollen tube penetration of the stigma (Gilissen 1976; Gilissen 1977; Gilissen and Hoekstra 1984), or from pollen–borne chemical messengers (Hoekstra and van Roekel 1988; Singh, Evensen et al. 1992). A number of potential primary signals have been tested, including the phytohormones ethylene (Singh, Evensen et al. 1992; O'Neill, Nadeau et al. 1993) and auxin (Zhang and O'Neill 1993; O'Neill 1997). Holden *et al.* (2003) have shown that ethylene production by the pistil shortly after pollen germination in *Petunia* accelerates tube growth during the autotrophic phase but not the heterotrophic phase, indicating that the initial phase of tube growth is influenced by the physiology of the pistil (Holden, Marty et al. 2003). Auxin was proposed to be the primary signal by the direct transfer of pollen-borne auxin to the stigma, from where it diffused to distal floral organs and promoted autocatalytic ethylene production throughout the flower leading to perianth senescence (Burg and Dijkman 1967). Considering that the phytohormone content of our four pollen types should be similar and that no hormone-related genes (either related to hormonal regulation, biosynthesis, or catabolism) were found in our data at 6 HAP when compared to the touch experiment, this suggests that the primary signal is related to tissue wounding and cell death, irrespective of the pollen type used. This is supported by the high overlap between the genes regulated by pollination with those regulated by wounding or MeJA treatments at 6 HAP ([Figures 5 and 7](#)).

Mid-style responses to pollination

At 24 HAP, the majority of all pollen tubes have reached 30 to 40% of the style's length, although SC, SeC and IS pollen tubes will continue growth, while SI pollen tubes have been mostly arrested.

Compared to 6 HAP, a much higher percentage of modulated genes was now specific to each pollination type. This is further supported by the distribution of the genes into functional categories. While genes involved in translation, embryonic development (EMB genes), lipid transport, response to water deprivation, unidimensional cell growth, gibberellic acid and auxin signaling functional categories characterized the SC pollination, the stress and defense response, carbohydrate metabolism, proteolysis, transcriptional regulation, protein folding, energy and binding characterized the IS pollination. These data suggest the specific emission of signaling molecules from the various pollen types and/or highly specific perception of the outcome of these different pollen-pistil interactions occurring in the transmitting tract of the style. The implication of primary and secondary signals in the pollination response has been reported in numerous plant species (reviewed in (O'Neill 1997)). The first signal, perceived in the stigma, is generally followed by a subsequent secondary signal that transmits and amplifies the primary pollination signal to distal floral organs. For example, in *Petunia* and some orchids, floral shape alteration implicates the role of secondary messengers that transduce and amplify the primary pollination signal (O'Neill 1997). Phytohormones have been proposed as such secondary signals (O'Neill 1997). At 24 HAP, enrichment in hormone-related genes could be observed in our dataset. Interestingly, a differential hormonal response could be observed between SC and SI pollinations. SC pollination was characterized by the expression of auxin- and GA-related genes while genes involved in ethylene signaling characterized SI pollination. It is possible that the primary and secondary signals in the pollination response are distinct, although it is also possible that a primary wound-related signal is followed by a secondary phytohormone signal that amplifies and specifies the pollination type. The primary pollination signals ethylene and auxin have been extensively evaluated as potential transmissible signals in pollinated flowers. Several studies on auxin translocation were contradictory, with one model of (Burg and Dijkman 1967) proposing that auxin diffused. Although ^{14}C -IAA applied to the stigma was mobilized to the column and labellum, subsequent research indicated that ^{14}C -IAA applied to *Angraecum* and *Cattleya* stigmas

was largely immobile (Strauss and Arditti 1982). However in some plants as *Pinus radiata* and orchids, it was suggested that, following pollination *in vivo*, auxin may diffuse from the germinated pollen tube into the nucellus, thereby triggering the processes which allow ovule and gametophyte development to proceed (Sweet and Lewis 1969; Zhang and O'Neill 1993). At 24 HAP in SC pollination, GA-responsive genes were found to be enriched. Several studies have shown the role of GA in parthenocarpic fruit development. In tomato, auxin and gibberellins are considered key elements in parthenocarpic fruit development. As an increased level of these hormones in the ovary can substitute for pollination and trigger fruit development (Gorguet, van Heusden et al. 2005; de Jong, Mariani et al. 2009).

In our dataset, three up-regulated ESTs in SC pollinations code for members of the alpha-expansin gene family, ATEXP3. Expansins were first identified as a cell wall loosening protein (Brummell, Harpster et al. 1999; Cosgrove 2000; Lee, Choi et al. 2001). Several studies have shown that, besides being involved in cell wall expansion, expansins are also involved in variety of plant processes including growth and ripening of tomato fruits (Rose, Cosgrove et al. 2000), endosperm weakening during tomato seed germination (Chen and Bradford 2000), softening of the fruits during ripening by hydrolysis of cell-wall polymers (Brummell, Harpster et al. 1999) and growth of the pollen tube through the stigma and the style of grasses (Cosgrove, Bedinger et al. 1997; Cosgrove 2000). An orthologue of the *Arabidopsis* AtGA2OX2, a GA signaling gene was found to be up-regulated. It was reported that an increase in gibberellin content after pollination could result from diminished bioactive gibberellin deactivation by GA 2-oxidases (GA2oxs) (de Jong, Mariani et al. 2009). In tomato, five *GA2ox* genes have been characterized and they are all expressed in the unpollinated ovary (Serrani, Sanjuan et al. 2007). However, transcript levels of these genes decreased not early after pollination (5 day old fruits), but transcript content reduction of all of them, mainly of *SlGA2ox2*, was found later (from 10 day after anthesis) suggesting that, during early fruit development, the increase in gibberellin biosynthesis is mainly caused by the up-regulation of *SlGA2ox1* and -2 expression, and not by a reduction of gibberellin deactivation. Both auxin and GA can

induce parthenocarpic fruit growth in tomato, although their possible interaction is not understood. Serrani et al (2008), indicated that the induction of parthenocarpic fruit growth by auxin is negated by GA biosynthesis inhibitors and that auxin induces fruit set by enhancing gibberellin biosynthesis and diminishing gibberellin inactivation, suggesting that auxin acts prior to gibberellin as the early post-pollination/fertilization signal (Serrani, Ruiz-Rivero et al. 2008). Several studies reported that GA might be part of long-distance signal, supported by its detection in phloem and xylem sap (reviewed in (Suarez-Lopez 2005)), and its transport from leaf to shoot apex (King, Moritz et al. 2001). The up-regulation of auxin and GA in the ovary after pollination suggests that these hormones may be part of the long distance signal acting to prepare the ovules for fertilization.

Later at 48 HAP, the highest number of modulated genes (828) was found in fertilized ovules observed in the SC pollination. Of these genes, 147 were also regulated at 6 and 24 HAP before the pollen tubes reach the ovule, suggesting a possible role in preparing the ovule for fertilization. Interestingly, SC pollination was characterized by the regulation of response to water-deprivation genes, indicating that the water plays an important role in pollination. These genes may be associated with a hydraulic signal to establish the gradient of the diffusible signal.

In semi-compatible pollinations, surprisingly only 36 genes were modulated after 24 HAP. At this time, SeC and SC pollen tubes have the almost same length. It is difficult to explain why the number of modulated genes decreased in SeC pollination between 6 and 24 HAP while it increased for all other pollination types. Perhaps either a form of signal interference between this composite SC and SI pollination, and/or a weaker or less statistically significant gene response precluded the identification of modulated genes with sufficient precision. More in depth approaches such as deep sequencing could reveal more subtle transcriptional responses.

For the interspecific pollination, a considerable increase in the number of regulated genes was observed from 6 to 24 HAP ([Figure 3B](#)). The very low number of IS regulated genes at 6 HAP is most probably directly related to the slower growth of IS pollen but once

actively growing in the style, the detection of specific pollen-associated molecular patterns (PoAMP) by analogy to pathogen recognition (Jones and Dangl 2006), led to a dramatic increase of genes modulated at a distance. This response was slightly dampened at 48 HAP since pollen tubes had not yet reached the ovules and had not effected fertilization. As mentioned previously, the large overlap between the genes expressed at 24 and 48 HAP (70%) in IS pollination ([Figure 3D](#)) reflects the fact that, due to its slower growth, IS pollinations perception is most probably perceived as a single continuous pollination event rather than a biphasic process. A large number of IS modulated genes were also in common with those from SC and SI pollinations suggesting that IS pollinations, though perfectly compatible, may leads to some side-effects due to the imperfect match between the pollen and the pistil, often referred to as incongruity (Hogenboom and Mather 1975). This hypothesis is supported by a reduction in seed production in IS pollination compared to conspecific pollinations (E. Lafleur and D. P. Matton, unpublished observations). It would also be of interest to determine the effect of other IS pollination with species presenting either strong unilateral incompatibility, for example *S. bulbocastanum*, and with more closely related species like *S. tarijense*.

For all pollination types, our data showed that, specific genes were found in each point time, suggesting that at least two different signals are perceived in the ovule: an early signal stemming from the initial pollination response (in the stigma) and a late signal, stemming from the cellular damage or elicited by pollen tube breakdown and cellular contens. The ensemble of these specific molecular signal, akin to pathogen-associated molecular patterns (PAMP), are by analogy here termed PoAMP (pollen-associated molecular patterns) ([Figure 8](#)).

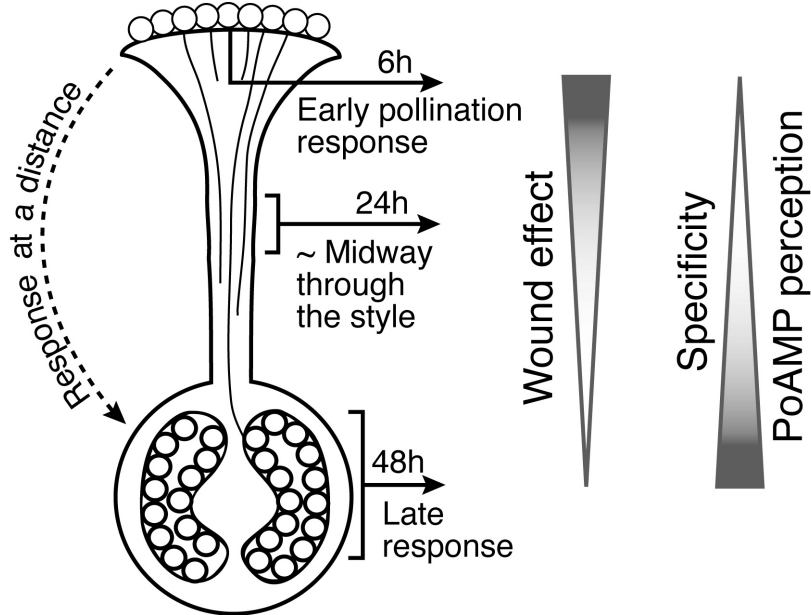


Figure 8: Summary of Pollination and wound effect at a distance in the ovary

Common elements shared by pollination and stress responses

To determine if pollination and wounding relay any common signals to the ovary, all pollinations were compared to stylar wounding at 6, 24 and 48 H. A large number of modulated genes were common and co-regulated between SC and SI pollinations and wounding, suggesting that pollination is at least partially perceived as a wound effect early during pollination (Figure 5 A-C). The deterioration of transmitting tissue cells induced by pollination has been postulated to contribute to pollen tube growth by providing more nutrients and the release of calcium, while other small molecules released from the dead cells have been hypothesized to play a role in pollen tube guidance (Wang, Wu et al. 1996). If cell death in the stylar transmitting tissue caused by the growing the pollen tube is the primary event that triggers gene modulation at a distance in the ovule, then wounding of the style without pollination would also partially produce a similar transcript profile. It has been reported that pollination and wounding induced nearly identical flavonol kinetics and patterns of the accumulation in the outer cell layers and exudates of the stigma (Vogt,

Pollak et al. 1994). Lan et al 2005, reported that 21% of genes regulated by pollination/fertilization were wounding-induced, including several regulatory proteins involved in signal transduction, indicating that the pollination and wounding do share some elements of a common signal transduction pathway (Lan, Li et al. 2005).

For the SeC and IS pollinations, a large number of genes were also shared with the wound effect at 6 HAP. Later at 24 HAP, the specific gene expression signature of SeC and IS pollinations became obvious with only few genes shared between SeC and IS and W. In IS pollination, fewer number of pollen tubes have traveled along the style, thus diminishing the wounding effect. This is reflected in the total number of seeds produced, which is lower than with a conspecific pollination. Thus, in contrast to incompatible pollinations, pollinations leading to fertilization are now clearly perceived as distinct from wounding.

The wounding response at the three time points revealed that a large number of specific genes is modulated at each time point and there is only a weak overlap between the time points ([Figure 6](#)). Wounding is thus not perceived as a single event and that the initial wound signal is either transformed and/or amplified during the time course, with more and more genes modulated at a distance from a single wounding event as time goes on. Wound perception probably involves long distance signals, similar to other developmental and physiological processes (flowering, tuberization, shoot development, leaf development, systemic acquired resistance, etc.). Wounded leaves of tomato and potato plants release systemin, an 18 amino acid peptide that promotes long distance defense response in unwounded leaves by amplifying jasmonate production in the vascular tissue (Ryan and Moura 2002; Ryan, Pearce et al. 2002). Other types of long distance signaling induced by wounding are electrical (Rhodes, Thain et al. 1996; Zimmermann, Maischak et al. 2009).

To explain gene modulation at a distance, many studies have focused on the role of chemical or electrical long-distance signals that move through the vascular system (Suarez Lopez 2005; Fromm and Lautner 2007; Heil and Silva Bueno 2007; Zimmermann, Maischak et al. 2009). Here, to determine if the gene modulation at a distance observed during wounding and from the various pollinations could be mediated by a diffusible stress

hormone, the volatile hormone MeJA was tested. Jasmonates are strong inducers of defense responses and may travel by airborne and vascular transports to mediate long-distance resistance (Farmer and Ryan 1990; Shulaev, Silverman et al. 1997; Karban, Baldwin et al. 2000; Park, Kaimoyo et al. 2007). Several studies have reported a dual role for jasmonic acid in defense and male and female fertility as well as in various developmental processes (Wilen, van Rooijen et al. 1991; Hause, Stenzel et al. 2000; Li, Li et al. 2001; Wasternack 2007). Although MeJA treatment induced a large modification in the ovary transcriptome, our data showed an important overlap between MeJA treatment, wounding and pollination, suggesting that jasmonates may not only mediate long distance signaling in defense responses but could also be involved in pollen-pistil interactions.

Taken together, our results confirm the existence of cross-talk between the genetic networks regulating pollination/fertilization and stress responses, as previously shown in rice (Lan, Li et al. 2005). Superimposed on these common genes is a large fraction of genes specifically modulated by each pollination type, and while this specificity is low at early times (6 HAP), it progresses during the time-course, indicating that additional genetic networks are involved and are specific to the pollination process ([Figure 8](#)). Our results also suggest that either pollen-borne signals, molecules secreted from pollen tubes or released after pollen tube death following self-recognition or incongruous heterospecific pollination, combined with those specifically released from the transmitting tract tissue of the style after various pollination type interactions may be responsible for the distinct responses observed.

Expression profiles obtained from compatible (SC), incompatible (SI), semi-compatible (SeC) and interspecific (IS) pollinations as well as from wounding and MeJA treatments revealed a precise and specific discrimination between pollination types early on after pollen germination from a distance in the ovary. By analogy to pathogen perception, we thus propose that during pollen-pistil interactions, along the path of the style, pollen-associated molecular patterns (PoAMP) are produced and recognized to elicit a specific response at a distance in the ovary in preparation for fertilization or to signal the presence

of incongruous or suboptimal pollen. These PoAMPs remain to be isolated, and, considering the very active and intimate interactions during pollen-pistil interactions, this will surely not be an easy task.

Chapitre 3.

Loss of ovule identity induced by overexpression of the Fertilization-Related Kinase 2 (ScFRK2), a MAPKKK from *Solanum chacoense*

By Madoka Gray-Mitsumune^{1*}, Martin O'Brien^{1*}, Charles Bertrand², Faiza Tebbji¹, André Nantel³, and Daniel P. Matton¹

¹Institut de recherche en biologie végétale, Département de sciences biologiques, Université de Montréal, 4101 rue Sherbrooke est, Montréal, Québec, Canada, H1X 2B2. ²Département d'Anatomie-Biologie Cellulaire, Université de Sherbrooke, 3001 12ème Avenue Nord, Sherbrooke, QC, Canada, J1H 5N4. ³Biotechnology Research Institute, National Research Council, 6100 Royalmount Avenue, Montreal, QC, Canada, H4P 2R2.

Short Running title: A new MAPKKK affects ovule identity

Participation des auteurs :

Dans le travail qui suit concernant l'implication de la kinase ScFRK2 dans l'identité des ovules, j'ai effectué la totalité des études transcriptomiques par microarray, incluant l'impression des puces, les extractions des ARNs, les hybridations ainsi que les analyses. J'ai participé aussi dans la rédaction de cet article.

Abstract

In order to gain information about protein kinases acting during plant fertilization and embryogenesis, we used a reverse genetic approach to determine the role of protein kinases expressed in reproductive tissues. Out of an EST library normalized for weakly expressed genes in fertilized ovaries, we isolated two cDNA clones named *ScFRK1* and *ScFRK2* (*Solanum chacoense* Fertilization-Related Kinase 1 and 2) that showed significant sequence similarities to members of the MAPKKK family. RNA gel blot and in situ RNA hybridization analyses confirmed the strong up-regulation of *ScFRK2* in ovules after fertilization. In addition, *ScFRK2* mRNAs accumulate during early ovule development in the megasporocyte of ovule primordium and in the integument of developing ovules. Overexpression of *ScFRK2* led to the production of fruits with a severely reduced number of seeds. The seeds that were produced also exhibited developmental retardation. Analysis of ovaries prior to fertilization showed that the seedless phenotype was caused by a homeotic conversion of ovules into carpel-like structures. Our observations are consistent with the role of *ScFRK2* in pre- and post-fertilization events. Furthermore, overexpression of *ScFRK2* lead to changes in the expression of the class D floral homeotic gene *ScFBP11*, suggesting that the *ScFRK2* kinase may interact, directly or indirectly, with the FBP7/11 pathway that direct establishment of ovule identity.

Keywords: MAPKKK, Ovule development, Carpel, Fruit development, *Solanaceae*.

Genbank Accession numbers: *ScFRK1*, AY427828; *ScFRK2*, AY427829; *ScFBP11*, DN980993.

Abbreviations: FRK, Fertilization-related kinase; MAPK, Mitogen-activated protein kinase; MAPKK, Mitogen-activated protein kinase kinase; MAPKKK, Mitogen-activated protein kinase kinase kinase; DAP, days after pollination; CS, carpelloid structure; RLK, Receptor-like kinase; SEM, scanning electron microscopy.

Introduction

The pivotal role played by protein phosphorylation in eukaryotic signal transduction is well illustrated by the wide range of phosphorylation cascades that involve Mitogen-Activated Protein Kinases (MAPK) (Treisman 1996; Robinson and Cobb 1997). In vertebrates, MAPK are typically activated in response to various mitotic agents such as hormone and growth factors (Piwien-Pilipuk, Huo et al. 2002). They have been shown to play an important role in the regulation of cell division and differentiation. The activation of MAPK occurs by phosphorylation of conserved threonine and tyrosine residues in the activation loop between the catalytic subdomain VII and VIII. This phosphorylation step is produced by dual specificity MAPK Kinases (MAPKK). These MAPK kinases are themselves activated on serine and/or threonine by serine/threonine MAPKK Kinase (MAPKKK) (Nishihama, Banno et al. 1995; Madhani and Fink 1998). In non-plant organisms, the activation of MAPKKK occurs either through phosphorylation by MAPKKK Kinase (MAPKKKK) (Sells, Knaus et al. 1997; Elion 2000), by the receiver domain of a two-component histidine kinase module (Posas and Saito 1997), or commonly by G proteins (Fanger, Gerwins et al. 1997) and G protein-coupled receptors (Sugden and Clerk 1997). Cell signals are thus transmitted through a chain of phosphorylation events. In plants, direct modulators of MAPKKK are yet unknown and complete cascade modules are only starting to unfold (Asai, Tena et al. 2002).

The vast majority of plant developmental mutants described so far have been found to be impaired in the expression of transcription factors, many from the MADS-box family (Jack 2001). Only few mutants affecting plant development have been described as encoding protein kinases although it would be reasonable to assume that post-translational modifications through phosphorylation of a protein involved in a key developmental pathway could be an important regulatory step for its intrinsic activity. Disruption of the signaling cascade would thus also lead to developmental defects. Among the protein kinases known to affect key developmental aspects of plant growth and development, most

belonged to the receptor-like kinase (RLK) family (Becraft 2002). Some have also been shown to affect reproductive development. These include the *Clavata 1* RLK gene involved in the regulation of meristem size and maintenance (Clark, Running et al. 1993); the *BRI1* RLK involved in brassinosteroid perception (Li and Chory 1997); the *Petunia PRK1* RLK involved in pollen and embryo sac development (Lee, Karunananada et al. 1996; Lee, Chung et al. 1997); the extra sporogenous cells (*EXS*) RLK which regulates male germ line cell number, tapetal identity, as well as promoting seed development (Canales, Bhatt et al. 2002); the maize *CRINKLY4* (*CR4*) RLK involved in aleurone cell fate (Becraft and Asuncion-Crabb 2000) and the *Arabidopsis CRINKLY4* (*ACR4*), required for proper embryogenesis (Tanaka, Watanabe et al. 2002) and involved in cell layer organization during ovule integument and sepal margin development (Gifford, Dean et al. 2003); the somatic embryogenesis receptor-like kinase (*SERK1*) involved in somatic embryogenesis (Schmidt, Guzzo et al. 1997), and expressed in developing ovules and embryo (Hecht, Vielle-Calzada et al. 2001); and the *Strubbelig* RLK that affects outer integument formation and organ shape although it does not encode a functional kinase domain (Chevalier, Batoux et al. 2005). Although downstream kinase modules transducing the initial signal from these RLKs could be expected, like MAPK transducing modules, none have yet been characterized in development, and only few MAPK family members have been shown to be involved in developmental processes (Hirt 2000). Recently, a mutation in the *Arabidopsis thaliana YODA* (*YDA*) gene, which codes for a MAPKKK, has been shown to cause early embryonic defect (Bergmann, Lukowitz et al. 2004; Lukowitz, Roeder et al. 2004). In this mutant, the zygote does not elongate properly and the suspensor cells are fused to the embryo. Mutant *yda* seedlings that can make it through maturity show overproduction and crowding of stomata cells (Bergmann, Lukowitz et al. 2004), reminiscent of the receptor kinase *two many mouths* (*tmm*) mutant phenotype (Nadeau and Sack 2002). This hints at the presence of a MAPK module involved in embryo development and stomata distribution. As for most MAPK cascades described so far, their involvement in limited to stress and

disease responses (Hirt 2000; Romeis 2001; Zhang and Klessig 2001; Asai, Tena et al. 2002), and hormone perception (Kieber, Rothenberg et al. 1993).

In this study we describe the isolation and functional characterization of a new MAPKKK from the MEKK subfamily in *S. chacoense*. Overexpression of this protein kinase named ScFRK2 affects ovule identity and is involved in seed and fruit development.

Material and Methods

Plant material

The diploid and self-incompatible wild potato *Solanum chacoense* Bitt. ($2n=2x=24$) was grown in greenhouse with 14-16 hours of light per day. The genotype used were V22 (S alleles S₁₁ and S₁₃) as pollen donor and G4 (S alleles S₁₂ and S₁₄) as female progenitor. Plants were hand-pollinated. Transgenic lines were generated in the G4 background.

DNA and RNA gel blot analysis

Total RNA was isolated as described previously (Jones, Dunsmuir et al. 1985) or with the Plant RNeasy RNA extraction kit from Qiagen (Mississauga, ONT, Canada). RNA concentration was determined by measuring its absorbance at 260 nm. Concentration and RNA quality were verified on agarose gel and ethidium bromide staining and RNA concentration adjustment was done if needed. For each tissue tested, ten µg of total RNA were separated on a formaldehyde/MOPS gel. RNA was then blotted on Hybond N+ membranes (GE Healthcare, Baie d'Urfée, QC, Canada), and were UV cross-linked with a Hoefer UV crosslinker (120 mJ/cm²). To confirm equal loading between RNA samples, a 1 kb fragment of *S. chacoense* 18S RNA was PCR amplified and used as a control probe. Pre-hybridization was performed at 45°C for three hours in 50% formamide solution (50% deionized formamide, 6X SCC, 5X Denhardt solution, 0.5% SDS and 200 µg ml⁻¹ of denatured salmon DNA). Hybridization of the membranes was performed overnight at 45°C in 50% formamide solution. Genomic DNA isolation was performed with the Plant DNeasy kit from Qiagen. Complete digestion of DNA (10 µg) was made overnight with 10 units of restriction enzymes as recommended by the supplier (New England Biolab, Beverly, MA, USA). DNA gel blot analysis was performed as previously described (Sambrook, Fritsch et al. 1989) and DNA was transferred to Hybond N+ membranes prior to cross-linking. Pre-hybridization was performed for three hours at 65°C in 50% phosphate solution (50% of 0.5 M Na₂ PO₄ pH 8.0, 1% BSA, 7% SDS and 1mM EDTA), while

hybridization was made overnight in the same conditions used for pre-hybridization. Probes for the RNA and DNA gel blot analysis were synthesized by random labeling using the Strip-EZ DNA labeling kit (Ambion, Austin, TX, USA) in presence of α -dATP- 32 P (ICN Biochemicals, Irvine, CA, USA). Following hybridization, membranes were washed 30 minutes at 25°C and 30 minutes at 35°C in 2X SSC/ 0.1% SDS, 30 minutes at 45°C and 30 minutes at 55°C in 1X SSC/ 0.1% SDS, and for 10 minutes at 55°C in 0.1X SSC/ 0.1% SDS. Prior to control hybridization with the 18S probe, the membranes were striped as recommended by the manufacturer (Ambion, Austin, TX, USA), and post-hybridization washes were done twice at 60°C for 30 minutes in 0.1X SSC/ 0.1% SDS. Autoradiography was performed at -86°C on Kodak Biomax MR film (Interscience, Markham, ONT, Canada).

Sequence analysis and phylogeny

The catalytic kinase domain structure of ScFRK2 was defined following the twelve kinase subdomains assignation described previously (Hanks and Hunter 1995). Protein secondary structure prediction needed for the ScFRK2 subdomain designation was performed with these four prediction tools: JUFO (<http://www.jens-meiler.de/jufo.html>), PORTER (<http://distill.ucd.ie/porter/>), PSIPred (<http://bioinf.cs.ucl.ac.uk/psipred/>) and SCRATCH (<http://www.igb.uci.edu/tools/scratch/>). Designations of subdomain boundaries were obtained from a consensus of all prediction tools and conserved amino acids specific to each domain. The phylogenetic analysis was accomplished with the trimmed catalytic kinase domain only. Alignment of the protein sequences was performed using ClustalX using default parameters (Thompson, Gibson et al. 1997). The phylogeny was reconstructed in SplitsTree4 (Huson and Bryant 2006) using the neighbor-joining algorithm (Saitou and Nei 1987) from both uncorrected distances and from distances corrected using a WAG + Γ + F model (Whelan and Goldman 2001). The phylogenies were validated using the nonparametric bootstrap with 1000 replicates.

Plant transformation

The *ScFRK2* cDNA was PCR amplified with Pwo polymerase (Roche Diagnostic, Laval, QC, Canada) with Kpn I overhang primers. Primers used were FRK2Kpn1: 5'-GGGGTACCGCGGTCGGCGCAATCTT-3' and FRK2Kpn2: 5'-GGGGTACCACTTCCATCAGGCTTG-3'. The PCR product was cleaved with Kpn I and inserted in a modified pBin19 transformation vector (Bussière, Ledû et al. 2003) with a double enhancer CaMV 35S promoter. Sense and antisense constructs were determined by plasmid digestion with Eco RI, which gives an asymmetric fragmentation according to the orientation of cloned PCR products. Sense and antisense constructs were individually transformed in *Agrobacterium tumefaciens* LBA4404 by electroporation. *S. chacoense* plants were transformed by the leaf disc method as previously described (Matton, Maes et al. 1997).

Tissue fixation and SEM observations

Dissected ovaries were fixed in 4% glutaraldehyde for 4 hours at room temperature in 0.1 M phosphate buffer (NaHPO₄, pH 7.0). After two rinsing steps in 0.1 M phosphate buffer, the tissues were dehydrated in an increasing ethanol series (from 30% to 100%) and critical-point-dried with CO₂, coated with gold-palladium, and viewed in a JEOL JSM-35 SEM.

Tissue fixation and optical microscopy observations

Pistils were fixed in FAA for 24 hours at 4°C (50 % ethanol, 1.35% formaldehyde and 5% glacial acetic acid). Samples were then dehydrated in increasing series of tert-butyl alcohol (from 70% to pure tert-butyl alcohol). Pistils were infiltrated with Paraplast Plus (Tyco Healthcare Group LP, Mansfield, MA, USA) at 60°C. Thin sections (10 µm) were prepared from embedded samples and tissue sections were stained in 0.5% Astra Blue and 1% safranine after removal of paraffin. Alternatively, thin sections (10 µm) were prepared from embedded samples and tissue sections were stained in 0.05% Toluidine Blue O (Figs. 4V-

Y). *In situ* hybridizations were performed as described previously (O'Brien, Chantha et al. 2005). Microscopic observations were taken on a Leica OrthoPlan microscope and pictures taken with a Leica DFC320 camera.

RNA extraction, probe preparation, cDNA array hybridization and data analysis

DNA microarrays were printed on UltraGAPSTM Slides (Corning) from 7741 expressed sequence tags (ESTs) corresponding to 6374 unigenes derived from a fertilized ovary cDNA libraries covering embryo development from zygote to late torpedo stages in *Solanum chacoense* (Germain, Rudd et al. 2005). This microarray was used to analyze gene expression profiles in ovaries prior to fertilization in WT and ScFRK2 mutant plants. Total RNA was extracted from unfertilized WT and ScFRK2 mutant ovaries using TRIzol ® Reagent (Invitrogen) according to the manufacturer's instructions. RNA yield and purity were assessed by absorbance determination at both 260 nm and 280 nm. RNA was only used when the ratio Abs260 nm/Abs280 nm was higher than 1.7. RNA integrity was determined with the RNA 6000 Nano Assay Kit and the Agilent 2100 Bioanalyzer. Thirty (30) µg of total RNA from WT ovaries were hybridized to microarrays along with the same amount of RNA from ScFRK2 mutant ovaries for 16h at 42°C. Each of the four pools of RNA from WT and ScFRK2-OX ovaries were compared to the control RNA in individual microarray hybridizations. Two hybridizations used a Cy3/Cy5 comparison, while the other two used a Cy5/Cy3 ratio. This strategy allowed us to obtain profiling data from four biological replicates while simultaneously negating any potential bias that could arise from the choice of labeling dyes. Labeling was performed with a cyanine 3-dCTP or cyanine 5-dCTP (1 mM; NEN Life Science, Boston MA, cat. no. NEL576 and 577). Hybridization and washing were performed as described in the CyScribe Post labeling Kit (Amersham Biosciences) in the CMTTM hybridization chamber (Corning). The DNA microarray slides were scanned with a ScanArray Lite scanner (Perkin Elmer-Cetus, Wellesley, CA; version 2.0) at 10-µm resolution. The resulting 16-bit TIFF files were quantified with QuantArray

software (Perkin Elmer-Cetus; versions 2.0 and 3.0). Normalization was performed with Lowess (Locally weighted scatter plot smoothing). Statistical analysis and visualization were performed with GeneSpring software (Silicon Genetics, Redwood City, CA) using the available statistical tools (Student's t test of replicate samples showing a variation different from 1).

Results

Isolation and sequence analysis of the *ScFRK1* and *ScFRK2* kinases

Using a negative selection screen targeting only weakly expressed genes expressed during fertilization and early embryogenesis, we have isolated 16 different protein kinase clones from the Mitogen-Activated Protein Kinase (MAPK) family in *Solanum chacoense*, a self-incompatible wild potato species close to potato and tomato (Germain, Rudd et al. 2005). Two of these, named *ScFRK1* and *ScFRK2*, were further investigated for their possible role in fertilization and embryogenesis. Both clones showed strong sequence similarity with the catalytic domain of various MAPKKK, but lacked a large regulatory domain characteristic of most of these MAPKKK (Tu, Barr et al. 1997; Wu, Leberer et al. 1999).

The *ScFRK1* kinase clone (accession number AY427828) is 1539 bp long (excluding the poly A tail) and is likely to represent the full-length *ScFRK1* mRNA since the size of this cDNA corresponded to the size of the mRNA as determined from RNA gel blot analyses (~1.5 kb, data not shown). It codes for an open reading frame of 320 amino acids with an estimated molecular weight of 36.2 kDa. A stop codon is found upstream and in frame with the first AUG initiation codon, indicating that the coding region is complete. The longest *ScFRK2* cDNA isolated (accession number AY427829) consisted of 1115 bp (excluding the poly A tail) and codes for a predicted 304 amino acids long protein with an estimated molecular weight of 34.3 kDa. A stop codon is also found upstream and in frame with the first AUG initiation codon, indicating that the coding region is also complete. Both proteins are composed of a catalytic domain that constitutes the major part of the protein (Fig. 1A). The kinase domain starts after the first 10 (for *ScFRK1*) and 5 (for *ScFRK2*) amino acids, and stops 42 (for *ScFRK1*) and 47 (for *ScFRK2*) amino acids before the end of the protein, leaving approximately 50 amino acids for putative regulatory domains.

The ScFRK2 deduced protein showed strongest amino acid sequence identity with ScFRK1 (45% identity, 60% overall similarity), and with a predicted protein kinase from *Arabidopsis thaliana* (At5g67080, renamed MAPKKK19), with 36% identity (51% overall similarity) (Fig. 1A). The ScFRK1 deduced protein showed greatest sequence identity (39%; 50% similarity) with the At3g50310 protein sequence (renamed MAPKKK20), a putative protein kinase from *A. thaliana*. Since initial Blast comparisons retrieved mostly protein kinases defined as MAPKKK, and since ScFRK1, ScFRK2 and their most similar *A. thaliana* putative orthologs were considerably smaller than most typical MAPKKK, lacking a large N- or C-terminal regulatory domain, we performed a phylogenetic analysis with representatives from the MAPK (as the outgroup), MAPKK, MAPKKK, and MAPKKKK families, in order to determine to which family of MAPK did ScFRK1 and ScFRK2 belonged. The phylogenetic analysis was achieved after aligning trimmed kinase domains based on previous sequence alignments and secondary structures predictions (Hanks and Quinn 1991). Protein kinases from *A. thaliana* previously classified into these various MAPK families were used for the analysis. Two members of the MAPK family were chosen (outgroup), as well as 10 MAPKK, 80 MAPKKK (48 from the RAF subfamily, 21 from the MEKK subfamily, and 11 from the ZIK subfamily), and six MAPKKKK. To simplify the display, and since the ScFRK1 and 2 kinases were closest to the MEKK, a phylogenetic tree obtained with only the MEKK subfamily from the MAPKKK family is shown in Figure 1B. Only the tree obtained from uncorrected distances is shown, but using corrected distances resulted in a tree with an identical topology (data not shown). This analysis clearly showed that both ScFRK1 and 2 are members of the MEKK subfamily of the MAPKKK.

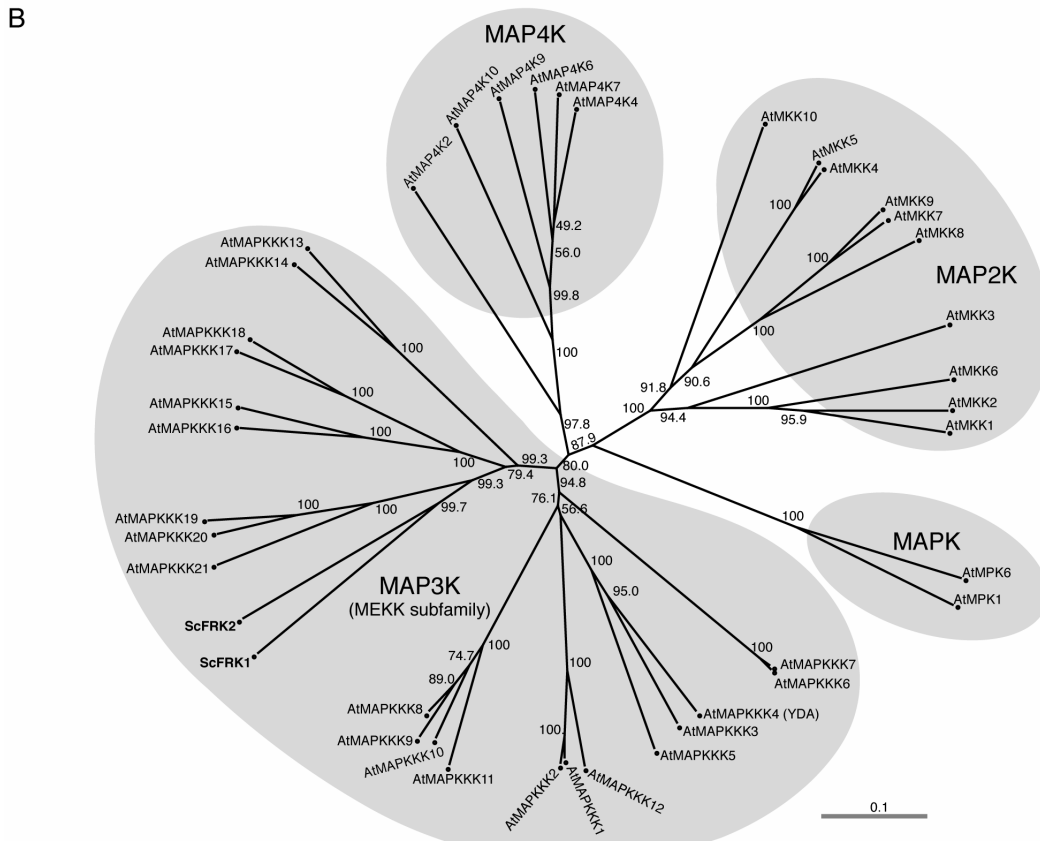
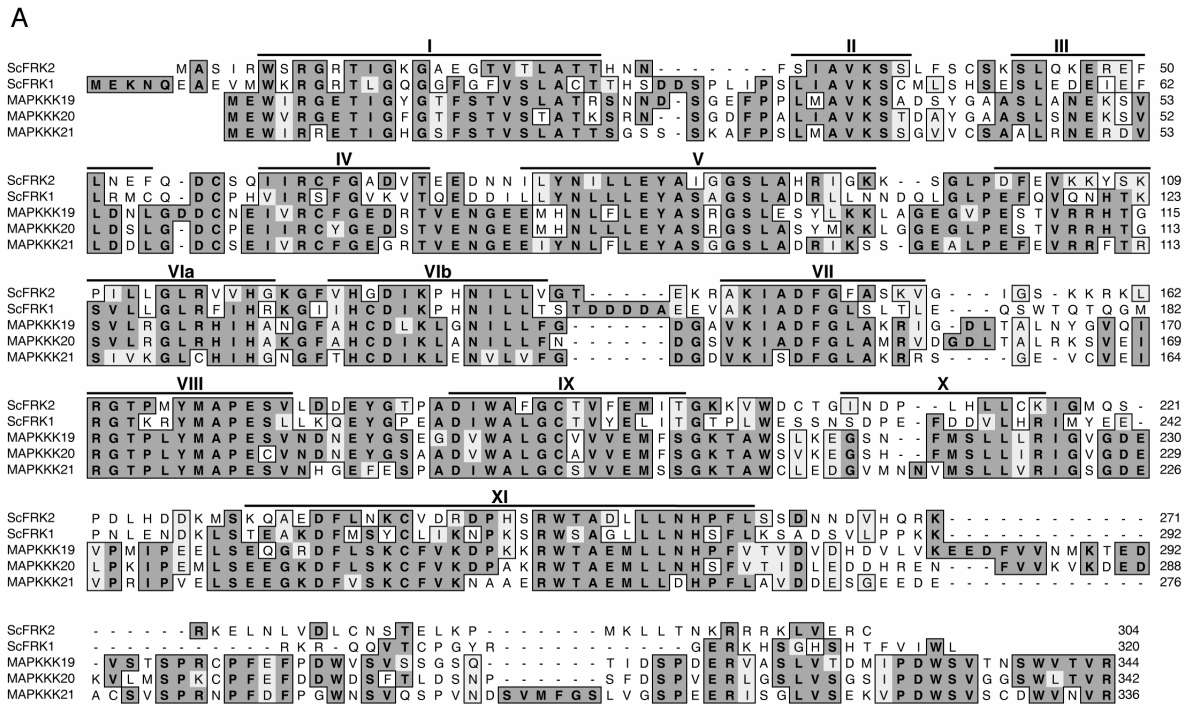


Figure 1. Sequence analyses of ScFRK1 and ScFRK2. **A.** Sequence alignment of the deduced protein sequences from *S. chacoense* ScFRK1 and ScFRK2, and with the three most similar MAPKKK from *A. thaliana*. Kinase subdomains are identified with thick black lines and were defined as described by Hanks and Hunter (1995), where alpha helices and beta sheets were deduced by four different prediction tools (see materials and methods). **B.** Phylogenetic tree obtained with the neighbor-joining method from uncorrected distances. Bootstrap support values from 1000 replicates are indicated beside the branches. All *A. thaliana* sequences were directly obtained from the TAIR website (<http://www.arabidopsis.org/>). The phylogenetic analysis was performed using the catalytic kinase domain. Tree branch length is proportional to the number of substitutions and the scale bar represents the expected number of substitution per site.

The genomic organization for *ScFRK2* was assayed by PCR amplification on genomic DNA and by restriction enzyme digestion of genomic DNA followed by DNA gel blot analyses. PCR amplification was achieved with primers that amplified the complete *ScFRK2* cDNA clone, including all available 5' and 3' UTR sequences. Genomic DNA and plasmid PCR amplifications were run side by side on an agarose gel and no differences in the length of the PCR products could be detected (data not shown), indicating the absence of an intron in the region defined by the primers used. In *A. thaliana* genome, At5g67080 (MAPKKK19), At3g50310 (MAPKKK20), and At4g36950 (MAPKKK21) are also intronless. DNA gel blot analyses of genomic DNA restriction fragments revealed a simple multi-banding pattern for *ScFRK2* hybridization (Fig. 2A). The Eco RI and Nco I digestions showed three bands, while the Bam HI and the Xba I digestions showed two bands. Since Eco RI and Bam HI cleave the *ScFRK2* cDNA once, and Nco I and Xba I do not cleave the *ScFRK2* cDNA, these results suggests that, in *S. chacoense*, the *ScFRK2* gene is present possibly in two to three copies if one of the Bam HI fragments contains two copies of *ScFRK2* in tandem.

Fertilization induces *ScFRK2* mRNA accumulation in ovules

ScFRK2 expression pattern was determined by RNA gel blot analysis (Fig. 2B) with various vegetative (stems and leaves), generative (petals) and reproductive tissues (stamens, pollen, pollen tubes, fertilized ovules, styles and ovaries). Prior to fertilization, strongest *ScFRK2* mRNA accumulation is observed in stamens and styles, although a basal level of mRNA can be detected in most tissues examined, including roots or tubers (Fig. 2B and data not shown). Fertilization had a dramatic effect on *ScFRK2* accumulation only in ovaries, as can be seen 2 days after pollination (DAP), and corresponding to ~12 hours after fertilization (Fig. 2B). Intriguingly, hybridization with the *ScFRK2* probe detected two transcripts, although not consistently in all experiments (for example, see Fig. 3A). The smaller transcript is estimated at 1.1 kb and corresponds to the expected size for the *ScFRK2* cDNA (1.11 kb). The larger 1.6 kb *ScFRK2* transcript is slightly less abundant in

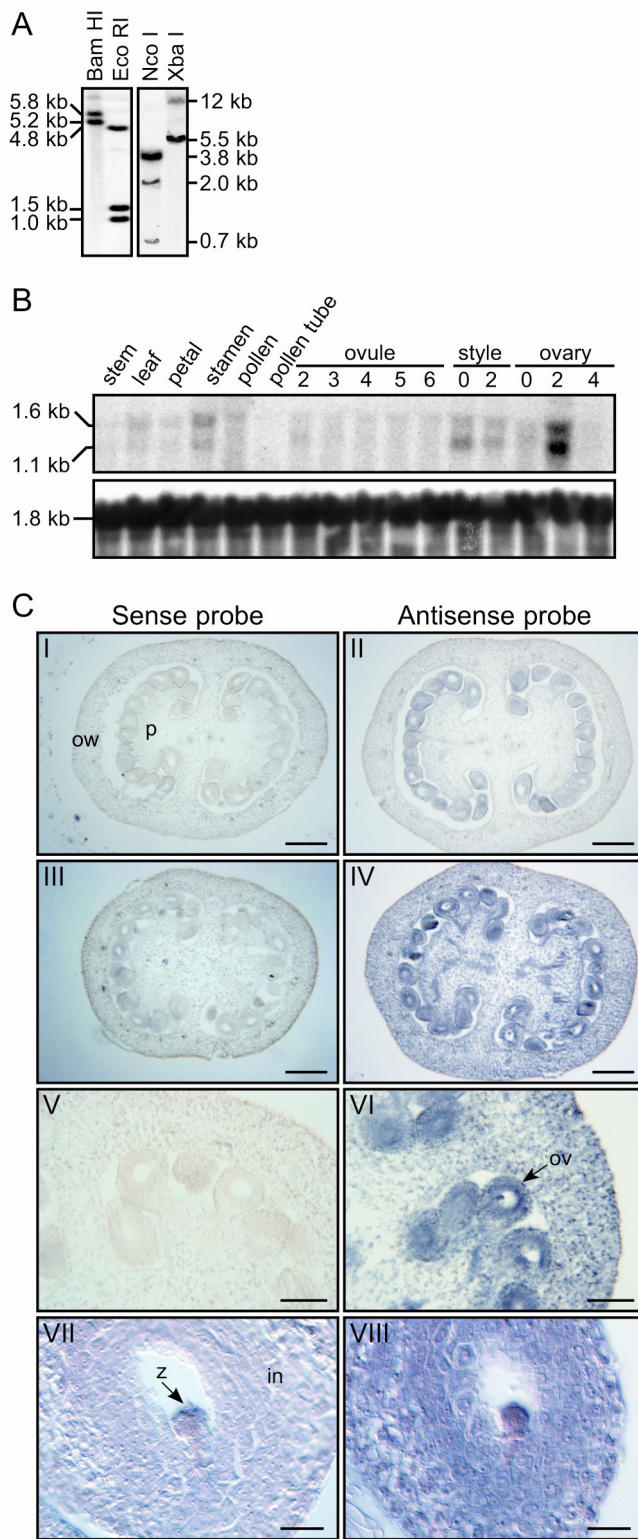


Figure 2. Transcript profile of *ScFRK2*. **A.** DNA gel blot analysis of the *ScFRK2* gene. Genomic DNA (10 µg) isolated from *S. chacoense* leaves was digested with Bam HI, Eco RI, Nco I or Xba I restriction enzyme, transferred onto membranes and probed with the complete 1.1 kb *ScFRK2* cDNA. Estimated molecular weights of the fragments obtained appear on the left of each DNA blot. **B.** RNA gel blot analysis of *ScFRK2* gene. All tissues were collected from greenhouse-grown plants. Pollen tubes were germinated *in vitro*. Fertilized ovules were dissected from ovaries 2 to 6 days after pollination (DAP). Pistils at 2 to 4 DAP were separated into styles and ovaries. Ten µg of total RNA isolated from *S. chacoense* tissues were blotted and probed using the full-length *ScFRK2* cDNA (upper panel). Membranes were stripped and re-probed using a partial 18S ribosomal RNA to ensure equal loading of each RNA sample (lower panel). **C.** *In situ* localization of *ScFRK2* transcripts in mature

ovaries. I and II, unfertilized mature ovary sections. III and IV, ovary sections 2 DAP (approximately 12 h post-fertilization). V and VI, magnifications of III and IV, respectively. VII and VIII, magnification of ovary sections 2 DAP showing staining in the zygote. I, III, V, and VII, control sense probe. II, IV, VI and VIII, antisense sense probe. Digoxigenin labeling is visible as red to purple staining. All hybridizations used 10 μm -thick sections and an equal amount of either *ScFRK2* sense or antisense probe. Scale bars, 250 μm (I to IV); 125 μm (V and VI); 20 μm (VII and VIII). In, integument; ov, ovule; ow, ovary wall (pericarp); p, placenta; zy, zygote.

all tissues tested except stamens. Since our previous result suggests that the gene has no introns, this suggests that the longer transcript is most probably not a splice variant. Nonetheless, since *ScFRK2* is part of a small gene family, this prompted us to attempt the isolation of a cDNA corresponding to the longer 1.6 kb transcript. One million phages from a cDNA library made from 2 DAP pistils were screened using the full length *ScFRK2* cDNA as a probe. All eight clones that were retrieved corresponded to the 1.1 kb transcript (data not shown). Thus the *ScFRK2* mRNA abundance can be estimated at 0.0008 % of total messenger RNAs in pistil tissues. This is reflected in the exposure time of the hybridization membranes, with four days exposure with the *ScFRK2* probe versus five minutes for the control 18S rRNA probe. A 5' RACE PCR was also attempted, but again, no product longer than the original *ScFRK2* cDNA could be isolated. Since it is unlikely that the larger *ScFRK2* hybridizing transcript corresponds to an unspliced *ScFRK2* pre-mRNA from the abovementioned results, the higher molecular weight band may correspond to a cross-hybridizing member of the *ScFRK2* family (Fig. 2A). Alternatively, we cannot exclude the possibility of an alternative transcription termination site that would generate a longer transcript, although again, this species should have been found in the library re-screening.

In order to determine spatial expression pattern of the *ScFRK2* gene, *in situ* RNA hybridizations were performed using ovaries taken before and after fertilization (Fig. 2C). Before fertilization, a weak *ScFRK2* mRNA signal was detected only in mature ovules (Fig. 2CII). After fertilization, much stronger *ScFRK2* mRNA signals were detected in ovules and, also, diffuse signals were detected in the placenta and ovary wall (Figs. 2CIV and VI). Although preservation and observation of the zygote is difficult in these paraffin embedded sections, staining can be occasionally observed in the embryo sac where the zygote would be located (for example see magnification in Fig. 2CVIII). Absence or very weak sense probe hybridization signals confirmed the specificity of the detection pattern obtained (Figs. 2CI, III, V, and VII).

ScFRK2 overexpression lines have defects in ovule development

We generated transgenic plants carrying sense or antisense construct of *ScFRK2*. The *ScFRK2* cDNA was placed downstream of a double enhancer 35S promoter in a modified pBin19 vector in a sense or antisense orientation (Bussière, Ledû et al. 2003). Kanamycin-resistant plants were grown to maturity in the greenhouse and the *ScFRK2* expression level was monitored by RNA gel blot analyses of stamen, leaf and ovary tissues. Identical results were obtained for the three tissues tested, indicating that the CaMV35S promoter used was equally active in ovaries, stamens and leaves. Among 13 transgenic lines containing the sense construct, one showed complete cosuppression for *ScFRK2* (Line S20 in Fig. 3A), while 12 others showed various levels of *ScFRK2* mRNA overexpression (*ScFRK2*-OX lines) (For example, lines S2 and S17 in Fig 3A). Plants containing the antisense construct showed reduced *ScFRK2* mRNA levels compared to wild-type (data not shown), but none showed mRNA down-regulation as severe as the cosuppression line S20 (Fig. 3A). No obvious developmental defects were detected either in cosuppression line S20 or in the antisense lines. Overall plant growth and development appeared unaffected in all *ScFRK2*-OX transgenic lines. However, they exhibited severe defects in seed and fruit development. Half of the *ScFRK2*-OX lines (OX lines S2, S17, S5, S7, S9 and S11) produced smaller than normal fruits containing fewer seeds (Figs. 3B and C, Table I). Two OX lines, S2 and S17, were selected for detailed phenotypic observation because they exhibited highest levels of *ScFRK2* mRNA. Development of the fruits started similarly in wild-type and transgenic lines, but significant differences in fruit size were detected from 10 DAP in OX lines (Fig. 3C). In wild-type *S. chacoense* plants, fruits develop to maturity in approximately 21 DAP. Thereafter, mature embryos start to desiccate in order to reach seed maturity around 40 DAP. At 21 DAP, fruit diameters from *ScFRK2* transgenic lines reached only to 60% of the normal wild-type fruits, weighed only 36% of normal WT fruits, and contained only 6.4 % of the total number of seeds normally produced in wild type fruits. The reduced seed set could explain the small fruit size observed. Furthermore, mature seeds obtained from OX lines bore embryos that were retarded in their

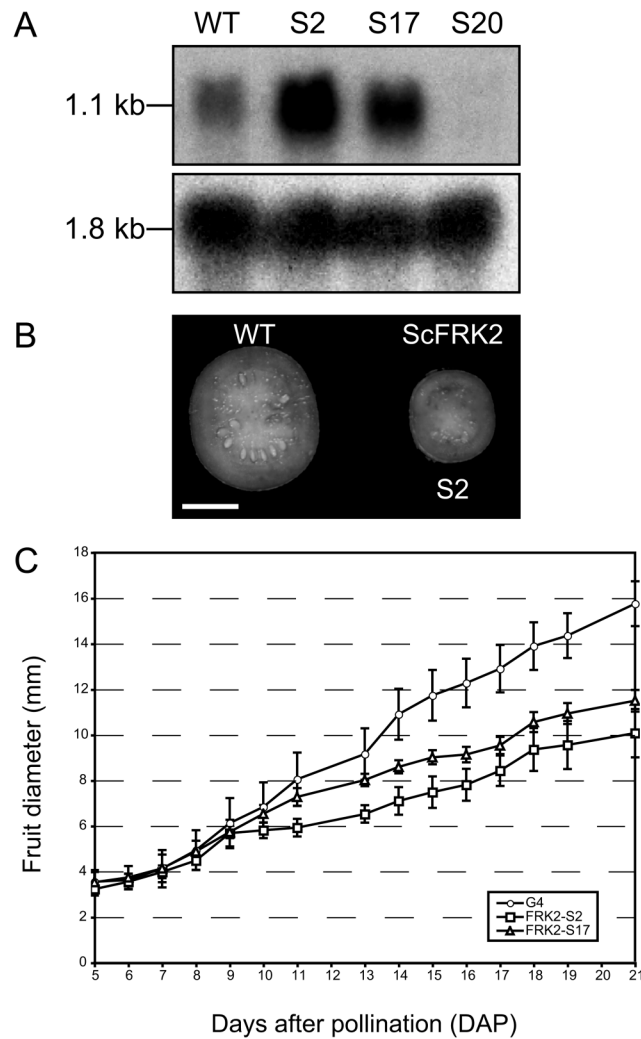


Figure 3. Analyses of *ScFRK2* transgenic plants carrying sense constructs. A. RNA gel blot analyses of *ScFRK2* mRNA (upper panel) and 18S rRNA (lower panel) of ovary tissues derived from wild-type plants (WT), overexpression lines S2 and S17, and cosuppression line S20. **B.** Comparison of fruit slices. Scale bar, 1 cm. **C.** Growth in fruit size after pollination.

development, most of them still being at the torpedo stage compared to mature embryos in wild-type plants (Table I). These embryos would eventually proceed to a mature stage and plants could be regenerated from these when hand dissected and placed on a sterile solid MS media (data not shown).

Table 1. Comparison of fruit size, weight, ovule number and embryo developmental stage between wild type and mutant plants.

Plant	Fruit diameter (mm) ¹	Fruit fresh weight (g) ¹	Number of ovule per fruit ¹	21 DAP Embryo mean developmental stage ²
Wild-type G4	15.8 ± 1.0	2.45 ± 0.24	106.2 ± 8.3	Mature
<i>ScFRK2-S2</i>	10.1 ± 1.1	0.89 ± 0.23	6.8 ± 1.9	Torpedo

¹ Each number represents the mean value of 24 fruits ± standard deviation.

² Developmental stage at which most embryos were found at 21 DAP, randomly taken from 24 dissected ovules. For wild-type, out of 24 embryos 19 were mature and 5 were at the torpedo stage. For the *ScFRK2* S2, 3 embryos were at the heart stage; 13 at the torpedo stage; 4 at the walking-stick stage; 4 at the mature embryo stage.

Further analyses of the *ScFRK2-S2* and *ScFRK2-S17* mutants revealed that overexpression of the *ScFRK2* led to the transformation of ovules into carpelloid structures (CS). In hand-dissected ovaries from the *ScFRK2* OX lines, the uppermost ovules in the ovary developed as filiform structures (Fig. 4B). A normal size ovule in this transgenic background is also visible indicated with a white arrow in Figure 4B. By comparison, a wild-type ovary containing normal ovules is shown in Figure 4A. Ovaries with a severe phenotype showed small bumps on their surface instead of a perfectly round and smooth surface as seen in control ovaries (data not shown). Inside these ovaries, the filiform structures filled most of the locular space, leaving few empty pockets. The transformed ovules took on a twisted spaghetti-like appearance due to the physical constraint of the

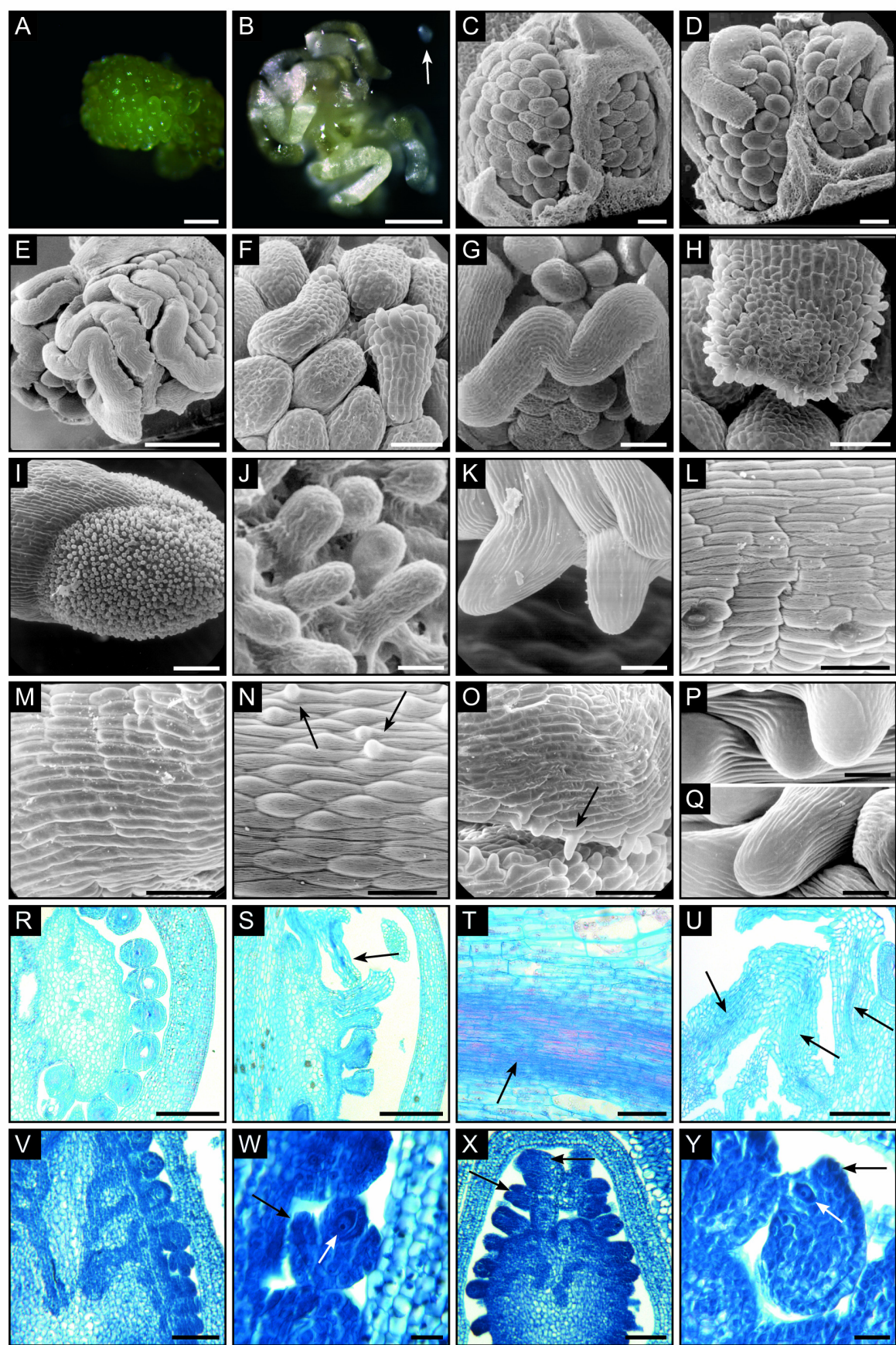


Figure 4. Fruit and ovule development of *ScFRK2-OX* plants. **A and B.** wild-type (**A**) and transgenic (**B**) ovaries. Ovary wall has been removed to expose ovules. The white arrow in **B** points to a normal ovule. **C-Q.** SEM images from wild-type (**C, H, J, L, N, and P**) and transgenic (**D-G, I, K, M, O and Q**) plants. **C.** Ovules from wild-type plant. **D and E.** Ovules from *ScFRK2-OX* plants, where **D** showing milder phenotype than **E**. **F.** Enlargement of emerging carpelloid structure (CS). **G.** Enlargement of an elongated CS. **H.** Papillae on wild-type stigma. **I.** Papillae on the CS extremity. **J.** Enlargement of stigmatic papillae. **K.** Enlargement of papillae on the CS extremity. **L.** Style cortex epidermis of a wild-type plant. **M.** Epidermis of the stylar section of CS. **N.** Small papillae on a wild-type style three days before anthesis. **O.** Small papillae from the stylar section of CS. In **N** and **O**, papillar cells are indicated by dark arrows. **P.** Enlargement of papillar ornamentations from the style of a wild-type plant. **Q.** Enlargement of papillar ornamentations from CS of a transgenic plant. **R through U.** Light microscopy of wild-type (**R**) and transgenic (**S-U**) plants. **R.** Ovary from a wild-type plant (only one locule shown). **S.** Ovary from a *ScFRK2-OX* plant (only one locule shown). **T.** Transverse section of a style from wild-type plant. The arrow indicates the transmitting tract. **U.** Transverse section of CS showing dense cells resembling the transmitting tract (indicated by arrows). **V.** Developing ovary from a wild-type plant. Section was taken from a flower bud approximately 2 mm in length. **W.** Enlargement of an ovule shown in **V**. The black arrow indicates the ovule integument and the white arrow indicates the megasporocyte. **X.** Developing ovary from a *ScFRK2-OX* plant. Section was taken from a flower bud approximately 2 mm in length. The black arrows indicate developing CSs. **Y.** Enlargement of the tip of CSs shown in **X**. The black arrow indicates the integument. Integuments were often enlarged. The white arrow indicates the megasporocyte. Scale bars, 1 mm (A and B); 100 µm (C , D, F-H, L-O, U, V, and X); 500 µm (E); 50 µm (I and T); 10 µm (J, K, P and Q); 250 µm (R and S); 20 µm (W and Y).

available growth space in the ovary (Fig. 4B). To identify the nature of these transformed ovules, we analyzed their morphology by scanning electron microscopy (SEM). Wild-type ovaries showed well-distributed ovules in the two locules (Fig. 4C). In contrast, mutant ovaries showed variable numbers of normal size ovules and ovules with abnormal growth. The severity of the defect was also influenced by environmental factors, such as day length or temperature; with more abnormal ovules observed in warmer periods during summer in the greenhouses (data not shown). The length of these modified ovules varied from small outgrowths to long and thin structure (Figs. 4D to G). Figure 4D shows modified ovules with a mild phenotype, while Figure 4E shows a more severe phenotype where filiform structures are longer and become twisted (Fig. 4G). These structures developed from the placenta as for normal ovules (Fig. 4F) and had an intrusive growth that disrupted ovule organization in their surroundings. Cells on the filiform structure were elongated without being wider than normal ovule cells (Fig. 4F). The tip of the filiform structure had cell projections (Fig. 4H) similar to stigmatic papillae found on WT pistil (Fig. 4I). As comparison, a magnification of stigmatic papillae of a wild-type style is shown in Fig. 4K. The papillae on the filiform structure resemble normal stigmatic papillae (Fig. 4J), except that no mucilage could be observed on their surface. Considering that the CS most probably corresponds to immature styles, this is not unexpected. We also compared cell morphology between wild-type stylar and CS cells (Figs. 4M, N and P, and L, O and Q, respectively). Cells from CS (Fig. 4L) showed rectangular cells that were more similar to stylar cells (Fig. 4M) than to ovule cells. Moreover, CS shared the same smaller triangular cells found on stylar cells (data not shown), but lacked guard cells and stomata that mature style shows along their length (compare Figs. 4L and M). Another feature of *S. chacoense* style is the presence of small papillae-like protrusions that develops as the style matures (O'Brien, Bertrand et al. 2002). Along their length, style (Fig. 4N) and CS (Fig. 4O) shared similar protruding papillae-like cells (Figs. 4N, O; black arrows). When magnified, these papillae-like cells showed similar cuticular ornamentations in both transgenic (Fig. 4Q) and wild-type cells (Fig. 4P).

To analyze the cell types present in the transformed ovules in more detail, we observed thin sections of fixed ovaries from *ScFRK2-OX* plants. The wild-type ovary contained ovules uniform in size and evenly arranged, extending from the placenta (Fig. 4R, only one locule shown). In contrast, ovaries in *ScFRK2-OX* plants contained irregularly shaped ovules as well as CSs similarly extending from the placenta (Fig 4S, only one locule shown). The locule organization was disrupted due to an excessive growth of the long filiform CS (Fig. 4S). These CSs showed a clearly different cellular organization than wild-type ovules. Transverse sections through the CS revealed strands of thin, long and more compacted cells (arrows in Figures 4S and U), reminiscent of the transmitting tissue cells found in wild-type style (arrow in figure 4T). CSs contained vessels through almost entire length of the filiform (Figs. 4 S and U). This is also similar to the transmitting tract of the wild-type style. On the other hand, wild-type ovules contained vessels only in the funiculus (data not shown). We have attempted to further identify CS using molecular markers for mature style transmitting tissue (*S-RNase*, *HT* gametophytic self-incompatibility modifier) (O'Brien, Kapfer et al. 2002). However, signal intensities of the marker transcripts were about the same between wild-type and mutant ovaries (data not shown). This may be because these CSs are more similar to immature styles and the expression of these genes had not yet initiated. At this stage, CS did not contain any structures resembling an embryo sac. In the section shown in Fig. 4S, most ovules, including those that are normal sizes, appeared abnormal and only a few would have led to seed formation, which explains the low seed yield in mature fruits (Table I). At 7 DAP, the filiform CS had already started to wither and turn brown and none could be observed at fruit maturity (data not shown).

We further investigated the ontogeny of CS in developing pistils. Ovule primordia of *ScFRK2-OX* plants appeared identical to those of wild-type plants (data not shown). First ovule abnormalities were detected when integument growth became apparent. Instead of forming a single layer integument characteristic of *Solanum* species (Fig. 4W, arrow), the stalk of ovule primordium continued to grow and expanded excessively forming enlarged ovules (Figs. 4X and Y, arrows). At this stage, the enlarged ovule still retained a

structure resembling the nucellus containing a megasporocyte at the tip (Fig. 4Y, white arrow). Some megasporocytes were undergoing meiosis, which appeared relatively normal (data not shown), suggesting that the conversion to carpelloids initiates from abnormal growth of the integument and stalk. Since no structures that resembled the megasporocyte or megagametophyte were visible in mature CS (Figs. 4S and U), the megagametophyte may either have degenerated or have been engulfed by the outgrowth of its surrounding tissues.

Expression of the *ScFRK2* gene in developing ovules

Since *ScFRK2* overexpression interfered with ovule development before fertilization (see above), we further investigated the *ScFRK2* expression pattern in developing ovules. RNA gel blot analyses using flower buds 1, 2, 3, 4 or 12 mm in length failed to detect any *ScFRK2* mRNA signals (data not shown), possibly because the cells expressing *ScFRK2* comprised only a small portion of the flower buds. However, *in situ* RNA hybridization revealed cell-specific accumulation of *ScFRK2* mRNA in early ovule development (Fig. 5). *ScFRK2* mRNA signals were detected in the ovule primordia of young pistil (Fig. 5B). Particularly intense signals were detected from the megasporocyte (Fig. 5D). Signals in megasporocyte weakened as the ovule developed and stronger signals were instead detected from the ovule integument (Fig. 5C). Intense signals were detected near the growing end of the ovule integument (Figs. 5C and E). Only diffuse signals were detected in the ovule integument after the integument reached full growth and little or no signal was detected from megagametophytes (Fig. 2CII).

As expected, *ScFRK2* mRNA signals were stronger in *ScFRK2*-OX plants than in wild-type plants (compare Figs. 5G and H). Surprisingly, transgenic plants retained a spatial expression pattern of *ScFRK2* that somewhat resembled the wild-type; i.e. strong expression in gametophytes. Ovule-specific signals in the transgenic plant are shown in Fig 5H. However, there were distinct differences in the cell specificity of *ScFRK2* distribution. Developing ovules of transgenic plants retained high levels of *ScFRK2* mRNA in

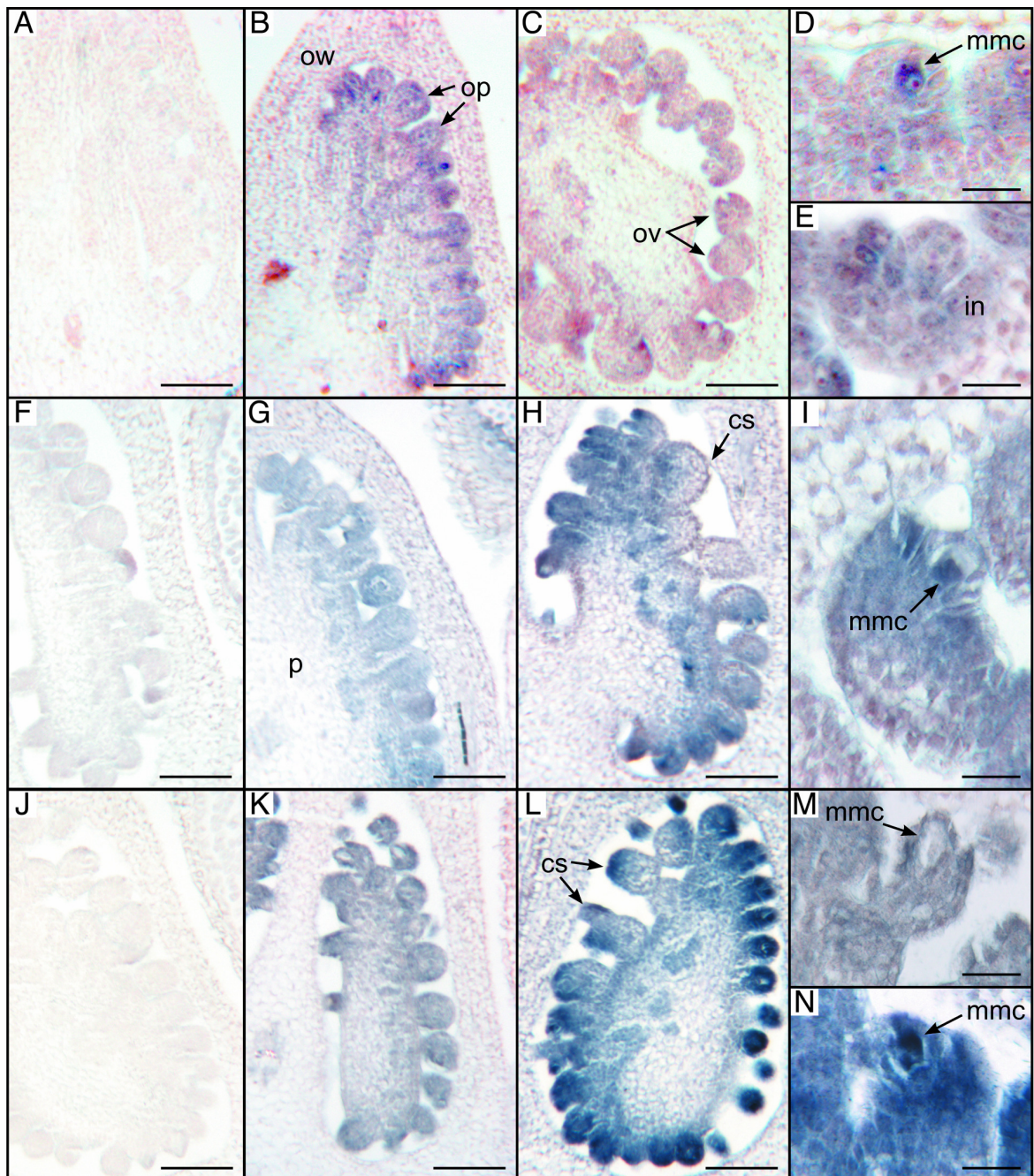


Figure 5. In situ RNA hybridization analyses in developing ovules.

A to E. *ScFRK2* expression in wild-type plants **A.** Sense probe. **B to E.** Antisense probe. **A and B.** Developing ovary showing ovule primordia arising from the placenta. Sections were taken from a flower bud approximately 1.5 mm in length. **C.** Ovary at a later stage showing developing ovule with growing integuments. The section was taken from a flower

bud approximately 2 mm in length. As ovules mature, the signal in the megasporocyte became weaker while the signal in the integument became stronger, particularly at the growing tip. **D.** Enlargement of B showing an intense *ScFRK2* mRNA signal in the megasporocyte. **E.** Enlargement of C. **F to I.** Comparison of *ScFRK2* expression between wild-type and *ScFRK2-OX* plants. *In situ* RNA hybridization was performed simultaneously using identical conditions to allow direct comparison. Sections were taken from ovaries at a similar stage as shown in C. **F.** Sense probe. **G-I.** Antisense probe. **F and G.** Wild-type plant. **H.** *ScFRK2-OX* plant. Arrow heads show developing CSs. Although signals are almost absent from the stalk, intense signals remain strong at the tip. **I.** Enlargement of H, showing the megasporocyte at the tip of the developing CS. The signal in the megasporocyte remains strong. **J to M.** *ScFBP11* expression in developing ovules. Tissue sections were taken from ovaries about the same stage as those in C-I. *In situ* RNA hybridization was performed simultaneously using identical conditions to allow direct comparison. **J.** Sense probe. **K to M.** Antisense probe. **J and K.** Wild-type plant. **K.** Diffuse signals were detected from the ovule integument while little signals were detected from the megasporocyte. **L.** Ovary from a *ScFRK2-OX* plant. Strong signals were detected in ovules that appear normal and also at the tip of the developing CS. Very little signals were detected in the stalk of CS. **M.** Enlargement of K. showing absence of signal in the megasporocyte. **N.** Enlargement of L, showing intense signals in the megasporocyte of CS.. cs, carpelloid; in, integument; mmc, megasporocyte; op, ovule primodium; ov, ovule; ow, ovary wall; p, placenta. Scale bars, 100 µm (A - C, F – H, J - L); 20 µm (D, E, I, M and N).

megasporocytes (Figs. 5H and I), whereas little or no signals were detected in the megasporocytes of wild-type ovules (Figs. 5C, E and G). Much weaker signals were detected in the stalk of developing CS, while intense signals were always associated with the megasporocyte and its surrounding tissues at the tip (Fig. 5H).

The expression of *ScFBP11*, a *Solanum* ortholog of *FBP7* and *FBP11*, is altered in *ScFRK2-OX* plants

In *Petunia*, down-regulation of the class D MADS-box genes *FBP7* and *FBP11* changes the fate of the ovule primordium to a carpel primordial and spaghetti-like structures in positions normally occupied by ovules (Angenent, Franken et al. 1995). These abnormal structures morphologically resemble style and stigma tissues, like the ones obtained in *ScFRK2-OX* lines. To determine if *ScFRK2* overexpression affected the class D MADS-box gene expression, we identified an EST corresponding to a putative *FBP7/11* ortholog from our *S. chacoense* ovary library and termed it *ScFBP11*. *ScFBP11* shares 87% amino acid sequence identity with both *FBP7* and *11*, and 86% with TAGL11, a tomato *FBP7/11* ortholog (Busi, Bustamante et al. 2003). A phylogenetic analysis confirmed the close association of *ScFBP11* with *Petunia* *FBP7* and *FBP11* as well as other class D MADS-box genes (data not shown). *In situ* RNA hybridization was performed using a partial *ScFBP11* cDNA sequence to determine spatial expression pattern of *ScFBP11*. In wild-type plants, diffuse *ScFBP11* mRNA signals were detected in the integument of the developing ovule and little or no signals were detected from megasporocytes (Fig. 5K). *ScFBP11* appeared to be up-regulated in the developing ovule of *ScFRK2-OX* transgenic plants. Ovule signals were much stronger in transgenic plants than in wild-type plants (compare Figs. 5L and K). More importantly, transgenic ovules retained *ScFBP11* signals in megasporocytes (Fig. 5N), in striking contrast with wild-type ovules (compare Figs. 5M and N). Developing CS retained intense signals in megasporocytes at the tip, while signals were mostly absent from the stalk (Fig. 5L).

cDNA microarray analyses

To determine whether the overexpression of *ScFRK2* showed any alterations in the expression of other genes, the mutant plants were compared with WT *S. chacoense* plants using DNA microarrays from a 7.7K array made from ovule-derived ESTs (Germain, Rudd et al. 2005). We used ANOVA testing, along with a Benjamini and Hochberg multiple testing correction algorithm, to select 389 ESTs that showed a statistically-significant difference in transcript abundance between the WT and the *ScFRK2*-overexpressing ovules. We initially used a Welch *t* test ($p < 0.05$) to compare the profiles from the *ScFRK2* vs. control and the control vs. control comparisons. They were then further restricted with a 1.5 fold-variation (1.5- cutoff up or down). We observed a relatively even split between up-regulated (160) and down-regulated (213) transcripts and this result is presented in Table S1. The observed changes in transcript abundance are relatively modest compared to what has been observed in other experiments (time-course analysis following fertilization in WT plants, data not shown). Since the phenotype in *ScFRK2*-OX lines is only observable in a fraction of the collected biological samples (see Figure 4, showing ovules at different stages of transformation into CS structures in the same ovary), it is possible that the changes in transcript abundance are somewhat “diluted” by contributions from unaffected tissue. Furthermore, for the microarray experiment, whole ovaries were used instead of isolated ovules, increasing the dilution effect. Nevertheless, statistically significant results were obtained for 373 ESTs. To determine whether the differentially expressed genes were involved in similar biological processes, these were categorized according to their Gene Ontology classification. Apart from a large class of hypothetical/unknown proteins (23.7%), the largest functional groups observed were implicated in metabolism (17.5%), protein with binding function, including RNA, DNA, protein, and ion binding (9.8%), development and organogenesis (8.5%), protein synthesis (7%), defense-response related proteins (6.9%), protein fate (8.5%), signal transduction (3.3%), transcription (5.1%) and transport (4.3%). Interestingly, of the selected genes, some have been previously shown to be involved in flower or fruit development. In the *ScFRK2*-OX down-regulated category,

among the genes involved in transcriptional regulation, homologs of LEUNIG and EIL2 transcription factors have been found. LEUNIG has been shown to negatively regulate AGMOUS during flower development (Conner and Liu 2000), while EIL2 (ETHYLENE INSENSITIVE3-like) is involved in ethylene perception, flower abscission, and fruit ripening (Tieman, Ciardi et al. 2001). Among the genes involved in signal transduction in the down-regulated category, three receptor-like kinases (RLKs) from *S. chacoense*, ORK3, 12, and 23, and an ethylene receptor homolog have been found. ORK3 and 12 transcript levels had been shown to increase after fertilization in the ovary, while transcript levels for ORK23 were induced at a distance in the ovary by pollination alone (Germain, Rudd et al. 2005). In the *ScFRK2-OX* up-regulated category, two RLKs and one serine/threonine kinase with records showing possible involvement in developmental processes were retrieved. The ORK6 RLK from *S. chacoense* was previously shown to be strongly induced (17 fold) following fertilization in ovaries (Germain, Rudd et al. 2005), while the second EST had significant sequence identity with putative orthologs of the phytosulfokine (PSK) receptor. PSKs are small peptide ligands that induce plant cells to dedifferentiate and reenter the cell cycle at nanomolar concentrations (Matsubayashi, Ogawa et al. 2002). Two PSK genes in maize, ZmPSK1 and ZmPSK3 were also detected in egg and central cells of the female gametophyte, while ZmPSK1 mRNA was present in synergids, indicating that the PSK peptide probably plays a role during gametogenesis and fertilization (Lorbiecke, Steffens et al. 2005). The other protein kinase was most similar to the APK1a kinase, a kinase very similar to the APK2a kinase, which gene was originally isolated as having cis-regulatory elements bound by AGAMOUS through an in vivo binding assay (Ito, Takahashi et al. 1997).

Discussion

ScFRK2 belong to the MEKK family of MAPKKK

Using the basic local alignment search tool on publicly available databases, both ScFRK1 and ScFRK2 were found to be most similar to the catalytic domain of numerous MAPKKK, as well as to three uncharacterized protein kinases from *Arabidopsis thaliana* (MAPKKK19, 20, and 21). When compared to most MAPKKK family members, these protein kinases (ScFRK1-2, MAPKKK19-21) lacked a typical regulatory domain. A phylogenetic analysis confirmed that these five MAPKKK belonged to the same subgroup inside the MEKK family of MAPKKK. Although kinase activity could be obtained from the ScFRK1 and ScFRK2 kinases after in vitro translation (data not shown), complementation in a yeast mutant background deficient for the Ste11 MAPKKK could not be achieved with either kinase (data not shown). This suggests that they may not be involved in a typical MAPK cascade, and/or that the lack of a large N-terminal regulatory domain, like in Ste11, might hamper proper function in yeast and make complementation ineffective.

Developmental defects caused by overexpression of ScFRK2

Overexpression of the *ScFRK2* gene leads to developmental defects in ovules, and delayed seed and fruit development. Although ectopic expression can sometime lead to pleiotropic effects on plant development, phenotypic abnormalities were found only in developing ovule and pollen (Gray-Mitsumune et al., manuscript in preparation) where *ScFRK2* was most strongly expressed during normal development. Ectopic expression of *ScFRK2* in vegetative tissues did not cause any visible changes in vegetative development. This suggests that the *ScFRK2* kinase acts only on the cells that contain its cognate signaling pathway partners and targets. Specific effects of *ScFRK2* overexpression may be explained partly by the ovule-specific accumulation of *ScFRK2* mRNAs in transgenic

plants (Fig. 5H). Although one would expect the activity of CaMV 35S promoter to be more ubiquitous, some tissue preferences have been reported previously (Wilkinson, Twell et al. 1997). Alternatively, the coding region of the *ScFRK2* gene might itself contain regulatory elements curbing the expression pattern obtained in ovules under the CaMV 35S promoter. In addition, steady state *ScFRK2* mRNA levels may be controlled post-transcriptionally by affecting mRNA processing and stability. Also, there may be a positive feedback mechanism that promotes up-regulation of endogenous *ScFRK2* transcription.

Nevertheless, there were distinctive differences in *ScFRK2* mRNA accumulation pattern in developing ovules between wild-type and transgenic plants. A schematic representation of *ScFRK2* mRNA distribution is shown in Figure 6. In wild type plants, *ScFRK2* mRNA signals in megasporocytes weakened after integument initiation while maintaining mRNA levels in integuments (Figs. 5C, E and G). In contrast, megasporocytes of transgenic ovules, including those that appeared of normal size, maintained high levels of *ScFRK2* mRNA levels (Figs. 5H and I). The abnormal elevation of *ScFRK2* in megasporocytes may hinder ovule maturation processes, possibly by preventing megagametogenesis and integument differentiation. This may be the reason why most ovules, including normal size ones, failed to mature in *ScFRK2*-OX plants (Fig. 4S). There were little *ScFRK2* mRNA signals in the stalk of developing CS (Figs. 5H and I). It is unlikely that the absence of *ScFRK2* is the cause of loss of ovule identity because *ScFRK2* down-regulation either by antisense or cosuppression does not cause ovule abnormality (see above). Instead, the down-regulation may have been caused by the loss of ovule identity itself. The abnormal elevation of *ScFRK2* in megasporocytes may have triggered the loss of identity in the integument, which in turn down-regulate *ScFRK2* expression in the CS. This scenario is also consistent with the persistence of *ScFRK2* mRNA in the nucellus-like structures at the tip of CS. Once the program for CS formation is initiated, the CS may have taken over the entire ovule to eliminate any structures reminiscent of megasporocytes or megagametophytes.

The *ScFRK2* expression in pistils prior to fertilization, taken together with a strong increase in expression observed in ovaries immediately after fertilization, suggest that this protein kinase has both pre- and post-fertilization roles. Unfortunately, the role of *ScFRK2* on post-fertilization ovule development could not be assessed thoroughly in this study since overexpression leads to the homeotic conversion of ovules into carpelloid structures that did not give rise to seeds. The few seeds that were obtained exhibited delayed development (Table I). Although this is consistent with the *ScFRK2* function on post-fertilization ovule development, it is difficult to distinguish a direct effect on embryo development from an indirect effect due to pre-fertilization ovule deficiency. To study the role of *ScFRK2* on post-fertilization ovule development, it will be necessary to direct *ScFRK2* expression only after fertilization using either a tissue-specific promoter or an inducible promoter.

Down-regulation of *ScFRK2* via antisense inhibition or cosuppression should have been more informative, however, no obvious defects were observed in these transgenic plants (data not shown). One explanation for this is functional redundancy shared with other related genes. Presence of such gene(s) was suggested by the DNA gel blot analysis (Fig. 2A). It will be interesting to see the effects of dominant negative mutations, which may overcome the functional redundancy problem. In this regard, it should be noted that the effect of *ScFRK2* overexpression may not always result in the enhancement the normal *ScFRK2* function. Proteins involved in MAPK cascades often function in protein complexes where MAPKKK, MAPKK and MAPK are anchored together and phosphorylate its targets within the complex (Murphy and Blenis 2006). Overexpression of one component may not always enhance the function of its complex as a whole. In an extreme situation, presence of excess proteins that do not participate in its cognate complex may actually hinder the complex function by competing for the same upstream targets. We do not know whether *ScFRK2* overexpression enhances or inhibit its downstream functions. Nor do we know whether *ScFRK2* overexpression results in accumulation of active *ScFRK2* kinase.

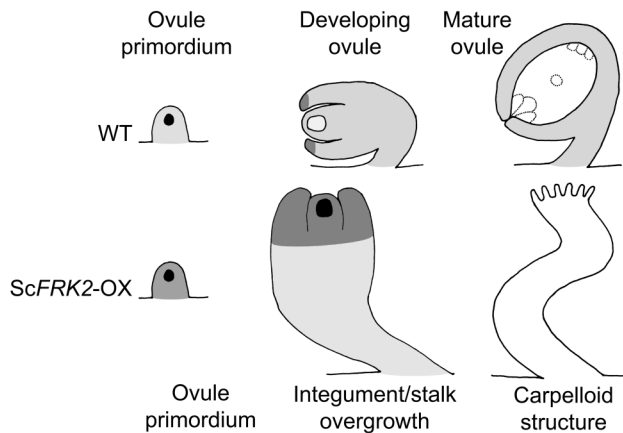


Figure 6. Schematic representation of *ScFRK2* mRNA distribution during wild type and *ScFRK2*-*OX* ovule development.

ScFRK2 *in situ* RNA hybridization signal distribution is represented by the gray scale, where black is strongest, and decreasing intensity of gray corresponds to lower expression levels. **Wild-type.** *ScFRK2* mRNA accumulates in the megasporocyte during ovule primordium formation. As ovules mature, *ScFRK2* mRNA levels decrease in megasporocyte and increase near the growing tip of the ovule's integument. When ovule reaches maturity, *ScFRK2* mRNA is only detected in the integument. ***ScFRK2*-*OX*.** In general, *ScFRK2* mRNA accumulates more than wild-type but the accumulation pattern during ovule primordium formation is identical to wild-type (i.e. accumulation mostly found in megasporocyte). *ScFRK2* mRNA remains abundant in megasporocyte during ovule/CS formation. Also, *ScFRK2* mRNA accumulates at the tip of overgrowing integument, whereas no or little *ScFRK2* mRNA is detected in the overgrowing funiculus (stalk of CS).

It will be necessary to identify downstream target proteins of ScFRK2. ScFRK2 function can then be monitored through the phosphorylation status of the target proteins.

Cells in multicellular organisms are equipped with an intricate network of signaling pathways that may interact to maintain a delicate balance of cell fate determination. This is why, unlike mutations in transcription factors, mutations in signaling pathways are difficult to interpret. Interplay of different MAPK cascades is illustrated by interactions between SIPK and WIPK, two closely related MAPKs in tobacco. Both SIPK and WIPK are phosphorylated after exposure to ozone, which trigger productions of ROS scavengers (Samuel and Ellis 2002). Stable overexpression of SIPK does not result in accumulation of phosphor-SIPK. SIPK is phosphorylated only after the exposure to ozone and, even then, the amount of phosphor-SIPK is not more than the wild-type. An unexpected side effect of SIPK overexpression was instead found in the phosphorylation status of WIPK. SIPK overexpression inhibits accumulation of phosphor-WIPK and, as a result, cells become hypersensitive to ozone stress. Inhibition of SIPK via RNAi also results in hypersensitivity to ozone. In this case, phosphor-WIPK accumulation is stimulated while phosphor-SIPK accumulation is inhibited (Samuel and Ellis 2002). Does the FRK2 pathway interact with other pathway(s) in a similar manner? Future biochemical analyses should reveal the web of FRK2 signaling pathways on ovule fate determination.

Gene mutations that result in loss of ovule identity

Overexpression of *ScFRK2* resulted in homeotic conversion of ovules into carpelloid structures (Fig. 4). Several genes coding for transcription factors have been identified as regulators of ovule development (Schneitz, Hulskamp et al. 1997; Gasser, Broadhurst et al. 1998), and misexpression of some of these genes lead to reiteration of carpel development instead of ovules to form of carpelloid structures and thus cause the loss of ovule identity. In many cases, the loss of ovule identity can be linked to either the misexpression class C MADS-box gene or down-regulation of class C and/or D MADS-

box genes. In *Arabidopsis*, a mutation in *APETALA2* (*AP2*), a negative regulator of class C MADS-box gene *AGAMOUS* (*AG*), causes the conversion of ovule to carpelloid structures within the gynoecium although at a low frequency (Modrusan, Reiser et al. 1994). *BELL1* (*BEL1*) is also postulated as a negative regulator of *AG* (Ray, Robinson-Beers et al. 1994). The *bell1* mutation likewise causes the loss of ovule identity, albeit at different timing as the *ap2* mutant (Modrusan, Reiser et al. 1994). In the *bell1* mutant, the ovule integument continues to grow and differentiate into structures with carpel-like morphology (Modrusan, Reiser et al. 1994). In the *ap2* mutant, homeotic conversion occurs at an earlier stage than in *bell1* mutants, as the carpelloid structure forms directly from ovule primordium projection (Modrusan, Reiser et al. 1994). *AG* is misexpressed in both *ap2* and *bell1* mutants and this may have caused the loss of ovule identity (Drews, Bowman et al. 1991; Ray, Robinson-Beers et al. 1994). Consistent with the idea, ectopic expression of *AG* orthologs results in homeotic conversion of ovule to CS in *Arabidopsis* (Ray, Robinson-Beers et al. 1994) and tobacco (Mandel, Bowman et al. 1992). Interestingly, the frequency of transformation in the *bell1* mutant decreases with lowering temperatures, as well as with reducing day-length (Modrusan, Reiser et al. 1994). Ovule to CS conversion in our *ScFRK2-OX* lines was also influenced by temperature and day-length (data not shown).

Involvement of the class D MADS-box genes in ovule identity determination was first identified in Petunia, a *Solanaceae* species like *Solanum chacoense*. Down-regulation of the class D MADS-box genes *FBP7* and *FBP11* via cosuppression changes the fate of the ovule primordia to the carpel primordia. Hence, CS develop on the placenta (Angenent, Franken et al. 1995). *Fbp7* and *Fbp11* works redundantly because neither *Fbp7* nor *Fbp11* single knockout mutant causes a similar phenotype (Vandenbussche, Zethof et al. 2003). Normally, the expression of *Fbp7* and 11 mRNAs are found in carpel. However, ectopic expression of the *Fbp11* gene causes ectopic ovule formation in the sepal, suggesting *Fbp11* is sufficient for ovule induction (Colombo, Franken et al. 1995). The *Arabidopsis* genome contains only one gene, *SEEDSTICK* (*STK*), that belongs to the class D MADS-box gene clade (Kramer, Jaramillo et al. 2004). *STK* alone does not determine

ovule identity but, instead, acts redundantly with three closely-related class C MADS-box genes, AG, *SHATTERPROOF1 (SHP1)* and 2 (*SHP2*) (Pinyopich, Ditta et al. 2003). In the *shp1 shp2 stk* triple mutant, ovules are converted into carpel- or leaf-like structures with style-like characteristics (Pinyopich, Ditta et al. 2003). Similar to *FBP11* in Petunia, ectopic expression of *STK*, *SHP1* or *SHP2* in *Arabidopsis* causes conversion of sepals to carpelloid organs with ectopic ovules (Favaro, Pinyopich et al. 2003). Interplay of class C and D MADS-box genes has further been demonstrated by protein interaction assays. Yeast two hybrid and three hybrid analyses have shown that, when the class E MADS-box transcription factor SEPALLATA 3 (SEP3) is present, AG forms complex with either STK, SHP1 or SHP2 and this complex (AG-SEP3-STK, AG-SEP3-SHP1 or AG-SEP3-SHP2) may be sufficient for promoting ovule identity (Favaro, Pinyopich et al. 2003). Similarly, FBP11 forms a higher-order complex with FBP2 (class E) and FBP6 (class C) transcription factors (Tonaco, Borst et al. 2006).

Possible interactions between *ScFRK2* and *FBP7/11* and/or AG pathways

ScFRK2 expression pattern in *S. chacoense* ovules was very similar to those of *FBP7* and *FBP11* in *Petunia* and *ScFBP11* in *S. chacoense*. Before fertilization, *ScFRK2* mRNAs are detected in ovule primordia in the young ovary (Fig. 5B) and ovule integuments of the mature ovary (Fig. 5C). Similarly, in *Petunia*, *FBP11* mRNA is detected in ovule primordia of the young ovary and the integuments of mature ovules (Angenent, Franken et al. 1995). We observed a similar distribution of *ScFBP11* mRNA in *S. chacoense* ovules (Fig. 5K). *ScFRK2* mRNA levels in ovules increased greatly after fertilization (2 DAP) and decreased back to pre-fertilization level by 4 DAP (Figs. 2B and C). *Petunia FBP7* and *FBP11* mRNA levels in ovules also increase after fertilization (Colombo, Franken et al. 1997). However, unlike *ScFRK2*, the levels of *FBP7* and *FBP11* remain high for several days and decrease after 7 DAP (Colombo, Franken et al. 1997).

ScFRK2 overexpression plants exhibit strikingly similar ovule defects as *FBP7/11* cosuppressed plants. In the ovary, ovules were transformed into filiform carpelloid

structures, with the uppermost ovules being more frequently transformed. An identical situation was also found in the *Petunia FBP7/11* cosuppression lines (Angenent, Franken et al. 1995). The filiform structures exhibit characteristics similar to the style, such as structures resembling transmitting tracts and cells projections at the extremity resembling stigmatic papillae (Fig. 4K). These were also characteristics found in CSs of *FBP7/11* cosuppressed plants (Angenent, Franken et al. 1995). The only difference is that the CSs found in *FBP7/11* cosuppressed plants were devoid of any structures resembling the nucellus (Angenent, Franken et al. 1995), whereas nucellus-like structures were found in the *ScFRK2* overexpression ovules at the beginning of abnormal growth (Fig. 4Y). This suggests that *ScFRK2* may be acting on ovule development at a later stage than *FBP7/11*.

FBP11 accumulation following fertilization has been associated with its role in seed development. Endosperm development is altered in *FBP7/11* cosuppression lines (Colombo, Franken et al. 1997). Between the time of pollination, and up to 9 DAP, seed development is unaffected. However, later on, the endothelium of the ovule starts to degenerate. By 18 DAP, the endothelium completely degenerates, which leads to disturbance of endosperm development and delayed embryo development (Colombo, Franken et al. 1997). *ScFRK2* overexpression lines also exhibited delay in embryo development. Wild type fruits 21 DAP contained a large proportion of mature embryos, the remaining embryos being at the walking-stick stage. In *ScFRK2-OX* lines, embryo development was delayed, and at 21 DAP, most embryos are still at the late torpedo stage (Table I). Although only a few ovules develop to mature seeds (around six per fruit compared to more than 100 seeds in WT plants), this delay has been consistently and repeatedly observed. These embryos would normally correspond to the ones observed 16 to 17 DAP in a WT plant. We also observed a small fruit phenotype (Figs. 3B and C). Mutations in *STK*, an *Arabidopsis* ortholog of *FBP7/11*, also causes defects in fruit (silique) development (Pinyopich, Ditta et al. 2003).

Phenotype similarities between *ScFRK2-OX* plants and *FBP7/11* cosuppressed plants suggested that *ScFRK2* may be interfering with the function of class D MADS-box

genes. On the contrary to our expectation, *ScFRK2* overexpression resulted in up-regulation of *ScFBP11* (Fig. 5L). If *ScFBP11* is up-regulated in our *ScFRK2-OX* plants, how do they phenocopy *FBP7/11* down-regulated plants and *AG* up-regulated plants? There are at least two possible explanations for this apparent discrepancy. Firstly, up-regulation of *ScFBP11* may cause ectopic expression of an *AG* ortholog, which subsequently may cause ovule to CS conversion in transgenic plants. In *Arabidopsis*, ectopic expression of class D gene *STK* causes ectopic accumulation of *AG* transcripts (Favaro, Pinyopich et al. 2003). Unfortunately, we do not have information regarding the expression levels of *AG* orthologs, because *AG* orthologs have not been cloned from *S. chacoense*. Secondly, ectopically-expressed *ScFBP11* may confer *AG* function due to functional redundancy between class C and D MADS-box genes. Functional redundancy between class C and D genes have been reported in *Arabidopsis* in which loss of ovule identity occurs only when both C and D gene functions are lost (Pinyopich, Ditta et al. 2003). Furthermore, *35S::STK* partially restores *AG* function in *ag1* mutants (Favaro, Pinyopich et al. 2003). In either way, the fact that *ScFBP11* expression was altered by *ScFRK2* overexpression suggests that there are at least some interactions, direct or indirect, between the *ScFRK2* and *ScFBP11* pathways.

To further identify target genes of the *ScFRK2* pathway, we examined global changes in gene expression levels in transgenic plants using a microarray analysis. We identified genes differentially regulated between transgenic and wild-type ovaries (Supplementary Table 1). Particularly interesting is the down-regulation of *LEUNIG* (*LUG*) in *ScFRK2-OX* ovaries. The *lug* mutation was initially identified as an enhancer of *ap2* mutant defects (Liu and Meyerowitz 1995). Like *ap2* and *bell* mutation, *lug* mutation causes ectopic expression of *AG*, suggesting that *LUG* is a negative regulator of *AG* (Liu and Meyerowitz 1995). The *lug* mutation alone causes abnormal gynoecium development where two carpel valves remain open (Liu, Franks et al. 2000). *LUG* mRNA accumulation in ovules suggest that *LUG* is also involved in ovule development (Conner and Liu 2000). *LUG* works redundantly with *AINTEGUMANTA* (*ANT*), another negative regulator of *AG*, to control ovule development. Double mutants of *lug* and *ant* causes complete abolishment

of ovules as well as other marginal tissues of gynoecium (Liu, Franks et al. 2000). Down-regulation of a LUG ortholog predicts up-regulation of AG ortholog in our transgenic plants and is consistent with the ovule phenotype. However further identification and expression analyses of AG orthologs will be necessary to confirm this point. Finally, it will be interesting to know if any of the differentially expressed genes are regulated by class C or D MADS box genes.

Discussion et perspectives

Dans cette thèse, les programmes transcriptionnels exprimés lors de la reproduction sexuée chez la solanacée modèle *Solanum chacoense* à différents stades de développement reproductifs ont été caractérisés. Ce programme inclus le développement du gamétophyte femelle, la pollinisation, la fécondation et tous les stades du développement embryonnaire du zygote à l'embryon mature. Une analyse de ces programmes transcriptionnelles a donné une vue globale sur les processus biologiques activés lors de la reproduction sexuée chez les plantes à fleur et peut être exploité chez d'autres espèces par orthologie de séquences afin de caractériser des gènes potentiellement impliqués dans ces processus. Il faut se rappeler que cette analyse représente un point de départ pour des études fonctionnelles détaillées. Une validation expérimentale des gènes candidats est nécessaire pour confirmer les résultats obtenus ici et pour définir les mécanismes moléculaires qui contrôlent la structuration cellulaire et biochimique de la différenciation des embryons chez les plantes ainsi que tous les événements contrôlant l'embryogenèse depuis le dépôt de pollen sur le stigma jusqu'à la fécondation. Ma thèse se structure en trois chapitres comprenant, l'effet de la surexpression d'une protéine kinase impliquée dans la reproduction sexuée sur le gamétophyte femelle, l'effet de différentes pollinisations à distance dans l'ovaire ainsi que l'effet d'autres traitements comme la blessure du style et le traitement par l'hormone volatile MeJA et finalement, l'étude globale du transcrit au cours de l'embryogenèse. Afin de comprendre les mécanismes de régulation pendant toutes les étapes de la reproduction sexuée, un projet de séquençage des ESTs à partir d'une banque d'ADNc d'ovules couvrant les stades de développement embryonnaire du zygote au stade torpédo chez *S. chacoense*, génotype G4 (allèles d'auto incompatibilité S₁₂S₁₄) a été initié au sein de notre laboratoire (Germain, Rudd et al. 2005). Les analyses des séquences ont révélé que 82% ces 7741 ESTs étaient de gènes à copie unique (unigènes) et ces derniers ont été exploités pour construire des puces à ADN. L'utilisation de cette technique permet de comparer le profil

d'expression des milliers de gènes simultanément. En effet, l'information obtenue à l'issue d'expériences de biopuces d'ADN s'est révélée très informative et a permis d'avoir une vision globale des mécanismes moléculaires impliqués dans les processus biologiques investigués.

La plus grande motivation biologique dans les expériences de puces à ADN est de détecter l'expression différentielle de centaines de gènes. Et ce, d'identifier les changements d'expression des gènes dans des conditions différentes ou de traitement entre les différents types d'échantillons de cellules. Avec des dizaines de milliers de sondes sur la puce, et le fait que chaque gène n'est pas une unité indépendante (i.e. plusieurs gènes sont co-regulés ou régulent l'expression d'autres gènes) le taux d'erreur mesuré par des méthodes statistique traditionnelles telles que la procédure de correction de Bonferroni peuvent être trop stringents. En 1995, Benjamini et Hochberg ont proposé une nouvelle mesure du taux d'erreur, le taux de fausses découvertes (FDR) qui est la proportion attendue de faux rejets de tous les rejets, et FDR contrôle une procédure par des tests statistiques indépendants. Si l'estimation de la proportion des hypothèses nulles vrai est incorporés dans la procédure de contrôle de Benjamini et Hochberg, le FDR peut être contrôlé à proximité d'un niveau de signification pré-sélectionné.

Dans nos études, plusieurs expériences ont été comparées et plusieurs de ces événements ne sont pas indépendants dans leur nature et représentent une succession d'étapes dans le même fond biologique (exp, embryogenèse, pollinisation....). Nous avons néanmoins choisi une analyse statistique beaucoup plus stringente que la normale afin de ramener le nombre de gènes à analyser à un niveau raisonnable. Ultimement, nous avons identifié les gènes avec une différence statistiquement significative en utilisant la méthode Welch ANOVA couplé à la correction des tests multiples de «Benjamini et Hochberg » avec un « False Discovery Rate» (FDR) inférieur à 1%. Cette méthode compare les profils de chaque expérience avec ceux mesurés dans les comparaisons contrôle contre contrôle. Théoriquement, environ 1% des gènes identifiés serait prévu de passer la restriction par

hasard pour chaque condition mais il est tenu de rappeler que ces conditions sont liées entre elles ce qui réduit grandement le nombre réel de faux positifs. L'utilisation d'autres méthodes d'analyse statistique change le nombre de gènes trouvés (surtout les transcrits ayant un plus faible taux de changement), mais ne modifie pas de façon significative les conclusions majeures de nos études. Par exemple, l'utilisation du test *t*, ou test de Student sans aucune stringence montre une modulation de 3458 gènes pendant l'embryogenèse. Le même test utilisé avec une correction des tests multiples de «Benjamini et Hochberg» sélectionne environ la moitié des gènes trouvés auparavant, soit 1645 gènes. Ce test compare les profils obtenu à un moment avec la présomption que ces transcrits ne sont pas modulés. Alors que l'utilisation de l'ANOVA, filtre plus les gènes modulés avec une diminution des faux d'erreur, soit 1888 gènes et 1442 gènes avec une correction des tests multiples de «Benjamini et Hochberg». Finalement, la stringence de notre analyses a été augmentées en limitant le «cutoff» de fold change choisi, soit 2-fold. L'utilisation de 4 réplicas biologiques indépendants et le fait que nous détectons de fortes corrélations avec les «GO term», nous confirme que nos résultats sont vrais avec un minimum de faux positif de 1%. L'utilisation d'autres techniques de validation statistique comme «post hoc» pourrait confirmer nos études. Cette analyse utilise des tests de multiples comparaisons (MCP) et utilise aussi les mêmes critiques que nous avons utilisé soit FDR afin d'obliger en général une augmentation des risques de l'analyse. Dans la biologie moderne, notamment, des tests MCP permettent de prendre en compte le risque de façon correcte malgré le grand nombre de tests effectués.

Les analyses de puces d'ADN ont permis tout d'abord d'identifier les gènes différentiellement régulés dans chacune des conditions étudiées. Ensuite, la classification des gènes dans des groupes fonctionnels permet de décrire les différentes fonctions cellulaires impliquées. Aussi, la comparaison des modes d'expression des gènes dans les différentes conditions et l'assemblage des gènes présentant des profils similaires au sein de groupes fonctionnels en utilisant les méthodes de “Clustering” a permis d'identifier les

gènes co-exprimés et ainsi de visualiser les interactions et les mécanismes de co-régulation. Le “Clustering” permet aussi d’attribuer une fonction putative aux gènes dont la fonction est inconnue. Enfin, l’analyse transcriptomique par biopuce est une approche globale pour la caractérisation des mécanismes moléculaires impliqués dans un processus biologique permettant de comprendre la problématique scientifique dans son intégralité en dégageant des hypothèses concernant le réseau de gènes et de protéines au niveau des systèmes biologiques.

Un grand nombre de bases de données indiquant les résultats d’expériences de biopuces menées sur différentes espèces végétales telles que GENEVESTIGATOR, TAIR, BarleyExpress ou encore SGMD (Soybean Genomics and Microarray Database) sont déjà disponibles *via* internet (Rhee, Beavis et al. 2003; Alkharouf and Matthews 2004; Zimmermann, Hirsch-Hoffmann et al. 2004; Tang, Shen et al. 2005). Des banques de données plus généralistes cataloguant l’ensemble des données d’expression génique obtenues chez diverses espèces ont également été développées, comme par exemple les bases des données ArrayExpress et NCBI GEO (Barrett, Suzek et al. 2005; Parkinson, Sarkans et al. 2005; Sarkans, Parkinson et al. 2005). Toutes ces initiatives, offrant un accès libre et facile à l’ensemble des données de profils transcriptionnels, ne permettent pas toutefois de les comparer aux résultats de nos propres analyses et de les intégrer à nos réflexions. En effet, étant donné le large éventail de procédés techniques disponibles pour réaliser ces analyses (type de puce à ADN utilisé, dispositif expérimental mis en œuvre, chimie de marquage des sondes et procédure d’hybridation, méthode d’analyse statistique), une uniformisation des protocoles expérimentaux semble indispensable afin que les résultats obtenus soient comparables entre eux.

L’objectif crucial des analyses de biopuces à ADN est la sélection, parmi les gènes différentiellement exprimés, de gènes candidats susceptibles de jouer des rôles clés dans le processus étudié. Dans l’espoir d’améliorer la sélection des gènes candidats et ainsi de

mieux appréhender le problème biologique posé, plusieurs projets dans ce sens ont déjà été entrepris avec, par exemple, la création de la banque de protéines non redondante PIR (Protein Information Resource) regroupant l'ensemble des informations concernant 283,000 protéines (Wu, Yeh et al. 2003), ou la base de donnée iProClass, qui intègre plusieurs données comprenant les relations familiales ainsi que structurelle et fonctionnelle de classifications et de fonctionnalités (Huang, Barker et al. 2003). Ou encore l'élaboration de Gene Ontology Consortium (GO) (<http://www.geneontology.org>) qui fournit une nomenclature contrôlée et structurée, décrivant les produits des gènes en fonction de leurs processus biologiques, les fonctions moléculaires et les composants cellulaires chez une espèce de manière indépendante (Ashburner, Ball et al. 2000). Cette nomenclature pouvant être notamment utilisée pour l'analyse automatisée des profils d'expression des gènes (Volinia, Evangelisti et al. 2004). Un autre projet original de regroupement d'informations est le MedBlast (Tu, Tang et al. 2004) permettant d'accéder à toute la bibliographie évoquant une séquence particulière, ou encore le projet développé chez *A. thaliana* par (Louis, Chiapello et al. 2002) associant des gènes en fonction de leur apparition commune dans la littérature selon l'hypothèse que des séquences citées conjointement sont susceptibles d'être engagées dans un même mécanisme. Ces initiatives prometteuses doivent être poursuivies dans le but de regrouper toutes les données disponibles et pouvoir intégrer les données dans des systèmes biologiques.

Chez la plupart des angiospermes, le gamétophyte femelle (appelé aussi, sac embryonnaire ou mégagamétophyte) contient sept cellules (huit noyaux) et est encastré dans le tissu maternel sporophytique. L'analyse du mégamétophyte est importante pour plusieurs raisons. Biologiquement, le sac embryonnaire est l'aspect intégral du cycle de vie de la plante et est essentiel pour la formation des graines. En plus, il joue un rôle essentiel dans chaque étape de la reproduction sexuée. Durant la fécondation, le mégagamétophyte participe au guidage des tubes polliniques (Hulskamp, Schneitz et al. 1995; Ray, Park et al. 1997; Shimizu and Okada 2000; Higashiyama, Yabe et al. 2001) et contrôle la fécondation

de la cellule centrale et de la cellule œuf (Russell 1992; Russell 1996). Après la fécondation, les gènes exprimés dans le gamétophyte femelle participe à l'induction du développement des graines (Ohad, Margossian et al. 1996; Chaudhury, Ming et al. 1997; Grossniklaus, Vielle-Calzada et al. 1998) et jouent un rôle dans le contrôle du développement de l'albumen et /ou de l'embryon (Drews, Lee et al. 1998; Chaudhury and Berger 2001; Chaudhury, Koltunow et al. 2001). Bien que les études cytologiques du gamétophyte femelle sont très bien détaillées, très peu est connu concernant les processus génétique et moléculaire contrôlant le développement et la fonction du sac embryonnaire.

Plusieurs milliers de gènes sont prédis être impliqués dans le développement du sac embryonnaire. Malgré des décennies de recherche sur la reproduction sexuée chez les plantes, les mécanismes génétiques qui contrôlent le développement du sac embryonnaire et les interactions entre le sac embryonnaire et le tube pollinique sont encore mal caractérisés. L'utilisation des mutants où le sac embryonnaire est absent ou ayant un développement anormal constitue un bon modèle pour identifier des gènes potentiellement impliqués dans l'initiation et le développement du mégagamétophyte. En effet, chez *Arabidopsis*, 225 gènes ont été identifiés comme étant dérégulés chez le mutant *spl/nzz* (Yu, Hogan et al. 2005), 71 chez *dif1* (Steffen, Kang et al. 2007), 398 chez *dif1* en utilisant tiling array, 77 chez *myb98* (Jones-Rhoades, Borevitz et al. 2007) et 527 chez *coa* (Johnston, Meier et al. 2007). Les auteurs ont utilisé les analyses par puces d'ADN pour comparer l'expression des gènes dans les ovules de type sauvage à celui des ovules dépourvus de sac embryonnaire ou qui montre une structure anormale du sac embryonnaire. Dans cette étude nous avons utilisé un mutants d *S. chacoense*: *Scfrk2* impliqué dans l'identité des ovules. Nous avons identifié respectivement 213 gènes chez *scfrk2* qui montraient une variation du niveau d'induction ou de répression de supérieure ou égale à au moins 1.5 fois par rapport à la plante sauvage. Ces résultats complémentent grandement les autres études récemment publiées. La détection de plusieurs gènes dont la fonction est inconnue limite l'ampleur de notre compréhension, mais donne de nouvelles pistes pour les analyses fonctionnelles.

Reste encore des milliers de gènes à identifier afin de mieux comprendre les mécanismes qui contrôlent la mégagaméto-génèse.

Le phénotype de *ScFRK2* chez *S. chacoense* est similaire à celui de *FBP7* et *FBP11*, deux MADS box impliquées dans le déterminisme de l'identité des ovules chez *Pétunia* (Angenent, Franken et al. 1995; Gray-Mitsumune, O'Brien et al. 2006). En effet, chez *Pétunia*, la répression des gènes de classe MADS-box D, *FBP7* et *FBP11* permet une transformation homeotiques des ovules en carpelles. Le fait que l'expression de l'orthologue de *FBP7/11* chez *S. chacoense* (*ScFBP11*) est altéré chez le mutant *ScFRK2*, ainsi que *FBP7/11* et *ScFRK2* montre la même signature transcriptionnelle ainsi que le même phénotype suggère que la protéine kinase *ScFRK2* pourrait intervenir avec les gènes MADS-box de la classe D du modèle ABCDE. De plus, parmi les gènes réprimés on trouve un des gènes de régulation négatif de *AG*, *LEUNIG* (Liu and Meyerowitz 1995), suggérant par conséquent une activation de l'orthologue de *AG* dans le mutant *Scfrk2*. D'autres études sont nécessaires pour confirmer l'interaction entre *ScFRK2* et les orthologues de la classe D chez les solanacées. Chez *A. thaliana*, trois orthologues de cette MAPKKK: At5g67080 (MAPKKK19), At3g50310 (MAPKKK20) et At4g36950 (MAPKKK21) présentent une similarité de séquence d'environ 50% en acides aminés. Une analyse détaillée de ces trois protéines kinases nous aidera à élucider leur fonction biologique chez *A. thaliana*. Ce projet est déjà en cours et plusieurs volets sont étudiés incluant la localisation cellulaire des protéines, l'expression spatiale des transcrits et les analyses de phénotypes des mutants d'insertions T-DNA.

Comme élucidé dans le premier chapitre de ma thèse, lors du développement embryonnaire des milliers de gènes sont modulés. Cependant, certains gènes sont régulés à distance dans l'ovaire avant même que les tubes polliniques n'atteignent les ovules, c'est-à-dire avant que la fécondation n'ait lieu (Lantin, O'Brien et al. 1999). Ces gènes doivent donc réagir à une signalisation de longue distance provenant d'autres phénomènes que la fécondation. Pour déterminer comment la régulation génique dans les ovules dépend de la

pollinisation, plusieurs types de pollinisations ont été testés en utilisant différentes sources de pollen (compatible, incompatible, semi-compatible et interspécifique) à différent temps après pollinisation (6, 24 et 48 HAP). Nos données suggèrent que l'ovaire perçoit le signal différemment dépendant du type de pollen et/ou de la distance parcourue par le pollen. Plusieurs types de signalisation de longue distance sont décrits dans la littérature. Parmi les plus étudiées dans différents processus biologiques, on retrouve la signalisation chimique, hydraulique et électrique. Le signal émis lors de la pollinisation est de nos jours encore mal connu. Nos données montrent l'implication de plusieurs hormones, suggérant ainsi des types de signaux, entre autre chimiques suite à une réponse à la pollinisation. Un autre résultat intéressant est le fait que la forme de régulation des gènes suite à une pollinisation est une répression plutôt qu'une activation. La croissance du tube pollinique incite la détérioration et la mort des cellules ou des tissus spécifiques dans le style. Afin de déterminer si la mort cellulaire pourrait aussi déclencher l'expression de gène à distance dans l'ovaire, nous avons mimé ce phénomène par une blessure au style. Nos résultats suggèrent que l'ovaire perçoit le signal en partie comme une blessure, tôt après la pollinisation et ce indépendamment du type de pollen utilisé, puis de façon plus précise après, selon le type de pollen utilisé. Nos résultats démontrent également que la pollinisation incompatible ressemble plus à une blessure que la pollinisation compatible. Cette ressemblance du signal est confirmée par le traitement par l'hormone de stress, le MeJA. L'ensemble des données montre en partie un chevauchement entre le programme génique suite à une pollinisation et une réponse au stress. Plusieurs études ont confirmé l'implication des gènes de stress et de défense dans plusieurs processus développementaux, tel que les LTP, les enzymes de la voie de biosynthèses de métabolites secondaires comme les flavonols.

Malgré que le séquençage de l'espèce modèle *A. thaliana* soit complet, rares sont les études portant sur le développement embryonnaire, dû aux difficultés liées à la manipulation des organes reproducteurs. Toutefois, des études prometteuses en utilisant des techniques de pointe combinées aux biopuces d'ADN ont pu donner des points de départ pour mieux comprendre la régulation génique au cours de l'embryogenèse. Ce type d'étude est

tellement sensible et exigeant qu'il a fallu plusieurs années de travail pour pouvoir compléter l'étude chez la plante modèle *A. thaliana*. Quoique le décryptage des gènes impliqués dans les processus de reproduction chez *Arabidopsis* puisse être exploité chez d'autres espèces ayant un impact économique important, les différences morphologiques et génétiques importantes entre cette plante modèle et la majorité des plantes d'intérêt économique cautionne l'utilisation d'autres modèles d'étude. Ainsi en était-il avant l'ère *Arabidopsis*. De plus, la diminution constante des coûts d'analyse génomique et de séquençage rend maintenant possible l'utilisation d'autres modèles performants. Ainsi, parmi la très grande famille des solanacées, nous avons utilisé comme plante modèle *Solanum chacoense*, une plante auparavant utilisé principalement dans notre laboratoire pour des études sur les barrières reproductives liées à l'auto-incompatibilité. *S. chacoense*, en plus d'être facilement manipulable au niveau génétique forme un fruit comme la tomate et une tubercule comme la pomme de terre, donc un modèle d'étude hybride. Quoique le séquençage complet de *S. chacoense* n'est pas encore envisagé, nous disposons actuellement au laboratoire de plusieurs milliers d'ESTs, issues des ovules couvrant différents stades d'embryogenèse du zygote jusqu'au stade torpédo. La banque représente 7741 ESTs dont 6347 unigènes répertoriés dans les banques de données publiques Genbank. De plus, plus de 700 000 ESTs de tomate, de pomme de terre et d'autres solanacées sont disponibles dans la base de données Genbank (http://www.ncbi.nlm.nih.gov/dbEST/dbEST_summary.html), et plusieurs projets de séquençages de génome sont en cours pour la tomate et la pomme de terre. Plusieurs autres projets de séquençage transcriptomique sont aussi en cours, dont ceux de notre laboratoire (pyroséquençage 454 d'ARNm d'ovules et de tubes polliniques). Une librairie de BAC (bacterial artificial chromosome) est aussi maintenant disponible dans le laboratoire du Professeur Mario Cappadocia. Ces ressources sont utilisées pour enrichir nos connaissances sur les différents stades de la reproduction sexuée.

Afin de mieux comprendre les voies de régulation impliquées lors de l'embryogenèse, nous avons évalué le changement transcriptomique dans les ovules de *S.*

chacoense type sauvage après différents temps de pollinisation de 0 à 22 jours après pollinisation à un intervalle de deux jours versus des plantes non pollinisées. L'utilisation de test statistique ANOVA (*t*-test) a révélé 1997 transcrits montrant un changement statistiquement significatif dans au moins un des points de temps comparés au contrôle ($p < 0.01$). Parmi eux, 1240 transcrits ont montré un taux d'induction de plus ou moins de 2-fold. Ces gènes différentiellement exprimés ont été regroupés selon la similitude de leur profil d'expression en utilisant la méthode du «two-dimentional hierarchical clustering». Les résultats obtenus montrent clairement une séparation de nos données en trois groupes majeurs de gènes qui spécifient le stade précoce (455 gènes), intermédiaire (602 gènes) et tardif (203 gènes) de l'embryogenèse (chapitre 1, figure 2a, 2b). Dans le but de sélectionner les gènes spécifiques aux ovules, une analyse comparative entre les gènes régulés dans l'ovule et ceux régulés dans des organes végétatifs (feuilles, étamines et styles) a été réalisée. De ce nombre, 93.2% (955 gènes) des gènes différentiellement exprimés spécifient le développement embryonnaire. La séparation de ces gènes en se basant sur leur profil d'expression durant les trois stades majeurs de développement embryonnaire a montré qu'un grand nombre de gènes sont spécifique à chaque stade de transition précoce, intermédiaire et tardif suggérant un très faible chevauchement et donc, la grande spécificité de chaque stade majeur du développement embryonnaire. En effet, parmi les groupes fonctionnels enrichis, nous avons montré que l'activation du cycle cellulaire et la biosynthèse des protéines caractérisent le stade précoce; la dégradation des protéines et le transport caractérisent le stade intermédiaire, alors que les protéines associées aux réserves spécifient le stade tardif.

Afin de pousser plus à fond notre étude, nous avons voulu voir si cette spécificité est liée au trois stades majeurs ou plutôt à des transitions de chaque stade de 0 à 22 DAP. Pour répondre à cette question, le regroupement par le “clustering” de type K-means a été effectué sur l'ensemble de gènes. Hennig et al. (2004) ont prédit neuf modèles dynamiques d'expression de gènes impliqués dans la reproduction et le développement d'*Arabidopsis* et a utilisé ce regroupement par profil d'expression pour sélectionner des gènes candidats

(Hennig, Gruisse et al. 2004). Cela semble être une amélioration en termes de sélection des gènes. Cependant, le nombre de points utilisés est d'une importance critique dans cette façon d'analyse. Utiliser trois points est le minimum et crée automatiquement 9 profils différents. Dans notre étude, nous avons voulu séparer dans le temps les différents profils d'expression des gènes d'une manière significative au cours du développement des embryons de 0 à 22 jours après pollinisation. Douze points ont été utilisés, et 15 groupes ont été définis. Cette façon nous a permis d'élucider plusieurs profils différents et ainsi d'isoler des groupes de gènes qui spécifient la transition d'un stade à l'autre. Pour confirmer ces résultats nous avons comparé, en utilisant les analyses par Volcano Plot, chaque stade de développement embryonnaire étant comparé au temps 0 (contrôle non fécondé). En gardant les mêmes critères de sélection ($FDR \leq 0.01$ et $\geq \pm 2$ fold cut-off), les stades 2, 4, 8 et 16 DAP montraient une spécificité plus intéressante par rapport au reste des points étudiés. À 2 DAP, la moitié des gènes spécifiques se sont révélés des membres du groupement fonctionnel spécifiant des gènes liés à la traduction des protéines. À 4 DAP, un enrichissement de gènes liés au stress et à la défense ainsi que des gènes codant pour des protéines qui ont des fonctions de liaison est remarqué. Les principaux groupes fonctionnels représentés à 8 DAP sont l'énergie, la biogénèse et l'organisation des chromosomes, ainsi que la régulation du cycle cellulaire. Finalement, le stade 16 DAP a été spécifiquement enrichi par trois groupes fonctionnels correspondant à la régulation hormonale, la transduction des signaux et le transport. Ces deux types d'analyses nous montrent en général, que plusieurs gènes et ainsi des processus biologiques spécifiques, sont impliqués dans plusieurs stades de développement embryonnaire et peu de gènes spécifient un stade de transition précis.

Grâce à cette étude transcriptomique, plusieurs hypothèses concernant les principaux processus biologiques impliqués lors du développement embryonnaire chez la pomme de terre sauvage peuvent être proposées. Nos résultats ont révélé que pendant l'embryogenèse plusieurs groupes fonctionnelles sont enrichis tel que, la différenciation, la communication

cellulaire, la régulation transcriptionnelle, la biosynthèse des protéines, la dégradation des protéines et l'énergie.

Bien que cette étude reflète des mécanismes de régulation transcriptionnelle contrôlant l'embryogenèse, d'autres types de régulation de l'activité génique ayant lieu au niveau post-transcriptionnel. En effet, l'observation parmi nos ESTs et dans nos gènes différemment régulés, d'un enrichissement de séquences codant pour des protéines jouant un rôle potentiel dans la dégradation des ARNm ou dans le catabolisme protéique tels que l'ubiquitine ou des éléments du système ubiquitine-protéasome confirme l'implication probable de ce type de contrôle au cours du développement embryonnaire. Il serait donc intéressant de mener, en complément de cette analyse du transcriptome, des études protéomiques et métabolomiques permettant de mettre en évidence des événements de régulation post-transcriptionnelle afin de mieux cibler les gènes et les voies métaboliques essentiels au bon déroulement de l'embryogenèse et ainsi intégrer toutes les données dans un ou plusieurs modèles en adoptant une approche de type biologie des systèmes. L'identification des gènes impliqués dans les processus de reproduction chez *S. chacoense* a un impact économique important, car leurs homologues dans les plantes cultivées sont des cibles potentielles en vue d'améliorer le rendement et la qualité des semences par la sélection conventionnelle ou approches biotechnologiques. Dans l'éventuelle conservation de ces mécanismes de régulation parmi l'ensemble des plantes dicotylédones, l'exploitation de ces connaissances pour des plantes modèles disposant d'un large arsenal d'outils génétiques et moléculaires permettrait de poursuivre cette étude plus aisément. Cette transposition permettrait d'appréhender ce processus dans sa globalité en effectuant, par exemple, des expériences de sur- et sous-expression de l'ensemble des gènes impliqués dans la voie de signalisation afin de caractériser la succession des événements moléculaire menant au développement correct de la graine.

Conclusion

Comprendre l'expression et la régulation des gènes pendant les différents stades de la reproduction sexuée chez les plantes à fleurs demande des expériences à grande échelle qui permettront de soustraire les contributions des cellules du sac embryonnaire du tissu sporophytique qui l'entoure. Dans notre laboratoire un projet de séquençage des ESTs issus des ovules couvrants différents stades d'embryogenèse (zygote au stade torpille) a été initié (Germain, Rudd et al. 2005). Nous avons utilisé ces banques de ESTs pour fabriquer une puce d'ADN possédant plus de 7000 ESTs. Cette dernière a été utilisée pour identifier un grand nombre de gènes candidats modulés: 1- dans l'embryon durant les différents stades d'embryogenèse; 2- à distance dans les ovaires après différents types de pollinisations ainsi que des traitements mécaniques par blessure de style ou hormonaux, en utilisant le MeJA; 3- et enfin dans les différents types de cellules du gamétophyte femelle par une stratégie de soustraction génétique.

Nous avons pu élargir la fenêtre du transcriptome du gamétophyte femelle en utilisant une comparaison de profils d'expression entre le type sauvage et le mutant *Scfrk2*. Ce dernier, montre une structure filiforme anormale des ovules qui réitère le programme génétique du carpelle entier. La majorité des gènes identifiés n'ont pas été identifiés dans d'autres études. D'un autre côté, avant même que les tubes polliniques n'arrivent aux ovules, nous avons pu montrer que certains gènes répondent à distance. Cette réponse est dûe fort probablement à un signal émis par la croissance du tube pollinique qui cause la mort cellulaire au niveau des tissus de style. D'autre côté, ce signal dépend du type de pollen et de la distance parcourus par le tube pollinique dans le style. Nous avons aussi constaté que la régulation génique lors de la pollinisation est en partie similaire à une réponse au stress, principalement, au tout début de la croissance des tubes dans le stigmate et le style, peu importe le type de pollinisation et plus spécifiquement, les pollinisations incompatibles. Ceci a aussi été confirmé par l'application de blessure physique dans la partie supérieure du style de même que lors de traitement avec une hormone de blessure comme le MeJA.

Durant l'embryogenèse, les résultats ont indiqué que l'embryon subit des changements dramatiques dans l'expression des gènes au cours du développement. Nous avons pu

montrer qu'en plus de spécificités liées aux transitions d'un stade à l'autre, le profil d'expression des gènes impliqués lors de l'embryogenèse suit trois transitions essentielles caractérisant : les stades de développement embryonnaire précoce, intermédiaire et tardif. Les données présentées permettent d'isoler plusieurs groupes fonctionnels, enrichis notamment dans les fonctions suivantes: la régulation de la transcription, la signalisation, le transport, l'énergie, le métabolisme, le cycle cellulaire, la biogénèse des protéines et la dégradation des protéines.

Les fonctions biologiques de la plupart des gènes restent à déterminer, et l'expression de données dans cette étude peut aider à identifier des fonctions putatives lors de la reproduction sexuée. L'inactivation de ces gènes, sera à entreprendre afin de comprendre leurs rôles précis dans le développement du sac embryonnaire et de l'embryon.

Bibliographie

- Abe, M., H. Katsumata, et al. (2003). "Regulation of shoot epidermal cell differentiation by a pair of homeodomain proteins in *Arabidopsis*." Development **130**(4): 635-643.
- Abe, M., T. Takahashi, et al. (1999). "Cloning and characterization of an L1 layer-specific gene in *Arabidopsis thaliana*." Plant Cell Physiol **40**(6): 571-580.
- Aharoni, A., L. C. Keizer, et al. (2002). "Novel insight into vascular, stress, and auxin-independent and -independent gene expression programs in strawberry, a non-climacteric fruit." Plant Physiol **129**(3): 1019-1031.
- Aida, M., T. Ishida, et al. (1999). "Shoot apical meristem and cotyledon formation during *Arabidopsis* embryogenesis: interaction among the CUP-SHAPED COTYLEDON and SHOOT MERISTEMLESS genes." Development **126**(8): 1563-1570.
- Aida, M., T. Vernoux, et al. (2002). "Roles of PIN-FORMED1 and MONOPTEROS in pattern formation of the apical region of the *Arabidopsis* embryo." Development **129**(17): 3965-3974.
- Alba, R., P. Payton, et al. (2005). "Transcriptome and Selected Metabolite Analyses Reveal Multiple Points of Ethylene Control during Tomato Fruit Development." Plant Cell **17**(11): 2954 - 2965.
- Alkharouf, N. W. and B. F. Matthews (2004). "SGMD: the Soybean Genomics and Microarray Database." Nucleic Acids Res **32**(Database issue): D398-400.
- Altmann, T., G. Felix, et al. (1995). "Ac/Ds transposon mutagenesis in *Arabidopsis thaliana*: mutant spectrum and frequency of Ds insertion mutants." Mol Gen Genet **247**(5): 646-652.
- Alvarez, J. and D. R. Smyth (1999). "CRABS CLAW and SPATULA, two *Arabidopsis* genes that control carpel development in parallel with AGAMOUS." Development **126**(11): 2377-2386.
- Angenent, G. C. and L. Colombo (1996). "Molecular control of ovule development." Trends in Plant Science **1**(7): 228-232.
- Angenent, G. C., J. Franken, et al. (1995). "A novel class of MADS box genes is involved in ovule development in petunia." Plant Cell **7**(10): 1569-1582.

- Angenent, G. C., J. Franken, et al. (1994). "Co-suppression of the petunia homeotic gene fbp2 affects the identity of the generative meristem." *Plant J* **5**(1): 33-44.
- Asai, T., G. Tena, et al. (2002). "MAP kinase signalling cascade in Arabidopsis innate immunity." *Nature* **415**(6875): 977-983.
- Ashburner, M., C. A. Ball, et al. (2000). "Gene ontology: tool for the unification of biology. The Gene Ontology Consortium." *Nat Genet* **25**(1): 25-29.
- Azumi, Y., D. Liu, et al. (2002). "Homolog interaction during meiotic prophase I in Arabidopsis requires the SOLO DANCERS gene encoding a novel cyclin-like protein." *Embo J* **21**(12): 3081-3095.
- Bajon, C., C. Horlow, et al. (1999). "Megasporogenesis in *Arabidopsis thaliana* L.: an ultrastructural study." *Sexual Plant Reproduction* **12**(2): 99-109.
- Balk, J., D. J. Aguilar Netz, et al. (2005). "The essential WD40 protein Cia1 is involved in a late step of cytosolic and nuclear iron-sulfur protein assembly." *Mol Cell Biol* **25**(24): 10833-10841.
- Barrett, T., T. O. Suzek, et al. (2005). "NCBI GEO: mining millions of expression profiles-database and tools." *Nucl. Acids Res.* **33**(suppl_1): D562-566.
- Barton, M. K. and R. S. Poethig (1993). "Formation of the shoot apical meristem in *Arabidopsis thaliana*: an analysis of development in the wild type and in the shoot meristemless mutant." *Development* **119**(3): 823-831.
- Becerra, C., P. Puigdomenech, et al. (2006). "Computational and experimental analysis identifies *Arabidopsis* genes specifically expressed during early seed development." *BMC Genomics* **7**: 38.
- Becker, J. D., L. C. Boavida, et al. (2003). "Transcriptional profiling of *Arabidopsis* tissues reveals the unique characteristics of the pollen transcriptome." *Plant Physiol* **133**(2): 713-725.
- Becraft, P. W. (2002). "Receptor Kinase Signaling in Plant Development." *Annu Rev Cell Dev Biol.*
- Becraft, P. W. and Y. Asuncion-Crabb (2000). "Positional cues specify and maintain aleurone cell fate in maize endosperm development." *Development* **127**(18): 4039-4048.

- Benschop, J. J., S. Mohammed, et al. (2007). "Quantitative phosphoproteomics of early elicitor signaling in Arabidopsis." *Mol Cell Proteomics* **6**(7): 1198-1214.
- Berardini, T. Z., S. Mundodi, et al. (2004). "Functional annotation of the Arabidopsis genome using controlled vocabularies." *Plant Physiol* **135**(2): 745-755.
- Berger, F., Y. Hamamura, et al. (2008). "Double fertilization - caught in the act." *Trends Plant Sci* **13**(8): 437-443.
- Bergmann, D. C., W. Lukowitz, et al. (2004). "Stomatal development and pattern controlled by a MAPKK kinase." *Science* **304**(5676): 1494-1497.
- Bih, F. Y., S. S. Wu, et al. (1999). "The predominant protein on the surface of maize pollen is an endoxylanase synthesized by a tapetum mRNA with a long 5' leader." *J Biol Chem* **274**(32): 22884-22894.
- Blein, J. P., P. Coutos-Thevenot, et al. (2002). "From elicitors to lipid-transfer proteins: a new insight in cell signalling involved in plant defence mechanisms." *Trends Plant Sci* **7**(7): 293-296.
- Boisson-Dernier, A., S. Frietsch, et al. (2008). "The peroxin loss-of-function mutation abstinence by mutual consent disrupts male-female gametophyte recognition." *Curr Biol* **18**(1): 63-68.
- Bowman, J., H. Sakai, et al. (1992). "SUPERMAN, a regulator of floral homeotic genes in Arabidopsis." *Development* **114**(3): 599-615.
- Bowman, J. L. (2000). "The YABBY gene family and abaxial cell fate." *Curr Opin Plant Biol* **3**(1): 17-22.
- Bowman, J. L., J. Alvarez, et al. (1993). "Control of flower development in Arabidopsis thaliana by APETALA1 and interacting genes." *Development* **119**(3): 721-743.
- Bowman, J. L., D. R. Smyth, et al. (1991). "Genetic interactions among floral homeotic genes of Arabidopsis." *Development* **112**(1): 1-20.
- Brand, U., J. C. Fletcher, et al. (2000). "Dependence of stem cell fate in Arabidopsis on a feedback loop regulated by CLV3 activity." *Science* **289**(5479): 617-619.
- Breton, C., A. Chaboud, et al. (1995). "PCR-generated cDNA library of transition-stage maize embryos: cloning and expression of calmodulin genes during early embryogenesis." *Plant Mol Biol* **27**(1): 105-113.

- Breyne, P., R. Dreesen, et al. (2002). "Transcriptome analysis during cell division in plants." *Proc Natl Acad Sci U S A* **99**(23): 14825-14830.
- Brucher, H. (1953). "Über das natürliche Vorkommen von Hybriden zwischen Solanum simplicifolium und Solanum subtilius im Aconquija Gebirge (On the natural occurrence of hybrids of Solanum simplicifolium and Solanum subtilius in the Aconquija range)." *Zeitschrift für induktive Abstammungs- und Vererbungslehre* **85**: 12-19.
- Brukhin, V., J. Gheyselinck, et al. (2005). "The RPN1 Subunit of the 26S Proteasome in Arabidopsis Is Essential for Embryogenesis." *Plant Cell* **17**(10): 2723-2737.
- Brummell, D. A., M. H. Harpster, et al. (1999). "Modification of Expansin Protein Abundance in Tomato Fruit Alters Softening and Cell Wall Polymer Metabolism during Ripening." *Plant Cell* **11**(11): 2203-2216.
- Burg, S. P. and M. J. Dijkman (1967). "Ethylene and Auxin Participation in Pollen Induced Fading of Vanda Orchid Blossoms." *Plant Physiol.* **42**(11): 1648-1650.
- Busi, M. V., C. Bustamante, et al. (2003). "MADS-box genes expressed during tomato seed and fruit development." *Plant Mol Biol* **52**(4): 801-815.
- Bussière, F., S. Ledû, et al. (2003). "Development of an efficient *cis-trans-cis* ribozyme cassette to inactivate plant genes." *Plant Biotechnology Journal* **1**(6): 423-435.
- Byrne, M. E., R. Barley, et al. (2000). "Asymmetric leaves1 mediates leaf patterning and stem cell function in Arabidopsis." *Nature* **408**(6815): 967-971.
- Calonje, M., R. Sanchez, et al. (2008). "EMBRYONIC FLOWER1 Participates in Polycomb Group-Mediated AG Gene Silencing in Arabidopsis." *Plant Cell*: tpc.106.049957.
- Canales, C., A. M. Bhatt, et al. (2002). "EXS, a putative LRR receptor kinase, regulates male germline cell number and tapetal identity and promotes seed development in Arabidopsis." *Curr Biol* **12**(20): 1718-1727.
- Carles, C. C. and J. C. Fletcher (2003). "Shoot apical meristem maintenance: the art of a dynamic balance." *Trends Plant Sci* **8**(8): 394-401.
- Casson, S., M. Spencer, et al. (2005). "Laser capture microdissection for the analysis of gene expression during embryogenesis of Arabidopsis." *Plant J* **42**(1): 111-123.

- Cazale, A.-C., M. Clement, et al. (2009). "Altered expression of cytosolic/nuclear HSC70-1 molecular chaperone affects development and abiotic stress tolerance in *Arabidopsis thaliana*." *J. Exp. Bot.* **60**(9): 2653-2664.
- Chandler, J. W., M. Cole, et al. (2007). "The AP2 transcription factors DORNROSCHEN and DORNROSCHEN-LIKE redundantly control *Arabidopsis* embryo patterning via interaction with PHAVOLUTA." *Development* **134**(9): 1653-1662.
- Chantha, S. C., B. S. Emerald, et al. (2006). "Characterization of the plant Notchless homolog, a WD repeat protein involved in seed development." *Plant Mol Biol* **62**(6): 897-912.
- Chantha, S. C., F. Tebbji, et al. (2007). "From the notch signaling pathway to ribosome biogenesis." *Plant Signal Behav* **2**(3): 168-170.
- Chanvivattana, Y., A. Bishopp, et al. (2004). "Interaction of Polycomb-group proteins controlling flowering in *Arabidopsis*." *Development* **131**(21): 5263-5276.
- Chaudhury, A. M. and F. Berger (2001). "Maternal control of seed development." *Semin Cell Dev Biol* **12**(5): 381-386.
- Chaudhury, A. M., A. Koltunow, et al. (2001). "Control of early seed development." *Annu Rev Cell Dev Biol* **17**: 677-699.
- Chaudhury, A. M., L. Ming, et al. (1997). "Fertilization-independent seed development in *Arabidopsis thaliana*." *Proc Natl Acad Sci U S A* **94**(8): 4223-4228.
- Chen, F. and K. J. Bradford (2000). "Expression of an Expansin Is Associated with Endosperm Weakening during Tomato Seed Germination." *Plant Physiol* **124**(3): 1265-1274.
- Chen, J.-G., H. Ullah, et al. (2001). "ABP1 is required for organized cell elongation and division in *Arabidopsis* embryogenesis." *Genes & Development* **15**(7): 902-911.
- Chen, Y.-H., H.-J. Li, et al. (2007). "The Central Cell Plays a Critical Role in Pollen Tube Guidance in *Arabidopsis*." *Plant Cell* **19**(11): 3563-3577.
- Cheong, Y. H., H. S. Chang, et al. (2002). "Transcriptional profiling reveals novel interactions between wounding, pathogen, abiotic stress, and hormonal responses in *Arabidopsis*." *Plant Physiol* **129**(2): 661-677.

- Cheung, A. Y. (1996). "The pollen tube growth pathway: its molecular and biochemical contributions and responses to pollination." *Sexual Plant Reproduction* **9**(6): 330-336.
- Cheung, A. Y., H. Wang, et al. (1995). "A floral transmitting tissue-specific glycoprotein attracts pollen tubes and stimulates their growth." *Cell* **82**(3): 383-393.
- Chevalier, D., M. Batoux, et al. (2005). "STRUBBELIG defines a receptor kinase-mediated signaling pathway regulating organ development in Arabidopsis." *Proc Natl Acad Sci U S A* **102**(25): 9074-9079.
- Christensen, C. A., S. W. Gorsich, et al. (2002). "Mitochondrial GFA2 is required for synergid cell death in Arabidopsis." *Plant Cell* **14**(9): 2215-2232.
- Christensen, C. A., E. J. King, et al. (1997). "Megagametogenesis in Arabidopsis wild type and the Gf mutant." *Sexual Plant Reproduction* **10**(1): 49-64.
- Christensen, C. A., S. Subramanian, et al. (1998). "Identification of gametophytic mutations affecting female gametophyte development in Arabidopsis." *Dev Biol* **202**(1): 136-151.
- Churchill, G. A. (2002). "Fundamentals of experimental design for cDNA microarrays." *Nat Genet Suppl*: 490-495.
- Clark, J. K. and W. F. Sheridan (1991). "Isolation and Characterization of 51 embryo-specific Mutations of Maize." *Plant Cell* **3**(9): 935-951.
- Clark, S. E. (2001). "Cell signalling at the shoot meristem." *Nat Rev Mol Cell Biol* **2**(4): 276-284.
- Clark, S. E., S. E. Jacobsen, et al. (1996). "The CLAVATA and SHOOT MERISTEMLESS loci competitively regulate meristem activity in Arabidopsis." *Development* **122**(5): 1567-1575.
- Clark, S. E., M. P. Running, et al. (1993). "CLAVATA1, a regulator of meristem and flower development in Arabidopsis." *Development* **119**(2): 397-418.
- Clark, S. E., M. P. Running, et al. (1995). CLAVATA3 is a specific regulator of shoot and floral meristem development affecting the same processes as CLAVATA1. *121*: 2057-2067.

- Clark, S. E., R. W. Williams, et al. (1997). "The CLAVATA1 gene encodes a putative receptor kinase that controls shoot and floral meristem size in *Arabidopsis*." *Cell* **89**(4): 575-585.
- Clarke, A. E. (1940). "Fertilization and early embryo development in the potato." *Am. Potato J.* **17**: 20-25.
- Coen, E. S. and E. M. Meyerowitz (1991). "The war of the whorls: genetic interactions controlling flower development." *Nature* **353**(6339): 31-37.
- Colombo, L., J. Franken, et al. (1995). "The petunia MADS box gene FBP11 determines ovule identity." *Plant Cell* **7**(11): 1859-1868.
- Colombo, L., J. Franken, et al. (1997). "Downregulation of ovule-specific MADS box genes from petunia results in maternally controlled defects in seed development." *Plant Cell* **9**(5): 703-715.
- Colombo, M., S. Masiero, et al. (2008). "AGL23, a type I MADS-box gene that controls female gametophyte and embryo development in *Arabidopsis*." *Plant J.* **54**(6): 1037-1048.
- Conner, J. and Z. Liu (2000). "LEUNIG, a putative transcriptional corepressor that regulates AGAMOUS expression during flower development." *Proc Natl Acad Sci U S A* **97**(23): 12902-12907.
- Cormier, P. (2000). "Translation factors : from protein synthesis to cell cycle regulation and tumorigenesis." *MS - Medecine sciences* **16**: 378-385.
- Cosgrove, D. J. (2000). "Loosening of plant cell walls by expansins." *Nature* **407**(6802): 321-326.
- Cosgrove, D. J., P. Bedinger, et al. (1997). "Group I allergens of grass pollen as cell wall-loosening agents." *Proceedings of the National Academy of Sciences of the United States of America* **94**(12): 6559-6564.
- de Jong, M., C. Mariani, et al. (2009). "The role of auxin and gibberellin in tomato fruit set." *J. Exp. Bot.* **60**(5): 1523-1532.
- Dearnaley, J. D. W. and G. A. Daggard (2001). "Expression of a polygalacturonase enzyme in germinating pollen of *Brassica napus*." *Sexual Plant Reproduction* **13**(5): 265-271.

- Desikan, R., A. H.-M. S, et al. (2001). "Regulation of the Arabidopsis transcriptome by oxidative stress." *Plant Physiol* **127**(1): 159-172.
- Devic, M., S. Albert, et al. (1996). "Induction and expression of seed-specific promoters in Arabidopsis embryo-defective mutants." *Plant J* **9**(2): 205-215.
- Dickinson, H. G. (2000). "Pollen stigma interactions: so near yet so far." *Trends Genet* **16**(9): 373-376.
- Dickinson, H. G., J. Doughty, et al. (1998). "Pollen-stigma interactions in Brassica." *Symp Soc Exp Biol* **51**: 51-57.
- Diener, A. C., H. Li, et al. (2000). "Sterol methyltransferase 1 controls the level of cholesterol in plants." *Plant Cell* **12**(6): 853-870.
- Ditta, G., A. Pinyopich, et al. (2004). "The SEP4 gene of Arabidopsis thaliana functions in floral organ and meristem identity." *Curr Biol* **14**(21): 1935-1940.
- Dnyansagar, V. R. and D. C. Cooper (1960). "Development of the Seed of Solanum phureja" *American Journal of Botany* **47**(3): 176-186.
- Doblin, M. S., L. De Melis, et al. (2001). "Pollen Tubes of Nicotiana alata Express Two Genes from Different {beta}-Glucan Synthase Families." *Plant Physiol.* **125**(4): 2040-2052.
- Dodds, P. N., A. E. Clarke, et al. (1996). "A molecular perspective on pollination in flowering plants." *Cell* **85**(2): 141-144.
- Dresselhaus, T., H. Lörz, et al. (1994). "Representative cDNA libraries from few plant cells." *The Plant Journal* **5**(4): 605-610.
- Drews, G. N., J. L. Bowman, et al. (1991). "Negative regulation of the Arabidopsis homeotic gene AGAMOUS by the APETALA2 product." *Cell* **65**(6): 991-1002.
- Drews, G. N., D. Lee, et al. (1998). "Genetic analysis of female gametophyte development and function." *Plant Cell* **10**(1): 5-17.
- Drews, G. N. and R. Yadegari (2002). "Development and function of the angiosperm female gametophyte." *Annu Rev Genet* **36**: 99-124.
- Durrant, W. E., O. Rowland, et al. (2000). "cDNA-AFLP reveals a striking overlap in race-specific resistance and wound response gene expression profiles." *Plant Cell* **12**(6): 963-977.

- Eeuwens, C. J. and W. W. Schwabe (1975). "Seed and podwall development in *P. sativum* L. in relation to extracted and applied hormones." Journal of Experimental Botany **26**(1-14).
- Elion, E. A. (2000). "Pheromone response, mating and cell biology." Curr Opin Microbiol **3**(6): 573-581.
- Elster, R., P. Bommert, et al. (2000). "Analysis of four embryo-specific mutants in *Zea mays* reveals that incomplete radial organization of the proembryo interferes with subsequent development." Dev Genes Evol **210**(6): 300-310.
- Errampalli, D., D. Patton, et al. (1991). "Embryonic Lethals and T-DNA Insertional Mutagenesis in *Arabidopsis*." Plant Cell **3**(2): 149-157.
- Esau, K. (1977). "Anatomy of Seed Plants." 2nd (Santa Barbara). des éditions John Wiley & Sons, Inc: 550.
- Espelund, M., S. Saeboe-Larsen, et al. (1992). "Late embryogenesis-abundant genes encoding proteins with different numbers of hydrophilic repeats are regulated differentially by abscisic acid and osmotic stress." Plant J **2**(2): 241-252.
- Fanger, G. R., P. Gerwins, et al. (1997). "MEKKs, GCKs, MLKs, PAKs, TAKs, and tpls: upstream regulators of the c-Jun amino-terminal kinases?" Curr Opin Genet Dev **7**(1): 67-74.
- Favaro, R., A. Pinyopich, et al. (2003). "MADS-box protein complexes control carpel and ovule development in *Arabidopsis*." Plant Cell **15**(11): 2603-2611.
- Feldmann, K. A. (1991). T-DNA insertion mutagenesis in *Arabidopsis*: mutational spectrum. 1: 71-82.
- Feldmann, K. A., D. A. Coury, et al. (1997). "Exceptional Segregation of a Selectable Marker (Kan(R)) in *Arabidopsis* Identifies Genes Important for Gametophytic Growth and Development." Genetics **147**(3): 1411-1422.
- Feng, J., X. Chen, et al. (2006). "Detection and transcript expression of S-RNase gene associated with self-incompatibility in apricot (*Prunus armeniaca* L.)." Molecular Biology Reports **33**(3): 215-221.
- Fletcher, J. C., U. Brand, et al. (1999). "Signaling of cell fate decisions by CLAVATA3 in *Arabidopsis* shoot meristems." Science **283**(5409): 1911-1914.

- Fowlkes, E. B. and C. L. Mallows (1983). "A Method for Comparing Two Hierarchical Clusterings." Journal of the American Statistical Association **78**(383): 553 -584.
- Friml, J., A. Vieten, et al. (2003). "Efflux-dependent auxin gradients establish the apical-basal axis of Arabidopsis." Nature **426**(6963): 147-153.
- Fromm, J. and S. Lautner (2007). "Electrical signals and their physiological significance in plants." Plant, Cell and Environment **30**(3): 249-257.
- Furutani, M., T. Vernoux, et al. (2004). "PIN-FORMED1 and PINOID regulate boundary formation and cotyledon development in *Arabidopsis* embryogenesis." Development **131**(20): 5021-5030.
- Galau, G. A., N. Bijaisoradat, et al. (1987). "Accumulation kinetics of cotton late embryogenesis-abundant mRNAs and storage protein mRNAs: coordinate regulation during embryogenesis and the role of abscisic acid." Dev Biol **123**(1): 198-212.
- Galau, G. A., D. W. Hughes, et al. (1986). "Abscisic acid induction of cloned cotton late embryogenesis-abundant (Lea) mRNAs." Plant Molecular Biology **7**(3): 155-170.
- Gasser, C. S., J. Broadhvest, et al. (1998). "Genetic analysis of ovule development." Annu. Rev. Plant Physiol. Plant Mol. Biol. **49**: 1-24.
- Gatehouse, J. A., I. M. Evans, et al. (1986). "Differential Expression of Genes During Legume Seed Development." Philosophical Transactions of the Royal Society of London. B, Biological Sciences **314**(1166): 367-384.
- Germain, H., S. Rudd, et al. (2005). "A 6374 unigene set corresponding to low abundance transcripts expressed following fertilization in *Solanum chacoense* Bitt, and characterization of 30 receptor-like kinases." Plant Mol Biol **59**(3): 515-532.
- Gifford, M. L., S. Dean, et al. (2003). "The *Arabidopsis* ACR4 gene plays a role in cell layer organisation during ovule integument and sepal margin development." Development **130**(18): 4249-4258.
- Gilissen, L. J. W. (1976). "The role of the style as a sense-organ in relation to wilting of the flower." Planta **131**(2): 201-202.
- Gilissen, L. J. W. (1977). "Style-controlled wilting of the flower." Planta **133**(3): 275-280.

- Gilissen, L. J. W. and F. A. Hoekstra (1984). "Pollination-Induced Corolla Wilting in *Petunia hybrida* Rapid Transfer through the Style of a Wilting-Inducing Substance." *Plant Physiol.* **75**(2): 496-498.
- Girke, T., J. Todd, et al. (2000). "Microarray analysis of developing *Arabidopsis* seeds." *Plant Physiol.* **124**(4): 1570-1581.
- Goldberg, R. B., S. J. Barker, et al. (1989). "Regulation of gene expression during plant embryogenesis." *Cell* **56**(2): 149-160.
- Goldberg, R. B., G. de Paiva, et al. (1994). "Plant Embryogenesis: Zygote to Seed." *Science* **266**(5185): 605-614.
- Golldack, D., P. Vera, et al. (2003). "Expression of subtilisin-like serine proteases in *Arabidopsis thaliana* is cell-specific and responds to jasmonic acid and heavy metals with developmental differences." *Physiol Plant* **118**(1): 64-73.
- Golz, J. F. and A. Hudson (1999). "Plant development: YABBYs claw to the fore." *Curr Biol* **9**(22): R861-863.
- Gomez, L. D., S. Baud, et al. (2006). "Delayed embryo development in the ARABIDOPSIS TREHALOSE-6-PHOSPHATE SYNTHASE 1 mutant is associated with altered cell wall structure, decreased cell division and starch accumulation." *Plant J* **46**(1): 69-84.
- Goodrich, J., P. Puangsomlee, et al. (1997). "A Polycomb-group gene regulates homeotic gene expression in *Arabidopsis*." *Nature* **386**(6620): 44-51.
- Gorguet, B., A. W. van Heusden, et al. (2005). "Parthenocarpic fruit development in tomato." *Plant Biol (Stuttg)* **7**(2): 131-139.
- Gown, A. M., J. J. Jiang, et al. (1996). "Validation of the S-phase specificity of histone (H3) in situ hybridization in normal and malignant cells." *J Histochem Cytochem* **44**(3): 221-226.
- Gray-Mitsumune, M., M. O'Brien, et al. (2006). "Loss of ovule identity induced by overexpression of the fertilization-related kinase 2 (ScFRK2), a MAPKK from *Solanum chacoense*." *J Exp Bot* **57**(15): 4171-4187.

- Griffith, M. E., A. da Silva Conceicao, et al. (1999). "PETAL LOSS gene regulates initiation and orientation of second whorl organs in the Arabidopsis flower." Development **126**(24): 5635-5644.
- Griffith, M. E., U. Mayer, et al. (2007). "The TORMOZ gene encodes a nucleolar protein required for regulated division planes and embryo development in Arabidopsis." Plant Cell **19**(7): 2246-2263.
- Grossniklaus, U., J.-P. Vielle-Calzada, et al. (1998). "Maternal Control of Embryogenesis by MEDEA, a Polycomb Group Gene in Arabidopsis." Science **280**(5362): 446-450.
- Gu, Q., C. Ferrandiz, et al. (1998). "The FRUITFULL MADS-box gene mediates cell differentiation during Arabidopsis fruit development." Development **125**(8): 1509-1517.
- Guignard, L. (1886). "Sur la pollinisation et ses effets chez les Orchidées." Annales des Sciences naturelles ser. 7. Botanique **4**: 202-240.
- Guignard, L. (1899). "Sur les anthérozoïdes et la double copulation sexuelle chez les végétaux angiospermes." C. R. Acad. Sci. Paris **128**: 864-871.
- Hadfi, K., V. Speth, et al. (1998). "Auxin-induced developmental patterns in *Brassica juncea* embryos." Development **125**(5): 879-887.
- Hamann, T., E. Benkova, et al. (2002). "The Arabidopsis BODENLOS gene encodes an auxin response protein inhibiting MONOPTEROS-mediated embryo patterning." Genes Dev **16**(13): 1610-1615.
- Hamann, T., U. Mayer, et al. (1999). "The auxin-insensitive bodenlos mutation affects primary root formation and apical-basal patterning in the Arabidopsis embryo." Development **126**(7): 1387-1395.
- Hanks, S. K. and T. Hunter (1995). "Protein kinases 6. The eukaryotic protein kinase superfamily: kinase (catalytic) domain structure and classification." Faseb J **9**(8): 576-596.
- Hanks, S. K. and A. M. Quinn (1991). "Protein kinase catalytic domain sequence database: identification of conserved features of primary structure and classification of family members." Methods Enzymol **200**: 38-62.

- Hardtke, C. S. and T. Berleth (1998). "The Arabidopsis gene MONOPTEROS encodes a transcription factor mediating embryo axis formation and vascular development." *EMBO J* **17**(5): 1405-1411.
- Hardtke, C. S., W. Ckushumova, et al. (2004). "Overlapping and non-redundant functions of the Arabidopsis auxin response factors MONOPTEROS and NONPHOTOTROPIC HYPOCOTYL 4." *Development* **131**(5): 1089-1100.
- Harmer, S. L. and S. A. Kay (2000). "Microarrays: determining the balance of cellular transcription." *Plant Cell* **12**(5): 613-616.
- Hecht, V., J. P. Vielle-Calzada, et al. (2001). "The Arabidopsis SOMATIC EMBRYOGENESIS RECEPTOR KINASE 1 gene is expressed in developing ovules and embryos and enhances embryogenic competence in culture." *Plant Physiol* **127**(3): 803-816.
- Heck, G. R., S. E. Perry, et al. (1995). "AGL15, a MADS domain protein expressed in developing embryos." *Plant Cell* **7**(8): 1271-1282.
- Heil, M. and J. C. Silva Bueno (2007). "Within-plant signaling by volatiles leads to induction and priming of an indirect plant defense in nature." *Proceedings of the National Academy of Sciences* **104**(13): 5467-5472.
- Hennig, L., W. Gruisse, et al. (2004). "Transcriptional programs of early reproductive stages in Arabidopsis." *Plant Physiol* **135**(3): 1765-1775.
- Herr, J., M, Jr. (1995). "The Origin of the Ovule." *American Journal of Botany* **82**(4): 547-564
- Herrero, M. and J. Hormaza (1996). "Pistil strategies controlling pollen tube growth." *Sexual Plant Reproduction* **9**(6): 343-347.
- Higashiyama, T., H. Kuroiwa, et al. (1998). "Guidance in vitro of the pollen tube to the naked embryo sac of torenia fournieri." *Plant Cell* **10**(12): 2019-2032.
- Higashiyama, T., S. Yabe, et al. (2001). "Pollen tube attraction by the synergid cell." *Science* **293**(5534): 1480-1483.
- Hildebrand, F. (1863). "Die Fruchtbildung der Orchideen, ein Beweis für die doppelte Wirkung des Pollen." *Botan. Zeitg.* **21**: 329-333.

- Hirt, H. (2000). "MAP kinases in plant signal transduction." Results Probl Cell Differ **27**: 1-9.
- Hiscock, S., D. Bown, et al. (2002). "Serine esterases are required for pollen tube penetration of the stigma in *Brassica*." Sexual Plant Reproduction **15**(2): 65-74.
- Hiscock, S. J. and A. M. Allen (2008). "Diverse cell signalling pathways regulate pollen-stigma interactions: the search for consensus." New Phytol **179**(2): 286-317.
- Hobbie, L., M. McGovern, et al. (2000). "The axr6 mutants of *Arabidopsis thaliana* define a gene involved in auxin response and early development." Development **127**(1): 23-32.
- Hoekstra, F. A. and T. van Roekel (1988). "Effects of Previous Pollination and Styler Ethylene on Pollen Tube Growth in *Petunia hybrida* Styles." Plant Physiol. **86**(1): 4-6.
- Hogenboom, N. G. and K. Mather (1975). "Incompatibility and Incongruity: Two Different Mechanisms for the Non-Functioning of Intimate Partner Relationships [and Comment]." Proceedings of the Royal Society of London. Series B, Biological Sciences **188**(1092): 361-375.
- Holden, M. J., J. A. Marty, et al. (2003). "Pollination-induced ethylene promotes the early phase of pollen tube growth in *Petunia inflata*." J Plant Physiol **160**(3): 261-269.
- Honma, T. and K. Goto (2001). "Complexes of MADS-box proteins are sufficient to convert leaves into floral organs." Nature **409**(6819): 525-529.
- Honya, D. and D. Twell (2003). "Comparative analysis of the *Arabidopsis* pollen transcriptome." Plant Physiol **132**(2): 640-652.
- Hormanza, J. L. and M. Herrero (1994). Gametophytic competition and selection. Genetic control of self-incompatibility and reproductive development in flowering plants. E. G. Williams, A. E. Clarke and R. B. Knox. Dordrecht, Kluwer: 372-400.
- Huang, B.-Q. and S. D. Russella (1992). "Female Germ Unit: Organization, Isolation, and Function." International Review of Cytology **140**: 233-293.
- Huang, B. Q. and W. F. Sheridan (1994). "Female Gametophyte Development in Maize: Microtubular Organization and Embryo Sac Polarity." Plant Cell **6**(6): 845-861.

- Huang, H., W. C. Barker, et al. (2003). "iProClass: an integrated database of protein family, function and structure information." Nucl. Acids Res. **31**(1): 390-392.
- Huck, N., J. M. Moore, et al. (2003). "The Arabidopsis mutant feronia disrupts the female gametophytic control of pollen tube reception." Development **130**(10): 2149-2159.
- Hulskamp, M., K. Schneitz, et al. (1995). "Genetic Evidence for a Long-Range Activity That Directs Pollen Tube Guidance in Arabidopsis." Plant Cell **7**(1): 57-64.
- Huson, D. H. and D. Bryant (2006). "Application of Phylogenetic Networks in Evolutionary Studies." Mol Biol Evol **23**(2): 254-267.
- Ito, T., N. Takahashi, et al. (1997). "A serine/threonine protein kinase gene isolated by an in vivo binding procedure using the Arabidopsis floral homeotic gene product, AGAMOUS." Plant Cell Physiol **38**(3): 248-258.
- Jack, T. (2001). "Plant development going MADS." Plant Mol Biol **46**(5): 515-520.
- Jack, T., L. L. Brockman, et al. (1992). "The homeotic gene APETALA3 of Arabidopsis thaliana encodes a MADS box and is expressed in petals and stamens." Cell **68**(4): 683-697.
- Jenik, P. D., C. S. Gillmor, et al. (2007). "Embryonic Patterning in Arabidopsis thaliana." Annu Rev Cell Dev Biol.
- Jeong, S., A. E. Trotochaud, et al. (1999). "The Arabidopsis CLAVATA2 gene encodes a receptor-like protein required for the stability of the CLAVATA1 receptor-like kinase." Plant Cell **11**(10): 1925-1934.
- Jofuku, K. D., B. G. den Boer, et al. (1994). "Control of Arabidopsis flower and seed development by the homeotic gene APETALA2." Plant Cell **6**(9): 1211-1225.
- Johnson, R., J. Narvaez, et al. (1989). "Expression of proteinase inhibitors I and II in transgenic tobacco plants: effects on natural defense against *Manduca sexta* larvae." Proceedings of the National Academy of Sciences of the United States of America **86**(24): 9871-9875.
- Johnston, A. J., P. Meier, et al. (2007). "Genetic subtraction profiling identifies genes essential for Arabidopsis reproduction and reveals interaction between the female gametophyte and the maternal sporophyte." Genome Biol **8**(10): R204.

- Johnstone, R. W., J. Wang, et al. (1998). "Ciao 1 is a novel WD40 protein that interacts with the tumor suppressor protein WT1." J Biol Chem **273**(18): 10880-10887.
- Jones-Rhoades, M. W., J. O. Borevitz, et al. (2007). "Genome-wide expression profiling of the Arabidopsis female gametophyte identifies families of small, secreted proteins." PLoS Genet **3**(10): 1848-1861.
- Jones, J. D. and J. L. Dangl (2006). "The plant immune system." Nature **444**(7117): 323-329.
- Jones, J. D. G., P. Dunsmuir, et al. (1985). "High level expression of introduced chimeric genes in regenerated transformed plants." EMBO J. **4**: 2411-2418.
- Jongedijk, E. (1985). "The pattern of megasporogenesis and megagametogenesis in diploid Solanum species hybrids; its relevance to the origin of 2n-eggs and the induction of apomixis." Euphytica **34**(3): 599-611.
- Josep, V., C. Francesc, et al. (1998). "Characterization of the wound-induced metallocarboxypeptidase inhibitor from potato1 The nucleotide sequence data reported here have been submitted to the GenBank Nucleotide Sequence Database and are available under accession number AF060551.1: cDNA sequence, induction of gene expression, subcellular immunolocalization and potential roles of the C-terminal propeptide." FEBS letters **440**(1): 175-182.
- Jürgens, G. (2001). "Apical-basal pattern formation in *Arabidopsis* embryogenesis." Embo J **20**(14): 3609-3616.
- Jürgens, G. (2003). "Growing up green: cellular basis of plant development." Mech Dev **120**(11): 1395-1406.
- Jürgens, G., Mayer U, Torres Ruiz R, Berleth T, Misera S (1991). "Genetic analysis of pattern formation in the *Arabidopsis* embryo." Dev Suppl **1**: 27-38.
- Jürgens G, M. U., Torres Ruiz R, Berleth T, Misera S (1991). "Genetic analysis of pattern formation in the *Arabidopsis* embryo." Dev Suppl **1**: 27-38.
- Jürgens, G., R. A. Torres Ruiz, et al. (1994). "Embryonic pattern formation in flowering plants." Annu Rev Genet **28**: 351-371.
- Kader, J.-C. (1997). "Lipid-transfer proteins: a puzzling family of plant proteins " Trends Plant Sci. **2**(2): 66-70.

- Kaothien, P., S. H. Ok, et al. (2005). "Kinase partner protein interacts with the LePRK1 and LePRK2 receptor kinases and plays a role in polarized pollen tube growth." *Plant J* **42**(4): 492-503.
- Kardailsky, I., V. K. Shukla, et al. (1999). "Activation tagging of the floral inducer FT." *Science* **286**(5446): 1962-1965.
- Kasahara, R. D., M. F. Portereiko, et al. (2005). "MYB98 is required for pollen tube guidance and synergid cell differentiation in Arabidopsis." *Plant Cell* **17**(11): 2981-2992.
- Kay Schneitz, M. H., Robert E. Pruitt, (1995). "Wild-type ovule development in *Arabidopsis thaliana*: a light microscope study of cleared whole-mount tissue." *The Plant Journal* **7**(5): 731-749.
- Kayes, J. M. and S. E. Clark (1998). "CLAVATA2, a regulator of meristem and organ development in Arabidopsis." *Development* **125**(19): 3843-3851.
- Kermicle, J. L. (1971). "Pleiotropic effects on seed development of the indeterminate gametophyte gene in maize." *Am. J. Bot* **58**: 1-7.
- Kieber, J. J., M. Rothenberg, et al. (1993). "CTR1, a negative regulator of the ethylene response pathway in Arabidopsis, encodes a member of the raf family of protein kinases." *Cell* **72**(3): 427-441.
- Kim, J., S. H. Shiu, et al. (2006). "Patterns of expansion and expression divergence in the plant polygalacturonase gene family." *Genome Biol* **7**(9): R87.
- Kim, S., J. Dong, et al. (2004). "Pollen tube guidance: the role of adhesion and chemotropic molecules." *Curr Top Dev Biol* **61**: 61-79.
- Kim, S., J. C. Mollet, et al. (2003). "Chemocyanin, a small basic protein from the lily stigma, induces pollen tube chemotropism." *Proc Natl Acad Sci U S A* **100**(26): 16125-16130.
- King, R. W., T. Moritz, et al. (2001). "Long-Day Induction of Flowering in *Lolium temulentum* Involves Sequential Increases in Specific Gibberellins at the Shoot Apex." *Plant Physiol*. **127**(2): 624-632.
- Kobayashi, Y., H. Kaya, et al. (1999). "A pair of related genes with antagonistic roles in mediating flowering signals." *Science* **286**(5446): 1960-1962.

- Komeda, Y. (2004). "Genetic regulation of time to flower in *Arabidopsis thaliana*." *Annu Rev Plant Biol* **55**: 521-535.
- Koo, A. J. and G. A. Howe (2009). "The wound hormone jasmonate." *Phytochemistry* **70**(13-14): 1571-1580.
- Kotake, T., Y. Q. Li, et al. (2000). "Characterization and function of wall-bound exo- β -glucanases of *Lilium longiflorum* pollen tubes." *Sexual Plant Reproduction* **13**(1): 1-9.
- Kramer, E. M., M. A. Jaramillo, et al. (2004). "Patterns of gene duplication and functional evolution during the diversification of the AGAMOUS subfamily of MADS box genes in angiosperms." *Genetics* **166**(2): 1011-1023.
- Krizek, B. A. and J. C. Fletcher (2005). "Molecular mechanisms of flower development: an armchair guide." *Nat Rev Genet* **6**(9): 688-698.
- Kushwaha, R., A. Singh, et al. (2008). "Calmodulin7 plays an important role as transcriptional regulator in *Arabidopsis* seedling development." *Plant Cell* **20**(7): 1747-1759.
- Labarca, C. and F. Loewus (1972). "The Nutritional Role of Pistil Exudate in Pollen Tube Wall Formation in *Lilium longiflorum*: I. Utilization of Injected Stigmatic Exudate." *Plant Physiol* **50**(1): 7-14.
- Lahmy, S., J. Guilleminot, et al. (2007). "QQT proteins colocalize with microtubules and are essential for early embryo development in *Arabidopsis*." *Plant J* **50**(4): 615-626.
- Lan, L., W. Chen, et al. (2004). "Monitoring of gene expression profiles and isolation of candidate genes involved in pollination and fertilization in rice (*Oryza sativa* L.) with a 10K cDNA microarray." *Plant Mol Biol* **54**(4): 471-487.
- Lan, L., M. Li, et al. (2005). "Microarray analysis reveals similarities and variations in genetic programs controlling pollination/fertilization and stress responses in rice (*Oryza sativa* L.)." *Plant Mol Biol* **59**(1): 151-164.
- Lantin, S., M. O'Brien, et al. (1999). "Pollination, wounding and jasmonate treatments induce the expression of a developmentally regulated pistil dioxygenase at a distance, in the ovary, in the wild potato *Solanum chacoense* Bitt." *Plant Mol Biol* **41**(3): 371-386.

- Lantin, S., M. O'Brien, et al. (1999). "Pollination, wounding and jasmonate treatments induce the expression of a developmentally regulated pistil dioxygenase at a distance, in the ovary, in the wild potato *Solanum chacoense* Bitt." Plant Molecular Biology **41**(3): 371-386.
- Lee, H.-S., Y.-Y. Chung, et al. (1997). "Embryo sac development is affected in *Petunia inflata* plants transformed with an antisense gene encoding the extracellular domain of receptor kinase PRK1." Sex Plant Reprod **10**: 341-350.
- Lee, H.-S., B. Karunanandaa, et al. (1996). "PRK1, a receptor-like kinase of *Petunia inflata*, is essential for postmeiotic development of pollen." Plant J **9**(5): 613-624.
- Lee, J. M., M. E. Williams, et al. (2002). "DNA array profiling of gene expression changes during maize embryo development." Funct Integr Genomics **2**(1-2): 13-27.
- Lee, J. Y., S. F. Baum, et al. (2005). "Activation of CRABS CLAW in the Nectaries and Carpels of *Arabidopsis*." Plant Cell **17**(1): 25-36.
- Lee, Y., D. Choi, et al. (2001). "Expansins: ever-expanding numbers and functions." Current Opinion in Plant Biology **4**(6): 527-532.
- Lehti-Shiu, M. D., B. J. Adamczyk, et al. (2005). "Expression of MADS-box genes during the embryonic phase in *Arabidopsis*." Plant Mol Biol **58**(1): 89-107.
- Lersten, N. R. (2004). Flowering plant embryology. Ames, Blackwell Publishing.
- Li, H. Y. and J. E. Gray (1997). "Pollination-enhanced expression of a receptor-like protein kinase related gene in tobacco styles." Plant Mol Biol **33**(4): 653-665.
- Li, J. and J. Chory (1997). "A putative leucine-rich repeat receptor kinase involved in brassinosteroid signal transduction." Cell **90**(5): 929-938.
- Li, M., W. Xu, et al. (2007). "Genome-Wide Gene Expression Profiling Reveals Conserved and Novel Molecular Functions of the Stigma in Rice." Plant Physiol **144**(4): 1797-1812.
- Lindsey, k. and j. F. Topping (1993). "Embryogenesis: a Question of Pattern." J. Exp. Bot. **44**(2): 359-374.
- Liu, B., D. Morse, et al. (2009). "Compatible Pollinations in *Solanum chacoense* Decrease Both S-RNase and S-RNase mRNA." PLoS ONE **4**(6): e5774.

- Liu, C., Z. Xu, et al. (1993). "Auxin Polar Transport Is Essential for the Establishment of Bilateral Symmetry during Early Plant Embryogenesis." Plant Cell **5**(6): 621-630.
- Liu, N. Y., Z. F. Zhang, et al. (2008). "Isolation of embryo-specific mutants in Arabidopsis: genetic and phenotypic analysis." Methods Mol Biol **427**: 101-109.
- Liu, Z., R. G. Franks, et al. (2000). "Regulation of gynoecium marginal tissue formation by LEUNIG and AINTEGUMENTA." Plant Cell **12**(10): 1879-1892.
- Liu, Z. and E. Meyerowitz (1995). "LEUNIG regulates AGAMOUS expression in Arabidopsis flowers." Development **121**(4): 975-991.
- Llop-Tous, I., C. S. Barry, et al. (2000). "Regulation of ethylene biosynthesis in response to pollination in tomato flowers." Plant Physiol **123**(3): 971-978.
- Long, J. A., C. Ohno, et al. (2006). "TOPLESS regulates apical embryonic fate in Arabidopsis." Science **312**(5779): 1520-1523.
- Long, J. A., S. Woody, et al. (2002). "Transformation of shoots into roots in Arabidopsis embryos mutant at the TOPLESS locus." Development **129**(12): 2797-2806.
- Lorbiecke, R., M. Steffens, et al. (2005). "Phytosulphokine gene regulation during maize (*Zea mays L.*) reproduction." J Exp Bot **56**(417): 1805-1819.
- Lord, E. M. (2003). "Adhesion and guidance in compatible pollination." J Exp Bot **54**(380): 47-54.
- Lotan, T., M. Ohto, et al. (1998). "Arabidopsis LEAFY COTYLEDON1 is sufficient to induce embryo development in vegetative cells." Cell **93**(7): 1195-1205.
- Louis, A., H. Chiapello, et al. (2002). "Deciphering *Arabidopsis thaliana* gene neighborhoods through bibliographic co-citations." Comput Chem **26**(5): 511-519.
- Lukowitz, W., A. Roeder, et al. (2004). "A MAPKK kinase gene regulates extra-embryonic cell fate in Arabidopsis." Cell **116**(1): 109-119.
- Lush, W. M., F. Grieser, et al. (1998). "Directional guidance of *nicotiana alata* pollen tubes in vitro and on the stigma." Plant Physiol **118**(3): 733-741.
- Lynn, K., A. Fernandez, et al. (1999). "The PINHEAD/ZWILLE gene acts pleiotropically in *Arabidopsis* development and has overlapping functions with the ARGONAUTE1 gene." Development **126**(3): 469-481.

- Ma, W., A. Smigel, et al. (2008). "Innate immunity signaling: cytosolic Ca²⁺ elevation is linked to downstream nitric oxide generation through the action of calmodulin or a calmodulin-like protein." *Plant Physiol* **148**(2): 818-828.
- Madhani, H. D. and G. R. Fink (1998). "The riddle of MAP kinase signaling specificity." *Trends Genet* **14**(4): 151-155.
- Maheshwari, P. (1950). "An introduction to the embryology of angiosperms." *New York, NY: McGraw-Hill Book Co.*
- Maheshwari, P. and B. M. Johri (1950). "Development of the embryo sac, embryo and endosperm in helixanthera ligustrina (wall.) dans." *Nature* **165**(4207): 978-979.
- Mahonen, A. P., M. Bonke, et al. (2000). "A novel two-component hybrid molecule regulates vascular morphogenesis of the *Arabidopsis* root." *Genes Dev* **14**(23): 2938-2943.
- Maldonado, A. M., P. Doerner, et al. (2002). "A putative lipid transfer protein involved in systemic resistance signalling in *Arabidopsis*." *Nature* **419**(6905): 399-403.
- Mandel, M. A., J. L. Bowman, et al. (1992). "Manipulation of flower structure in transgenic tobacco." *Cell* **71**(1): 133-143.
- Mansfield, S. G. and L. G. Briarty (1991). "Early embryogenesis in *Arabidopsis thaliana*. II. The developing embryo." *Canadian journal of botany* **69**(3): 461-476
- Martineau, B., K. E. McBride, et al. (1991). "Regulation of metallocarboxypeptidase inhibitor gene expression in tomato." *Molecular and General Genetics MGG* **228**(1): 281-286.
- Marton, M. L., S. Cordts, et al. (2005). "Micropylar pollen tube guidance by egg apparatus 1 of maize." *Science* **307**(5709): 573-576.
- Mascarenhas, J. P. and L. Machlis (1999). "Chemotropic Response of *Antirrhinum majus* Pollen to Calcium." *Nature* **126**(23): 5431-5440.
- Matsubayashi, Y., M. Ogawa, et al. (2002). "An LRR receptor kinase involved in perception of a peptide plant hormone, phytosulfokine." *Science* **296**(5572): 1470-1472.
- Matton, D. P., O. Maes, et al. (1997). "Hypervariable domains of self-incompatibility RNases mediate allele-specific pollen recognition." *Plant Cell* **9**: 1757-1766.

- Mayer, U., G. Buttner, et al. (1993). Apical-basal pattern formation in the *Arabidopsis* embryo: studies on the role of the *gnom* gene. **117**: 149-162.
- Mayer, U., R. A. T. Ruiz, et al. (1991). "Mutations affecting body organization in the *Arabidopsis* embryo." *Nature* **353**(6343): 402-407.
- McClure, B. (2009). "Darwin's foundation for investigating self-incompatibility and the progress toward a physiological model for S-RNase-based SI." *J Exp Bot* **60**(4): 1069-1081.
- McElver, J., I. Tzafrir, et al. (2001). "Insertional mutagenesis of genes required for seed development in *Arabidopsis thaliana*." *Genetics* **159**(4): 1751-1763.
- Meinke, D. W. (1985). "Embryo-lethal mutants of *Arabidopsis thaliana*: analysis of mutants with a wide range of lethal phases." *TAG Theoretical and Applied Genetics* **69**(5): 543-552.
- Meinke, D. W. (1991). "Perspectives on Genetic Analysis of Plant Embryogenesis." *Plant Cell* **3**(9): 857-866.
- Metzker, M. L. (2010). "Sequencing technologies - the next generation." *Nat Rev Genet* **11**(1): 31-46.
- Modrusan, Z., L. Reiser, et al. (1994). "Homeotic Transformation of Ovules into Carpel-like Structures in *Arabidopsis*." *Plant Cell* **6**(3): 333-349.
- Moore, I., T. Diefenthal, et al. (1997). "A homolog of the mammalian GTPase Rab2 is present in *Arabidopsis* and is expressed predominantly in pollen grains and seedlings." *Proc Natl Acad Sci U S A* **94**(2): 762-767.
- Moore JM, Calzada JP, et al. (1997). "Genetic characterization of hadad, a mutant disrupting female gametogenesis in *Arabidopsis thaliana*." *Cold Spring Harbor Laboratory, New York 11724, USA*. **62**: 35-47.
- Mu, J. H., J. P. Stains, et al. (1994). "Characterization of a pollen-expressed gene encoding a putative pectin esterase of *Petunia inflata*." *Plant Mol Biol* **25**(3): 539-544.
- Murphy, L. O. and J. Blenis (2006). "MAPK signal specificity: the right place at the right time." *Trends Biochem Sci* **31**(5): 268-275.

- Muschietti, J., Y. Eyal, et al. (1998). "Pollen tube localization implies a role in pollen-pistil interactions for the tomato receptor-like protein kinases LePRK1 and LePRK2." *Plant Cell* **10**(3): 319-330.
- Nadeau, J. A. and F. D. Sack (2002). "Control of stomatal distribution on the *Arabidopsis* leaf surface." *Science* **296**(5573): 1697-1700.
- Navarro, L., C. Zipfel, et al. (2004). "The transcriptional innate immune response to flg22. Interplay and overlap with Avr gene-dependent defense responses and bacterial pathogenesis." *Plant Physiol* **135**(2): 1113-1128.
- Nawaschin, S. G. (1898). "Resultate einer Revision der Befruchtungsvorgänge bei *Lilium Martagon* und *Fritillaria tenella*." *Bull. Acad. Sci. St Petersburg* **9**: 377-382.
- Neuffer, M. G. and W. F. Sheridan (1980). "Defective Kernel Mutants of Maize. I. Genetic and Lethality Studies." *Genetics* **95**(4): 929-944.
- Newman, K. L., A. G. Fernandez, et al. (2002). "Regulation of axis determinacy by the *Arabidopsis* PINHEAD gene." *Plant Cell* **14**(12): 3029-3042.
- Ng, M. and M. F. Yanofsky (2001). "Function and evolution of the plant MADS-box gene family." *Nat Rev Genet* **2**(3): 186-195.
- Nielsen, M. E., F. Lok, et al. (2006). "Distinct developmental defense activations in barley embryos identified by transcriptome profiling." *Plant Mol Biol* **61**(4-5): 589-601.
- Nieuwland, J., R. Feron, et al. (2005). "Lipid transfer proteins enhance cell wall extension in tobacco." *Plant Cell* **17**(7): 2009-2019.
- Nishihama, R., H. Banno, et al. (1995). "Plant homologues of components of MAPK (mitogen-activated protein kinase) signal pathways in yeast and animal cells." *Plant Cell Physiol* **36**(5): 749-757.
- Nuccio, M. L. and T. L. Thomas (1999). "ATS1 and ATS3: two novel embryo-specific genes in *Arabidopsis thaliana*." *Plant Mol Biol* **39**(6): 1153-1163.
- O'Brien, M., C. Bertrand, et al. (2002). "Characterization of a fertilization-induced and developmentally regulated plasma-membrane aquaporin expressed in reproductive tissues, in the wild potato *Solanum chacoense* Bitt." *Planta* **215**(3): 485-493.
- O'Brien, M., S. C. Chantha, et al. (2005). "Lipid signaling in plants. Cloning and expression analysis of the obtusifoliol 14alpha-demethylase from *Solanum chacoense* Bitt., a

- pollination- and fertilization-induced gene with both obtusifoliol and lanosterol demethylase activity." *Plant Physiol* **139**(2): 734-749.
- O'Brien, M., C. Kapfer, et al. (2002). "Molecular analysis of the stylar-expressed Solanum chacoense small asparagine-rich protein family related to the HT modifier of gametophytic self-incompatibility in Nicotiana." *Plant J* **32**(6): 985-996.
- O'Neill, S. D. (1997). "Pollination Regulation of Flower Development." *Annual Review of Plant Physiology and Plant Molecular Biology* **48**(1): 547-574.
- O'Neill, S. D., J. A. Nadeau, et al. (1993). "Interorgan regulation of ethylene biosynthetic genes by pollination." *Plant Cell* **5**(4): 419-432.
- Ohad, N., L. Margossian, et al. (1996). "A mutation that allows endosperm development without fertilization." *Proc Natl Acad Sci U S A* **93**(11): 5319-5324.
- Okamuro, J. K., B. G. den Boer, et al. (1996). "Flowers into shoots: photo and hormonal control of a meristem identity switch in Arabidopsis." *Proc Natl Acad Sci U S A* **93**(24): 13831-13836.
- Okuda, S., H. Tsutsui, et al. (2009). "Defensin-like polypeptide LUREs are pollen tube attractants secreted from synergid cells." *Nature* **458**(7236): 357-361.
- Palanivelu, R., L. Brass, et al. (2003). "Pollen tube growth and guidance is regulated by POP2, an Arabidopsis gene that controls GABA levels." *Cell* **114**(1): 47-59.
- Parcy, F., O. Nilsson, et al. (1998). "A genetic framework for floral patterning." *Nature* **395**(6702): 561-566.
- Park, S. Y., G. Y. Jauh, et al. (2000). "A lipid transfer-like protein is necessary for lily pollen tube adhesion to an in vitro stylar matrix." *Plant Cell* **12**(1): 151-164.
- Parkinson, H., U. Sarkans, et al. (2005). "ArrayExpress--a public repository for microarray gene expression data at the EBI." *Nucleic Acids Res* **33**(Database issue): D553-555.
- Peiffer, J. A., S. Kaushik, et al. (2008). "A spatial dissection of the Arabidopsis floral transcriptome by MPSS." *BMC Plant Biol* **8**: 43.
- Pelaz, S., G. S. Ditta, et al. (2000). "B and C floral organ identity functions require SEPALLATA MADS-box genes." *Nature* **405**(6783): 200-203.
- Peña-Cortes, H., J. Sanchez-Serrano, et al. (1988). "Systemic induction of proteinase-inhibitor-II gene expression in potato plants by wounding." *Planta* **174**(1): 84-89.

- Perez-Amador, M. A., P. Lidder, et al. (2001). "New molecular phenotypes in the dst mutants of Arabidopsis revealed by DNA microarray analysis." *Plant Cell* **13**(12): 2703-2717.
- Pezzotti, M., R. Feron, et al. (2002). "Pollination modulates expression of the PPAL gene, a pistil-specific beta-expansin." *Plant Mol Biol* **49**(2): 187-197.
- Pina, C., F. Pinto, et al. (2005). "Gene family analysis of the Arabidopsis pollen transcriptome reveals biological implications for cell growth, division control, and gene expression regulation." *Plant Physiol* **138**(2): 744-756.
- Pinyopich, A., G. S. Ditta, et al. (2003). "Assessing the redundancy of MADS-box genes during carpel and ovule development." *Nature* **424**(6944): 85-88.
- Pislariu, C. I. and R. Dickstein (2007). "An IRE-like AGC kinase gene, MtIRE, has unique expression in the invasion zone of developing root nodules in *Medicago truncatula*." *Plant Physiol* **144**(2): 682-694.
- Piwien-Pilipuk, G., J. S. Huo, et al. (2002). "Growth hormone signal transduction." *J Pediatr Endocrinol Metab* **15**(6): 771-786.
- Porceddu, A., H. Stals, et al. (2001). "A plant-specific cyclin-dependent kinase is involved in the control of G2/M progression in plants." *J Biol Chem* **276**(39): 36354-36360.
- Posas, F. and H. Saito (1997). "Osmotic activation of the HOG MAPK pathway via Ste11p MAPKKK: scaffold role of Pbs2p MAPKK." *Science* **276**(5319): 1702-1705.
- Przemeck, G. K., J. Mattsson, et al. (1996). "Studies on the role of the Arabidopsis gene MONOPTEROS in vascular development and plant cell axialization." *Planta* **200**(2): 229-237.
- Putterill, J., F. Robson, et al. (1995). "The CONSTANS gene of Arabidopsis promotes flowering and encodes a protein showing similarities to zinc finger transcription factors." *Cell* **80**(6): 847-857.
- Qin, Y., A. R. Leydon, et al. (2009). "Penetration of the stigma and style elicits a novel transcriptome in pollen tubes, pointing to genes critical for growth in a pistil." *PLoS Genet* **5**(8): e1000621.

- Quiapim, A. C., M. S. Brito, et al. (2009). "Analysis of the Nicotiana tabacum Stigma/Style Transcriptome Reveals Gene Expression Differences between Wet and Dry Stigma Species." *Plant Physiol.* **149**(3): 1211-1230.
- Ray, A., K. Robinson-Beers, et al. (1994). "Arabidopsis floral homeotic gene BELL (BEL1) controls ovule development through negative regulation of AGAMOUS gene (AG)." *Proc Natl Acad Sci U S A* **91**(13): 5761-5765.
- Ray, S. M., S. S. Park, et al. (1997). "Pollen tube guidance by the female gametophyte." *Development* **124**(12): 2489-2498.
- Rea, A. C. and J. B. Nasrallah (2008). "Self-incompatibility systems: barriers to self-fertilization in flowering plants." *Int J Dev Biol* **52**(5-6): 627-636.
- Redei, G. P. (1965). "NON-MENDELIAN MEGAGAMETOGENESIS IN ARABIDOPSIS." *Genetics* **51**(6): 857-872.
- Rees-Leonard, O. L. (1935). "Macrosporogenesis and Development of the Macrogametophyte of Solanum tuberosum" *Botanical Gazette* **96**(4): 734-750.
- Regan, S. M. and B. A. Moffatt (1990). "Cytochemical Analysis of Pollen Development in Wild-Type Arabidopsis and a Male-Sterile Mutant." *Plant Cell* **2**(9): 877-889.
- Reiser, L., Z. Modrusan, et al. (1995). "The BELL1 gene encodes a homeodomain protein involved in pattern formation in the Arabidopsis ovule primordium." *Cell* **83**(5): 735-742.
- Rhee, S. Y., W. Beavis, et al. (2003). "The Arabidopsis Information Resource (TAIR): a model organism database providing a centralized, curated gateway to Arabidopsis biology, research materials and community." *Nucleic Acids Res* **31**(1): 224-228.
- Rhodes, J. D., J. F. Thain, et al. (1996). "The pathway for systemic electrical signal conduction in the wounded tomato plant." *Planta* **200**(1): 50-57.
- Riechmann, J. L., B. A. Krizek, et al. (1996). "Dimerization specificity of Arabidopsis MADS domain homeotic proteins APETALA1, APETALA3, PISTILLATA, and AGAMOUS." *Proc Natl Acad Sci U S A* **93**(10): 4793-4798.
- Robinson-Beers, K., R. E. Pruitt, et al. (1992). Ovule Development in Wild-Type Arabidopsis and Two Female-Sterile Mutants. *4*: 1237-1249.

- Robinson, M. J. and M. H. Cobb (1997). "Mitogen-activated protein kinase pathways." *Curr Opin Cell Biol* **9**(2): 180-186.
- Roe, J. L., T. Durfee, et al. (1997). "TOUSLED is a nuclear serine/threonine protein kinase that requires a coiled-coil region for oligomerization and catalytic activity." *J Biol Chem* **272**(9): 5838-5845.
- Roe, J. L., J. L. Nemhauser, et al. (1997). "TOUSLED participates in apical tissue formation during gynoecium development in *Arabidopsis*." *Plant Cell* **9**(3): 335-353.
- Roe, J. L., C. J. Rivin, et al. (1993). "The Tousled gene in *A. thaliana* encodes a protein kinase homolog that is required for leaf and flower development." *Cell* **75**(5): 939-950.
- Rojo, E., V. K. Sharma, et al. (2002). "CLV3 is localized to the extracellular space, where it activates the *Arabidopsis* CLAVATA stem cell signaling pathway." *Plant Cell* **14**(5): 969-977.
- Romeis, T. (2001). "Protein kinases in the plant defence response." *Curr Opin Plant Biol* **4**(5): 407-414.
- Rose, J. K. C., D. J. Cosgrove, et al. (2000). "Detection of Expansin Proteins and Activity during Tomato Fruit Ontogeny." *Plant Physiol* **123**(4): 1583-1592.
- Rotman, N., F. Rozier, et al. (2003). "Female control of male gamete delivery during fertilization in *Arabidopsis thaliana*." *Curr Biol* **13**(5): 432-436.
- Rounsley, S. D., G. S. Ditta, et al. (1995). "Diverse Roles for MADS Box Genes in *Arabidopsis* Development." *Plant Cell* **7**(8): 1259-1269.
- Russell, D. S. (1996). "Attraction and transport of male gametes for fertilization." *Sexual Plant Reproduction* **V9**(6): 337-342.
- Russell, S. D. (1992). "Double fertilization." *Int Rev Cytol* **140**: 357-388.
- Russell, S. D. (1993). "The Egg Cell: Development and Role in Fertilization and Early Embryogenesis." *Plant Cell* **5**(10): 1349-1359.
- Russell, S. D. (1996). "Attraction and transport of male gametes for fertilization." *Sex Plant Reprod* **9**: 337-342.

- Saitou, N. and M. Nei (1987). "The neighbor-joining method: a new method for reconstructing phylogenetic trees." Mol Biol Evol **4**(4): 406-425.
- Samach, A., H. Onouchi, et al. (2000). "Distinct roles of CONSTANS target genes in reproductive development of Arabidopsis." Science **288**(5471): 1613-1616.
- Sambrook, J., E. F. Fritsch, et al. (1989). Molecular cloning: a laboratory manual. Cold Spring Harbor, New York, Cold Spring Harbor Laboratory Press.
- Samuel, M. A. and B. E. Ellis (2002). "Double jeopardy: both overexpression and suppression of a redox-activated plant mitogen-activated protein kinase render tobacco plants ozone sensitive." Plant Cell **14**(9): 2059-2069.
- Sanchez, A. M., M. Bosch, et al. (2004). "Pistil Factors Controlling Pollination." Plant Cell **16**(suppl_1): S98-106.
- Sanchez, A. M. and C. Mariani (2002). "Expression of the ACC synthase and ACC oxidase coding genes after self-pollination and incongruous pollination of tobacco pistils." Plant Molecular Biology **48**(4): 351-359.
- Sandaklie-Nikolova, L., R. Palanivelu, et al. (2007). "Synergid cell death in Arabidopsis is triggered following direct interaction with the pollen tube." Plant Physiol **144**(4): 1753-1762.
- Sarkans, U., H. Parkinson, et al. (2005). "The ArrayExpress gene expression database: a software engineering and implementation perspective." Bioinformatics **21**(8): 1495-1501.
- Sarowar, S., Y. J. Kim, et al. (2009). "Overexpression of lipid transfer protein (LTP) genes enhances resistance to plant pathogens and LTP functions in long-distance systemic signaling in tobacco." Plant Cell Rep **28**(3): 419-427.
- Scanlon, M. J., P. S. Stinard, et al. (1994). "Genetic analysis of 63 mutations affecting maize kernel development isolated from Mutator stocks." Genetics **136**(1): 281-294.
- Schenk, P. M., K. Kazan, et al. (2000). "Coordinated plant defense responses in Arabidopsis revealed by microarray analysis." Proc Natl Acad Sci U S A **97**(21): 11655-11660.

- Scheres, B., L. Di Laurenzio, et al. (1995). Mutations affecting the radial organisation of the Arabidopsis root display specific defects throughout the embryonic axis. **121**: 53-62.
- Schmid, M., N. H. Uhlenhaut, et al. (2003). "Dissection of floral induction pathways using global expression analysis." *Development* **130**(24): 6001-6012.
- Schmidt, E. D., F. Guzzo, et al. (1997). "A leucine-rich repeat containing receptor-like kinase marks somatic plant cells competent to form embryos." *Development* **124**(10): 2049-2062.
- Schneitz, K., M. Hulskamp, et al. (1997). "Dissection of sexual organ ontogenesis: a genetic analysis of ovule development in *Arabidopsis thaliana*." *Development* **124**(7): 1367-1376.
- Schoof, H., M. Lenhard, et al. (2000). "The stem cell population of *Arabidopsis* shoot meristems is maintained by a regulatory loop between the CLAVATA and WUSCHEL genes." *Cell* **100**(6): 635-644.
- Schrick, K., U. Mayer, et al. (2000). "FACKEL is a sterol C-14 reductase required for organized cell division and expansion in *Arabidopsis* embryogenesis." *Genes Dev* **14**(12): 1471-1484.
- Sells, M. A., U. G. Knaus, et al. (1997). "Human p21-activated kinase (Pak1) regulates actin organization in mammalian cells." *Curr Biol* **7**(3): 202-210.
- Serrani, J. C., O. Ruiz-Rivero, et al. (2008). "Auxin-induced fruit-set in tomato is mediated in part by gibberellins." *Plant J* **56**(6): 922-934.
- Serrani, J. C., R. Sanjuan, et al. (2007). "Gibberellin Regulation of Fruit Set and Growth in Tomato." *Plant Physiol* **145**(1): 246-257.
- Sheoran, I. S., D. J. Olson, et al. (2005). "Proteome analysis of embryo and endosperm from germinating tomato seeds." *Proteomics* **5**(14): 3752-3764.
- Sheridan, W. F. and M. G. Neuffer (1980). "Defective Kernel Mutants of Maize II. Morphological and Embryo Culture Studies." *Genetics* **95**(4): 945-960.
- Shimizu, K. K., T. Ito, et al. (2008). "MAA3 (MAGATAMA3) helicase gene is required for female gametophyte development and pollen tube guidance in *Arabidopsis thaliana*." *Plant Cell Physiol* **49**(10): 1478-1483.

- Shimizu, K. K. and K. Okada (2000). "Attractive and repulsive interactions between female and male gametophytes in *Arabidopsis* pollen tube guidance." Development **127**(20): 4511-4518.
- Sieber, P., J. Gheyselinck, et al. (2004). "Pattern formation during early ovule development in *Arabidopsis thaliana*." Dev Biol **273**(2): 321-334.
- Simpson, G. G. and C. Dean (2002). "Arabidopsis, the Rosetta stone of flowering time?" Science **296**(5566): 285-289.
- Singh, A., K. B. Evensen, et al. (1992). "Ethylene Synthesis and Floral Senescence following Compatible and Incompatible Pollinations in *Petunia inflata*." Plant Physiol. **99**(1): 38-45.
- Skriver, K. and J. Mundy (1990). "Gene expression in response to abscisic acid and osmotic stress." Plant Cell **2**(6): 503-512.
- Smyth, D. R., J. L. Bowman, et al. (1990). "Early flower development in *Arabidopsis*." Plant Cell **2**(8): 755-767.
- Spellman, P. T., G. Sherlock, et al. (1998). "Comprehensive identification of cell cycle-regulated genes of the yeast *Saccharomyces cerevisiae* by microarray hybridization." Mol Biol Cell **9**(12): 3273-3297.
- Spencer, M. W., S. A. Casson, et al. (2007). "Transcriptional profiling of the *Arabidopsis* embryo." Plant Physiol **143**(2): 924-940.
- Springer, P., W. McCombie, et al. (1995). "Gene trap tagging of PROLIFERA, an essential MCM2-3-5-like gene in *Arabidopsis*." Science **268**(5212): 877-880.
- Sprunck, S., U. Baumann, et al. (2005). "The transcript composition of egg cells changes significantly following fertilization in wheat (*Triticum aestivum* L.)." Plant J **41**(5): 660-672.
- Steffen, J. G., I. H. Kang, et al. (2007). "Identification of genes expressed in the *Arabidopsis* female gametophyte." Plant J **51**(2): 281-292.
- Stephenson, A. G., S. E. Travers, et al. (2003). "Pollen performance before and during the autotrophic-heterotrophic transition of pollen tube growth." Philos Trans R Soc Lond B Biol Sci **358**(1434): 1009-1018.

- Strauss, M. and J. Arditti (1982). "postpollination phenomena in orchid flowers. X. transport and fate of auxin." *Bot. Gaz.* **143**: 286-293.
- Suarez Lopez, P. (2005). "Long-range signalling in plant reproductive development." *Int. J. Dev. Biol.* **49**(5-6): 761-771.
- Sugden, P. H. and A. Clerk (1997). "Regulation of the ERK subgroup of MAP kinase cascades through G protein-coupled receptors." *Cell Signal* **9**(5): 337-351.
- Swanson, R., T. Clark, et al. (2005). "Expression profiling of *Arabidopsis* stigma tissue identifies stigma-specific genes." *Sexual Plant Reproduction* **18**(4): 163-171.
- Swanson, R., A. F. Edlund, et al. (2004). "Species specificity in pollen-pistil interactions." *Annu Rev Genet* **38**: 793-818.
- Sweet, G. B. and P. N. Lewis (1969). "A diffusible auxin from *Pinus radiata* pollen and its possible role in stimulating ovule development." *Planta* **89**(4): 380-384.
- Sweetlove, L. J., J. L. Heazlewood, et al. (2002). "The impact of oxidative stress on *Arabidopsis* mitochondria." *The Plant Journal* **32**(6): 891-904.
- Takada, S. and G. Jurgens (2007). "Transcriptional regulation of epidermal cell fate in the *Arabidopsis* embryo." *Development* **134**(6): 1141-1150.
- Takase, T., M. Nakazawa, et al. (2004). "ydk1-D, an auxin-responsive GH3 mutant that is involved in hypocotyl and root elongation." *Plant J* **37**(4): 471-483.
- Takeda, S., N. Matsumoto, et al. (2004). "RABBIT EARS, encoding a SUPERMAN-like zinc finger protein, regulates petal development in *Arabidopsis thaliana*." *Development* **131**(2): 425-434.
- Tanaka, H., P. Dhonukshe, et al. (2006). "Spatiotemporal asymmetric auxin distribution: a means to coordinate plant development." *Cellular and Molecular Life Sciences* **63**(23): 2738-2754.
- Tanaka, H., M. Watanabe, et al. (2002). "ACR4, a putative receptor kinase gene of *Arabidopsis thaliana*, that is expressed in the outer cell layers of embryos and plants, is involved in proper embryogenesis." *Plant Cell Physiol* **43**(4): 419-428.
- Tang, X., L. Shen, et al. (2005). "BarleyExpress: a web-based submission tool for enriched microarray database annotations." *Bioinformatics* **21**(3): 399-401.

- Tanimoto, E. Y., T. L. Rost, et al. (1993). "DNA Replication-Dependent Histone H2A mRNA Expression in Pea Root Tips." *Plant Physiol* **103**(4): 1291-1297.
- Tebbji, F., A. Nantel, et al. (2010). "Transcription profiling of fertilization and early seed development events in a solanaceous species using a 7.7K cDNA microarray from Solanum chacoense ovules." *BMC Plant Biology submitted*.
- Theissen, G., A. Becker, et al. (2000). "A short history of MADS-box genes in plants." *Plant Mol Biol* **42**(1): 115-149.
- Thomas, T. L. (1993). "Gene expression during plant embryogenesis and germination: an overview." *Plant Cell* **5**(10): 1401-1410.
- Thompson, J. D., T. J. Gibson, et al. (1997). "The CLUSTAL_X windows interface: flexible strategies for multiple sequence alignment aided by quality analysis tools." *Nucleic Acids Res* **25**(24): 4876-4882.
- Tieman, D. M., J. A. Ciardi, et al. (2001). "Members of the tomato LeEIL (EIN3-like) gene family are functionally redundant and regulate ethylene responses throughout plant development." *Plant J* **26**(1): 47-58.
- Tonaco, I. A., J. W. Borst, et al. (2006). "In vivo imaging of MADS-box transcription factor interactions." *J Exp Bot* **57**(1): 33-42.
- Topping, J. F., V. J. May, et al. (1997). "Mutations in the HYDRA1 gene of Arabidopsis perturb cell shape and disrupt embryonic and seedling morphogenesis." *Development* **124**(21): 4415-4424.
- Torres-Ruiz, R. A., A. Lohner, et al. (1996). "The GURKE gene is required for normal organization of the apical region in the Arabidopsis embryo." *Plant J* **10**(6): 1005-1016.
- Treisman, R. (1996). "Regulation of transcription by MAP kinase cascades." *Curr Opin Cell Biol* **8**(2): 205-215.
- Treub, M. (1883). "L'action des tubes polliniques sur le développement des ovules chez les Orchidées." *Annales du jard. bot. de Buitenzorg* **3**: 122-128.
- Trevino, M. B. and O. C. MA (1998). "Three drought-responsive members of the nonspecific lipid-transfer protein gene family in *Lycopersicon pennellii* show different developmental patterns of expression." *Plant Physiol* **116**(4): 1461-1468.

- Tu, H., M. Barr, et al. (1997). "Multiple regulatory domains on the Byr2 protein kinase." Mol Cell Biol **17**(10): 5876-5887.
- Tu, Q., H. Tang, et al. (2004). "MedBlast: searching articles related to a biological sequence." Bioinformatics **20**(1): 75-77.
- Tung, C. W., K. G. Dwyer, et al. (2005). "Genome-wide identification of genes expressed in Arabidopsis pistils specifically along the path of pollen tube growth." Plant Physiol **138**(2): 977-989.
- Tzafrir, I., R. Pena-Muralla, et al. (2004). "Identification of genes required for embryo development in Arabidopsis." Plant Physiol **135**(3): 1206-1220.
- van Eldik, G. J., W. H. Reijnen, et al. (1997). "Regulation of flavonol biosynthesis during anther and pistil development, and during pollen tube growth in Solanum tuberosum." Plant J **11**(1): 105-113.
- Van Sint Jan, V., G. Laublin, et al. (1996). "Genetic analysis of leaf explant regenerability in Solanum chacoense." Plant Cell, Tissue and Organ Culture **47**(1): 9-13(15).
- van Went JL and W. MTM (1984). "Fertilization. In B Johri, ed, Embryology of Angiosperms." Springer-Verlag, Berlin: 273-318.
- Vandenbussche, M., J. Zethof, et al. (2003). "Toward the analysis of the petunia MADS box gene family by reverse and forward transposon insertion mutagenesis approaches: B, C, and D floral organ identity functions require SEPALLATA-like MADS box genes in petunia." Plant Cell **15**(11): 2680-2693.
- Vidaurre, D. P., S. Ploense, et al. (2007). "AMP1 and MP antagonistically regulate embryo and meristem development in Arabidopsis." Development **134**(14): 2561-2567.
- Vogt, T., P. Pollak, et al. (1994). "Pollination- or Wound-Induced Kaempferol Accumulation in Petunia Stigmas Enhances Seed Production." Plant Cell **6**(1): 11-23.
- Volinia, S., R. Evangelisti, et al. (2004). "GOAL: automated Gene Ontology analysis of expression profiles." Nucleic Acids Res **32**(Web Server issue): W492-499.
- Vriezen, W. H., R. Feron, et al. (2008). "Changes in tomato ovary transcriptome demonstrate complex hormonal regulation of fruit set." New Phytol **177**(1): 60-76.

- Vroemen, C. W., S. Langeveld, et al. (1996). "Pattern Formation in the Arabidopsis Embryo Revealed by Position-Specific Lipid Transfer Protein Gene Expression." *Plant Cell* **8**(5): 783-791.
- Vroemen, C. W., A. P. Mordhorst, et al. (2003). "The CUP-SHAPED COTYLEDON3 gene is required for boundary and shoot meristem formation in Arabidopsis." *Plant Cell* **15**(7): 1563-1577.
- Wagner, D., R. W. Sablowski, et al. (1999). "Transcriptional activation of APETALA1 by LEAFY." *Science* **285**(5427): 582-584.
- Wagner, D., F. Wellmer, et al. (2004). "Floral induction in tissue culture: a system for the analysis of LEAFY-dependent gene regulation." *Plant J* **39**(2): 273-282.
- Walling, L., G. N. Drews, et al. (1986). "Transcriptional and post-transcriptional regulation of soybean seed protein mRNA levels." *Proc Natl Acad Sci U S A* **83**(7): 2123-2127.
- Wang, H., N. Ngwenyama, et al. (2007). "Stomatal development and patterning are regulated by environmentally responsive mitogen-activated protein kinases in Arabidopsis." *Plant Cell* **19**(1): 63-73.
- Wang, H., H.-m. Wu, et al. (1996). "Pollination induces mRNA poly(A) tail-shortening and cell deterioration in flower transmitting tissue." *The Plant Journal* **9**(5): 715-727.
- Wang, H., H. M. Wu, et al. (1993). "Development and Pollination Regulated Accumulation and Glycosylation of a Stylar Transmitting Tissue-Specific Proline-Rich Protein." *Plant Cell* **5**(11): 1639-1650.
- Wang, Y., W. Z. Zhang, et al. (2008). "Transcriptome analyses show changes in gene expression to accompany pollen germination and tube growth in Arabidopsis." *Plant Physiol* **148**(3): 1201-1211.
- Weigel, D., J. Alvarez, et al. (1992). "LEAFY controls floral meristem identity in Arabidopsis." *Cell* **69**(5): 843-859.
- Weigel, D. and E. M. Meyerowitz (1994). "The ABCs of floral homeotic genes." *Cell* **78**(2): 203-209.
- Weijers, D., E. Benkova, et al. (2005). "Developmental specificity of auxin response by pairs of ARF and Aux/IAA transcriptional regulators." *EMBO J* **24**(10): 1874-1885.

- Weijers, D., A. Schlereth, et al. (2006). "Auxin triggers transient local signaling for cell specification in *Arabidopsis* embryogenesis." *Dev Cell* **10**(2): 265-270.
- Wellmer, F., M. Alves-Ferreira, et al. (2006). "Genome-wide analysis of gene expression during early *Arabidopsis* flower development." *PLoS Genet* **2**(7): e117.
- Wellmer, F., J. L. Riechmann, et al. (2004). "Genome-wide analysis of spatial gene expression in *Arabidopsis* flowers." *Plant Cell* **16**(5): 1314-1326.
- Went, J. and M. Cresti (1988). "Pre-fertilization degeneration of both synergids in *Brassica campestris* ovules." *Sexual Plant Reproduction* **1**(4): 208-216.
- West, M. and J. J. Harada (1993). "Embryogenesis in Higher Plants: An Overview." *Plant Cell* **5**(10): 1361-1369.
- Western, T. L. and G. W. Haughn (1999). "*BELL1* and *AGAMOUS* genes promote ovule identity in *Arabidopsis thaliana*." *The Plant Journal* **18**(3): 329-336.
- Weterings, K., M. Pezzotti, et al. (2002). "Dynamic 1-aminocyclopropane-1-carboxylate-synthase and -oxidase transcript accumulation patterns during pollen tube growth in tobacco styles." *Plant Physiol* **130**(3): 1190-1200.
- Weterings, K. and S. D. Russell (2004). "Experimental analysis of the fertilization process." *Plant Cell* **16 Suppl**: S107-118.
- Wheeler, M. J., S. Vatovec, et al. (2010). "The pollen S-determinant in *Papaver*: comparisons with known plant receptors and protein ligand partners." *J Exp Bot*.
- Whelan, S. and N. Goldman (2001). "A general empirical model of protein evolution derived from multiple protein families using a maximum-likelihood approach." *Mol Biol Evol* **18**(5): 691-699.
- White, J. A., J. Todd, et al. (2000). "A new set of *Arabidopsis* expressed sequence tags from developing seeds. The metabolic pathway from carbohydrates to seed oil." *Plant Physiol* **124**(4): 1582-1594.
- Wilhelmi, L. K. and D. Preuss (1996). "Self-sterility in *Arabidopsis* due to defective pollen tube guidance." *Science* **274**(5292): 1535-1537.
- Wilkinson, J., D. Twiss, et al. (1997). "Activities of CaMV 35S and nos promoters in pollen: implications for field release of transgenic plants." *J. Exp. Bot.* **48**(307): 265-275.

- William, D. A., Y. Su, et al. (2004). "Genomic identification of direct target genes of LEAFY." Proc Natl Acad Sci U S A **101**(6): 1775-1780.
- William F. Sheridan, B.-Q. H. (1997). "Nuclear behavior is defective in the maize *Zea mays* lethal ovule2 female gametophyte." The Plant Journal **11**(5): 1029-1041.
- Williams, E. J. (1955). "Seed failure in the Chippewa variety of *Solanum tuberosum*." Bot. Gaz. **10**: 10-15.
- Wolters-Arts, M., W. M. Lush, et al. (1998). "Lipids are required for directional pollen-tube growth." Nature **392**(6678): 818-821.
- Wu, C., E. Leberer, et al. (1999). "Functional characterization of the interaction of Ste50p with Ste11p MAPKKK in *Saccharomyces cerevisiae*." Mol Biol Cell **10**(7): 2425-2440.
- Wu, C. H., L. S. Yeh, et al. (2003). "The Protein Information Resource." Nucleic Acids Res **31**(1): 345-347.
- Wu, H. M. and A. Y. Cheung (2000). "Programmed cell death in plant reproduction." Plant Mol Biol **44**(3): 267-281.
- Wu, H. M., H. Wang, et al. (1995). "A pollen tube growth stimulatory glycoprotein is deglycosylated by pollen tubes and displays a glycosylation gradient in the flower." Cell **82**(3): 395-403.
- Xing, S., M. G. Rosso, et al. (2005). "ROXY1, a member of the plant glutaredoxin family, is required for petal development in *Arabidopsis thaliana*." Development **132**(7): 1555-1565.
- Yadegari, R. and G. N. Drews (2004). "Female Gametophyte Development." Plant Cell **16**(suppl_1): S133-141.
- Yamaoka, S. and C. J. Leaver (2008). "EMB2473/MIRO1, an *Arabidopsis* Miro GTPase, is required for embryogenesis and influences mitochondrial morphology in pollen." Plant Cell **20**(3): 589-601.
- Yanofsky, M. F., H. Ma, et al. (1990). "The protein encoded by the *Arabidopsis* homeotic gene agamous resembles transcription factors." Nature **346**(6279): 35-39.

- Yoshida, K., M. Endo, et al. (2005). "cDNA microarray analysis of gene expression changes during pollination, pollen-tube elongation, fertilization, and early embryogenesis in rice pistils." *Sexual Plant Reproduction* **17**(6): 269-275.
- Yu, H. J., P. Hogan, et al. (2005). "Analysis of the female gametophyte transcriptome of Arabidopsis by comparative expression profiling." *Plant Physiol* **139**(4): 1853-1869.
- Zhang, S. and D. F. Klessig (2001). "MAPK cascades in plant defense signaling." *Trends Plant Sci* **6**(11): 520-527.
- Zhang, X., B. Feng, et al. (2005). "Genome-wide expression profiling and identification of gene activities during early flower development in Arabidopsis." *Plant Mol Biol* **58**(3): 401-419.
- Zhang, X. S. and S. D. O'Neill (1993). "Ovary and Gametophyte Development Are Coordinately Regulated by Auxin and Ethylene following Pollination." *Plant Cell* **5**(4): 403-418.
- Zimmerman, J. L. (1993). "Somatic Embryogenesis: A Model for Early Development in Higher Plants." *Plant Cell* **5**(10): 1411-1423.
- Zimmermann, M. R., H. Maischak, et al. (2009). "System potentials, a novel electrical long-distance apoplastic signal in plants, induced by wounding." *Plant Physiol* **149**(3): 1593-1600.
- Zimmermann, P., M. Hirsch-Hoffmann, et al. (2004). "GENEVESTIGATOR. Arabidopsis microarray database and analysis toolbox." *Plant Physiol* **136**(1): 2621-2632.
- Zinkl, G. M., B. I. Zwiebel, et al. (1999). "Pollen-stigma adhesion in Arabidopsis: a species-specific interaction mediated by lipophilic molecules in the pollen exine." *Development* **126**(23): 5431-5440.
- Zybailov, B., H. Rutschow, et al. (2008). "Sorting signals, N-terminal modifications and abundance of the chloroplast proteome." *PLoS One* **3**(4): e1994.